ALFRED-WEGENER-INSTITUT
HELMHOLTZ-ZENTRUM FÜR POLAR- UND MEERESFORSCHUNG

736
2019

Berichte
zur Polar- und Meeresforschung

Reports on Polar and Marine Research

The Expedition PS119 of the Research Vessel POLARSTERN to the Eastern Scotia Sea in 2019

Edited by

Gerhard Bohrmann

with contributions of the participants

HELMHOLTZ

Die Berichte zur Polar- und Meeresforschung werden vom Alfred-Wegener-Institut, Helmholtz-Zentrum für Polar- und Meeresforschung (AWI) in Bremerhaven, Deutschland, in Fortsetzung der vormaligen Berichte zur Polarforschung herausgegeben. Sie erscheinen in unregelmäßiger Abfolge.

Die Berichte zur Polar- und Meeresforschung enthalten Darstellungen und Ergebnisse der vom AWI selbst oder mit seiner Unterstützung durchgeführten Forschungsarbeiten in den Polargebieten und in den Meeren.

Die Publikationen umfassen Expeditionsberichte der vom AWI betriebenen Schiffe, Flugzeuge und Stationen, Forschungsergebnisse (inkl. Dissertationen) des Instituts und des Archivs für deutsche Polarforschung, sowie Abstracts und Proceedings von nationalen und internationalen Tagungen und Workshops des AWI.

Die Beiträge geben nicht notwendigerweise die Auffassung des AWI wider.

Herausgeber
Dr. Horst Bornemann

Redaktionelle Bearbeitung und Layout
Birgit Reimann

Alfred-Wegener-Institut
Helmholtz-Zentrum für Polar- und Meeresforschung
Am Handelshafen 12
27570 Bremerhaven
Germany

www.awi.de
www.awi.de/reports

The Reports on Polar and Marine Research are issued by the Alfred Wegener Institute, Helmholtz Centre for Polar and Marine Research (AWI) in Bremerhaven, Germany, succeeding the former Reports on Polar Research. They are published at irregular intervals.

The Reports on Polar and Marine Research contain presentations and results of research activities in polar regions and in the seas either carried out by the AWI or with its support.

Publications comprise expedition reports of the ships, aircrafts, and stations operated by the AWI, research results (incl. dissertations) of the Institute and the Archiv für deutsche Polarforschung, as well as abstracts and proceedings of national and international conferences and workshops of the AWI.

The papers contained in the Reports do not necessarily reflect the opinion of the AWI.

Editor
Dr. Horst Bornemann

Editorial editing and layout
Birgit Reimann

Alfred-Wegener-Institut
Helmholtz-Zentrum für Polar- und Meeresforschung
Am Handelshafen 12
27570 Bremerhaven
Germany

www.awi.de
www.awi.de/en/reports

Titel: Blick in den Steuer-Container des ROV MARUM QUEST während des Tauchganges Nummer 449 in Hydrothermalfeldern der untermeerischen Kemp Kaldera im vulkanischen Bogen der Südsandwich Inseln (Foto: H. von Neuhoff).

Cover: View into the control container of ROV MARUM QUEST during dive number 449 in hydrothermal fields of the submarine Kemp caldera in the volcanic arc of the South Sandwich Islands (Photo: H. von Neuhoff).

The Expedition PS119 of the Research Vessel POLARSTERN to the Eastern Scotia Sea in 2019

Edited by
Gerhard Bohrmann
with contributions of the participants

Please cite or link this publication using the identifiers

http://hdl.handle.net/10013/epic.d1422e80-2643-40cf-a794-d5b4c73bbbdc
https://doi.org/10.2312/BzPM_0736_2019

ISSN 1866-3192

PS119

15 April 2019 – 31 May 2019

Punta Arenas – Port Stanley

Chief Scientist
Gerhard Bohrmann

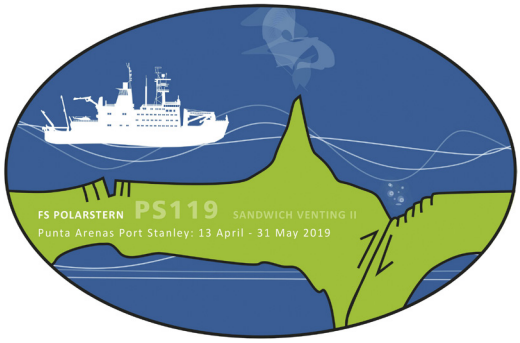

Coordinator
Rainer Knust

Contents

Appendix

1. ZUSAMMENFASSUNG UND FAHRTVERLAUF

Gerhard Bohrmann MARUM, Bremen

Zusammenfassung

Die 119. Expedition der *Polarstern* begann am 15. April 2019 in Punta Arenas, Chile, und endete auf den Falkland-Inseln in Port Stanley am 31. Mai 2019. Südgeorgien wurde nach 5 Tagen Transit erreicht, wobei die Anfahrtszeit für hydroakustische Messungen (Parasound und Hydrosweep) genutzt wurde. In Südgeorgien wurden mehrere Schwerelot- und Multicorer-Stationen am südlichen Kontinentalhang und im Bereich des Drygalski-Fjords bzw. Schelftroges durchgeführt.

Das Hauptarbeitsgebiet lag im Bereich der Sandwich-Platte, die durch den Vulkanbogen der 11 Südsandwich Inseln sowie zahlreiche submarine Vulkane gekennzeichnet ist. Erstmals wurde MARUM ROV QUEST 4000 an Bord von *Polarstern* in der Südhemisphäre zur Untersuchung von Hydrothermalsystemen eingesetzt. Weitere Themen waren der Vulkanologie der Saunders Insel und der Erfassung von Walen, insbesondere Finnwalen, gewidmet. Aufgrund recht kleinräumiger, wechselnder Wetterbedingungen wurden die Untersuchungslokationen durch die Wetterprognosen extrem bestimmt, wobei die häufigen Wechsel zur hydroakustischen Vermessung genutzt wurden. Insgesamt wurden 4 ROV-Tauchgänge auf dem Ost-Scotia Rückensegment E2 in 2.600 m Wassertiefe und 3 Tauchgänge in der Kemp Caldera, einem submarinen Inselbogenvulkan in 1.600 m Wassertiefe, durchgeführt. Dabei wurde der AWI-eigene TV-Schlitten OFOBS, der mit einem Sidescan-Sonar ausgestattet ist, vor allem zur Registrierung der Mikro-Bathymetrie mehrfach eingesetzt. Im Bereich E2 wurden Schwarze Raucher mit bis zu 344°C heißen Fluiden beprobt und ein neues Hydrothermalfeld mit 50°C heißen Fluidaustritten entdeckt, das wir „Alexander von Humboldt-Feld“ benannten. In der Kemp Caldera wurden vorwiegend Weiße Raucher mit geringer temperierten Fluidaustritten bis zu 230°C registriert. Elementarer Schwefel wurde sowohl als Präzipitat beprobt, als auch in flüssiger Form an Austritten beobachtet. Erstmals wurden die Tauchgänge über Telepräsenz ins Internet live gestreamt und Wissenschaftler, die nicht an Bord waren, wurden so erfolgreich an einzelnen Tauchgängen beteiligt. Weiterhin konnte die Telepräsenz für 4 Live-Schaltungen zu Veranstaltungen in Deutschland im Rahmen der Öffentlichkeitsarbeit sehr erfolgreich genutzt werden. Insgesamt haben wir 20 Schwerelot- , 3 Kolbenlot-, 18 CTD-, 13 Multicorer-Stationen, 10 OFOBS-Profile und 7 ROV Tauchgänge von insgesamt 46 Stunden Bodenzeit durchgeführt. Zusätzlich wurden entlang einer Stecke von 6.700 nautischen Meilen Fächerecholotdaten zur Bathymetrie und Sedimentecholotdaten zur Sedimentkartierung vermessen.

Fahrtverlauf

Am Montag, den 15. April 2019, verließ *Polarstern* um 13:48 Uhr Ortszeit die Ankerposition C auf Reede im Hafen von Punta Arenas, um nach einem dreitägigen Transit ein erstes Forschungsgebiet in den Gewässern um die subantarktische Insel Süd-Georgien zu erreichen.

Dem Auslaufen von *Polarstern* zur 119. Expedition war eine Liegezeit von einer Woche an verschiedenen Orten im Hafen von Punta Arenas vorausgegangen, um all die logistischen Herausforderungen zu meistern. Eine erste Hürde musste schon zuvor in Deutschland genommen werden, denn eine Teilnahme an der diesjährigen Europawahl am 26. Mai war vom Schiff aus nicht möglich. Im Bundesland Bremen wurde die Europawahl zusammen mit der Wahl zur neuen Bürgerschaft durchgeführt, und so war es uns ein Anliegen bereits vor dem Auslaufen noch wählen zu können. Obwohl die Bürgerschaftskandidaten erst am 1. April bekannt gegeben wurden und die Wahlscheine noch gedruckt werden mussten, hat das Wahlamt in Bremen große Anstrengungen unternommen, uns die Wahl am 8. April im Landesamt An der Weide 14-16 zu ermöglichen. Ein großer Dank geht daher an den Referatsleiter Herrn Martin Kesper, der mit seinem Team die Wahl für uns vorbereiten ließ, und wir daher unserer Bürgerpflicht auch nachkommen konnten.

Die weiteren Herausforderungen, die Schiff und Mannschaft leisteten, wurden durch die Hafenlogistik bestimmt. Die vorhergehende Reise mit *Polarstern* konnte zwar früher als geplant beendet werden, das Schiff allerdings musste auf Reede liegen, da die einzige Pier mit Tiefwasser, die Mardones Pier, von einem Frachter belegt war. So wurden die ankommenden Wissenschaftler mit Shuttle-Booten ausgeschifft und erst am Donnerstag, den 11. April, konnte die Ladung, vor allem der 4 Container mit der ROV-Ausrüstung, an der Mardones Pier erfolgen. Aufziehendes schlechtes Wetter erforderte die Verlegung des Schiffes auf Reede und erst am Samstag, den 13. April, konnten die restlichen zwei Container geladen werden, nachdem *Polarstern* abermals an der Mardones Pier anlegen konnte. Den Sonntag verbrachte das Schiff an der Bunker Pier Cabo Negro von Punta Arenas, wo wir tagsüber 2.000 Tonnen Treibstoff aufnahmen, um in den kommenden Wochen das Schiff betreiben zu können. *Polarstern* verholte noch in der Nacht wieder zur Ankerpier auf Reede, sodass wir am Montag, den 15. April, die abschließenden Decksarbeiten durchführen konnten. Nachdem das letzte Paket Luftfracht um 13:30 von der lokalen Agentur angeliefert wurde, konnte das Schiff ausklariert werden und seinen Ankerpunkt verlassen.

Nach dem Auslaufen in Punta Arenas und der 8-stündigen Passage durch die Magellan Straße begab sich *Polarstern* auf einen 4-tägigen Transit in Richtung Südgeorgien (Abb. 1.1). Diese Zeit ohne Stationsarbeiten wurde von den 51 Wissenschaftlern aus Deutschland, USA, Costa Rica, Österreich, Großbritannien, Bosnien und Herzegowina, Chile, Taiwan, Frankreich, Indien, Slowenien, Spanien und der Schweiz zur weiteren Einrichtung der Labore und zum intensiven Austausch über die wissenschaftlichen Themen der Fahrt genutzt. So wurden täglich Vorträge gehalten, die in die Diskussion der relevanten Themen unserer Fahrt einführten. *Polarstern* dampfte über den breiten argentinischen Schelf nach Osten, wobei wir nach knapp 2 Tagen größere Wassertiefen von mehr als 3.000 m im Falklandtrog, einer lang gestreckten Einkerbung zwischen dem Falklandplateau und der Burdwood Bank bzw. des nördlichen Scotia Rückens, erreichten. Nach Überquerung des ebenfalls flacher als 1.000 m aufragenden Nord-Scotia Rückens begannen wir im Scotiameer mit bathymetrischen und sedimentechographischen Vermessungen durch die schiffseigenen Hydrosweep- und Parasound -Anlagen. Dabei wählten wir auf unserem Weg nach Osten Kurslinien aus, die noch unkartierte Meeresbodenareale überdeckten, um so die noch vorhandenen großen Lücken der Meeresbodenvermessung in diesem Gebiet zumindest teilweise zu schließen.

Nachdem wir am vierten Tag, am Freitag den 19. April, die südwestlich Südgeorgiens vorgelagerte Tiefsee erreichten, begannen wir am frühen Samstagmorgen mit der Parasoundvermessung von Sedimentwellen. Diese Sedimentwellen, die sehr wahrscheinlich durch die Bodenströmungen moduliert wurden, dokumentieren durch höhere Sedimentationsraten die Paläozeanographie des antarktischen Zirkumpolarstromes und wurden daher zur Beprobung ausgesucht. Zwei Schwerelot- und eine Multicorer-Beprobung dieser Strukturen führten wir daher im Verlaufe des Samstags bei recht unruhiger See und

Winden zwischen Beaufort 6 und 7 durch (Abb. 1.2). Die am AWI geplanten multi-proxy Untersuchungen dieser Sedimente sollen neue Erkenntnisse zur räumlichen Variabilität der Oberflächen– und Tiefwasserzirkulation während des letzten orbitalen Klimazyklus aufzeigen. Die Meeresbereiche in der Umrandung von Südgeorgien sind aufgrund eines möglichen Eiseneintrages und der damit zusammenhängenden möglichen erhöhten Produktivität von besonderem Interesse für die Paläozeanographie. Für Sonntag, den 21. April, sollte das Wetter sich etwas bessern, und wir planten unseren ersten Tauchgang mit MARUM ROV QUEST, um an der sogenannten Paradise Flare die Austrittsstelle von Gasblasen zu untersuchen. Paradise Flare wurde während der *Meteor* Expedition M134 im Jahre 2017 auf einer von Eisbergen zerfurchten Ebene südlich von Paradise Beach in 170 m Wassertiefe in akustischen Aufnahmen der Wassersäule über dem Meeresboden entdeckt und konnte aufgrund schlechten Wetters nicht näher untersucht werden.

Wiederum hat uns das Wetter am Sonntag und Montag für eine detaillierte Untersuchung keine Gelegenheit gegeben. Wir konnten allerdings den neuen Multifunktionsschlitten der Tiefseegruppe des AWI, genannt OFOBS an der Lokation einsetzen (Abb. 1.2) und neben einer optischen Begutachtung der Umgebung der Paradise Flare am Boden auch eine bathymetrische Vermessung des Meeresbodens mit dem Fächerecholot des Schlittens durchführen. Am Nachmittag des Ostersonntags ging es in den Drygalski Fjord, der sich vom südöstlichsten Ende von Südgeorgien tief in die Insel einschneidet. Während der Eingang zum Fjord 2 km breit ist, verjüngt sich der Fjord auf ca. 800 m und von *Polarstern* aus hatte man einen fantastischen Ausblick auf die steilen Bergflanken, die Gletscher, und die geologischen Formationen dieser ältesten Gesteine Südgeorgiens gewinnen können. In der Mitte des Fjords haben wir einen Sedimentkern (GC-03; Abb. 1.2) in einem eng umgrenzten Becken gewonnen, dessen chemische Signatur besonders interessant für unsere Geochemiker ist. Die Beprobung gelang.

Am Ostermontag, den 22. April, war es wie erwartet leider auch zu stürmisch, um unseren ersten Tauchgang am Paradise Flare durchzuführen und wir nutzten diesen Tag, um eine Serie von Sedimentkernen aus den verschiedenen Subbecken des Drygalski Troges und einen Multicorer zu bergen. Hohe Sedimentablagerungen in einigen Fjorden und glazial erodierten Kanälen von Südgeorgien haben hervorragend das jüngere Gletscherverhalten und Klimaveränderungen archiviert. Die subpolare Südgeorgische Eiskappe reagiert empfindlicher auf klimatische Veränderungen als die viel größeren und isolierteren antarktischen Eisschilde und ist daher ein Hauptziel für Untersuchungen der Sedimentkernuntersuchungen zum besseren Verständnis der Klimaschwankungen der südlichen Hemisphäre. Leider erlaubte uns die Wetterlage frühestens am Mittwoch den ersten Tauchgang durchzuführen, und so haben wir uns dazu entschieden, am Dienstag zum Ost-Scotia-Rücken zu dampfen, um dort an den Hydrothermalquellen des Segmentes E2 mit dem Tauchen zu beginnen. Ein Hochdruckkeil aus Norden, der sich westlich von uns einschob, versprach ein paar Tage besseres Wetter, welches wir gerne zum Tauchen intensiv nutzen wollten.

Am Dienstag, den 23. April, dampften wir unter Nutzung der akustischen Vermessungssysteme in Richtung Osten und erreichten am Abend den Ost-Scotia Rücken. Dieser generell Nord-Süd verlaufende Rücken wird durch Spreizung des Meeresbodens um etwa 5 - 6 cm pro Jahr und austretende Lava in Form von Kissenbasalten neu gebildet. Der Rücken, der durch ein rückenparalleles Schollenmosaik ein kompliziertes morphologisches Gebilde mit z.T. sehr steilen Hängen bildet, trennt die Scotia-Platte im Westen von der Süd-Sandwich-Platte im Osten. In Nord-Süd Erstreckung wird der Rücken in 10 Segmente von jeweils 30 bis 90 km Länge aufgeteilt (E1 bis E10). In zwei der Segmente, in E2 und E9, wurden von unseren britischen Kollegen aktive Hydrothermalquellen entdeckt. In diesen Bereichen liegen Magmenkammern in 2 - 3 km Krustentiefe, von denen im Spreizungsbereich Magma sehr leicht aufsteigen kann und am Meeresboden ausfließt.

Nach Ankunft im Segment E2 des Ost-Scotia Rückens am Dienstagabend den 23. April haben wir zunächst mit dem OFOBS und mit einer CTD-Sonde mit Wasserschöpfern versucht, chemische Signale für heiße Quellen am Meeresboden in der Wassersäule zu finden (Abb. 1.3). Dabei waren vor allem unsere sogenannten Mapper, die neben Trübung auch Temperatur und Redoxpotential detektieren, eine große Hilfe. Als autonom-registrierende Messinstrumente wurden sie bei fast allen Geräteeinsätzen mit eingesetzt. Diese Sucharbeiten wurden am Mittwoch, den 24. April, fortgesetzt und am Donnerstag, den 25. April, kam es dann endlich zu dem ersten Einsatz des ROV QUEST (ROV 444; Abb. 1.3). Wir tauchten in dem bekannten Hydrothermalfeld, welches während der *James Clark Ross* Expedition 224 vor 10 Jahren entdeckt wurde. Mit etwas Mühe konnten wir die meisten der bekannten Hydrothermalstrukturen wiedererkennen, wobei sehr bald während des Tauchgangs klar wurde, dass es in den letzten 10 Jahren große Veränderungen gegeben haben muss. Einige der damals aktiven Schwarzen Raucher waren jetzt nicht mehr aktiv und andere zeigten aktive Fluidaustritte heute, die vor 10 Jahren inaktiv waren. Entsprechend haben sich auch die Besiedlungen der chemosynthetisch-lebenden Faunen verändert. Trotzdem konnten wir ausgewählte Organismen wie einige Schnecken der Gattung *Gigantopelta* und eine sogenannte *Kiwa*-Krabbe für geplante Aquariumsversuche erfolgreich bergen. Während des Tauchganges nutzten wir erstmals eine sogenannte Telepräsenz, die von unserem ROV Projektleiter Volker Ratmeyer und seinem Team für diese Reise installiert wurde.

Dazu war eine spezielle Hardware angeschafft worden, die über die Antennenanlage der *Polarstern* eine stabile Satelliten-Übertragung der beim Tauchgang anfallenden Bilder mit 5 Mbit upload erlaubt, sodass Kollegen in Bremen und anderswo über das Internet sich online beim Tauchgang beteiligen konnten, indem sie die Audiokommunikation, die Datei-Übertragung und das interaktive Geographische Informationssystem in Echtzeit nutzten. Beim 2. Tauchgang mit QUEST am Samstag, den 27. April, konnte zusätzlich im Rahmen eines Live-Streams über das Internet die Öffentlichkeit mit einer Verzögerung von 30 Minuten an dem Tauchgang teilnehmen. Wie wir erfahren haben, wurde dies auch zu nächtlicher Zeit in Deutschland zwischen 22 Uhr abends bis 04 Uhr morgens genutzt. Auch der 2. Tauchgang (ROV 445; Abb. 1.3) war ein voller Erfolg, denn wir hatten in einem unbekannten Gebiet ein wohl abklingendes Hydrothermalfeld entdeckt, wobei Mineralschlote mit gemessenen Fluidtemperaturen von 30 - 50°C assoziiert sind.

Die neue Woche begannen wir am Montag, den 29. April, mit einem langen Tauchgang zur Beprobung von Raucherschloten und Ventorganismen des Hydrothermalfeldes von Segment E2 Süd (ROV 446; Abb.1.3). Dabei konzentrierten wir uns auf aktive Ventsysteme um Dog's Head, einem komplexen Gebilde aus 4 Schloten, die in einer Reihe hintereinander im Bodenbereich zusammengewachsen und in 12 - 15 m Höhe durch einzelne Austritte von „schwarzem Rauch" gekennzeichnet sind. Südlich von Dog's Head clustern zahlreiche erloschene Reliktschornsteine sowie aktive Fluidschlote, die sehr unterschiedlich mit Anemonen, Schnecken, Krebsen und anderen Organismen besiedelt sind. Auffällig sind vor allem die weißen Bakterienmatten, die einzelne Raucher wie schneebedeckte Berge aussehen lassen.

Mit unseren speziellen Fluidprobennehmern aus chemisch inertem Titan konnten wir 2 der austretenden Fluidströme der schwarzen Raucher beproben. Die Fluidprobennehmer sind gasdicht. Beim Auftauchen des ROV und der damit zusammenhängenden Druckentlastung kann das Gas nicht entweichen und wir können die Konzentrationen der Gase an Bord mit einem Gaschromatographen messen. Der Schnorchel des Fluidprobennehmers, mit dem das heiße Fluid aus dem geöffneten Schlot sehr gezielt beprobt werden kann, ist weiterhin mit einem Temperatursensor gekoppelt, sodass wir auch sehr genau die Temperaturen der Fluide messen können. Die erste Probe war 320°C heiß und enthielt in der Gasphase hohe Wasserstoff- und Methankonzentrationen. Nur etwa die Hälfte der Gaskonzentrationen wurden in einem zweiten Fluid bei einer Austrittstemperatur von 344° C gemessen. Diese hohen Temperaturwerte werden nur im Fluidstrom unmittelbar an der Austrittsstelle

gemessen, während das umgebende Meerwasser nur leicht erwärmt ist. Vent-unbeeinflusstes Meerwasser hat am Boden des Seegebietes eine Temperatur von 0° Celsius, die je nach Nähe zu fokussiertem und diffusem Ausfluss auf einige wenige Grad C ansteigen kann. Neben den Fluidproben wurden auch Gesteinsproben der Schornsteine mit dem Greifarm des ROV QUEST geborgen, die neben Anhydrit auch metallisch glänzende Sulfidminerale wie Kupferkies, Pyrit und Zinkblende enthielten. Insgesamt war es ein sehr erfolgreicher Tauchgang, der in Bremen durch die Möglichkeit der Telepräsenz von Kollegen aktiv mitverfolgt wurde.

Die anschließende Nacht wurde zur Suche von Sedimentkernpositionen genutzt, die wir in mit Sediment gefüllten Becken zwischen tektonischen Hochschollen der magmatischen Kruste in verschiedenen Wassertiefen fanden. Zwei Sedimentkernpositionen wurden ausgewählt, an denen wir am Dienstag, den 30. April, Schwerelotkerne und Multicorerproben (GC-12, -13 und MUC-06; Abb. 1.3) nahmen. Die Untersuchung der Porenwässer dieser Sedimentkerne und die der Vortage sowie der Chemie der Eisenminerale wird zur Erfassung der „Plume“-artigen Verdriftung der Eisenminerale aus den heißen Quellen in die Umgebung beitragen. In der Nacht von Dienstag auf Mittwoch kartierten wir einen Streifen Meeresboden vom Spreizungszentrum E2 nach Osten, den Inselbogen der Südlichen Sandwich Inseln nördlich von Zavodovski Island querend über den Forearc-Bereich bis in die Tiefseerinne der Südsandwich-Subduktionszone (Abb. 1.3). Diese ist in ihrem nördlichen Teil besonders tief und erreicht im sogenannten Meteor-Tief eine Wassertiefe von 8.264 m. Das Tief wurde von der 1. *Meteor* auf seinem südlichsten West-Ost-Profil während der Expedition 1925-1927 entdeckt und als tiefste Stelle im Südatlantik vermessen. Mit einem CTD-Profil (CTD-06; Abb.1.3) mit Wasserproben zur Bestimmung der Methankonzentrationen begann der Mittwoch, der 1. Mai.

Wiederum wurde eine Nacht und ein Vormittag in Richtung Süden entlang des Forearc-Bereiches kartiert und gleichzeitig nach Indikatoren für Fluid- und Gasaustritte gesucht, bis wir am Nachmittag Saunders Island, das Ziel unserer Vulkanologen, erreichten (Abb. 1.3). Die vulkanische Insel ist die drittgrößte der Südsandwich Inseln, die von Norden nach Süden in einem nach Osten zeigenden Bogen parallel der Tiefseerinne aufgereiht sind. Während die nördlichen Vulkaninseln mit russischen Namen von Admiral Fabian Gottlieb von Bellingshausen entdeckt wurden, hat James Cook die südlichen entdeckt und mit britischen Namen versehen. Der Mount Michael auf Saunders Island ist wie viele der Inselvulkane aktiv und zeigte sich in Teilen erst nach einer Weile. Weder die geplante Vermessung der Insel mit Drohnen noch ein Besuch der Vulkanologen auf der Insel war aufgrund des schlechten Wetters möglich. So haben wir in immer enger werdenden Kreisen den Meeresboden um die Insel vermessen, um bei einem späteren Besuch das Vulkanprogramm besser verwirklichen zu können.

Am Sonntag, den 5. Mai, erreichten wir die Kemp Caldera, die am Südende des Südsandwich Vulkanbogens eine prominente vulkanische Kraterstruktur darstellt. Die Caldera mit einem mittleren Durchmesser von 7,4 km ist im Zentrum 1.600 m tief und hat einen breiten Rand mit etlichen Parasitärkegeln in 800 - 900 m Wassertiefe (Abb. 1.4). Ein jüngerer Vulkankegel überragt den westlichen Kraterboden um ca. 200 m. An seinen Flanken hatten unsere britischen Kollegen hydrothermale Aktivitäten beobachtet. Eine erste CTD-Sonden Messung (CTD-07; Abb. 1.4) am Sonntag über dem bekannten Hydrothermalfeld bestätigte, dass hydrothermale Aktivität weiterhin besteht. Neben einer deutlich erhöhten Trübung wurden erhöhte Temperaturen sowie Anomalien im Redoxpotenzial und im Methangehalt des Wasserkörpers nahe der Hydrothermen festgestellt. Am Montag, den 6. Mai, führten wir zunächst eine Schwerelot- und Multicorer-Beprobung auf dem halben Weg zwischen der Caldera im Osten zum Segment E9 des Ost-Scotia Rückens im Westen durch. Es folgte in der Nacht von Montag auf Dienstag eine weitere CTD-Beprobung sowie eine Profilvermessung mit dem OFOBS (Ocean Floor Observation Bathymetry System; OFOBS-04). Am Dienstag, den 7. Mai, war es endlich soweit, und wir konnten einen langen Tauchgang mit dem Tauchroboter QUEST in der Kemp Caldera mit über 11 Stunden Bodenzeit durchführen (ROV-447; Abb. 1.4). Begonnen hatten wir den Tauchgang an einer Lokation namens „Great Wall“, die ihren Namen

von einem herausgewitterten Ganggestein hat, das an vielen Stellen mit gelbem Schwefel bzw. mit weißen Bakterienmatten überdeckt ist. Einzelne Schornsteine scheinen vollkommen aus Schwefel zu bestehen und beim Abbrechen von Schwefelstücken zeigte sich die frische gelbe Farbe elementaren Schwefels. Schwefel konnten wir ebenfalls in einem weiteren Gebiet 100 m südöstlich, das als „Winter Palace“ bekannt ist, sehen. Der Schwefel trat direkt vor unseren Kameralinsen in flüssiger Tropfenform auf, bevor er sich zu perlenartigen Strukturen in dem kalten Meerwasser verfestigte.

Die Region ist durch zahlreiche weiße Raucher gekennzeichnet, die eine helle Trübung im Bodenwasser verursachen. Mit unseren Fluid-Probennehmern haben wir die austretenden Fluide beprobt, um ihre chemische Zusammensetzung zu analysieren. Das heiße austretende Wasser, in dem verschiedene Stoffe in hohen Konzentrationen gelöst enthalten sind, vermischt sich mit dem kalten Meerwasser. Dabei scheiden sich die gelösten Substanzen in Form von feinen Mineralpartikeln ab, die einerseits die Schornsteine selbst aufbauen und zum anderen helle Wolkenkegel bilden. Die Weißen Raucher haben generell geringere Temperaturen als die Schwarzen Raucher, und in den weißen Wolken werden helle Minerale, wie Anhydrit, Opal und Baryt präzipitiert, während bei den Schwarzen Rauchern sulfidische Metalle abgeschieden werden. Welche Minerale durch die Weißen Raucher der Kemp Caldera ausgeschieden werden, können wir erst nach der Analyse der Fluide und der Gesteinsproben wissen. Der fantastische Tauchgang, der über die Telepräsenz von zahlreichen Interessierten an Land begleitet wurde, war nicht nur am Meeresboden spannend, sondern auch auf der Brücke. Dort wurde ein 700 m langer Tafeleisberg etwa 2,5 nautische Meilen südlich unserer ROV-Position beobachtet, der sich langsam auf uns zubewegte und etwa nach der ersten Hälfte des Tauchganges auf 1,6 Meilen herangedriftet war. Beinahe hätten wir früher als geplant auftauchen müssen. Doch zum Glück änderte der Eisberg seine Richtung und passierte *Polarstern* an der Backbordseite in genügend großem Abstand.

Als Teil des wissenschaftlichen Programms führen unsere Biologen Experimente zum Verständnis der Biologie von hydrothermal-assoziierten Organismen durch. Dazu wurden im Sediment lebende vesicomyide Muscheln der Art *Laubiericoncha puertodeseadoi* mit ROV QUEST lebend geborgen und in Aquarien auf dem Schiff weiter versorgt. Das Bodenwasser der Caldera hat eine Temperatur von 1°C, und der vulkanische Einfluss erwärmt das Sediment auf etwa 5°C. Die Tiere wurden an Bord in 2 Temperaturklassen aufgeteilt, wobei eine Gruppe bei 2°C und die andere bei 10°C gehalten wurde. Verschiedene Messungen, z.B. des Sauerstoffverbrauchs der Tiere, lassen Rückschlüsse auf die Temperaturverträglichkeit zu.

Am Mittwoch, den 8. Mai, beprobten wir ein Sedimentbecken östlich der Riftachse von Segment E9, das von zwei Hochschollen magmatischer Gesteine eingegrenzt wird. Die hervorragende akustische Eindringung der Parasoundanlage zeigte uns eine Sedimentabfolge von mehr als 50 m. Mit dem Kolbenlot (PC-02; Abb. 1.3) konnten wir fast 12 m hervorragend geschichtete Ablagerungen beproben, die eine bunte Abfolge von hemipelagischen Sedimenten mit teilweise vulkanischen und hydrothermalen Komponenten beinhalten. Unsere Geochemiker erfreute dies, denn sie untersuchen in mehreren Sedimentkernen, wie weit hydrothermale Partikel mit der Ostströmung vom Spreizungsrücken entfernt transportiert werden können. Am Donnerstag, den 9. Mai, verließen wir dieses südlichste Arbeitsgebiet für 2 Tage, um im Rückensegment E5 (Abb. 1.3) nach hydrothermalen Aktivitäten zu suchen. Dieses Rückensegment besitzt wie E2 und E9 eine Magmenkammer, die in relativ geringem Abstand zum Meeresboden liegt, sodass die Existenz einer hydrothermalen Zirkulation mit Fluidaustritten und anderen Hot Vent Erscheinungen am Meeresboden wahrscheinlich ist. Die größte Wahrscheinlichkeit neue Fluidaustritte zu finden, lag in der Untersuchung einer axialen Hochlage des Rifttals im zentralen Bereich. Dort führten wir eine CTD-Messung (CTD-09) und ein Messprofil mit dem OFOBS (OFOBS-05; Abb. 1.3) durch. Kleine Anomalien in der Trübung und auch im Methangehalt waren zwar prinzipiell zu sehen, sie waren aber zu unspezifisch, sodass wir beschlossen, hier nicht weiter nach Vents zu suchen.

Wie in der Woche zuvor, verbrachten wir auch die 6. Woche im südlichsten Bereich der Südsandwich Platte vom Backarc Spreizungsrücken der Segmente 8 und 9 im Westen bis zur Kemp Caldera. Die Wetterbedingungen, die von Sonntag bis Dienstagmorgen weitere Tauchgänge verhinderten, erlaubten uns erst wieder am Dienstag mit ROV QUEST zum Meeresboden abzutauchen. Die Zeit nutzten wir zum Einsatz anderer Beprobungsgeräte. So haben wir am Sonntag, den 12. Mai, mit einem 3 m Schwerelot und einem Multicorer den tiefsten Bereich der Kemp Caldera beprobt (GC-16; Abb. 1.4). Die bis dahin vermessenen Parasoundprofile über den Krater zeigten im tiefsten Bereich geringmächtige Sedimentlagen an, deren mineralogische und chemische Zusammensetzung im Hinblick auf hydrothermale Einlagerungen von großem Interesse ist. Mit den Kerngeräten gelang es, eine Sedimentabfolge von 230 cm zu beproben, die uns aufgrund ihrer Farben und unterschiedlichen Sedimentzusammensetzungen überraschte.

Reinste biogene Opalschlämme kamen zum Vorschein, die aus Diatomeen-Skeletten aufgebaut werden. Kieselalgen werden in großen Mengen im Oberflächenwasser des Südozeans südlich der Polarfront gebildet und ihre Skelette werden nach dem Absterben am Meeresboden im sogenannten Opalgürtel abgelagert. Besonders auffällig in unserem Kern sind Matten der Diatomeen-Gattung *Thalassiotrix*, welche als extrem nadelförmige Zellhüllen aus Biogenopal aufgebaut sind und bei monospezifischem Auftreten im Sedimentkern wie nasse Papiertaschentücher aussehen. Die reinen Opalschlämme sind in einigen Abschnitten durch Metallsulfide stark verfärbt, sodass die Abfolge insgesamt die Hydrothermalaktivität innerhalb der Caldera über die Zeit dokumentiert. Am Montag, den 13. Mai, haben wir etwa 60 km westlich der Kemp Caldera an der östlichen Flanke von Rückensegment E8 Sedimente mit einem Kolbenlot (PC-02; Abb. 1.3) beprobt. Die Ablagerungen des 8,70 m langen Kernes haben hohe Anteile an vulkanischen Komponenten und unsere Geochemiker sind daran interessiert, den Einfluss hydrothermaler Aktivität und besonders die Eisengeochemie daran zu untersuchen. Aus diesem Interesse heraus werden im Abstand von jeweils 10 cm Porenwasserproben gewonnen, an denen Alkalinität und Eisenkonzentrationen bereits an Bord bestimmt werden. Die weiteren Nährstoffe und spezifische gelöste Komponenten werden nach der Reise in den Laboren der Heimatinstitute gemessen.

Am Dienstag, den 14. Mai, stand die Kemp Caldera erneut im Mittelpunkt unserer Forschung. Es wurden mehrere CTD-Stationen (CTD-11, -12, -13; Abb. 1.4) mit Wasserschöpfer-beprobungen nahe dem Hydrothermalgebiet, im Zentrum der Kraterstruktur und in ihrem Randbereich, durchgeführt. Anhand der Anomalien in Trübung, Redoxpotential, Temperatur und im Methangehalt wollen wir den Einfluss des aktiven Hydrothermalgebietes auf die Meerwasserchemie untersuchen. Es folgte dann der ROV Tauchgang ROV-449 am nördlichen Rand der Kemp Caldera in 1.100 m Wassertiefe an einer Lokation, an der wir mehrfach in der Wassersäule Gasblasenaustritte akustisch detektieren konnten. Beim Tauchen mit ROV QUEST konnten wir allerdings den Austritt der Gasblasen am Meeresboden nicht finden und haben uns auf die Beprobung von neu entdeckten Schornsteinen mit Fluidaustritten konzentriert. Ein Schwarzer Raucher, dessen Fluidaustrittstemperatur bei 230°C lag, hatte einen hohen Eisengehalt und den bisher geringsten pH-Wert von 2,3, während ein zweiter Schornstein bei einer Temperatur von 200°C kaum Eisen enthielt und einen pH von 5,5 zeigte.

Obwohl sich während der 3 Tauchgänge in der Kemp Caldera weitere Tauchzielwünsche ergeben haben, mussten wir im Hinblick auf weitere Ziele der Expedition am Mittwoch, den 15. Mai, die Kemp Caldera verlassen. Die Route führte uns in den nordwestlichen Bereich der Südsandwichplatte, an den Inseln Leskov, Visokoi and Zavadovski vorbei in den Forearc-Bereich (Abb. 1.3). Es wurde ein OFOBS-Profil über einem Forearc-High durchgeführt, um Indikatoren für mögliche kalte Quellen zu finden. Dort haben in früheren Jahren britische Wissenschaftler serpentinisierte Mantelgesteine gedredgt, die in anderen Meeresgebieten auch mit Fluidaustritten am Meeresboden assoziiert sind. In der Nacht ging es weiter nach Süden, wo wir am Morgen des 17. Mai die Vulkaninsel Saunders erreichten. Unsere

Vulkanologen planten einen Besuch mit Probennahme und photogrammetrischer Vermessung durch Drohnenflüge. Aufgrund des Wetters, das sich im Laufe des Tages sehr verbesserte, konnten Drohnenvermessungsflüge von der *Polarstern* durchgeführt werden, vor allem nachdem *Polarstern* ihren Weg in die Cordelia-Bucht fand und dort sehr nahe an die Insel heran kam.

Ein weiterer Tauchgang in dem Hydrothermalgebiet E2 Süd konnte am Samstag, den 18. Mai, (ROV-450; Abb. 1.3) sehr erfolgreich abgeschlossen werden, bevor sich das Wetter in der Nacht wesentlich verschlechterte. Da ein orkanartiger Sturm für die 2. Nachthälfte und den anschließenden Morgen angekündigt wurde, sind wir mit *Polarstern* in der Nacht nach Osten gedampft und haben uns am Sonntagmorgen in den Windschatten der Vulkaninsel Zavodovski zum Abwettern gelegt. Bei Windstärken 10 bis 11 mit gelegentlichen Spitzenwerten nach Beaufort 12 haben wir im Schutze der Insel 3 - 4 Meter hohe Wellen, während außerhalb z.T. über 8 m hohe Wellen abgeschätzt werden.

Die rasche Wetteränderung, die uns am letzten Wochenende heimsuchte, war beispielhaft für die gesamte letzte Woche. Am Samstag konnten wir zwar noch den 450. Tauchgang des MARUM ROV QUEST im Spreizungsegment E2 des Ost-Scotia Rückens durchführen, aber den Sturm am Sonntag mussten wir im Windschatten der Insel Zavodovski abwetterten. Erst am Montag, den 20. Mai, um 04:00 Schiffszeit verließen wir den Schutz der nördlichsten der 11 Südsandwich Inseln, um nach Westen in Richtung unseres Hydrothermalgebietes E2 zu dampfen. Von zwei geplanten Schwerelot-/Multicorer-Stationen konnten wir aus Zeitgründen nur eine verwirklichen, wobei Sandlagen vulkanischer Komponenten beprobt wurden, deren Ursprung im Vulkanbogen liegt. In E2 angekommen, war zunächst ein OFOBS-Profil geplant, wobei wir in Ost-West-Richtung das bereits bekannte Hydrothermalgebiet mit hochauflösender Mikro-Bathymetrie vermessen wollten. Die Wettervorhersage vom Montagmorgen führte uns zu einer anderen Entscheidung.

Zum sicheren Tauchen mit ROV QUEST brauchen wir stabile Wetterbedingungen mit Wellenhöhen unter 3 m für mehrere Stunden. Wir schauen daher nach solchen Bedingungen im gesamten Arbeitsgebiet der Südsandwichplatte 2 - 3 Tage im Voraus. Das Arbeitsgebiet erstreckt sich allerdings über 5 Breitengrade und 8 Längengrade und unser Meteorologe war eifrig bemüht uns die günstigsten Tauchbedingungen in allen Regionen des Arbeitsgebietes vorherzusagen. Aufgrund der kleinräumigen Hochs und Tiefs und ihrer Wanderung war dies nicht sehr einfach. So wurde am Montagmorgen klar, dass am morgigen Dienstag und Mittwoch nur Tauchbedingungen im südlichsten Teil im Bereich der Kemp Caldera zu finden sein werden. Da im Norden auch die längere Wetterprognose den Einsatz des ROV nicht möglich erscheinen ließ, dampfte *Polarstern* sofort in Richtung Süden zur Kemp Caldera. Dabei konnte ein breiter Streifen Multibeamkartierung an die bereits vorhandene Kartierung des zentralen Spreizungszentrums angeschlossen werden. Am Abend des 21. Mai sollte dann der nächste Tauchgang beginnen.

Wir mussten allerdings lernen, dass aus technischen Gründen mit dem Fahrzeug kein Tauchgang auf dieser Reise mehr möglich war und dampften daher sogleich in Richtung Saunders Island. Dort konnte das Team der Vulkanologen am Mittwoch, den 22. Mai, die photogrammetrische Kartierung der Vulkaninsel fortsetzen. Während bei der Vermessungszeit zuvor die Nordost-Seite der Cordelia Bucht und Teile der Südost-Flanke mit den Ashen Hills kartiert wurden, konnten mit Drohnenflügen die westlichen und nördlichen Inselbereiche aufgenommen werden. Wichtige Daten, die eine topographische Karte in bis zu 10 cm Auflösung erlauben, wurden mit optischer Kamera und Infrarotkamera durch Drohnenvermessung gewonnen. Nach Sonnenuntergang dampfte *Polarstern* nach Nordwesten zum Spreizungsrücken. Dort wurden am Donnerstag, den 23. Mai, mehrere Sediment- und Wasserbeprobungen in einer Region durchgeführt, die Plume-artige Strukturen in der Wassersäule zeigte. Schon in der Nacht zum Freitag kam der nächste Sturm, dem wir aus Zeitgründen nicht ausweichen konnten. Die

Bordwetterwarte hatte uns Zeitpunkt und Verlauf des Sturms vorausgesagt, sodass wir die Geräteeinsätze sehr gut nach der meteorologischen Vorhersage planen konnten. Obwohl das Wettermodel des Deutschen Wetterdienstes nur wenige Bodenstationen sowie die Schiffs- und Satellitendaten nutzt, ist es erstaunlich genau. Sehr wichtige Basisdaten dafür, wie Temperatur, Feuchte, Luftdruck und mittels GPS-Analyse auch Geschwindigkeit und Richtung der Luftpartikel werden durch die täglichen Radiosonden-Aufstiege bis in 30 - 35 km über der Wasseroberfläche durch die Mitarbeiter des DWD auf *Polarstern* selbst ermittelt. Zweimal am Tag bekommen wir eine aktuelle Wettervorhersage, die uns auf der Reise ein sehr wichtiges Entscheidungskriterium zur Stationsauswahl ist.

Auch das Team der Walbeobachter der Universität Hamburg ließ sich von den Wetterbedingungen nicht beirren. Auf Grund von häufiger Vereisungsgefahr und starken Stürmen war der Einsatz des Helikopters für gezielte Zählflüge über dem offenen Meer nicht immer möglich. So wurde auch das Krähennest über der Brücke von *Polarstern* für systematische Walerfassungen genutzt. Den Umweltbedingungen trotzend, konnten so wichtige Daten zum Vorkommen und zur Verteilung von Walen, insbesondere Finnwalen, in der Region gesammelt werden. Zusammen mit Daten aus vorherigen Erfassungskampagnen an Bord von *Polarstern* wird es demnächst möglich sein, eine verlässliche Abschätzung zum Vorkommen und zur Verteilung von Walen im Untersuchungsgebiet zu erstellen.

Nach unserem Sturm am letzten Freitag, den 24. Mai, erholte sich die See nur sehr langsam und Stationsarbeiten waren erst spät in der Nacht zum Samstag mit zwei CTD-Stationen (CTD-12 und -13; Abb. 1.3) möglich. Die Messungen wurden etwa 60 km westlich des Spreizungszentrums an seiner Flanke durchgeführt. Dort ist der Meeresboden durch Nord/Süd-orientierte parallele Störungen in Schollen zergliedert und mit jungen Sedimenten bedeckt. Wir haben sowohl in diesen Sedimenten als auch in der Wassersäule Anzeichen für eine Fluidzirkulation in unseren Parasound-Aufzeichnungen entdeckt. Eine Fluidzirkulation, bei der Meerwasser in die Erdkruste eindringt und durch die Wärmeaufnahme in der jungen Kruste zirkuliert und als warmes oder heißes Fluid an anderen Stellen am Meeresboden wieder ausfließt, ist nicht nur von Spreizungsrücken bekannt, sondern wird mehr und mehr auch an den Flanken weit ab von dem gerade aktiven Spreizungssegment beobachtet. In den Wasserproben der CTD wurden schon leicht erhöhte Methanwerte am Boden gemessen, die auf einen Ausstrom hindeuten. Auch die ersten Sedimentkerne, die wir vor drei Wochen dort genommen haben, zeigen Porenwasserprofile, die Hinweise sowohl auf einströmendes, an anderer Stelle auch auf ausströmendes Fluid geben, welches wir gerne durch weitere Proben bestätigen oder verifizieren wollten. Nachdem es klar wurde, dass der wichtige Sedimentkern aufgrund des Seegangs auch Samstagmorgen nicht genommen werden konnte, fuhren wir nach Osten und führten unser früher geplantes OFOBS-Profil in Ost-West-Richtung im Spreizungssegment E2 am Samstag, den 25. Mai, (OFOBS-10; Abb. 1.3) durch. Danach ging es in der Nacht zurück zur CTD-Station, wo wir einen fast 8 m langen Sedimentkern nehmen konnten.

Alsbald verließ die *Polarstern* das Gebiet des Ost-Scotia Rückens in Richtung Süd-Georgien, was leider nur unter recht ruppigen Seeverhältnissen möglich war. Am Sonntag, den 26. Mai, haben wir bereits bei Dunkelheit im Drygalski Trog den letzten Sedimentkern (GC-20; Abb.1.2) aus dieser Reise genommen. Danach hat *Polarstern* seinen Rückweg angetreten und nachdem wir die Nordostseite von Süd-Georgien erreicht hatten, ging es entlang der langgestreckten Insel auf dem Schelf nach Westen geradewegs auf die Falkland Inseln zu (Abb. 1.1). Diese Strecken des Rückwegs nutzten wir von Montag bis Donnerstag für weitere Vermessungen mit dem Fächerecholot Hydrosweep und dem Parasound Sedimentecholot. Die stationsfreie Zeit nutzten wir zur Auswertung der Daten, für den Fahrtbericht, zum Packen, zum Reinigen der Labore und für Präsentationen während des täglichen Meetings im Kinoraum des Schiffes. Am Freitag, den 31. Mai, erreichte die *Polarstern* Port Stanley auf Reede, wo die Wissenschaftler von Bord gingen.

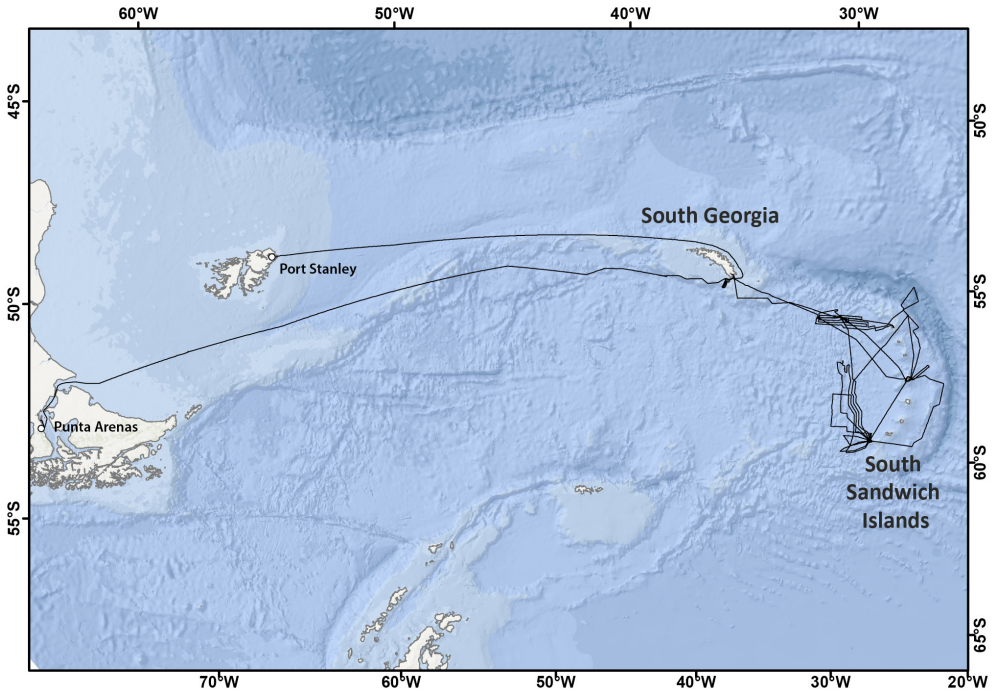

Abb. 1.1: Fahrtroute der Polarstern-Expedition PS119 im Bereich der Scotia Sea. Siehe https://doi.pangaea.de/10.1594/PANGAEA.904050 für eine Darstellung des master tracks in Verbindung mit der Stationsliste für PS119.

Fig. 1.1: Cruise track of Polarstern during expedition PS119 in the Scotia Sea area. See https://doi.pangaea.de/10.1594/PANGAEA.904050 to display the master track in conjunction with the list of stations for PS119.

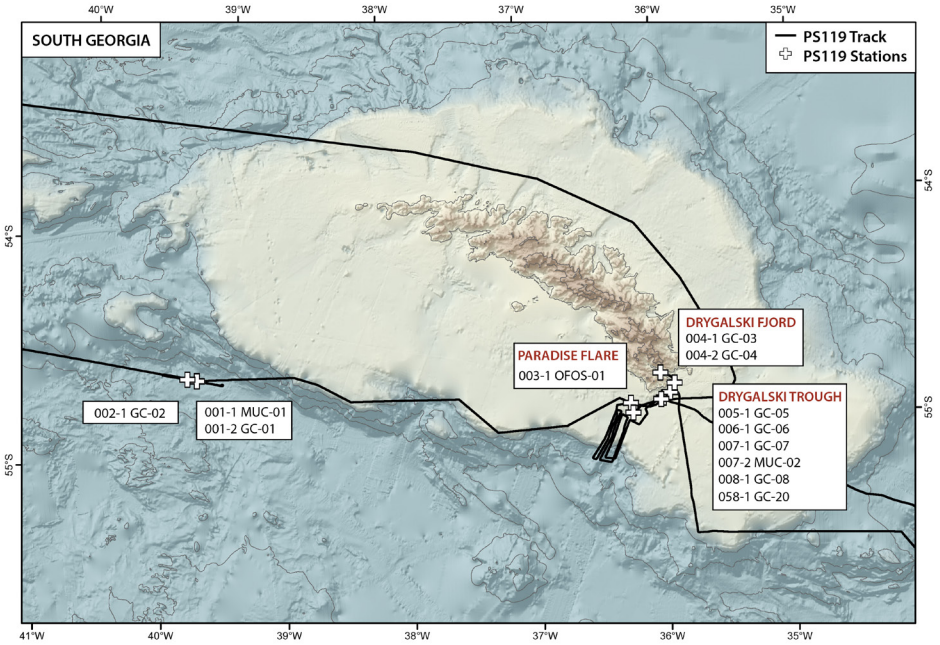

Abb. 1.2: Fahrtverlauf und Beprobungsstationen in der Umgebung Süd-Georgiens

Fig. 1.2: Track lines and stations during Polarstern cruise PS119 around South Georgia

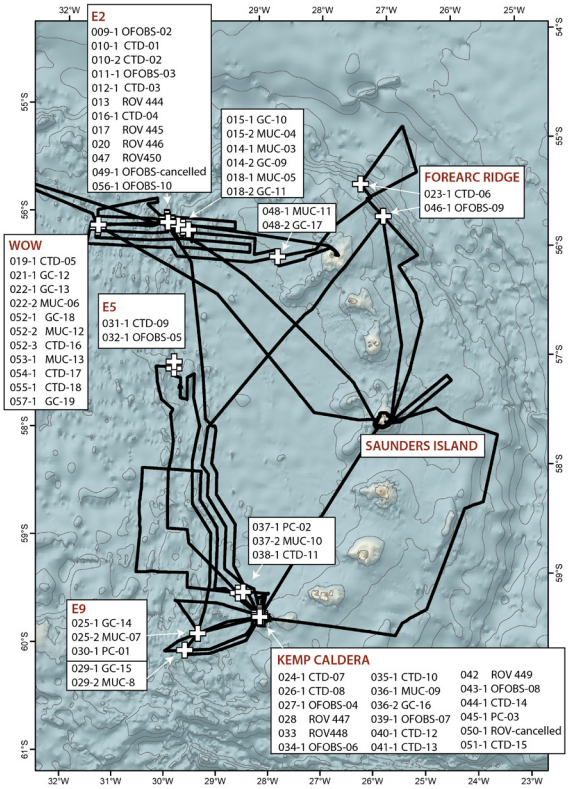

Abb. 1.3: Fahrtroute und Beprobungslokationen im Bereich der Scotia Platte
Fig. 1.3: Track lines and stations during Polarstern cruise PS119 in the Scotia Plate area

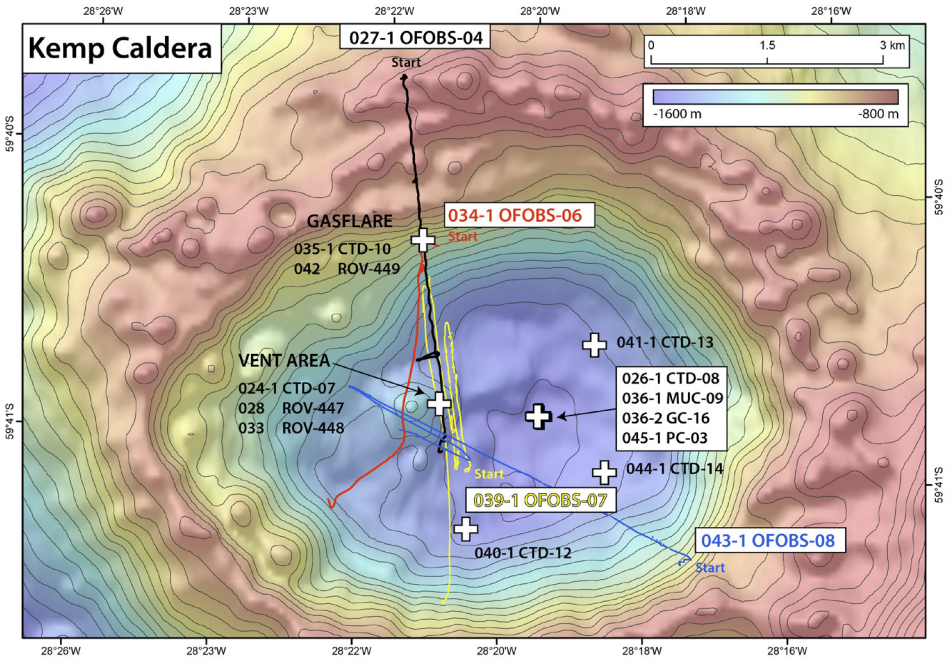

Abb. 1.4: Bathymetrie der Kemp Caldera mit Stationen der PS119
Fig. 1.4: Bathymetry of the Kemp Caldera with stations performed during PS119

SUMMARY AND ITINERARY

Polarstern's 119th expedition started in Punta Arenas, Chile on April 15, 2019 and ended on the Falkland Islands in Port Stanley on May 31, 2019. South Georgia was reached after 5 days of transit, during which hydro-acoustic measurements using Parasound and Hydrosweep were performed. At South Georgia, several gravity core and multi-corer stations were deployed on the southern continental slope and in the area of the Drygalski Fjord and Drygalski shelf trough, respectively. The main research area was located on the South Sandwich plate area, which is characterized by the volcanic arc of the 11 South Sandwich Islands as well as numerous submarine volcanoes. For the first time MARUM ROV QUEST 4000 was used on board *Polarstern* in the southern hemisphere for the investigation of hydrothermal systems. Other topics included the volcanology of Saunders Island and the recording of whales, especially finback whales. Due to very small-scale changing weather conditions, the study locations were extremely determined by the weather forecasts, the frequent changes were used for hydro-acoustic surveying. A total of 4 ROV dives were conducted on the East Scotia back segment E2 at 2,600 m water depth and 3 dives in the Kemp Caldera, a submarine island arc volcano at 1,600 m water depth. The AWI-owned TV sled OFOBS, which is equipped with a side scan sonar, had been used several times especially for the registration of micro-bathymetry. In the area E2, black smokers were sampled with fluids up to 344°C and a new hydrothermal vent field with 50°C hot fluid spills was discovered, which we called "Alexander von Humboldt"-Field. In the Kemp Caldera predominantly white smokers with low tempered fluid outlets up to 230° C were registered. Elemental sulfur was sampled both as precipitates and observed in video footage leaking in liquid form. For the first time, the dives were streamed live via telepresence to the internet and scientists who were not on board were so successfully involved in individual dives. Furthermore, the telepresence for 4 live circuits for events in Germany could be used very successfully in the context of public relations. In total, we performed 20 gravity corer, 3 piston corer, 18 CTD stations, 13 multi-corer, 10 OFOBs profiles and 7 ROV dives with a total of 46 hours of ground time. In addition, multi-beam data on bathymetry and sediment echo sounding data for sediment mapping were acquired along a distance of 6,700 nautical miles.

Cruise Narrative

On Monday, April 15, 2019, at 13:48 local time *Polarstern* left her mooring at position C in front of the harbor of Punta Arenas for a 3-day transit toward her first research area in the waters of the sub-Antarctic island of South Georgia. Ahead of the departure for her 119th expedition, *Polarstern* had a week of mooring at different positions in the harbor of Punta Arenas to fulfil various logistic challenges. The first hurdle had already to be taken in Germany, as the participation in the vote for the European election on the May 26 is not possible while being on board. In the state of Bremen the European election was at the same time as the voting for the State's House of Representatives and therefore we wanted to vote already prior to departure. Despite the fact that the candidates for representatives were only announced on April 1 and the voting forms had still to be printed, the voting office in Bremen did their best and enabled us to vote at the state office at An der Weide 14 - 16 on the April 8. Our major acknowledgements go to the Head of Office, Mr. Martin Kesper, who together with his team prepared the voting for us and we were able to exercise our citizen right and duty to vote.

The further challenges that the vessel and her crew had to master were directed by harbor logistics. The previous cruise with *Polarstern* had to arrive earlier than planned but the vessel

had to stay on an outer mooring as the only deep-water wharf, the Mardones Wharf, was occupied by freight vessels. The disembarking scientists had to be shuttled to land by the pilot boat and only 3 days later on Thursday, April 11 loading of cargo, especially of the four containers carrying the ROV and its equipment, could start at Mardones Wharf. Emerging bad weather forced the move of the vessel to an outer berth and not until on Saturday, April 13 the last two containers could be loaded on board, after *Polarstern* had been allowed to moor at Mardones Wharf again. The Sunday was spent with the vessel bunkering fuel at the pier of the Cabo Negro refinery near Punta Arenas, where we received 2.000 tons of marine fuel during the day, so the vessel would be able to sail for the following weeks. During the night *Polarstern* moved again to an outer mooring position which enabled us to finish the last pre-departure tasks on the working deck on Monday, April 15. After the last piece of airfreight was delivered by the local agent at 13:30, the vessel was checked out and able to leave anchorage.

After the departure from Punta Arenas and an 8-hourly passage through the Magellan Strait *Polarstern* started a 4-day transit bound for South Georgia (Fig. 1.1). This time without station work was used by our 51 scientists from Germany, USA, Costa Rica, Austria, UK, Bosnia & Herzegovina, Chile, Taiwan, France, India, Slovenia, Spain and Switzerland to further set up laboratories and to intensely exchange talks on the various research aims of this expedition. Every day, lectures were given between afternoon coffee break and dinner, which introduced discussions into the subjects relevant to this expedition. *Polarstern* steamed over the wide Argentine continental shelf eastwards and after about 2 days, we reached deeper water depths of more than 3,000 m in the Falklands Trough, an elongated groove separating the Falkland Plateau from Burdwood Bank and the northern Scotia Ridge. After crossing the shallow North Scotia Ridge, which rises to shallower than 1,000 m water depth, we started our bathymetric and sediment-profiling surveys with the vessel's own hydro-acoustic Hydrosweep and Parasound systems in the Scotia Sea. We selected our transit line to the East by choosing a course to cover yet uncharted seafloor areas, in order to contribute to closing the still significant gaps in the seafloor surveys of this region.

After we reached the deep-sea area to the south-west of South Georgia on our fourth day, Friday, April 19, we started the Parasound survey of the sediment waves very early Saturday morning. These sediment waves, which are thought to have formed through bottom currents, document through high sedimentation rates the Paleo-oceanography of the Circum-Antarctic Current and were therefore chosen as targets for sampling. We sampled these structures via two gravity corer and one multi-corer deployments throughout Saturday despite a lively sea state and winds of 6 to 7 on the Beaufort scale. Multi-proxy examinations at the AWI on these sediment cores shall deliver new knowledge on the temporal variability of the surface and seafloor circulation during the last orbital climate cycle. The oceanographic regions around South Georgia are of special interest for Palaeo-oceanography because of the possibility of iron influx and a linked raised primary productivity. On Sunday, April 21, the weather was to brighten and calm down and we planned our first dive with the MARUM ROV QUEST to dive at Paradise Flare and investigate a gas emission site. Paradise Flare was discovered in the course of hydro-acoustic surveys of the water column during *Meteor* Expedition M134 in 170 m water depth in 2017 but bad weather had stopped a closer investigation.

Again, weather conditions on Sunday and Monday denied us the chance of a detailed investigation of the site. But we were able to use the new multi-function sled OFOBS of the AWI deep-sea group at the location (Fig. 1.2) and next to an optical assessment in the neighborhood of Paradise Flare to do a bathymetric survey of the seafloor with the sled's side-scan sonar. In the afternoon of Easter Sunday we steamed into Drygalski Fjord, which is penetrating deep into the island at the south-easterly end of South Georgia. While the entrance to the fjord is 2 km wide, it narrows to just about 800 m width, and from board of *Polarstern* one had a fantastic view to the steep mountain sides, the glaciers, and onto the geological formations formed by the oldest rocks of South Georgia. Right in the middle of the fjord, we took a sediment core

(GC-03; Fig. 1.2) within a tightly confined basin, which chemical signature is of special interest to our geochemists. The sampling was a success.

Unfortunately, Easter Monday, April 22, was, like expected, still too stormy to proceed with our first dive at Paradise Flare. Therefore, we used the day for a series of sediment cores by gravity corer in various sub-basins of the Drygalski Trough and by a multicorer with 12 shorter sediment cores. Thick sediment layers in some of the fjords and glacially eroded troughs of South Georgia have exceptionally well archived recent glacier behavior and climate change. The sub-polar ice-cap on South Georgia reacts more sensitive to climatic changes than the much larger and more isolated Antarctic ice shelves and are therefore a central target for studies on sediment cores to better understand the climate variations in the Southern Hemisphere. Unfortunately, the weather system would have allowed us to commence the first dive on Wednesday at the earliest and therefore we decided to use the Tuesday to steam to the East Scotia Ridge, to start our diving there on the hydrothermal vents of the ridge segment E2. A westerly wedge of a high pressure system lying to the north would reach us and was promising a few calmer days which we wanted to use for ROV dives.

On Tuesday, 23 April 23, we steamed eastwards while using acoustic survey systems and reached the East Scotia Ridge in the evening. This N to S running ridge is created through the fracture of the seafloor by 5 - 6 cm each year and the resulting outflow of pillow lava. The ridge, which is characterized by a mosaic of ridge-parallel flows building an comprehensive morphological structure with at parts extremely steep slopes, separates the Scotia Plate in the west from the South Sandwich Plate in the East. Running from North to South the ridge is split into 10 segments of 30 to 90 km length each (E1 to E10). On two of these segments, E2 and E9, our British colleagues had discovered active hydrothermal springs. In these areas the magma chambers lie only in 2 - 3 km deep in the Earth's crust and in fracture areas magma can rise easily and flow out on the seafloor.

On arrival at the segment E2 of the East Scotia Ridge on the evening of Tuesday, April 23, we started to find chemical signals of these hot springs in the water column, first with the OFOBS system and later by CTD and water rosette. A big help in this search were our so called MAPRs (self-contained miniature autonomous plume recorders), sensors that detect next to turbidity and temperature also the redox potential. As independently recording instruments they were deployed on almost all deployments of equipment. Our search was continued on Wednesday, April 24, and on Thursday, April 25, the first dive of the ROV QUEST (ROV 444; Fig. 1.3) was able to happen. We dived on a known hydrothermal vent field which was discovered during an expedition JR224 of *James Clarke Ross* 10 years ago. With some teething troubles we were able to recognize most of the known hydrothermal structures but it became also clear during this dive that huge changes had happened during the last 10 years. Some of the then active black smokers were not active anymore and others showed active fluid exits which had been inactive 10 years ago. Following the assemblage structure of the chemosynthetic fauna had changed. Despite all odds we were able to collect selected target species like snails of the genus *Gigantopelta* and crabs of the genus *Kiwa* (so-called Hoff crab) for experiments in our aquaria. During this dive we used a so-called telepresence for the first time in from a scientific Southern Ocean expedition, which technical set-up had been installed prior to this expedition by our ROV project lead Volker Ratmeyer and his team. A specialized hardware had been bought which enabled a stable satellite connecting via *Polarstern's* arial dome system to upload the dive images of 5 Mbit and enabled colleagues in Bremen and elsewhere to interact online via the internet with the dive using real-time audio communication, data transfer and interactive georeferenced positioning systems. During the second dive of QUEST on Sunday, April 27, the public was able to follow the dive in the frame of a public viewing event via the internet, with a delay of 30 minutes. We heard that this opportunity was even used at night in Germany between 22:00 in the night and 4:00 in the morning. Also the second dive (ROV 445; Fig. 1.3) was a full success; we discovered in an unknown area a cooling down hydrothermal

vent field with mineral chimneys, gushing out of fluid temperatures of 30 - 50°C.

We started the new week on Monday, April 29, with a long dive to sample smoking chimneys and vent animals in the known hydrothermal field of the segment E2-South (ROV 446; Fig. 1.3). Here we concentrated our efforts on the active vent systems around Dog's Head, a complex structure consisting of 4 chimneys, which are lined up nicely one after the other, fused on their bases and characterized by single black smoking orifices in 12 - 15 m height. South of Dog's Head, several extinct relict chimneys and active fluid smokestacks cluster, which are colonized in very different patterns by anemones, snails, yeti crabs, and other organisms. Obvious are especially the white bacterial mats, which cover single chimneys like snow-covered mountains.

Our specialized fluid sampler made from chemically inert titanium enabled us to collect the extruding fluids from two black smokers. The fluid samplers are gas-tight, which means that gases cannot escape when the ROV rises and the pressure drops, and we are able to measure the gas concentrations on board in a gas chromatograph. The snorkel of the fluid sampler, which is used to collect the hot fluids from the opened orifice in a much-directed way, is linked to a temperature sensor, so that we can measure the precise fluid temperature. The first sample was hot and contained in its gas phase high hydrogen and methane concentrations. Only about half of the former gas concentrations were measured in the second fluid sample, which was collected from a site with an exit temperature of 344°C. These high temperature measurements are only measured in the fluid flow directly in the exit orifices, while the surrounding seawater is only slightly warmed up. The off-vent seawater on the seafloor of this oceanic region has a temperature of 0°C, which can rise up to a few degrees C depending on the proximity to focused and diffuse flow exits. Next to the fluid samples, we also collected rock samples of the chimneys, which were taken with the manipulator arms of ROV QUEST; these contained, next to anhydrite, shiny metal sulphide minerals, like chalcopyrite, pyrite and sphalerite. Overall, it was a very successful dive, actively followed by our colleagues in Bremen as the telepresence link enabled this.

The following night was used for surveying the area for suitable sediment corer positions, which we discovered in different water depths in sediment-covered basins between tectonic high blocks of the magmatic crust. Two sediment-coring positions were selected, which we sampled on Tuesday, April 30, with gravity corer and multicorer (GC-12, -13, and MUC-06; Fig. 1.3). The investigation of the pore waters in these sediment cores and in those of the past days, together with the chemistry of the iron minerals, will contribute to the charting of the "plume"-like drift of the iron minerals originating from the hot springs in the surrounding. In the night from Tuesday to Wednesday, we surveyed the seafloor on a line from the spreading center E2 to the East, crossing the island arc of the South Sandwich Islands north of Zavodovski Island over the forearc area into the deep-sea trench of the South Sandwich subduction zone (Fig. 1.3). This zone is in its northern part especially deep and reaches a depth of 8,264 m in the so-called Meteor Deep. The German survey vessel *Meteor I* discovered the deep on its southernmost West-East transect during its expedition in 1925 - 1927 and mapped it as deepest area of the South Atlantic. Wednesday, May 1, started with a CTD profile (CTD-06; Fig. 1.3) including water sampling to measure methane concentrations.

Again a night and a morning were used surveying the seafloor of the forearc and in parallel searching for indicators of fluid and gas exits, while we were steaming southward bound until we reached Saunders Island, the target of our volcanologists, in the afternoon. This volcanic island is the third largest of the South Sandwich Islands, which are running from North to South in an eastwards bend arc parallel to the deep-sea trench. While the northernmost volcanic islands, with Russian names, were discovered by Admiral Fabian Gottlieb von Bellingshausen, James Cook discovered the southern islands and gave them British names. Mount Michael on Saunders Island is, like many of these island volcanoes, active and partly reveals itself only after a while. Neither the planned surveying of the island by drones nor a visit of our

volcanologists to the island was able due to bad weather; therefore, we surveyed the seafloor of the island in closer and closer circles, hoping this improved seafloor mapping will support a future landing and enable the volcanic research project.

On Sunday, May 5, we arrived at the Kemp Caldera, a prominent crater of volcanic origin at the southern end of the South Sandwich volcanic arc. The caldera, which has an average diameter of 7.4 km, has a depth of 1,600 m in its center and has a wide rim with several secondary cones in 800 - 900 m water depth. A younger volcanic cone rises up to about 200 m from the western bottom of the crater. A first measurement with the CTD sensors (CTD-07; Fig. 1.4) over a known hydrothermal vent field confirmed that hydrothermal activity was still present. Next to a distinctly increased turbidity, also increased temperatures and an anomaly in the redox potential of the water column near the thermal area were observed. On Monday, May 6, we deployed a gravity corer and a multicorer half way between the caldera to the East and the segment E9 of the East Scotia Ridge to the West. In the night from Monday to Tuesday, a further CTD followed as well as seafloor survey with the OFOBS (Ocean Floor Observation Bathymetry System; OFOBS-04). On Tuesday, May 7, at last we were able to conduct a long ROV dive in the Kemp Caldera with more than 11 hours on the seafloor (ROV 447; Fig. 1.4). We started the dive at the location “Great Wall”, which got its name from an altered hypabyssal rock covered at many places with either yellow sulphur or white bacterial mats. Single chimneys appeared to fully consist of sulphur and on breaking off sulphur pieces, the fresh yellow color of elemental sulphur became visible. We also saw sulphur in an area about 100 m to the southeast known as “Winter Palace”. The sulphur dripped into the cold seawater in liquid form right in front our camera lenses, before it solidified into pearl-like structures.

The area is characterized by multiple white smokers, which cause a light turbidity of the bottom water. With our fluid samplers we collected the expelling fluids to analyze their chemical composition. The hot expelling fluids, which contain different components in solution and high concentrations, is mixing with the cold seawater. In this process, some of the components in solutions flock out, which on one hand build the smokers themselves and on the other form the light cloud cones. In general, these white smokers have a lower temperature than the black smokers do; and in white smokers, lighter minerals like anhydrite, opal and barite are precipitated while black smokers expel sulphidic minerals. What type of minerals the white smokers of the Kemp Caldera expel, we will only know after we will have analyzed the fluid and rock samples. The fantastic dive time, which was broadcasted to numerous interested parties back on land via the telepresence was not only exciting on the seafloor but also on the bridge. From there, they watched a 700 m long table iceberg, about 2.5 nautical miles south of our ROV position, which slowly made its way towards us and halfway throughout the drifted to a distance of only 1.6 miles and threatened us with an early abortion of the dive. Luckily, it changed its direction and passed the vessel on portside in a wide enough distance.

As part of the scientific programme on this cruise, we were undertaking experiments to understand the biology of hydrothermal vent associated animals. In the Kemp Caldera we collected vesicomyid clams, *Laubiericoncha puertodeseadoi*, living in the seafloor sediments using the ROV QUEST and were able to bring the clams back to the ship alive and in good condition. The water temperature at the seafloor in the caldera is about 1°C, but the volcanic influence makes the sediment warmer at about 5°C. The animals were then divided into two temperature conditions, at 2°C and 10°C in the laboratory facilities on board, and experiments done to measure how their oxygen consumption might change in warmer conditions.

On Wednesday, May 8, we sampled a sediment basin east of the rifting axis of the E9 segment, which was enclosed by magmatic rocks of two fault ridges. The impressive acoustic penetration of the Parasound system showed us a sediment layering of more than 50 m. With the piston corer (PC-02; Fig. 1.3) we were able to collect almost 12 m of brilliantly layered sediments, which showed a colorful mix of hemipelagic sediments with partially volcanic and

hydrothermal components. Our geochemists were pleased by this, as they examined in several sediment cores how far these hydrothermal particles are transported away from the rift axis by the easterly current. On Thursday, May 9, we left our southernmost work area for 2 days to investigate the ridge segment E5 for hydrothermal activities. This ridge segment, like E2 and E9, has a magma chamber that sits in relatively short distance to the seafloor so the existence of hydrothermal circulation with fluid orifices and further hot vent indicators on the seafloor are predictable. The highest probability to find new fluid orifices was in the investigation of an axial high in the central area of the rift valley. There we carried out a CTD (CTD-09; Fig. 1.3) and an OFOBS survey (OFOBS-05; Fig. 1.3). Small anomalies of turbidity as well as in the methane concentration were present in general but not specific enough to be localized, so we decided not to search further for vent sites here.

Like last week, we spent the sixth week in the southernmost area of the South Sandwich Plate, from the backarc spreading ridge of the segments 8 and 9 in the west to the Kemp Caldera. The volcano of Kemp Caldera is part of the collision zone with the South American plate to the East. A look to our expedition logo shows symbolically the spreading ridge on the left and flowing to the right the volcanoes, forearc area and subduction zone. The weather conditions, which denied from Sunday to Tuesday morning further dives, permitted not until Tuesday to dive down with ROV QUEST to the seafloor. We used the dive-free time for the deployment of other sampling gear. On Sunday, May 12, we sampled the deepest area of the Kemp Caldera with a 3 m long gravity corer and the multi-corer (GC-16; Fig. 1.4). The Parasound profiles over the caldera surveyed until then showed narrow sediment layers in the deepest area, whose mineral and chemical composition in references to hydrothermal deposits are of huge interest. With our corers we were able to sample sediment layers of 230 cm depth, which surprised us by their coloring and diverse sediment compositions.

Pure biogenic opal ooze came to show, which are composed of diatom skeletons. These diatoms are growing in huge numbers in the surface waters of the Southern Ocean, south of the Polar Front, and after death, their skeletons are deposited on the sea floor along the so-called Opal Belt. The mats of the diatom genus *Thalassiotrix* are especially obvious in our core. They are built from needle-like cell covers of biogenic opal and if appearing with a single species in the sediment core, look like wet paper tissues. The pure opal ooze is strongly coloured in some layers by metal sulphides, documenting the hydrothermal activity in the caldera over time. On Monday, May 13, we sampled sediments by piston corer about 60 km to the west of the Kemp Caldera on the eastern flank of the ridge segment E8. The sediments of the 8.70 m long core (PC-02; Fig. 1.3) had high contents of volcanic components and our geochemists are interested in investigating the influence of the hydrothermal activity and especially that of the iron geochemistry. Based on this interest, pore water samples were taken every 10 cm along the length of the core to measure alkalinity and iron concentrations already on board. Further nutrients and specific dissolved components will be analyzed after the expeditions in the labs of the home institutes.

On Tuesday, May 14, the Kemp Caldera was back in the center of our research. Several CTD (CTD-11, -12, -13; Fig. 1.3) and water rosette stations were taken near the hydrothermal area, in the caldera center and on the rim area. Based on anomalies of turbidity, redox potential, temperature and methane content we wanted to analyze the influence of the active hydrothermal area on the seawater chemistry. ROV dive (ROV 449) followed located at the northern, inner rim of the Kemp Caldera in 1,100 m depth, over an area where we had detected gas bubble streams several times in the water column. Diving with ROV QUEST, we were unable to find the original exit of the gas bubbles on the seafloor, and therefore we concentrated our efforts on sampling the hydrothermal fluids of new discovered smokers. A black smoker, the fluid temperatures of which were measured as 230°C, had a high iron concentration and the lowest pH values of 2.3, while a second chimney which we sampled had a temperature of 200°C contained almost no iron and had a pH of 5.5. We will have to wait until after the detailed fluid

analyses at home to find out if the fluid chemistry is in line with the precipitate content.

Despite the newly detected dive target wishes, which emerged during our 3 dives in the Kemp Caldera, we had to leave the Kemp Caldera on May 15 in view of our further expedition objectives. Our route led us along the northwestern part of the South Sandwich Plate to the forearc, passing the islands of Leskov, Visokoi and Zavadovski. We ran an OFOBS profile over a forearc high in the hope to find indicators for cold seepage. There, British scientists had dredged up serpentinite crustal rocks a few years ago, which are associated with active seafloor fluid exits in other oceans. During the night we progressed southwards, reaching the volcanic Saunders Island in the morning of May 17. Our volcanologists had planned a visit with sampling and a photogrammetrically survey via drone flights. In light of the weather, which improved as the day went by, drone flights starting from *Polarstern* were possible, especially after *Polarstern* made her way through Cordelia Bay and stopped very close to the island.

A further successful ROV dive (ROV 450; Fig. 1.3) took place in the hydrothermal area E2-South on Saturday, May 18, before the weather got bad during the night. As a strong storm of up to hurricane level was forecasted for the second part of the night and the following morning, we steamed with *Polarstern* westwards and found shelter behind the volcanic island Zavodovski. With a wind strength of 10 to 11 Beaufort with occasional gusts of 12, we had waves of 3 - 4 m height in the shelter of the island while further out waves of more than 8 m height were forecasted.

The rapid changes in weather condition, which hit us last weekend, was exemplar for the entire week. While we were able to achieve the 450th dive of MARUM ROV QUEST on the ridge segment E2 of the East Scotia Ridge on Saturday, the storm on Sunday, which we endured in the alley of Zavodovski Island, showed us that Antarctic winter had started. It was not until Monday, 4 am on May 27, that we left our shelter behind the northernmost of eleven the South Sandwich Islands to steam westwards to our hydrothermal work area E2. Of the two planned gravity- and multi-corer stations, we were only able to do one because of time constraints, sampling sandy layers with volcanic components, which seem to originate from the volcanic arc. On arrival at E2, initially an OFOBS profile running from East to West was planned to survey the known hydrothermal venting area with high-resolution micro-bathymetry. However, the weather forecast on Monday morning made us to decide differently. For a safe and secure dive with ROV QUEST we require stable weather conditions with wave heights below 3 m for several hours. We were looking for these conditions for 2 - 3 days ahead throughout our entire working area on the South Sandwich microplate. The working area extends over 5 degrees of latitude and 8 degrees of longitude and our meteorologist was busy finding us the forecast for the best diving conditions in all of its regions. Because of the small-scale highs and lows and their movement this is not always easy. On Monday morning, it became evident that on Tuesday and Wednesday diving conditions were only possible in the southernmost part, in the area of the Kemp Caldera. As the multiday forecast did not permit ROV dives in the North, *Polarstern* left at ones to steam southwards bound to the Kemp Caldera. This enabled us to add a wide-scale line of a multi-beam survey to the already existing survey of the central spreading ridge. In the evening of May 21, the next ROV dive was meant to commence.

However, we had to realize that because of unforeseeable technical problems with the ROV no further dives during this expedition were possible, immediately leaving towards Saunders Island. There our team of volcanologists was able to proceed with their photogrammetry survey on Wednesday, May 22. While during the previous survey time, the north-eastern side of Cordelia Bay and part of the south-eastern flank of Ashen Hills were surveyed, this time drone flights to the western and northern areas of the island were achieved. Important data, which enable the making of a topographic map of down to 10 cm resolution, were collected by optical and infra-red cameras during the drone surveys. After sunset, *Polarstern* steamed to the northwest to the spreading ridge. On Thursday, May 23, several sediment and water column sampling

events happened, which showed plume-like structures in the water column. Already in the night to Friday, the next storm arrived, which we could not avoid because of time constraints. As the meteorologist office on board was able to predict time and composition of the storm, we were able to plan gear deployments in line with the meteorological forecast. Although the weather model of the German Weather Service (DWD) can only use a few terrestrial base stations as well as vessel and satellite data, it is extremely correct. Very important base-line data for the model are temperature, humidity, air pressure and using GPS-analyses also speed and direction of air particles. These data are taken daily on *Polarstern* by staff of the DWD with radio sounder deployments via balloons which reach 30-35 km height above sea level. Twice per day, we received updated weather forecasts, which were enormously important information during this expedition to make decisions regarding the selection of station positions.

The whale observation team from Hamburg University did not succumb to the storm, even though the helicopter could not be deployed often for dedicated surveys due to severe threat of icing. The group thus intensified their research effort to dedicated surveys from the crow's nest of *Polarstern* whenever conditions did not allow helicopter operations. Valuable data sets on occurrence and distribution of cetaceans were collected in spite of the adverse weather situation. Once pooled with records from previous surveys on board of *Polarstern*, the forthcoming analysis will produce reliable and robust estimates of the occurrence, distribution and density of whales (and finbacks in particular) within the study area.

After our storm on last Friday, May 24, the sea only calmed down very slowly and station work was only possible with two CTD stations (CTD-12, and -13; Fig. 1.3) in the late night towards Saturday. The deployments were made about 60 km to the West of the spreading center on its flank. There, the seafloor is parted by North-South orientated, parallel faults covered by young sediment, and we discovered both in the sediments as well as in the water column indications for fluid circulation in the Parasound recordings. The type of fluid circulation whereby sea water is penetrating the Earth's crust, then circulates in the young crust, and rises as warm or hot fluid at different areas of the ocean's floor is not only known from spreading centers but also has been observed along the flanks far away from currently active spreading centers. The water samples taken by CTD showed slightly raised methane concentrations, which hinted to a fluid outflow. In addition, the first sediment cores, which we had taken there 3 weeks ago, showed profiles of pore water content, which gave hints toward inflowing and at a different site also outflowing fluids, a phenomena, which we wanted to verify or confirm by further sampling. When it became obvious that the most important sediment core could not be taken even on Saturday morning because of the sea state, we steamed eastwards and carried out our OFOBS profile (OFOBS-10; Fig. 1.3) in East to West direction across the spreading segment E2 on Saturday, May 25. At night we moved back to the CTD station and successfully took an almost 8 m long sediment core.

Shortly after *Polarstern* left finally the area of the East Scotia Ridge towards South Georgia, which unfortunately was only able during rough sailing conditions. In the darkness of Sunday, May 26, we took our last sediment core of this expedition in the Drygalski Trough (GC-20; Fig. 1.2). Afterwards *Polarstern* started her return journey, and after we reached the north-eastern side of South Georgia, steamed along the elongated island shelf directly toward the Falkland Islands in the West (Fig. 1.1). The track of the return journey we used from Monday to Thursday for further acoustic surveys with the multi-beam system Hydrosweep and the sediment penetrating sounding system Parasound. We used the station-free time to analyze data, write the cruise report, pack the expedition cargo, clean the labs and give presentations during the daily meetings on the conference room of the vessel. On Friday, May 31, *Polarstern* reached the harbor of Port Stanley, where the scientists left the vessel.

2. WEATHER CONDITIONS DURING PS119

Harald Rensch, Juliane Hempelt DWD

On Monday, April 15, 2019, *Polarstern* left Punta Arenas (52.9°S, 70.8°W) for the expedition PS119 to first steam in transit to the research area west of South Georgia (Paradise Flare: ~54.9°S/~36.5°W). All research then took place in the well-known latitudes between 50°S and 60°S, also known as Furious Fifties, where frequently cyclones are produced and move as strong storms preferred eastwards, influencing so the different working areas by stormy winds and partly very rough seas. This scenario often happened in a one- or two-days' time period.

One of the main tasks of the forecaster during the expedition was to find out those research areas days in advance that would provide suitable working conditions during a given possible long lasting calmed sea state-weather window. By help of the available German Global-sea model (ICON) in combination with the ECMW Global-sea model we accomplished this challenge in the best possible way.

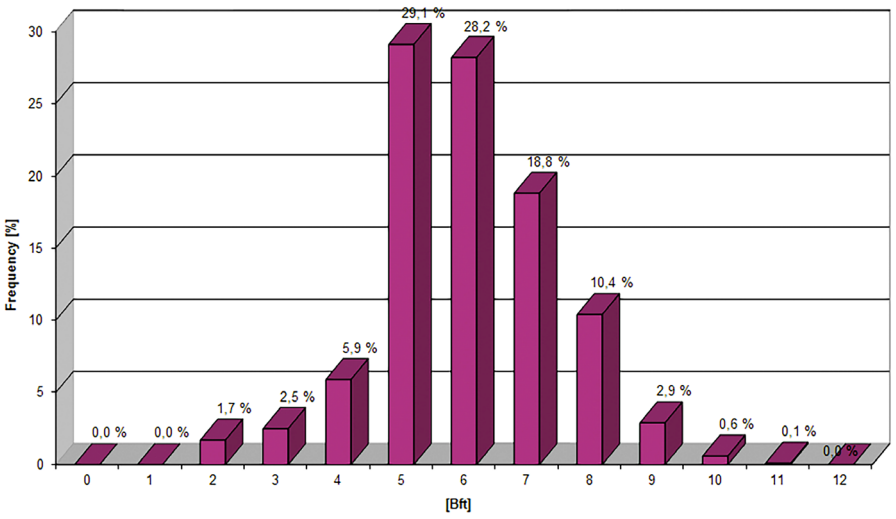

Fig. 2.1: Distribution of wind force during PS119

Transit Punta Arenas – South Georgia (April 15 - 21)

For the first part of the expedition the ship steamed on transit or a period of nearly 5 days over Scotia Sea to the first main working areas South Georgia and Paradise Flare. Under the influence of cyclonic westerlies 5 to 6 Bft (wind force in Beaufort = Bft) there were often slightly rain showers observed. During the transit towards east wind speed raised up day by day, after

all reached 7 to 8 Bft on April 18 at noon. Short time after that, wind veered to southwesterly directions and continued at same wind force. The maximum gusts of the day were measured nearby 45kt (9 Bft). The significant wave heights rose up to 1.5 to 2.5 m, observed during first two transit-days, to nearly 6 m on April 19 in the late morning. During the same period the air cooled down from 9-10°C at the beginning of the cruise to 0-2°C at the end of transit. Corresponding precipitation fell nearly every day, but it came first as rain, later most as sleet or snow, often in form of showers.

Research area Paradise Flare - nearby 50 sm to South Georgia (April 21 – 23)

In an area of moist and cold air from Antarctic, where snow- and rain showers were often produced, the westerlies of wind force around 6 Bft and a sea around 3.5 m (swell up to 2.5 m) dominated the weather conditions during the first working areas.

After entering Drygalski-Fjord on Easter Sunday, the swell fell suddenly below 2 m and the wind calmed down very fast. The glaciers nearby cooled the air down to values below -5°C. One day later back at Paradise Flare southwesterly winds of 7 Bft and waves of 5.5 m (swell around 3 m) prevent the planned first dive with the ROV 4000 (Remote Operated Vehicle).

Research area ridge segment E2 (April 23 – 29)

A cyclonic cold and moist southwesterly wind flow dominated this part of expedition. Wind speed around Bft 6 and significant waves of heights of 3.5 to 4 m were observed at E2-arrival. Also, one day later the sea remains high, around 4 m, many showers with risk of icing prevented all helicopter-flights. An eastward shifting ridge of high provided calmed sea conditions, the swell was lower than 2 m. This allowed the first ROV-dive of this expedition.

Also flight conditions were sufficient until the afternoon, as frontal snowfall began. During the day of April 26 a low pressure system and its fronts snow showers produced a strong south-westerly wind of 7-8 Bft caused significant waves of more than 5 m. Already next day a passing ridge of high brought decreasing values of wind speed and swell (2 to 3 m). Following Sunday/ Monday we sailed on the edge of a high pressure area over South Georgia. The sea-level did not much change during this period and westerly winds below 20kt opened the next opportunity for ROV-divings, for example used on Monday, April 29.

Transit to E2 – Research at areas Forearc seeps, Saunders I. (April 30 – May 03)

Strong northerly, later northeasterly winds of force around 8 Bft, often snow- and rain showers and significant waves of more than 4 m accompanied us on our way to next working area Forearc seeps on Wednesday, May 1. A 5-day ahead ECMW-model forecast showed an eastward shifting ridge of subtropical high causing a useable fine weather window of around one day (May 2 to 3, conditions: wind variable < 5 Bft, broken high level clouds, swell below 2.5 m). But in reality the weather-window was reduced to a time span of one night, the wind came from north around 6 Bft and the swell was estimated by around 3 m, too high waves to go with Zodiac safe on shore. So, too bad weather conditions impeded all kinds of wind- and cloud-sensitive research at Saunders I.

Transit and research at E5 and at Kemp Caldera (May 03 – 14)

During the night to May 4, transit to next working area, a storm low of 950 hPa nearby 50°S/50°W moved southeastward towards *Polarstern*, causing stormy northerly winds of 9 Bft and a total wave of nearly 6 m. On the evening of transit-day waves of about 5 m were observed at our goal. Snow and rain showers, a fully cloud-covered sky, gusty southwesterly winds of 5 variable 8 Bft, and a swell of around 3 m were the dominant features also next two

days. The approach of a ridge of subtropical high on May 7 was the beginning of a one-day period of following fine weather and sea-conditions: southwesterly winds around 6 Bft, sea around 3 m, seldom cooled rain showers, also sunny moments. This all included the necessary conditions for a long lasting and successful ROV-dive. Besides relatively good meteorological flight conditions, alone the strong icing-conditions were the reason for preventing all helicopter flights for whale-watching during this time.

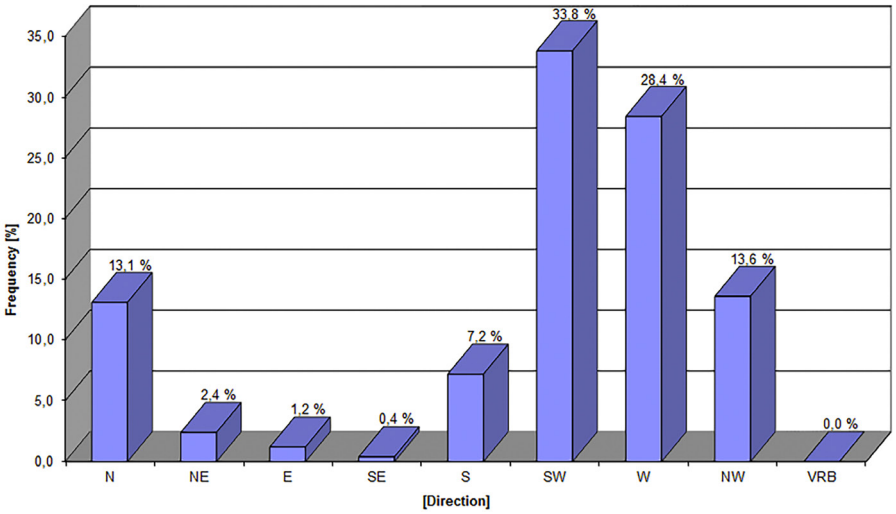

Fig. 2.2: Distribution of wind direction during PS119

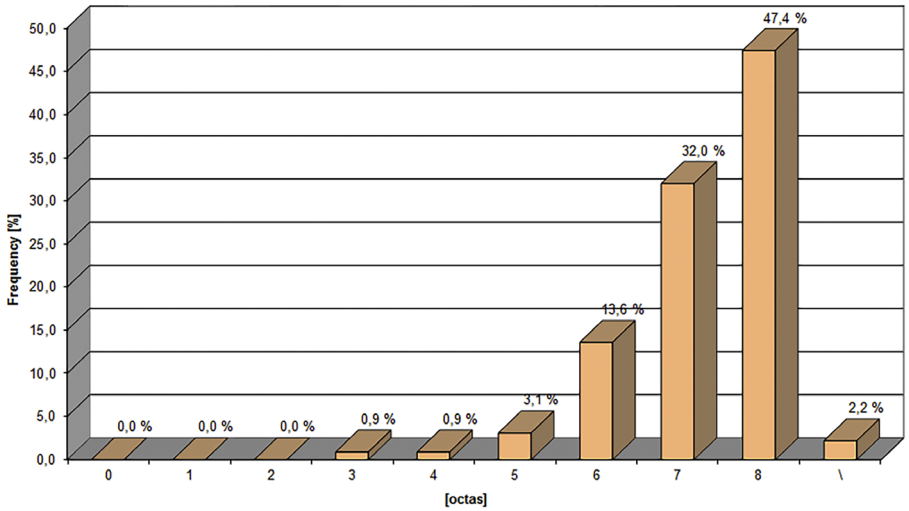

Fig. 2.3: Distribution of cloud coverage during PS119

On May 8 research went on despite of influences of frontal precipitation (snow- and sleet), a strong northwesterly wind of 6 to 7 wind forces caused slowly increasing wave heights of 3.5 to 4 m, which were also seen in the following working area E5 one day later. There waves reached already 5 m. On the ground that negative temperatures caused more showers and sleet accompanied the ship all the time. Again, icing in the lower layers of the atmosphere was the main reason for stopping of all long distance flights. The westerlies were very strong again during this period reaching around 7 Bft. On the rear sides of fronts during our track back to the old dive area, which we reached on May 10, the sea and swell went down, swell-values around 2.5 m, wind-sea 1.5 m: those conditions were stable and good enough for ROV-diving until the early afternoon of this day.

On Sunday May 12, stormy winds came within a cold front from northwest reaching 8 to 9 Bft and the maximum waves did nearly outrun 6 m: this was the weather-scenario which led to a nearly completely failure of research. On Monday, the day after was dominated by very low clouds first, but later some cloud spells were opened on the rear of the eastward moving bad weather area, and before a ridge of high had approached. On May 14, another cold front passed the ship until noon causing heavy snowfalls. During the day isolated showers were observed in vicinity of the ship, and decreasing waves of below 3 m enabled a 12-hour ROV-dive at relatively weak northwesterly winds of 5 Bft.

Transit Kemp Caldera, transit to Saunders I., research at E2 (May 15 – 20)

Under influence of low pressure in eastern Weddell Sea and its northward moving fronts cold air from Antarctic was brought to the working areas causing often snow showers. By moderate westerly to south-westerly winds waves reached nearly 5 m during the night to May 16, and additional: directions of wind-sea and swell were strong different, that's why the ship moved at times uncontrolled. Between May 17 and 19, a dynamically ridge of high pressure was present and brought calmed conditions with westerly winds below 5 Bft, so it hindered the production of low clouds and showers. Also sea calmed down on May18 to values below 3 m, which makes the diving by ROV and use of Zodiac possible, as well in the lee of Saunders I. as at area E2.

The strongest storm low of this cruise developed between May 18 and 19 southeast of South-Orkney Islands and approached E2. Warm air moved on May 18 towards north causing fog, drizzle and very low clouds, so the helicopter had to stay further on in the hangar. The forecast of high waves up to 8 m in open seas let it advisable to protect the ship and people by stashing in the lee of the nearby located Zavodovski Island. On Sunday in the afternoon the storm moved by stepping up southerly from E2 eastward and caused at its high stage gusts in hurricane forces of nearly 83 kt, but only <53kt = 11 Bft (10 s averaged-storm wind values) were measured. At the same time waves up to 6 m were seen. Thus, research had to pause during the weathering. On the following Tuesday, May 21, the ship steamed to Kemp Caldera, where weak winds and a sea below 3 m were found, conditions, good enough for ROV-diving. Unfortunately, an unforeseen serious technical defect prevented the use of the ROV until the end of the voyage.

Transit Kemp Caldera to Saunders I., research at E2; transit to Falkland-Islands (May 21 – 31)

On May 22, more cyclones and snow showers accompanied us to Saunders Island, which were surveyed by drone again. Later on, as we reached E2 the sea was lower than 3 m. Southerly winds brought colder air from Antarctic latitudes and temperatures fell down to -6°C.

The further on strong icing-probability on helicopters and very low layered stratus clouds tolerated only seldom short flights nearby the ship.

Between May 23 and 24, next autumn-storm moved easterly of E2 southwards. South-westerlies of wind force 11 Bft, snowfalls and possible icing-conditions on the ship by freezing spindrift (temperatures around -6°C) in combination with waves up to 7 m forced the ship to weathering loco citato. On May 25 researches were finished at E2 by calmed winds, the swell of 4 to 5 m was not much perturbing. The transit to Falkland via South Georgia began on May 26 as frontal influences dominated already, wind of 8 Bft blew, waves of 3.5 m existed, later 5 m were observed nearby the south of the island.

The intensifying of the storm during the following night with gusts up to 12 Bft were unfortunately not predicted by all available forecast-models, and this happened more times during this expedition (e.g. May 3, 19, 25- 26, 27).

Next day transit to Port Stanley was continued at stormy westerly winds 8-9 Bft and significantly waves of more than 5 m with route north of the island.

Last strong storm during the cruise occurred from May 27 to 28, westerly winds of more than 10 Bft (averaged wind) prevailed, and again, the sea was higher than 5 m. As well last 2 days of the voyage to our goal stormy winds prevailed, often snow or rain fell, and a sea of around 4 m was appreciated. Finally, on May 31 in the morning, we entered Port Stanley at a calmed sea, southeasterly winds of around 5 Bft and snow showers. The temperatures ranged between -1 and -3°C.

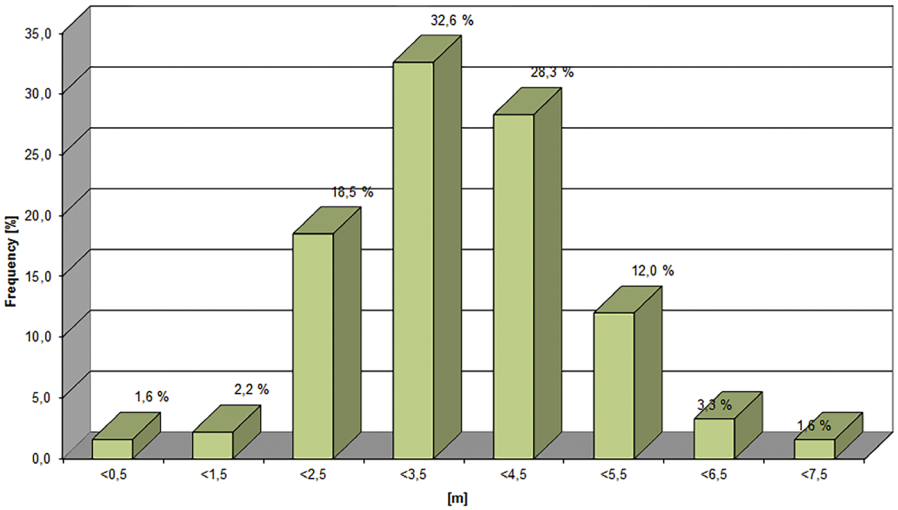

Fig. 2.4: Distribution of sea state during PS119

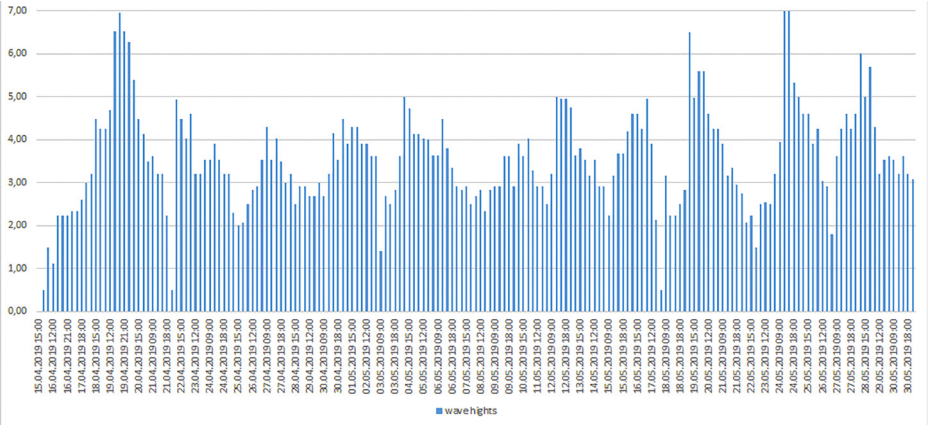

Fig. 2.5: Significant wave heights

3. MULTIBEAM ECHOSOUNDER BATHYMETRY

Paul Wintersteller[2,1] Stefanie Gaide[1], Ines Vejzovic[2], Victoria Kürzinger[2], Nontje Rücker[2], Martin Meschede[3], Nicole Richter[4], Crispin Little[5], Anna Lichtschlag[6]

[1]MARUM, Bremen
[2]GeoB, Bremen
[3]IGG-UG, Greifswald
[4]GFZ, Potsdam
[5]SEE-UL, Leeds
[6]NOC, Southampton

Grant-No. AWI_PS119_00

Objectives

During *Polarstern* cruise PS119, April 13, 2019 to May 31, 2019, we acquired bathymetric data with the hull-mounted TELEDYNE HS-DS3 multi beam echosounder (MBES) in the Southern Oceans Scotia Sea. The research area was located between the eastern part of the Scotia Plate, along the East Scotia Ridge, and within the South Sandwich Plate including its most eastern part, the forearc and the South Sandwich Trench area. The focus of the cruise was the investigation of hydrothermal vents and potential cold seeps at the Sandwich micro-plate utilizing the remotely operated vehicle (ROV) MARUM-QUEST for sampling and habitat mosaicking. A number of other different sampling methods like piston and gravity corer, CTD rosettes and OFOBS were used to explore the areas of interest. The main purpose of the hydroacoustic methods was the search for anomalies in the water column as indicator of active fluid or gas seep sites as well as mapping the deep-sea basins, flare sites and plate-tectonic driven magmatic mounts and ridges. In addition, for planning station work and OFOBS/ROV dives bathymetry was a necessary basis.

Work at sea

System and Acquisition

Bathymetry and MBES water column as well as backscatter were recorded with the hull-mounted Teledyne HS-DS3 MBES. At *Polarstern*, the MBES transducer arrays are arranged in a Mills cross configuration of 3 m (transmit unit) by 3 m (receive unit) behind an ice-shield. The combined motion, position (with Trimble GNSS D-GPS correction signal), and time data comes from an iXBlue Hydrins INS (Inertial Navigation System). The signal goes directly into the Processing Unit (SPM & CM) of the MBES to do real-time motion compensation for pitch, during transmit, and roll, during receive. No yaw stabilization is applied. This echosounder system uses nominal sounding frequencies of 14 to 17 kHz and was therefore used in water depths (WD) ranging between 30 – 8250 m. Depending on the WD the amount of beams varies. In average about 600 beams per swath with an acoustical footprint of 2°(TX)/2°(RX) are formed for each ping in general. During the cruise the swath width was set in the deep sea to a coverage of 4 times and in the shallower areas of 5 times the water depth. For further information about the echosounder consult https://www.teledyne.com/.

One of our main purposes were investigations in the water column with respect to gas flare search and/or findings of anomalies that may give a hint to hydrothermal or other fluid escape activities. Due to that reason, a recording next to the old-fashioned ASD format was established using the rather new and on board available Teledyne Software PDS. Besides the PDS own format (*.pds) we recorded the so called Teledyne-Reson standard *.S7k. Main advantage of this modern format in version 3.x is full binary habit (for metadata and data section) which provides a rather slim size and a fast handling within the post processing for all four acquired datasets: bathymetry, amplitude, beam time series and water column. The handling of this format has recently been implemented to CARIS Hips & Sips as well as MB System.

The HSDS-3 was recording continuously during the cruise besides some station work and transits within EEZs where acquisition has not been applied. During the hydroacoustic surveys the vessel speed was conducted up to 8 kn, within transits up to 11 kn. Due to a problem with the multi-ping mode during the cruise the data was recorded in single ping only. Bad weather conditions and interferences with the Parasound PS70 affected the data quality during the cruise at times.

Post-Processing

The open source software MB-System suite (Caress & Chayes, 2017) was utilized for post-processing purposes. A tide correction was applied, based on the Oregon State University (OSU) tidal prediction software (OTPS) which is retrievable through MB-System. CTD and SVP measurements were conducted between or during the MBES surveys to receive sound velocity profiles (SVP) and were applied during the acquisition. A roll, pitch and heave correction were applied while ray tracing (sound velocity correction) in accordance to the given values from the last calibration of the echosounder. More details can be found in the detailed description of processing (process.cmd - file). By using the Mbeditviz tool, artefacts were cleaned manually. NetCDF (GMT) grids of the edited data as well as statistics were created with mbgrid. This grids represent digital terrain models (DTMs) with a certain raster grid cell size. The published bathymetric grid of the cruise PS119 will have a resolution of 70 m. Currently, due to discussions with the vendor, no total propagated uncertainty (TPU) has been calculated to gather vertical or horizontal accuracy. A higher resolution is achievable and for scientific purposes, a current resolution of 35 m is used. The grid extended with _num represents a raster dataset with the statistical number of beams/depths taken into account to create the depth of the cell. The extended _sd -grid contains the standard deviation for each cell. The DTMs projections are given in Geografic Coordinate System Lat/Lon; Geodetic Datum: WGS84. All grids produced will be retrievable through the PANGAEA database (*www.pangaea.de*) after a moratorium for scientific purposes.

Since the handling of the new format *.S7k required some implementation time into the existing post processing tools we worked in parallel to MB-System with CARIS Hips and Sips™. Especially water column investigation is covered by this tool, since there are currently no other software packages that can deal with this data format.

For this reason, data from this cruise are processed within projects in both mentioned software packages.

Preliminary (expected) results

Throughout the cruise, 645.996 pings were released recording in total 364.871.740 beams within 1,064 hours (without station time), along a track length of 10,329 km (without station time). The average speed was 5.25 knots. Fig. 3.1 gives an overview of the covered region of an area of 75,923 km². To avoid dwell time due to adverse weather we used the transits between stations to consequently fill gaps or improve existing bathymetry with new hydroacoustic surveys.

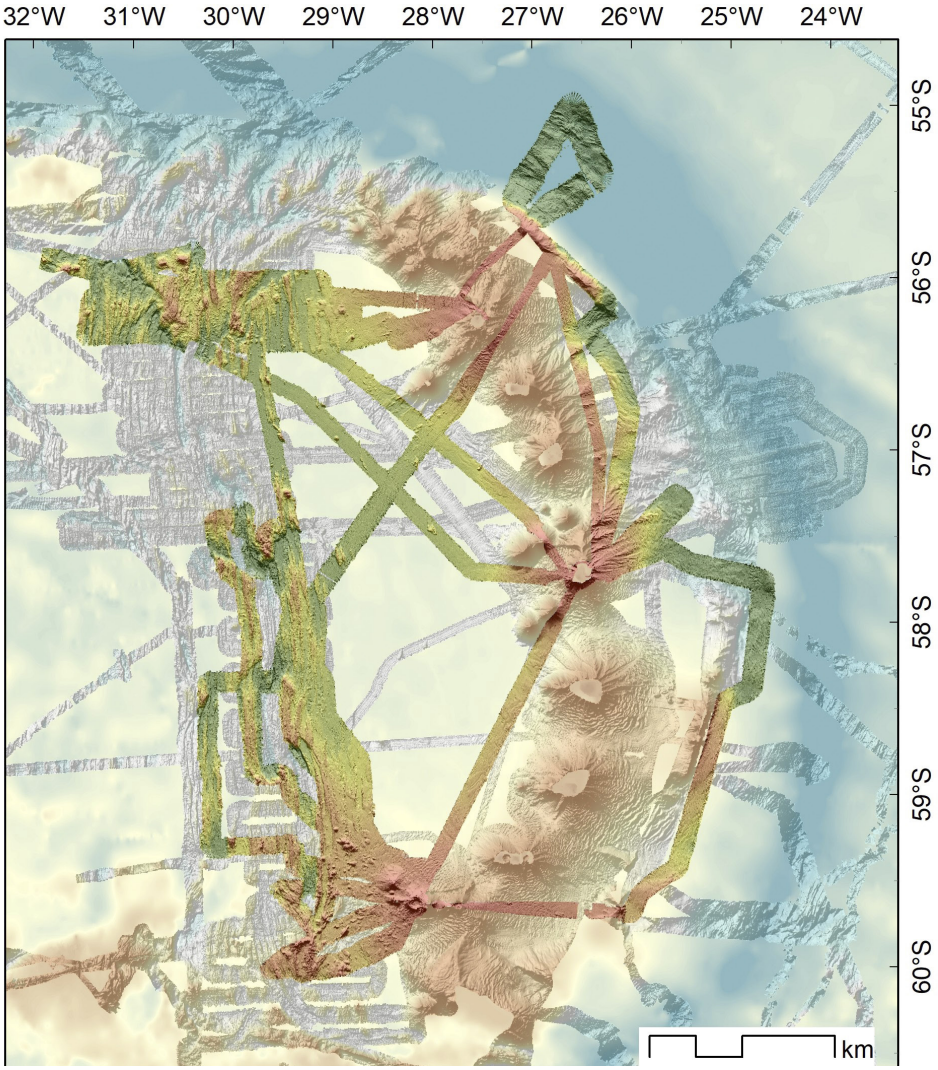

Fig. 3.1: Overview of the recorded data. Wherever possible we tried to add new data to already existing records on the South Sandwich Plate and along the trench.

With the surveys, we gained new insights to the area of E2, in general along the East Scotia Ridge (E2-E9), the Kemp Caldera (E8), in the direct vicinity of Saunders Island and in some areas of the forearc and in the trench.

Information: Within the Five Deeps Expedition (https://fivedeeps.com/) Mr. Vescovo and his team mapped the South Sandwich Trench along its deepest areas in February 2019. He signed a memorandum of understanding to provide the data to the scientific community by participating the Seabed 2030 project.

One of our main areas of investigation was the Kemp Caldera. We therefore used the opportunity to re-survey the caldera (Fig. 3.2) for a detailed comparison of the geomorphology.

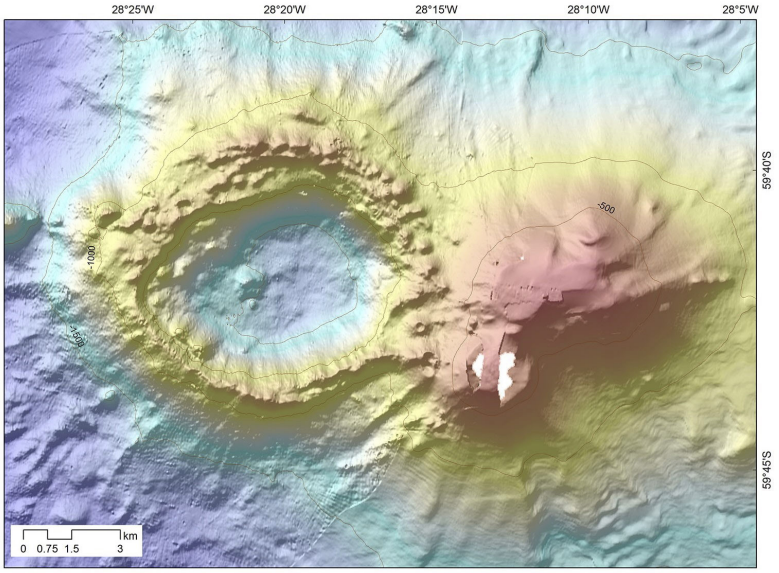

Fig. 3.2: Compilation of the re-surveyed Kemp Caldera and data provided by BAS (Leat et al., 2016)

During the cruise, Saunders Island was in the focus of a group of scientists around Nicole Richter to map the island with unmanned aerial vehicles (UAVs) and to enter the island for sampling and further investigations. In the course of accomplishing this task, the captain Moritz Langhinrichs had to lead the vessel beyond known waters. Focusing security reasons we started to map the waters around the island and manage to cover a good portion in the E, SE, S and W of the island (Fig. 3.3). While entering Cordelia Bay we crossed a ridge that seems to surround the bay towards the open waters. The rim has an altitude up to 38 m below the water depth. The bay itself has greater depths to around 100 m WD.

Fig. 3.3: Bathymetry around Saunders Island

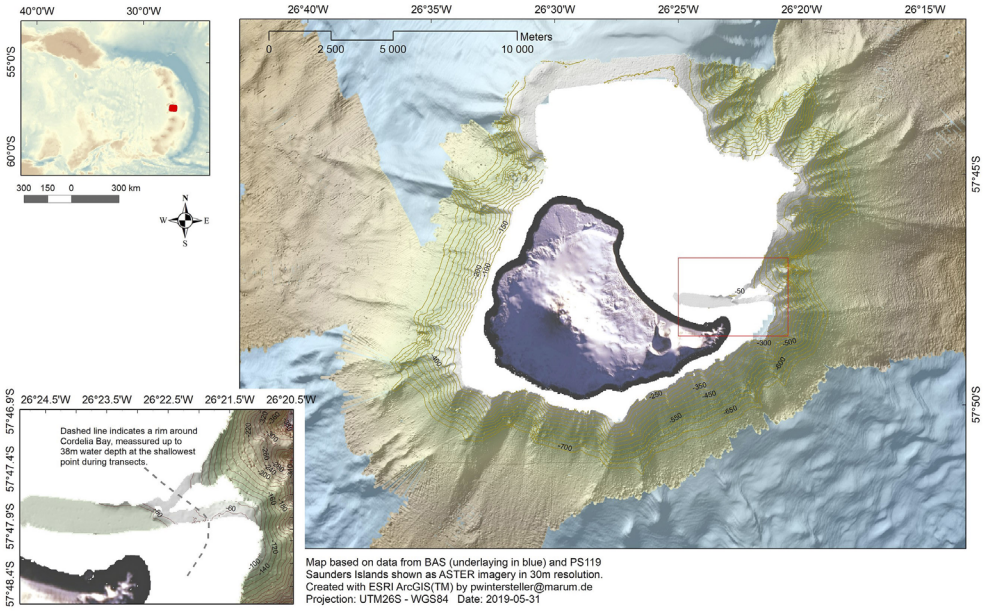

Sound velocity profiles

A number of CTD (conductivity, temperature, depth) casts were conducted to investigate in the water column but also to measure the water sound velocity. The sound velocity is influenced by density and compressibility, both depending on pressure, temperature and salinity. Wrong or outdated sound profiles led to erroneous vertical and horizontal localization of the beams.

The CTD measures conductivity, temperature, and depth through pressure in the water column while it is lowered to the seafloor. From these parameters, the sound velocity is calculated ideally by utilizing the UNESCO formula or the once based on Del Grosso, Wilson or Chen & Millero.

The sound velocity profiles obtained by the CTD were immediately processed and applied to the MBES & Parasound system for correct beamforming during the survey.

Throughout PS119, a total of 18 sound velocity profiles (SVP) were applied on the collected MBES data. The SVPs were retrieved from the CTD data while several synthetic SVPs were generated from the World Ocean Atlas 2013 (e.g. on transits). A selection of the profiles is shown in Fig. 3.4. Over the time period of almost 2 months and the distances between the stations a certain variation of the sound velocity, especially in the upper part of the water column, reflects a domination of different water masses. The values vary enough for visible issues if the correct SVPs are not applied for ray tracing.

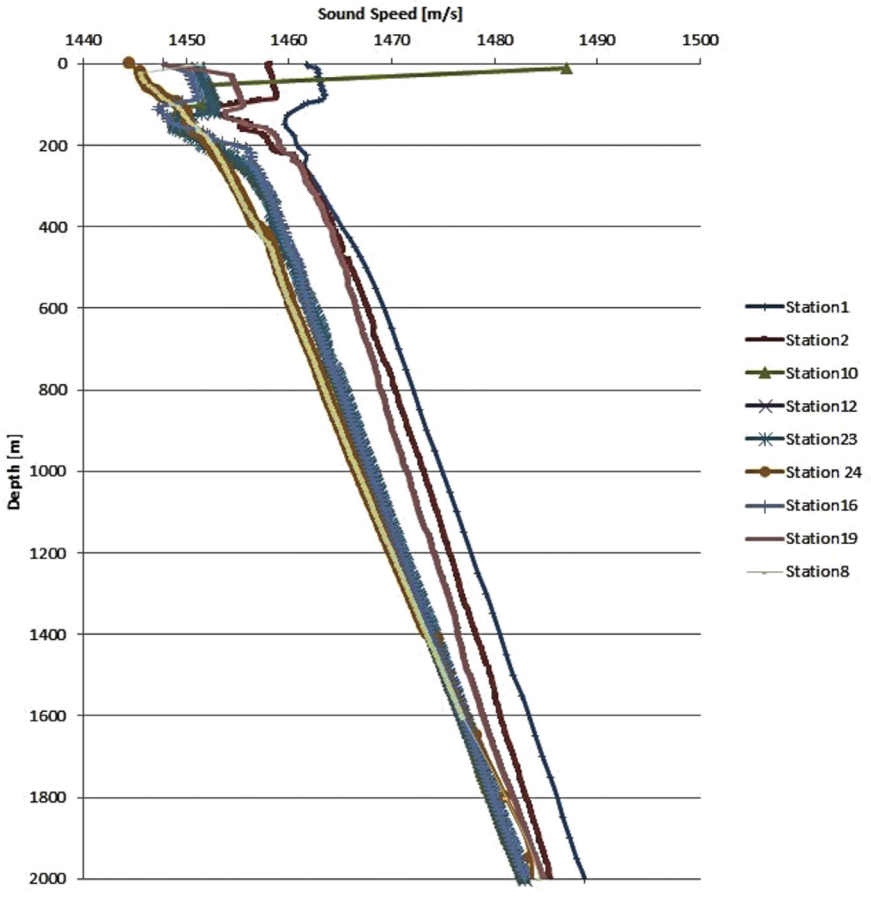

Fig. 3.4: SV profiles from several stations. Station numbers are given according to the ship stations

Data management

Hydroacoustic data collected during PS119 will be under moratorium for about 36 months for scientific purposes. Meanwhile the raw data (format *.asd and *.s7k) and products (grids) will be made available via the World Data Center PANGAEA Data Publisher for Earth & Environmental Science (www.pangaea.de) with a secured access. A DOI will be given for the data set and is therefore citable. Furthermore, the data will be provided to mapping projects and included in regional data compilations such as IBCSO (International Bathymetric Chart of the Southern Ocean) and GEBCO (General Bathymetric Chart of the Ocean). Bathymetric data will also be provided to the Nippon Foundation – GEBCO Seabed 2030 Project. In total the raw data volume of the Hydrosweep is 588 GB with 1833 separate files in S7k format but around 6-7 TB for the ASD files. Both include water column information.

References

Caress DW & Chayes DN (2017) MB-System: Mapping the Seafloor, https://www.mbari.org/products/research-software/mb-system

Leat PT, Fretwell PT, Tate AJ, Larter RD, Martin TJ, Smellie JL, Jokat W & Bohrmann G (2016) Bathymetry and geological setting of the South Sandwich Islands volcanic arc. Antarctic Science, 28(4), 293-303. doi:10.1017/S0954102016000043

4. SUB-BOTTOM PROFILING AND WATER COLUMN IMAGING

Paul Wintersteller[1,2], Miriam Römer[2], Stefanie Gaide[2], Ines Vejzovic[1], Victoria Kürzinger[1], Nontje Rücker[1], Martin Meschede[3], Nicole Richter[4], Crispin Little[5], Anna Lichtschlag[6]

[1]GeoB Bremen
[2]MARUM, Bremen
[3]IGG-UG, Greifswald
[4]GFZ Potsdam
[5]SEE-UL, Leeds
[6]NOC, Southampton

Grant-No. AWI_PS119_00

Objectives

The main purpose of the hydroacoustic methods was the search for anomalies in the water column as indicator of active fluid or gas seep sites as well as mapping the deep-sea basins, flare sites and the sediment coverage of plate-tectonic driven magmatic mounts and ridges. In addition, for planning station work, like piston- and gravity core sites sub-bottom profiles were an essential basis. Sub-bottom profiler data were acquired with the hull-mounted TELEDYNE PARASOUND P70 echosounder.

Work at sea

System and acquisition

The P70 system (the label is derived from P for parametric and a max. transmission power of 70kW, capable to penetrate up to 200 m of sediments) is utilized not only as a sediment echosounder but also for single beam echosounder investigations in the water column. The device utilizes the parametric effect based on the nonlinear relation of pressure and density during sonar propagation (Spiess and Breitzke, 1990). Two similar high intensity acoustic waves, transmitted as a sequence of sinusoidal wave pulses, with frequencies of 18 - 20 kHz, the so called primary high frequency (PHF), and a 22 - 24 kHz frequency were used to create a secondary high (40 - 42 kHz) and a secondary low (~4 kHz) frequency (referred to as SLF). The SLF signal travels within the narrow 19 kHz beam, which is much narrower than e.g. the 30° beam of a 4 kHz signal when emitted directly. Therefore, a higher lateral resolution can be achieved, and imaging of small-scale structures on the seafloor is superior to conventional systems. While the SLF is used for the sub-bottom profiling, the PHF can be used to image gas bubbles, plankton, fish or nepheloid layers in the water column. The opening angle of the transducer array is 4° by 5°, which corresponds to a footprint size of about 7 % of the water depth. Therefore, the footprint varies in a range between 2.4 to 650 m in 30 to 8,250 m water depth. The pulse shape was kept rectangular, with a duration of 1-2 periods and lengths of 0.25 - 0.5 ms. The receiver amplifications were 30 dB (PHF) and 12 dB (SLF) for most of the in deep sea recorded data. Less amplification was used for the upper continental slope and shelf areas. The given values are recorded in the header of the *.asd raw-data.

The data acquisition was performed using measured real-time values of surface sound velocity and sound velocity profiles derived from CTD measurements during the cruise. The SLF penetration at the ridges was rather low due to the steep slopes and a low sediment coverage. However, inside valleys and basins a better penetration was accomplished.

During regular surveys, single rectangular shaped pulses with a continuous wave pulse type were emitted. Special settings were used during the exploration of the Kemp Caldera. These profiles were recorded in quasi-equidistant mode with a FM chirp pulse type. (Due to very low transmit power (50 %) from a former shallow water survey the data is rather difficult to interprete). To avoid signal interferences in general, all used hydroacoustic systems were synchronized using the on-board K-Sync-Unit. The vessel speed while surveying was conducted to 8 -10 kn besides for particular water column investigation. Therefore, a vessel speed of < 5 kn according to the weather conditions was chosen. The data quality was in general fair; weather conditions were the most limiting factors while the utilization of the installed ice-window, an 8 cm Titanium shield, was not necessary and impeded attenuation.

The acquisition software PARASTORE is used to store and display the echograms. It stores raw files (.asd/.asx) in the main window and the formats .ps3 and .segy within the particular PHF/ SLF echogram windows. Auxiliary data files (.aux) were recorded along with the .asd files. They contain navigation in a selected frequency. These .ps3 files were converted into SEGY formats and further processed using PS32SEGY (by H. Keil and V. Spiess, University of Bremen) to be used e.g. in the Kingdom™ software. For further information about the system consult the following link: https://epic.awi.de/id/eprint/26733/7/ATLAS_PARASOUND_2015-02.pdf

Preliminary (expected) results

Recognizing that very small anomalies in the water column can hardly be seen on the MBES HS-DS3, most probably due to the settings preferring good bathymetric coverage and bottom detection than high resolution in the water column, we focused on investigations above (PHF) and of course below (SLF) the seafloor onto the PARASOUND system.

Fig. 4.1 shows principle findings and its appearance in the very shallow waters around South Georgia. Although the horizontal footprint of the parametric system (see above) is rather large a vertical resolution of about 12cm can be achieved.

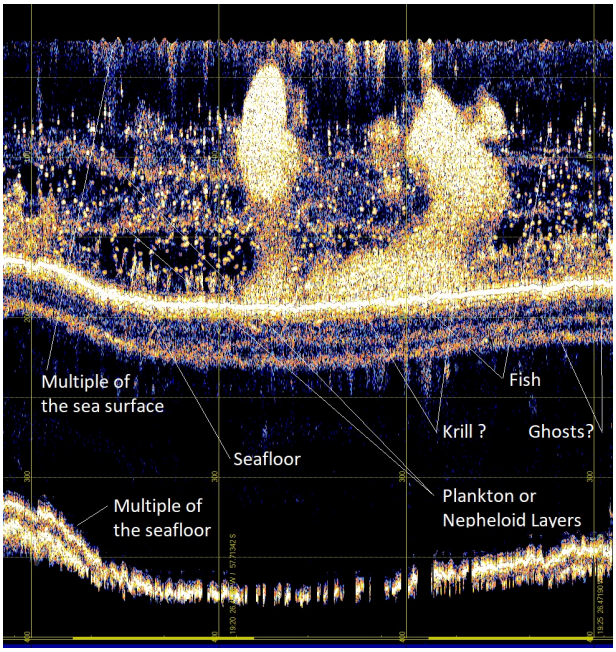

Fig. 4.1: PHF recording of the water column on the shelf of South Georgia

One of the anomalies, which we found west of E2, in the so-called WOW area, is what we believe, evidence for weak fluid and/or gas escape (Fig. 4.2). While the SLF shows a clear blanking within the layered sediments, the PHF signal reveals a small but reproducible acoustic illumination in the near vicinity to the seafloor (Fig.4. 2).

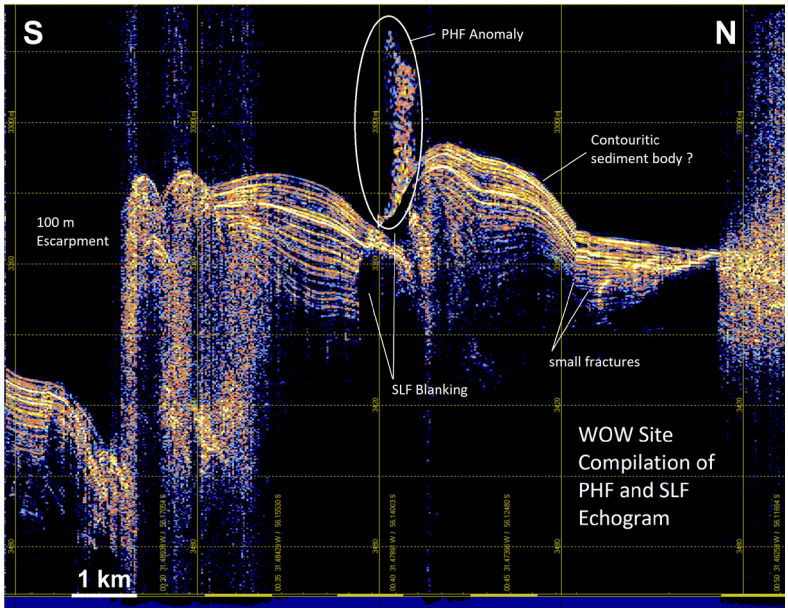

Fig. 4.2: Compilation of SLF (4kHz) and PHF (18kHz) echogram over the WOW site

Within the forearc and trench area investigation was clearly focusing on possible release of abiotic methane driven by serpentinization of ultramafic rocks within the subduction processes. While we found 2-3 promising sites almost as expected, on the ridges west of the trench in about 1,300 – 2,500 m WD, no signals in the water column were observed during our little excursion around the Meteor Deep (Fig. 4.3). Recently, Mr. Vescovo found an even little deeper site (8,266 m) about 1-2 miles away, during his FiveDeeps-Expedition.

A former Topas™ profile (a Kongsberg parametric SBP) was conducted in the deep sea basin west of the continental rise of South Georgia and was the basis of a AWI-MARUM joint proposal. With that respect, we rerun the profile to find the best site for coring the sediments, particular on elevated/ridge-like features. The very nice profile is shown in Fig. 4.4, highlighting the position of gravity corer GC-01 and GC-02.

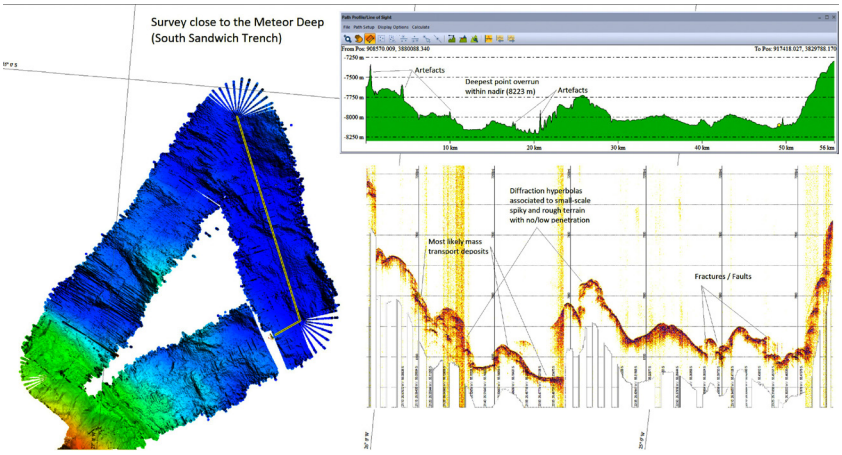

Fig. 4.3: Observations around the Meteor Deep. Next to the bathymetry (left) a profile is given (upper right corner, position is indicated in the bathymetry). In parallel (lower left), the SLF recording is shown.

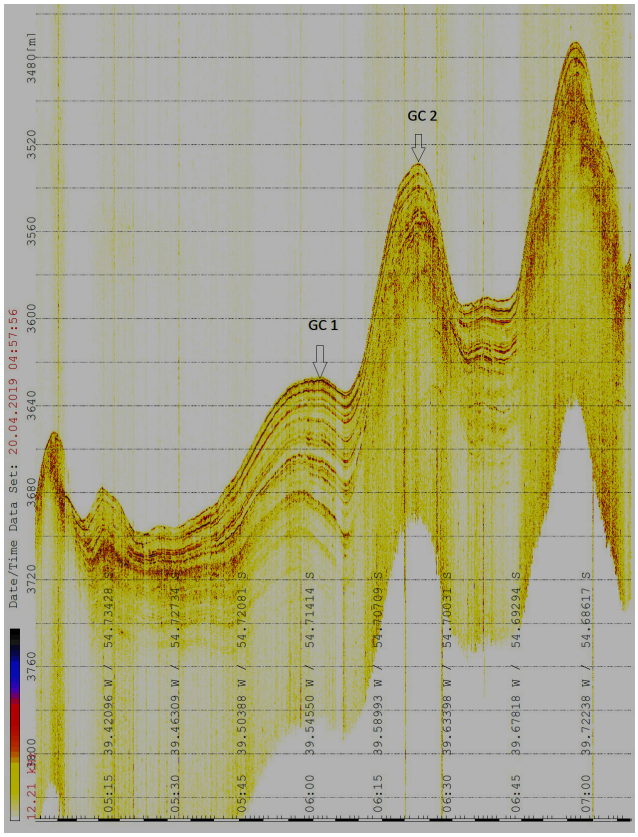

Fig. 4.4: SLF profile in parallel to the pre-existing Topas™ profile

Data management

PARASOUND data sets will be under moratorium for about 36 months for scientific purposes. Meanwhile the data, including raw data recordings of the format *.asd and post-processed SegY will be transferred and stored at the World Data Center PANGAEA Data Publisher for Earth & Environmental Science (www.pangaea.de) with a secured access. A DOI will be given for the data set and is therefore citable. Around 700 GB of data were recorded on the cruise, including *.asd, *.ps3 and *.segy files.

References

Spiess V & Breitzke M (1990) Das Parasound-Sedimentecholotsystem - Funktionsweise, Anwendungsbeispiele und digitale Datenerfassung, Jahrestagung der Deutschen Geologischen Gesellschaft, Bremen. hdl:10013/epic.21196

5. PHYSICO-CHEMICAL CHARACTERIZATION OF THE WATER COLUMN (CTD WORK)

Thomas Pape[1], Yiting Tseng[1], Alexander Diehl[2]

[1]MARUM, Bremen
[2]GeoB, Bremen

Grant-No. AWI_PS119_00

Objectives

Objectives of the CTD work during PS119 were

- to identify general water masses in the working area
- to assess physico-chemical characteristics, water depth intervals, and spatial extent of plumes in the water column that are fueled by hydrothermal emissions
- to evaluate physico-chemical characteristics of fluids emitted at hydrothermal vents.

Work at sea

Oceanographic data and water samples were collected using a SBE911plus CTD underwater unit and a carousel water sampler (SBE 32) connected to a CTD deck unit SBE11 from AWI, Bremerhaven – Physical Oceanography. The CTD was comprised of double sensor packages of conductivity (SBE4c) and temperature (SBE3plus) with pumps (SBE5T), a pressure sensor as well as an oxygen sensor (SBE43), a transmissometer (WET Labs C-Star, 25 cm), and a fluorometer (WET Labs ECO-FLR). Distance to seafloor was measured with an altimeter (Benthos, PSA900D). Data from the fluorometer were not investigated during PS119. Measured oxygen concentrations are not reported.

In contrast to the typical configuration of the carousel water sampler that includes 24 ten liter Niskin bottles, during PS119 two bottles were demounted from the frame in order to give way for a MAPR sensor (chapter 9). During PS119, 17 CTD-rosette stations were completed; station CTD-15 at Kemp Caldera was aborted due to time constraints. Because the major objectives of the CTD-rosette deployments during the cruise were the characterization of seafloor fluid emissions into the water column, water was sampled for onboard analyses of dissolved methane in up to 22 different water depths from close to the seafloor to close to the sea-surface to obtain vertical concentration profiles of methane.

Here we show temperature and salinity, while methane concentrations in discrete water samples and continuous profiles of beam transmission values are reported in chapter 13.

Preliminary results

East Scotia Ridge - E2 West

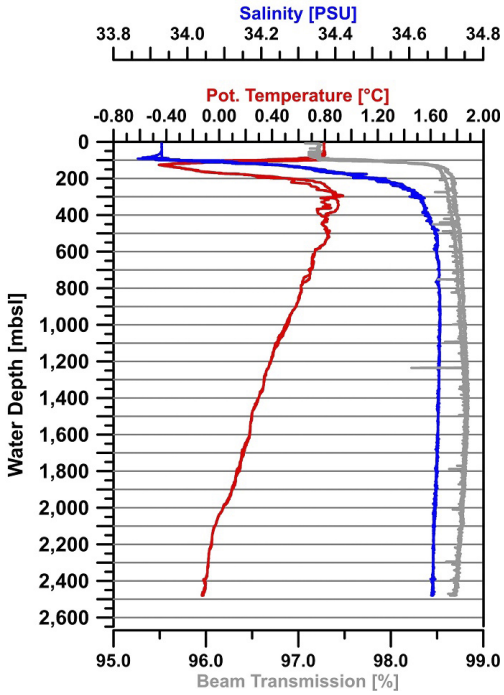

Fig. 5.1: Salinity, Potential Temperature, and Beam Transmission vs. Water Depth at station CTD-01 (down- and upcast; dissolved CH4 was not measured at this station)

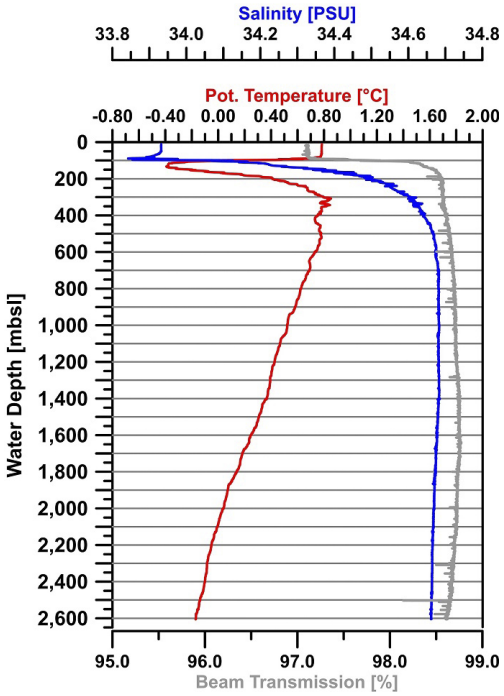

Fig. 5.2: Salinity, Potential Temperature, and Beam Transmission versus Water Depth at station CTD-02 (upcast; dissolved CH4 was not measured at this station)

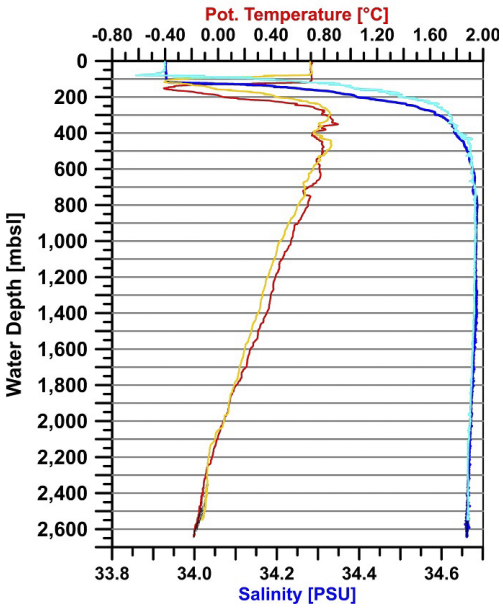

Fig. 5.3: Salinity and Potential Temperature vs. Water Depth at station CTD-03 (several down- and upcast in deep waters – tow yo-method)

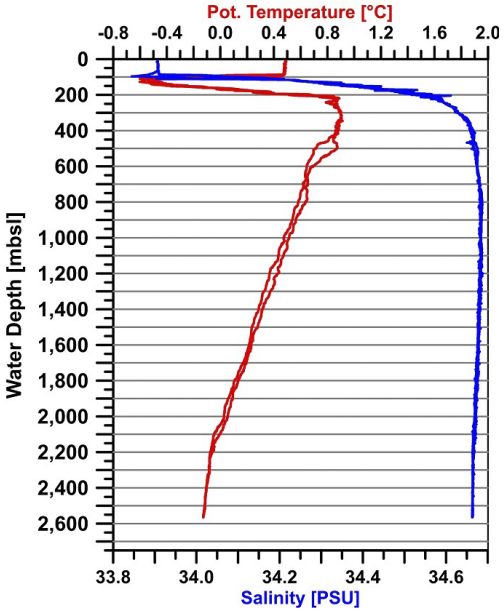

Fig. 5.4: Salinity and Potential Temperature vs. Water Depth at station CTD-04 (several down- and upcast)

East Scotia Ridge - E2 West (WOW area)

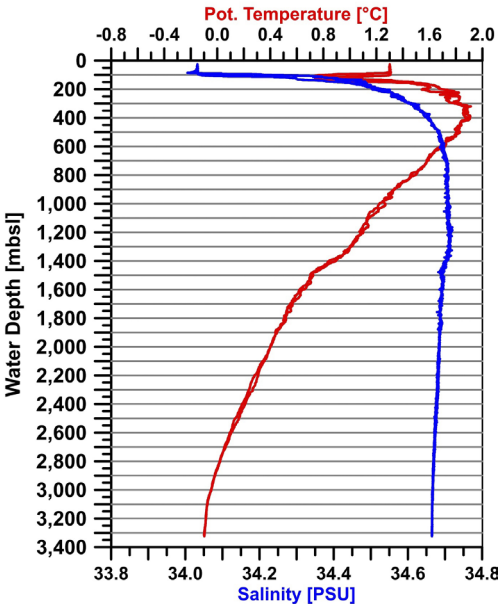

Fig. 5.5: Salinity and Potential Temperature vs. Water Depth at station CTD-05 (down- and upcast)

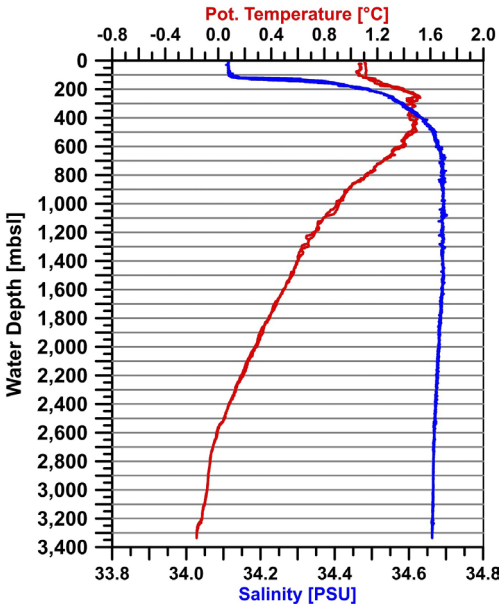

Fig. 5.6: Salinity and Potential Temperature vs. Water Depth at station CTD-16 (down- and upcast)

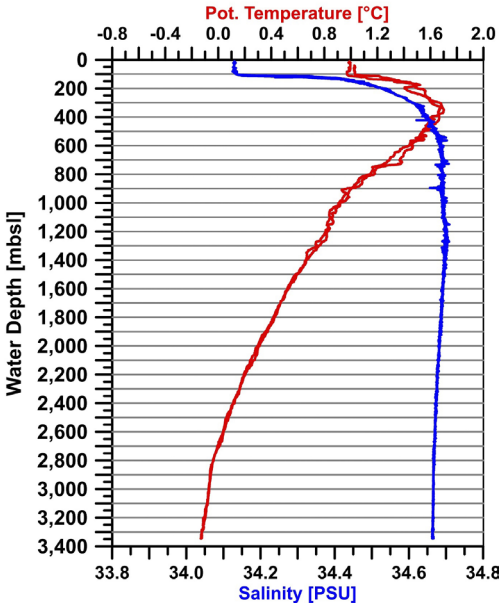

Fig. 5.7: Salinity and Potential Temperature vs. Water Depth at station CTD-17 (down- and upcast)

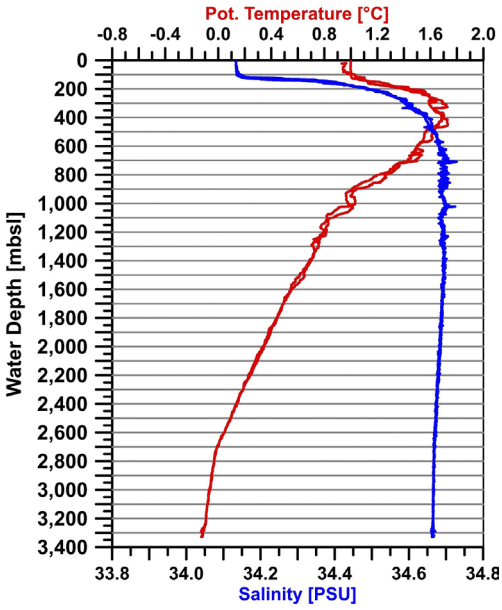

Fig. 5.8: Salinity and Potential Temperature vs. Water Depth at station CTD-18 (down- and upcast)

East Scotia Ridge – E5

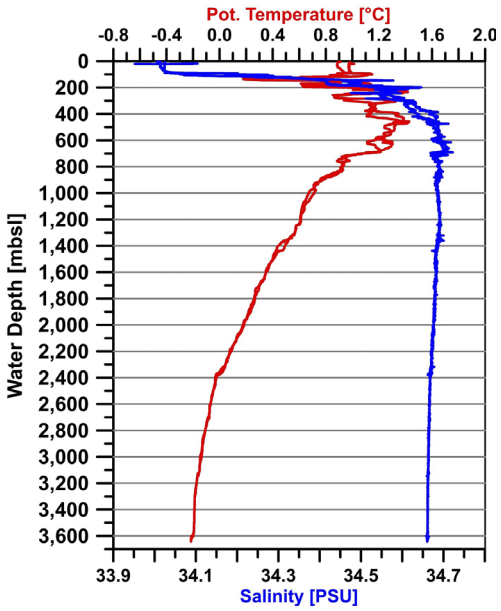

Fig. 5.9: Salinity and Potential Temperature vs. Water Depth at station CTD-09 (down- and upcast)

East Scotia Ridge – E8

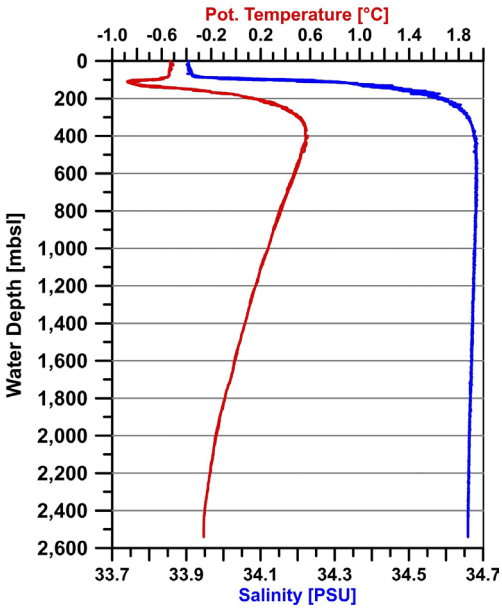

Fig. 5.10: Salinity and Potential Temperature vs. Water Depth at station CTD-11 (down- and upcast)

Kemp Caldera

Positive anomalies in bottom water temperature and strong scattering in salinity indicated the presence of near-bottom plume caused by injection of hydrothermal fluids at sites CTD-07 and CTD-10.

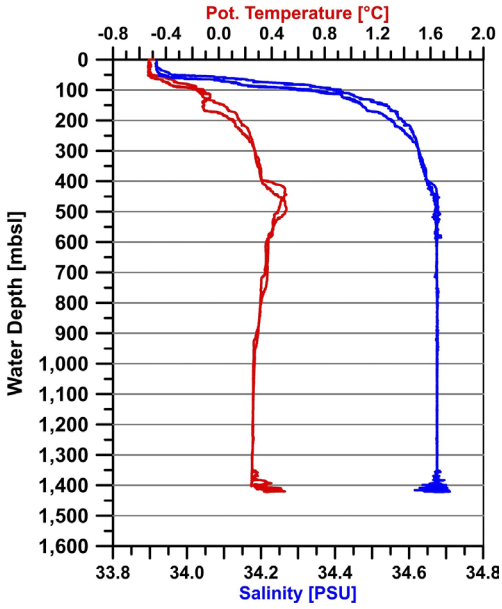

Fig. 5.11: Salinity and Potential Temperature vs. Water Depth at station CTD-07 (down- and upcast)

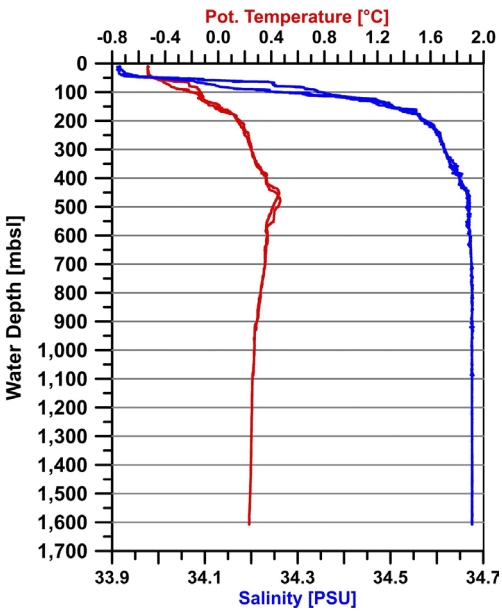

Fig. 5.12: Salinity and Potential Temperature vs. Water Depth at station CTD-08 (down- and upcast)

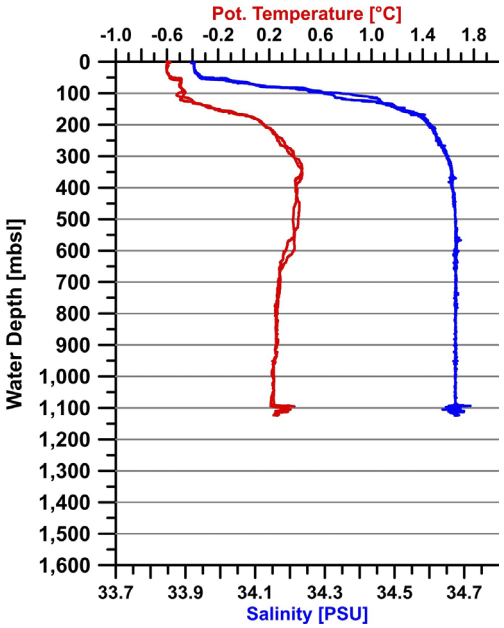

Fig. 5.13: Salinity and Potential Temperature vs. Water Depth at station CTD-10 (down- and upcast)

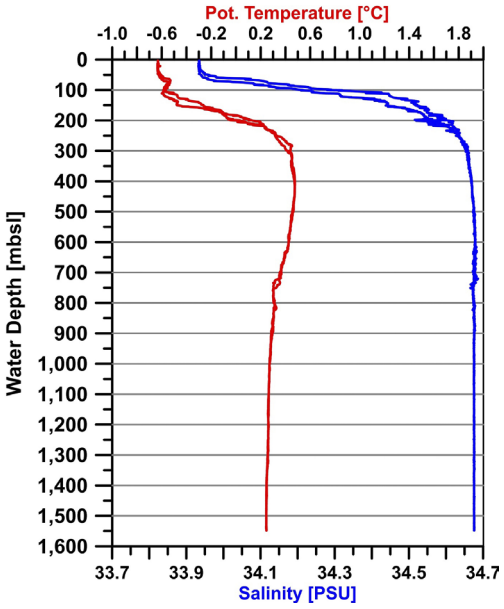

Fig. 5.14: Salinity and Potential Temperature vs. Water Depth at station CTD-12 (down- and upcast)

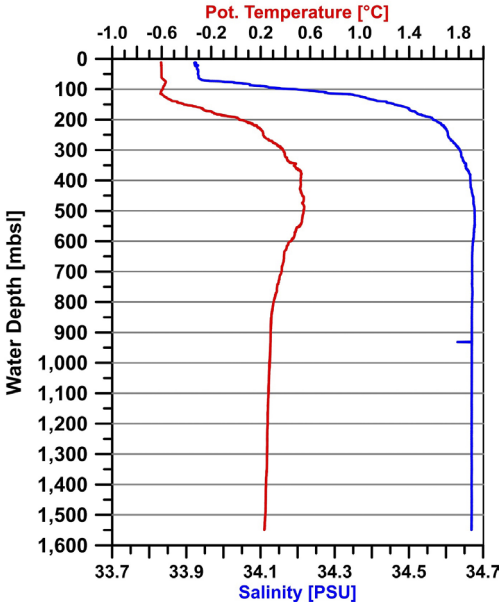

Fig. 5.15: Salinity and Potential Temperature vs. Water Depth at station CTD-13 (down- and upcast)

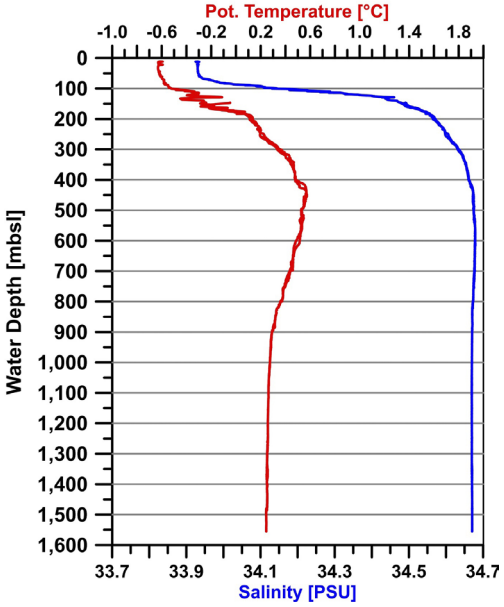

Fig. 5.16: Salinity and Potential Temperature vs. Water Depth at station CTD-14 (down- and upcast)

South Sandwich forearc

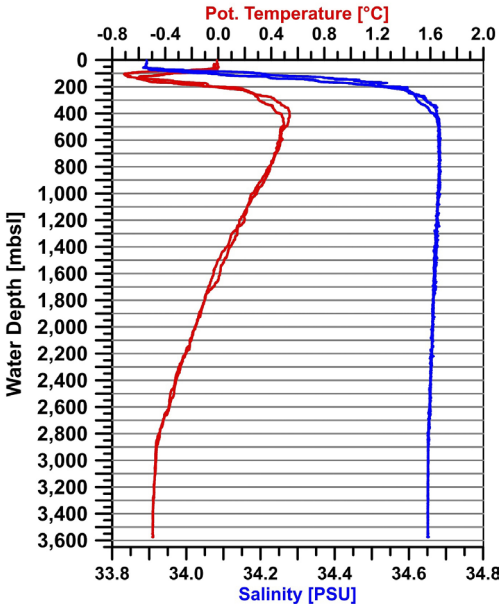

Fig. 5.17: Salinity and Potential Temperature vs. Water Depth at station CTD-06 (down- and upcast)

Data management

All data collected and generated by this project will be made publicly available via the World Data Center PANGAEA Data Publisher for Earth & Environmental Science (www.pangaea.de).

6. OCEAN FLOOR OBSERVATION AND BATHYMETRY SYSTEM (OFOBS)

Miriam Römer[1], Paul Wintersteller[2,1], Yiting Tseng[2], Ines Vejzovic[2], Victoria Kürzinger[2], Stefanie Gaide[1], Nontje Rücker[2], Crispin Little[3]

[1]MARUM, Bremen
[2]GeoB, Bremen
[3]SEE-UL, Leeds

Grant-No. AWI_PS119_00

Objectives

During PS119, a towed camera platform integrating additional acoustical devices called ocean floor observation and bathymetry system (OFOBS) was used (Purser et al., 2019). The system is deployed with a continuous direct communication through the ship's fiber optic cable and operational at depths up to 6,000 m. The objective for the OFOBS deployments was mainly the acquisition of high-resolution bathymetry and additionally to get a visual impression of the seafloor in areas of special interest.

The OFOBS frame is equipped with a deep-sea underwater telemetry system including 4 LED lamps, 2 flashes, 3 laser pointers, a high-resolution digital camera (iSiTEC, CANON EOS 5D Mark III) for still pictures and a HD color video camera (Sony FCB-H11). A USBL Posidonia transponder and a Tritech altimeter are mounted for underwater positioning and depth control. However, the altimeter did not function during the first 7 dives of PS119. In the upper front of the OFOBS frame, a forward-looking sonar (Teledyne BlueView M900-130) with a maximum range of 100 m is installed. The bathymetry unit of the OFOBS consists of an Edgetech 2205 bathymetric side scan sonar supported by an iXblue PHINS 6000 INS navigation setup. Auxiliary sensors include an AML Micro-X sound velocity sensor, an AML Micro-X pressure sensor (which did not work within the first 6 dives) and a iXblue Doppler Velocity Log (DVL), also installed to aid with acoustics and navigation. Finally, we installed during PS119 a MAPR (see chapter 9) in the lower front part of the OFOBS frame and three temperature loggers during each deployment. These sensors are self-recording and were not attached to the power supply of the OFOBS.

Work at sea

During PS119, in total 10 OFOBS deployments were successfully conducted. One deployment had to be cancelled before entering the water, when it was recognized that the fibre optic cable termination was not working properly during the deck dry test. At South Georgia, in the Forearc region as well as in E5, we conducted one OFOBS dive each, whereas at Kemp Caldera and E2 several OFOBS dives were carried out. In total, about 16.4 hours have been spent close enough to the seafloor to acquire video footage and 29.9 hours for bathymetric mapping.

Tab. 6.1: OFOBS deployment list during PS119 including area, date, deployment time and time spans for seafloor imaging and micro-bathymetry mapping.

OFOBS	Station PS119_	Area	Date	Start Time	End Time	Seafloor imaging	Bathymetry (at ~40 m)
-1	003-1	South Georgia	21.04.2019	09:16	13:21	11:35 - 12:26	12:26 - 13:07
-2	009-1	E2	23.04.2019	20:37	02:00	-	22:50 - 01:11
-3	011-1	E2	24.04.2019	17:34	19:31	19:01 - 19:07	-

OFOBS	Station PS119_	Area	Date	Start Time	End Time	Seafloor imaging	Bathymetry (at ~40 m)
-4	027-1	Kemp Caldera	07.05.2019	01:10	08:24	07:26 - 07:38	03:06 - 07:26
-5	032-1	E5	10.05.2019	23:22	10:36	02:26 - 02:30 06:23 - 06:57	02:30 - 06:27 06:57 - 09:01
-6	034-1	Kemp Caldera	11.05.2019	17:00	23:50	18:59 - 20:18 22:11 - 22:42	20:18 - 22:11
-7	039-1	Kemp Caldera	14.05.2019	00:51	09:36	01:58 - 02:02 07:52 - 08:03	02:02 - 07:52 08:03 - 08:52
-8	043-1	Kemp Caldera	15.05.2019	03:40	09:30	06:10 - 08:57	04:34 - 06:10
-9	046-1	Forearc	16.05.2019	17:49	22:50	18:43 - 22:17	-
cancelled	049-1	E2	21.05.2019	00:05	01:37	-	-
-10	056-1	E2	25.05.2019	16:39	01:14	17:35 - 17:38 17:51 - 23:59	17:38 - 23:59

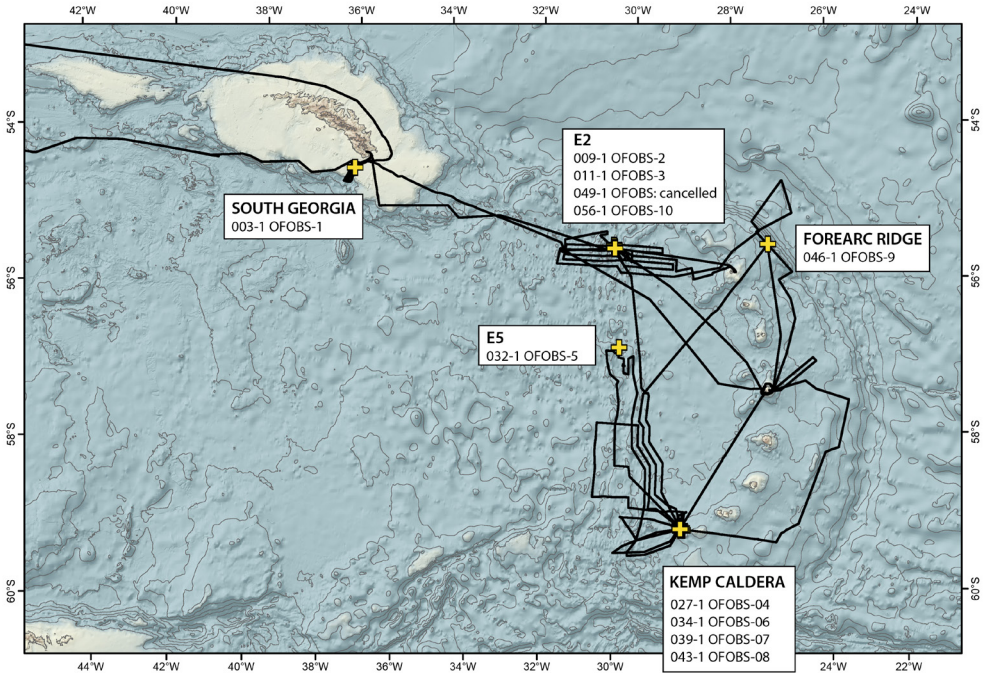

Fig. 6.1: Map of the Locations of OFOBS deployments during PS119

Preliminary (expected) results

OFOBS-01

Station: PS119_003-1

Location: South Georgia

Objective: Seafloor imaging and high-resolution bathymetry at Paradise Flare

The first OFOBS deployment was conducted at a flare position detected during *Meteor* Cruise M134 and which was confirmed to be actively degassing when passing over during this cruise. The OFOBS was deployed for ROV dive preparation and divided into two parts. The first part was dedicated to seafloor imaging when passing over the presumed location of the

gas emissions. The second part was planned to conduct first micro-bathymetric mapping in different water depth to test the side scan sonar performance and results in different altitudes regarding coverage and grid resolution. The towed track was a straight line from ESE to WNW about 1.3 km long. Unfortunately, the USBL Posidonia transponder did not work during this first deployment and only ships position is available.

Seafloor imaging revealed no clear evidence of gas emissions. The seafloor with fine sediment and scattered stones was colonized by *Aphrodite* polychaetes, brittlestars, *Labidiaster* and other starfish, cidaroid sea urchins, *Paralomis* crabs, and numerous filter feeding organisms, including bryozoans, anemones, sponges octocorals, and many comatulid crinoids. The only intriguing observation was in an area where filter-feeders were less abundant and ~cm sized holes were seen in the seafloor sediments; this could be interpreted as resulting from bubble escape.

The second part of the deployment was conducted at an altitude of first ~10-15 m and at the end at 40 m. A height of 40 m resulted in a bathymetric coverage of ~180 m of flat seafloor with a resolution about 800 depths/swath and was therefore defined as the desired performance for later deployments with the purpose of micro-bathymetric mapping.

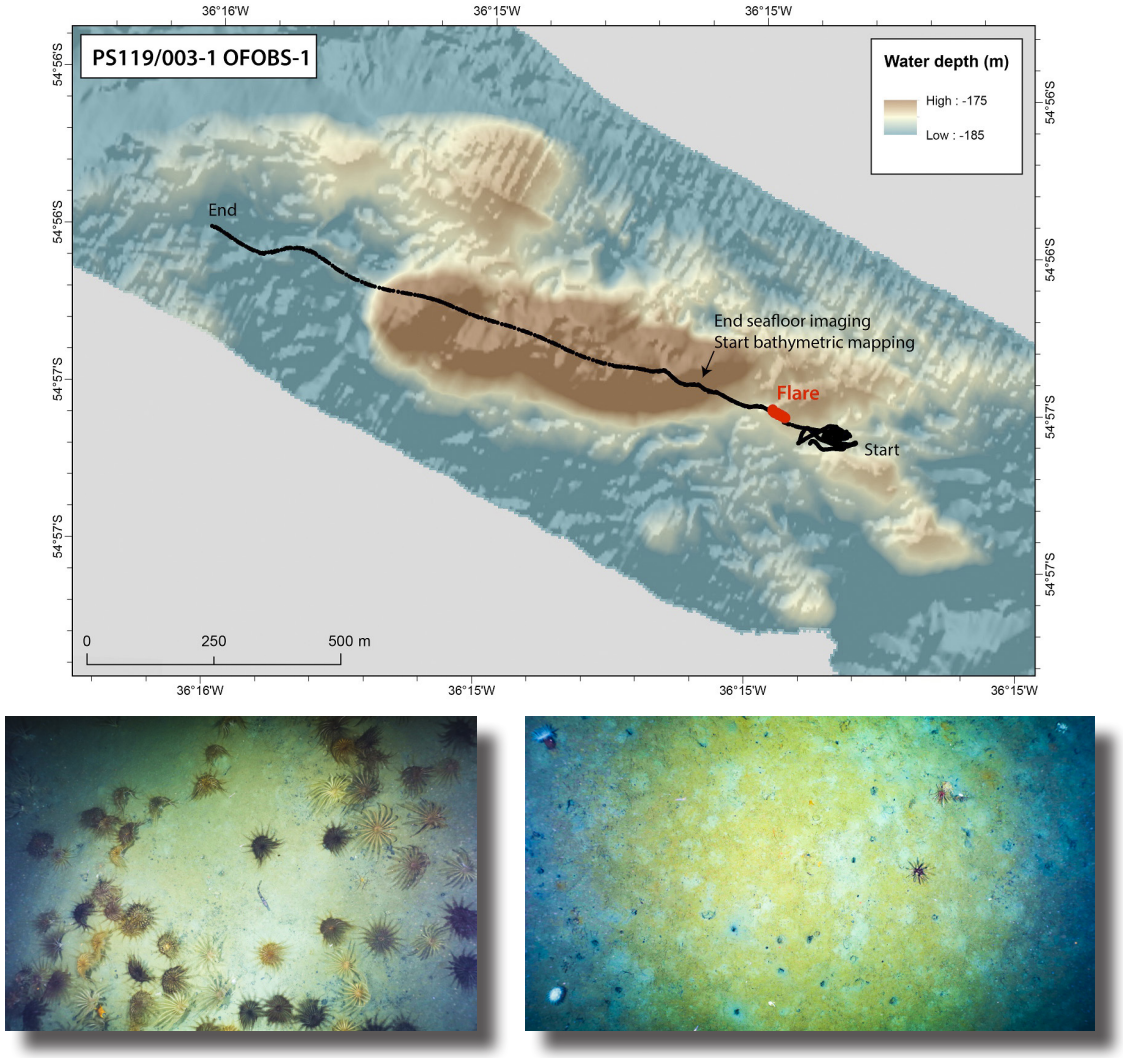

Fig. 6.2: Above: Map of the deployment of OFOBS-1. Note: the track line shown is ship's positioning, as the Posidonia transponder was not working. Below: Two seafloor images of the area in the beginning of the deployment showing many comatulid crinoids (left) and at the presumed flare location (right).

OFOBS-02

Station: PS119_009-1

Location: E2

Objective: Micro-bathymetry mapping of a N to S transect west extending the maps from NOC to W

This first deployment at E2 was planned as a N-S transect, exclusively for micro-bathymetric mapping in 40 m altitude to acquire a new map extending the information available for E2 north and E2 south west of existing NOC ISIS-ROV bathymetry. When close to the seafloor the system had to be restarted before starting the transect. When passing the presumed vent area at E2 north, some morphological features were observed. A transect of about 3.5 km was conducted in ~2.5 hours.

OFOBS-03

Station: PS119_011-1

Location: E2

Objective: Micro-bathymetry mapping of a transect from NW to SE ending at the known vent area

After reaching the seafloor and having a first visual impression, micro-bathymetric mapping in 40 m altitude was planned. However, the bathymetric side scan sonar unit did not work properly and several restarts of the entire system did not solve the problem of not having communication to the OFOBS modules. It was suspected that the fibre optical cable caused the issues but first two cable connections within the OFOBS caused a ground fault and later also the fibre optical cable had issues and needed a retermination. The deployment was cancelled and the OFOBS recovered without starting the transect.

OFOBS-04

Station: PS119_027-1

Location: Kemp Caldera

Objective: Survey a N-S transect from the rim over the newly detected flare site to the known vent area in the center of the caldera

The first OFOBS dive at the Kemp Caldera covered two sites of fluid escape: a) a flare site at the inner rim of the caldera detected by the Parasound echosounder during prior surveys, and b) the known hydrothermal vent area at the cone in the center of the caldera. The deployment was planned to acquire high-resolution micro-bathymetry as basis for coming ROV dives. At the very end of the dive, when reaching the vent area and recognizing smoke in the video footage, the OFOBS was lowered to the seafloor to gain the first visual impressions of the vent area. The system had to be restarted several times during the deployment, as three times the connection to USBL Posidonia as well as the Phins was lost.

OFOBS-05

Station: PS119_032-1

Location: E5

Objective: Long transect from N to S along the rift axis

The transect started ~7 km north of the highest elevation along the rift axis at segment E5. Before heading southwards, the OFOBS was lowered close to the seafloor to get a short visual impression. Heavily sedimented pillows were seen, with a few soft corals and brittlestars. The sediment between the pillows were habitat for some rat-tailed fish, holothurians, stalked crinoids, brittlestars, sponges and an acorn worm (Fig. 6.3). The following 4 hours were used

to map for micro-bathymetry in 40 m altitude towards the highest point of the rift axis. One kilometer before reaching the highest point, the OFOBS was again lowered to the seafloor to gain visual seafloor information. The seafloor is covered by pillow lavas and more sediment cover than expected. Not many organisms were observed, only few sea cucumbers, brittlestars, and sponges were seen. The pillow lavas formed rough landscapes and it was difficult to keep the OFOBS close to the seafloor to image it, without touching the ground. After about half an hour without remarkable findings, the micro-bathymetric mapping proceeded at 40 m altitude for about 3 hours, until the highest elevation of the rift axis was passed.

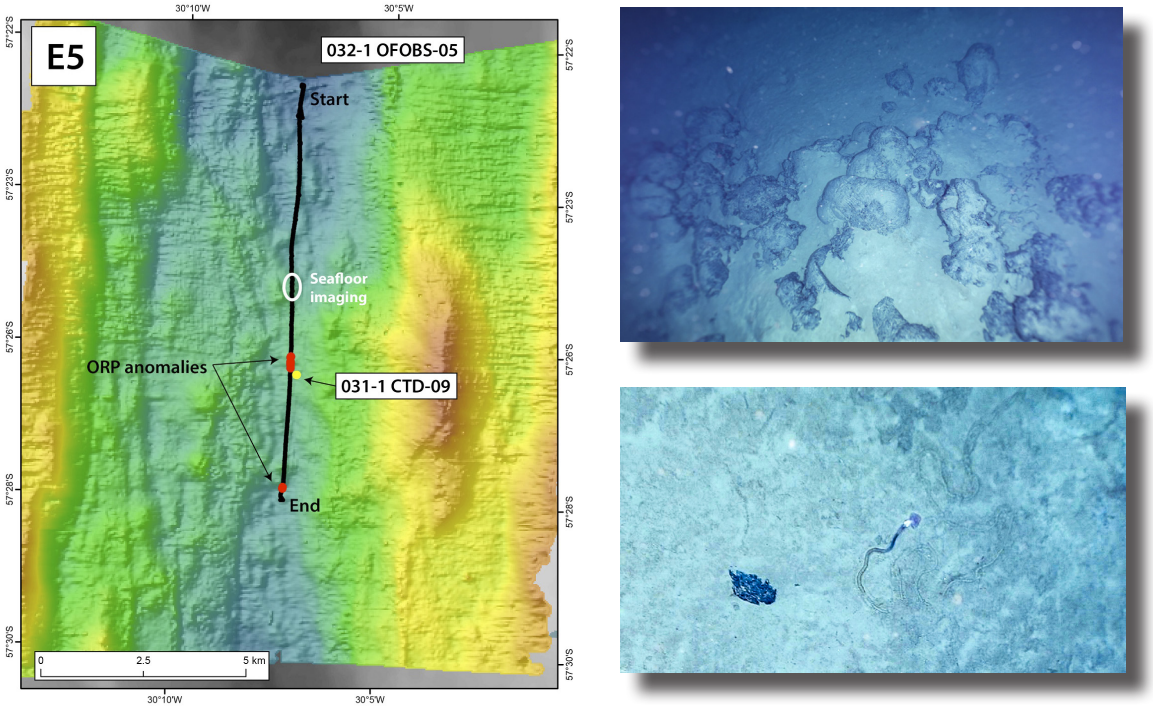

Fig. 6.3: Left: Map of E5 showing the transect of OFOBS-05. Upper right: Seafloor image showing pillow lava covered by hemipelagic sediments. Lower right: Acorn worm and ejected sediment.

OFOBS-06

Station: PS119_034-1

Location: Kemp Caldera

Objective: First half of the deployment was dedicated to seafloor imaging of the flare site, the second half for a micro-bathymetry transect from the flare site to the central cone.

After reaching the bottom, the first hour was dedicated to observation of the seafloor in the area of the flare imaged in the ship's echosounder. The OFOBS was towed by the ship with only minor deviations of about 50 m around the central coordinate of the flare position. The seafloor was rocky with some patches of gravel, sometimes brightly colored. White anemones settled on rocks and nearby sediments, rat-tailed and elongate fish, brisingid sea star and many brittlestars. Numerous vent related structures, such as extinct chimneys, were seen. However, beside microbial mats seen in several areas indicating some diffuse fluid flow, there was no indication of an active vent area including black or white smokers.

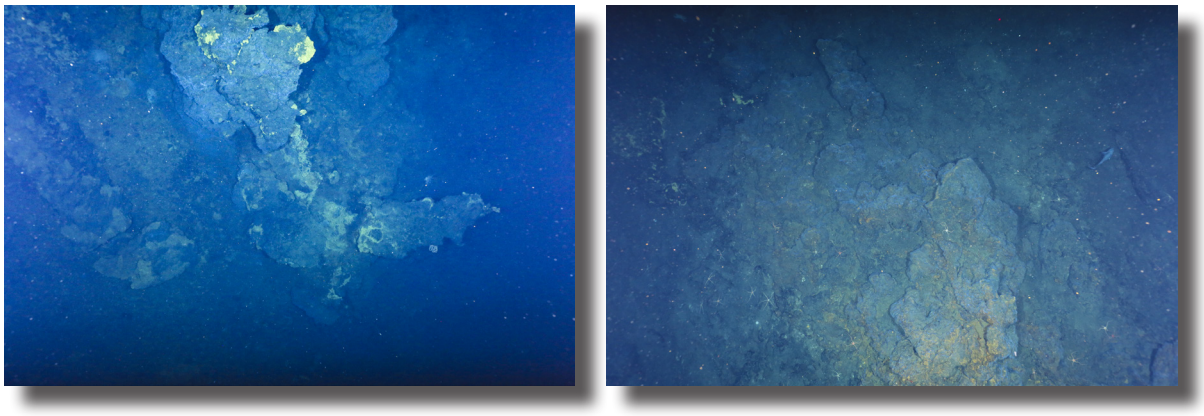

Fig. 6.4: Seafloor images taken in the area of the flare detected in ship's echosounder records. Left: Chimney structures formed of an unknown yellow material. Centre: Extinct rusty colored vent site covered with lighter colored microbial mats.

The second part of the deployment was a transect at 40 m altitude directed southward to the western side of the central cone in the caldera, an area not yet mapped or investigated. Before starting the transect, a system restart was necessary to reconnect all modules. After ~1.5 hours, the cone area was reached and the OFOBS was lowered again to the seafloor. The seafloor in this area was colonized by soft corals, anemones, brittlestars, brisingid starfish and other starfish. Black smoke appeared at some point. When leaving the seafloor and heaving through the water column, high turbidity was apparent up to ~800 m below sea level.

OFOBS-07

Station: PS119_039-1

Location: Kemp Caldera

Objective: Covering the vent area at the central cone for micro-bathymetry with 4 parallel lines

The system had to be restarted several times due to connection lost. On the decent at 1500 m large red tentacles were seen in the camera which probably belong to the of large jellyfish *Stygiomedusa gigantea*. Smoke was seen in the camera systems while mapping in an altitude of ~40 m. The seafloor was imaged during two short time periods. For the first period the seafloor consisted of variably colored sediment, dark rocks and pillow lava, with some pink echinoids and brittlestars. The second seafloor set of images showed variably colored sediments and scattered rocks with microbial mats. Sponges, anemones, rat-tailed fish and red shrimp were present. One image clearly showed the skull of an Antarctic minke whale and some associated bones (Fig. 6.5), which were described during an earlier British dive to this area (Amon et al., 2013). Towards the end of the deployment the seafloor had dense beds of living and dead vesicomyid clams and large dark red actinostolid anemones, and in a later stage small upstanding structures formed of white precipitate were visible, very similar to the ones in the Great Wall area (see ROV dive 447)(Fig. 6.5).

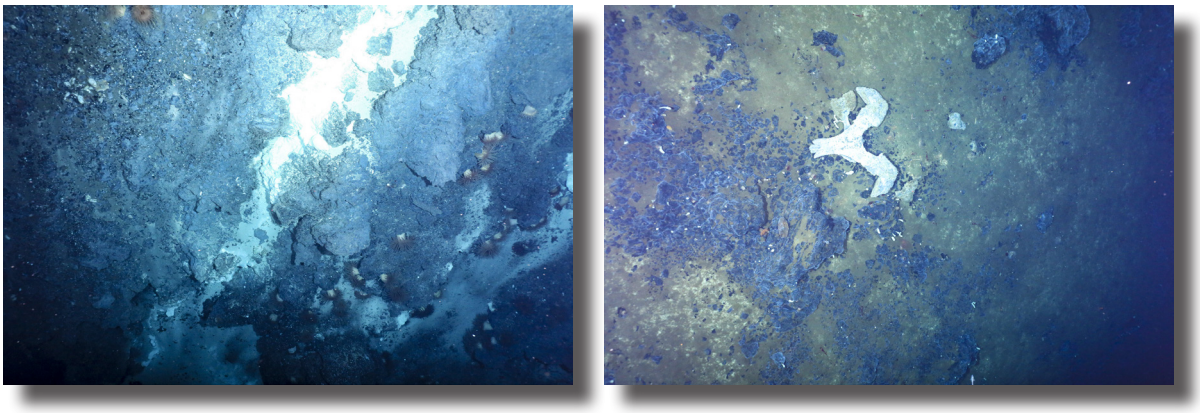

Fig. 6.5: Left: White precipitates and actinostolid anemones. Right: Antarctic minke whale skull and associated bones that were first detected during a British expedition.

OFOBS-08

Station: PS119_043-1

Location: Kemp Caldera

Objective: Micro-bathymetry transect from the south-western rim towards the central cone

The last OFOBS deployment at the Kemp Caldera was dedicated to gain more micro-bathymetric data connecting the south-western rim of the caldera with the central cone. For the first part of the deployment, the OFOBS was towed at ~40 m altitude; for the second part seafloor observations were in focus. Smoke was seen several times when passing the known vent area. Numerous squid and/or their yellow ink was seen in the water column (Fig. 6.6).

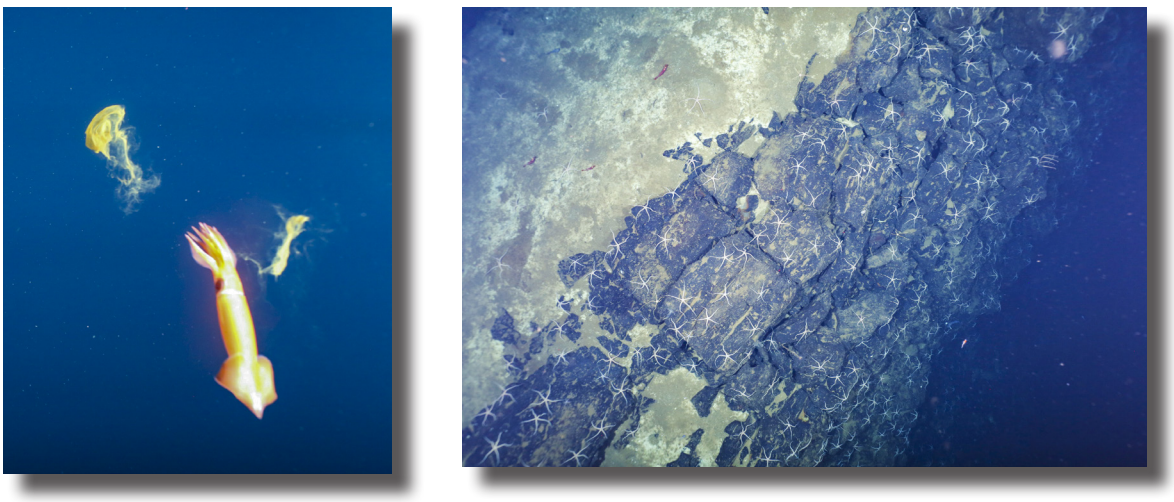

Fig. 6.6: Left: Orange colored squid and its ink imaged in the water column. Right: Steep slope of volcanic material colonized by thousands of brittlestars.

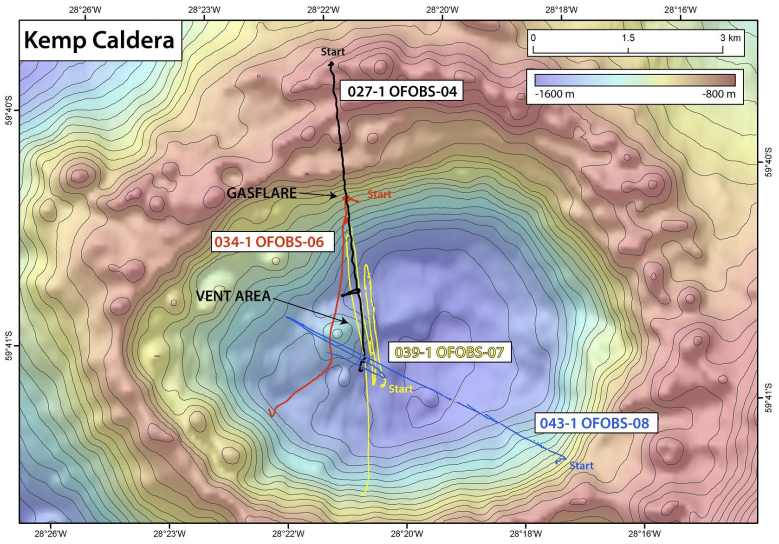

Fig. 6.7: OFOBS dive tracks in Kemp Caldera

OFOBS-09

Station: PS119_046-1

Location: Forearc

Objective: Investigating an area where Parasound records indicated a water column anomaly interpreted as a plume

OFOBS-09 was planned in the Forearc area at an arc-parallel ridge where serpentinite rocks had been dredged during a former cruise. Mapping along this ridge crest during this cruise revealed the existence of three water column anomalies that could indicate serpentinization-related fluid escape. The OFOBS deployment was therefore conducted at the most prominent water column anomaly. A first transect was planned for seafloor imaging, whereas the rest of the dive was meant to construct a micro-bathymetric map. However, the entire dive was finally dedicated to seafloor visualization.

Dark colored rock outcrops and light colored sediments were seen throughout the deployment. Especially along the northern transect and in the south-eastern part of the mapped area small scarps and outcrops of rough dark colored rocks where visibly colonized by numerous filter-feeder animals (crinoids, brisingids, sponges, octocorals, sea whips). More sediment occurred in the flatter areas but no indication for fluid seepage was recognized during the dive. Post-deployment investigation of the high-resolution still images revealed two pictures showing accumulations of small white oblate objects occurring along the edge of an elongate rock outcrop (Fig. 6.8). Unfortunately, these objects were not in focus in either image, but one interpretation is that they are white clams in living position within the sediment. The size and geometry of the objects support this interpretation, as does their location, being right in the center of the water column anomaly. If this is correct, this finding might indicate active fluid flow in the sediments.

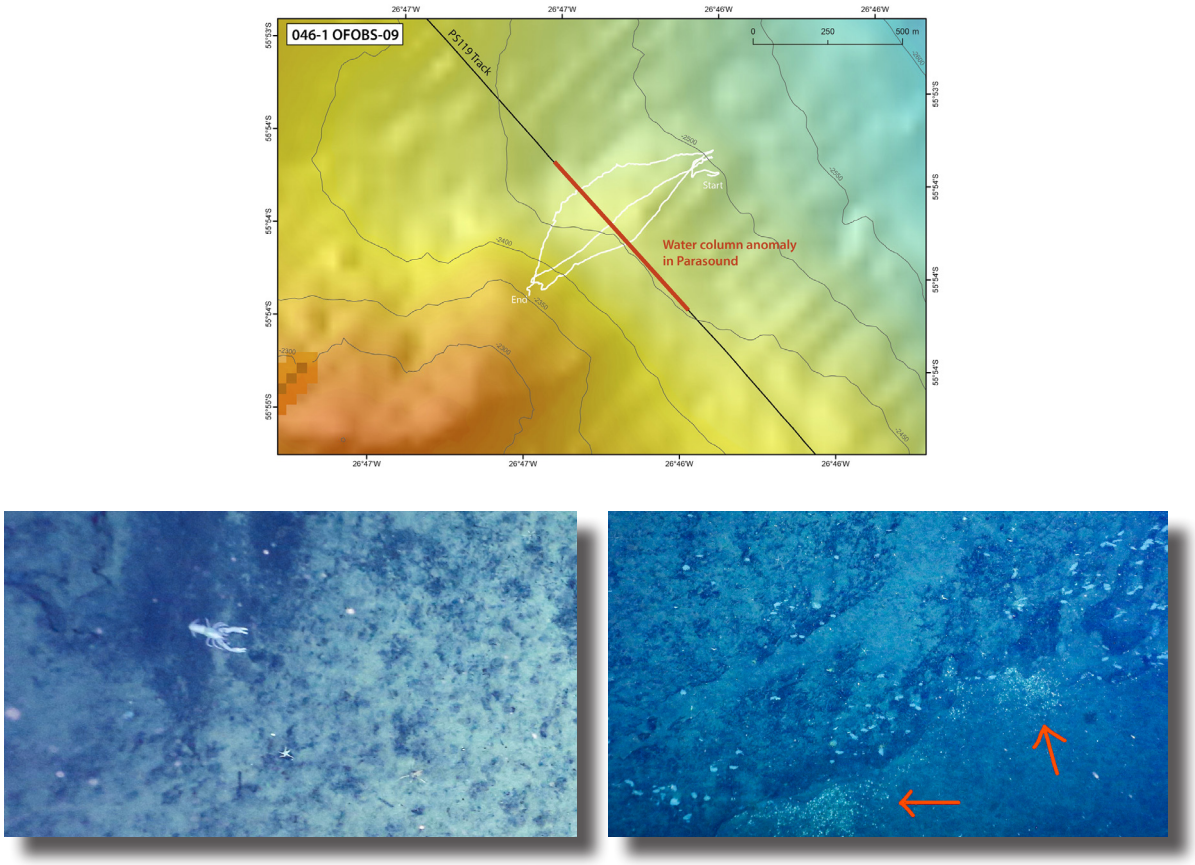

Fig. 6.8: Upper: Bathymetric map of the surveyed area during OFOBS-9. Lower left: one of five white lobsters were seen in the area surveyed. Lower right: image taken when passing close to the most central points of the echogram anomaly showing a ridge made up of dark rock and accumulations of small white objects (red arrows), which could be clams in living position in the sediment

OFOBS-cancelled

Station: PS119_049-1

Location: E2 (South)

Objective: Micro-bathymetry mapping of the known vent area

This deployment started as usual with a deck dry test, which this time failed completely as the signal was not received through the fibre optical cable. After testing and checking for about 1 hour, it turned out a new termination was needed. The deployment had to be postponed for several days.

OFOBS-10

Station: PS119_056-1

Location: E2 (South)

Objective: Micro-bathymetry mapping of the known vent area

As several NOC ISIS-ROV dives were conducted in the vent area in E2 South, a great micro-bathymetry map has been acquired. Obviously, the area has changed drastically during the

past about 10 years with respect to the presence or absence of biomasses but also with focus to hydrothermal activities. For that reason, the last OFOBS dive was dedicated to re-survey the area. The newly terminated fibre optic cable was tested successfully and technical performance of the OFOBS was good after a restart of the system at the beginning of the mapping at 40 m altitude. Mapping was conducted closer to the seafloor, at around 20 m above seafloor, allowing for seafloor imaging several times during this deployment. Vent structures became visible occasionally (Fig. 6.9), as well as areas covered by pillow lavas and, at the end of the deployment as expected by ship's bathymetry, a steep but surprisingly vertical and unruffled wall at the western side of the ridge axis (Fig. 6.9).

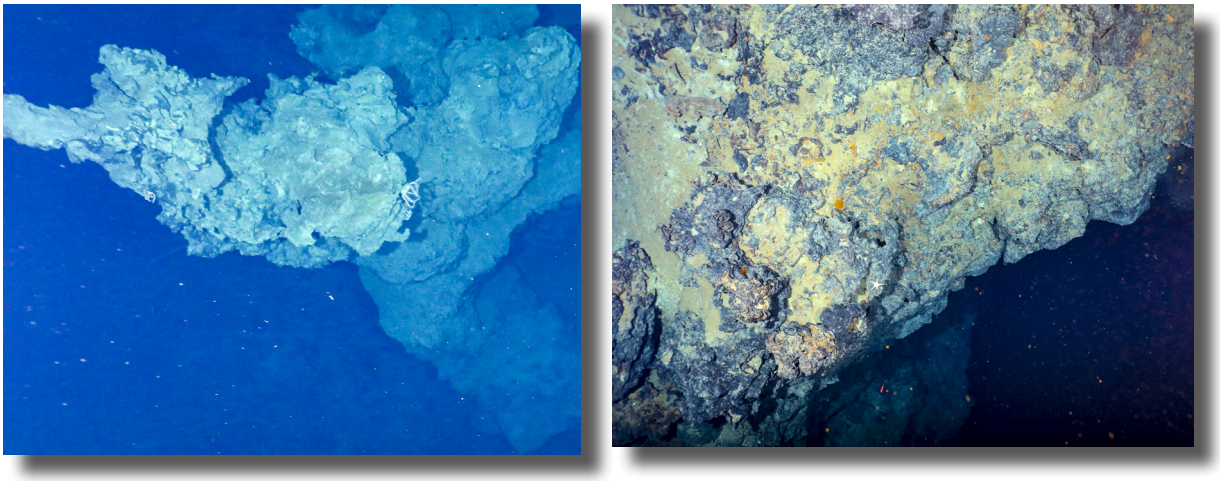

Fig. 6.9: Left: Inactive chimney with brisingid starfish. Right: Top of wall of ridge axis

Data management

OFOBS data sets will be under moratorium for 36 months for scientific purposes. Meanwhile the data, including images, videos and hydroacoustic recordings will be transferred and stored in the World Data Center PANGAEA Data Publisher for Earth & Environmental Science (www.pangaea.de) with a secured access. A DOI will be given for each dive data set and is therefore citable.

References

Amon DJ, Glover AG, Wiklund H, Marsh L, Linse K, Rogers AD, Copley JT (2013) The discovery of a natural whale fall in the Antarctic deep sea, Deep Sea Research Part II: Topical Studies in Oceanography, 92, 87-96, doi.org/10.1016/j.dsr2.2013.01.028.

Purser A, Marcon Y, Dreutter S, Hoge U, Sablotny B, Hehemann L, Lemburg J, Dorschel B, Biebow H, Boetius A (2019) Ocean Floor Observation and Bathymetry System (OFOBS): A New Towed Camera/Sonar System for Deep-Sea Habitat Surveys. IEEE Journal of Oceanic Engineering 44, 87-99.

7. REMOTELY OPERATED VEHICLE (ROV) MARUM QUEST 4000M

Grant-No AWI_PS119_00

7.1. Technical description and performance during PS119

Volker Ratmeyer, Frauke Ahrlich, Hauke Büttner, Philipp Koschinsky, Tom Leymann, Christian Reuter, Michael Reuter, Tobias Schade, Marcel Schröder

MARUM, Bremen

Objectives

The scientific deepwater ROV (remotely operated vehicle) “MARUM QUEST 4000m” was used aboard *Polarstern* during PS119. The system is hosted at and operated by MARUM, Center for Marine Environmental Sciences at the University of Bremen, Germany. The QUEST ROV is based on a former commercially available 4,000 m rated deepwater robotic vehicle designed and built by Schilling Robotics, Davis, USA. Since installation at MARUM in May 2003, it was set up as a mobile system specifically adapted to the requirements of scientific work aboard marine research vessels for worldwide operation. Today, QUEST has a total record of 450 dives during 38 expeditions, including this cruise.

During PS119, QUEST performed 7 dives to depths between approx. 1,700 m and 2,700 m. Dive tasks included rock and fluid sampling, biological sampling, high quality photographic and HDTV video documentation, optical 3D structure reconstruction and online *in-situ* measurements of fluid temperatures around hydrothermal vents. QUEST was operated by a team of 9 pilots/technicians on a 12-hour basis. Only few weather windows allowed diving, mainly due to high swell and waves almost during the entire expedition. When diving was possible, close cooperation between ROV team and ship’s crew through all departments allowed a safe and routinely performed handling especially during deployment and recovery in remaining high swell, as well as precise navigation, underwater positioning and an always clear and friendly communication prior and during dives.

The expected rough weather conditions in the southern ocean at this time of year required an extensive preparation of the deck setup for the entire ROV system, which was discussed and planned prior to the cruise almost one year in advance in Bremerhaven in close cooperation between MARUM, the vessel’s crew, the shipping company Laeisz, the Lloyd wharf and AWI. During mobilization in Punta Arenas a sheltered parking and maintenance “hangar” could be created underneath the helideck, containing a simple rail system to pull the ROV into safe position after each dive. Towards the aft, a large reinforced curtain was mounted underneath a special designed protector shield which guided the umbilical during deployment and recovery. Towards the side a stack of containers provided shelter. The control van with the power conditioning compartment was safely positioned in 2nd level, being accessible safely over a specially designed stairway / platform array. During mobilization in Punta Arenas, all planned work could be finished within 5 days with extra support from Laeisz / Lloyd and the ship’s crew. During the expedition the setup proved to be functional and provided substantial shelter for preparation and maintenance of the ROV in strong weather conditions.

Fig. 7.1: ROV QUEST installation with rails, hangar under helideck, protector shield. Reinforced curtain not mounted. Winch and LARS not visible.

QUEST System description

The total QUEST system weighs about 45 tons (including the vehicle, control van, workshop van, electrical winch, 5,000 m umbilical, Launch and Recovery System, and transportation vans) and can be transported in four standard ISO 20 foot vans. Using a MacArtney Cormac electric storage winch to manage the 5,000 m of 17.6 mm NSW umbilical, no hydraulic connections are necessary to host the entire handling system. For installation on *Polarstern*, the launch and recovery frame (LARS) has to be mounted on a special traversal adapter structure in the A-Frame, providing mechanical mounts to host LARS and umbilical block, as well as an external hydraulic lift winch assembly.

The QUEST uses a Doppler velocity log (DVL, 1200 kHz) to perform Stationkeep, Displacement, and other auto control functions. The combination of 60-kW propulsion power with DVL-based auto control functions provides exceptional positioning capabilities at depth. Designed and operated as a free-flying vehicle, QUEST system exerts such precise control over the electric propulsion system that the vehicle could maintain relative positioning hold within decimeters. Absolute GPS-based positioning is carried out using the shipboard IXBLUE Posidonia USBL positioning system.

The QUEST control system provides transparent access to all RS-232, network data and video channels. The scientific data system used at MARUM feeds all ROV- and ship-based science and logging channels into a real-time database system (DSHIP-ROV), a version of the database software commonly used aboard the German research vessels. During operation, data such as the navigation, CTD and high temperature data, sonar screen, and underwater video including 3 HDTV feeds are distributed to the vessels winch control room and ships TV system (tiled pilot video screen only). Due to the limited space in the Control Van, the winch control room was setup to allow scientists to take part in the dive with access to all images and data, including a QGIS client and acoustic intercom to communicate with the 2 scientists and pilots inside the Control Van, as well as with the remote scientists in Bremen in real-time.

Work at sea

Scientific payloads

During PS119, the following scientific equipment was used onboard MARUM QUEST:

- ROV based standard tools, installed on vehicle:
- 2 hydraulic manipulators for sampling and experiment handling
- 2 hydraulic drawers for probe and sample storage
- toolskid center section setup for vertical mapping with cameras and lights
- ROV starboard-side basket frame for rock and fluid sampling
- high temperature probe “T-Lance” with logger and online data display
- various nets and shovels with T-handles
- up to 12 push cores

PS119 specific payloads, installed on vehicle:

- up to 4 “IGT” type gas tight fluid samplers with online temperature data display (up to 2 ICL data connection paddles were used)
- MAPR autonomous sensor loggers
- Biobox in drawer
- Gas Samplersww
- “T-Stick” autonomous sediment temperature probe

Table 7.1: Positions and dive times obtained during PS119

DIVE LOG Summary: **PS119** Dates/Times UTC								
No.	**Dive No.**	**Date**	**Site Lat**	**Site Lon**	**Depth (m)**	**Time Launch**	**Bottom hours**	**Total Dive hours**
1	444	25.04.2019	56°05.28441‘	30°19.12189‘	2611	11:29	5,05	12,65
2	445	27.04.2019	56°04.62171‘	30°19.41366‘	2596	17:27	5,05	10,83
3	446	29.04.2019	56°05.27687‘	30°19.13552‘	2571	11:15	10,45	15,18
4	447	07.05.2019	59°41.67402‘	28°21.09645‘	1407	10:12	11,82	16,10
5	448	11.05.2019	59°42.02108‘	28°21.25022‘	1463	10:10	2,97	6,05
6	449	14.05.2019	59°40.56149‘	28°21.40589‘	1138	14:32	9,17	12,63
7	450	18.05.2019	56°05.27229‘	30°19.14507‘	2590	10:00	6,97	11,55
				Max. Dive depth (m):	**2596**		**46,42**	**72,35**

New developments used during PS119

To enhance the video imaging capabilities of QUEST and to be prepared for high quality documentary filming tasks required during PS119, a number of developments were undertaken and tested in Bremen prior to the cruise and were installed over the duration of the expedition onto the ROV. Among these the most important ones are two new ultra-low latency HDTV cameras, a new 4k tiling system for the projection display in the control van and streaming output, as well as a new stereo camera with corrected optics and a new still camera prototype (so far without corrected optics). The stereo camera was successfully tested during 3 dives, but due to limited time not used for scientific or documentary filming on the manipulator arm so far.

New MARUM developments, installed on vehicle during PS119

- Enhanced 4k video tiling, overlay and distribution system
- Integration of a professional digital 4K/HDTV recording unit
- 2 HDTV h.264 network cameras on upper and lower front pan tilt units
- Upgrade of ZEUS HDTV tilt mount with new pan function on starboard drawer
- New Still Camera 15 Megapixel on starboard drawer (prototype)

- 3D HDTV Stereo h.264 camera on T-handle for manipulator deployment (former cooperation with IFREMER, France / EUROFLEETS)
- Hydrophone with mp3 network audio stream and topside realtime frequency domain filtering and spectrogram display (prototype)

Telepresence video streaming and participation of land based scientist and the general public in ROV dives during PS119

Within a dedicated initiative ("Telepresence in the German marine science", started in May 2017 by MARUM and GEOMAR) to establish high bandwidth telepresence aboard the large German research vessels, two test phases were funded in 2018 and 2019 by the German Ministry of Research and Education (BMBF), including the installation of a large C-Band antenna aboard *Sonne* and offshore testing during 2 expeditions. To proof the concept of remote science participation, PS119 was chosen to host the previously tested technical setup for the first time in Germany within a real-world deepsea research application. A number of scientists at MARUM and MPI in Bremen pronounced their interest to take part remotely in the proposed dives during PS119. In addition, a variety of public events was prepared to take advantage of live video streaming from the deep seafloor in Antarctic waters, being the first setup of its kind.

To reach this goal, a bulk bandwidth of 5 Mbit/s ship-to-shore and 3 Mbit/s shore to ship was requested prior to the cruise, of which a 3 Mbit/s uplink upgrade was funded. Together with the 2 Mbit/s existing standard link between *Polarstern, Neumayer Station* and AWI, this resulted in 5Mbit/s during PS119. The downlink unfortunately could not be upgraded.

During extensive tests aboard the vessel in Bremerhaven prior to the cruise, in Bremen at the provider and at MARUM, we could establish a stable satellite link, a state of the art video streaming setup and a dedicated distribution server. A workflow was designed at MARUM including new encoding hardware (incl. a dedicated PC, HDMI/HD-SDI signal conversion, Haivision SRT based HEVC streaming encoder) and open source software (ffmpeg, nginx, Open Broadcast Studio, VLC, Next Cloud) packages to be setup in the vessel's winch control room after leaving Punta Arenas. For us it was important to keep the normal ships internet access fully functional without restrictions while performing a routine high quality video streaming service. This goal in mind, we could establish full HDTV 1080p30 streaming at a bulk bandwidth of 2.9 Mbit/s, leaving the original 2 Mbit/s ships link untouched. During the dives, online participation of scientists via the webbased DFNconf German science network (DFN) infrastructure could be established for audio communication with only 1.5-3 seconds delay. The 7-camera tiled underwater video pilot screen could be streamed routinely to MARUM and to the public in 1080p and 720p resolutions, respectively with latency between 5 and 20 seconds. File transfer of dozens of gigabytes could be transferred after selected dives to allow land based 3D reconstruction of *in situ* filmed smoker structures and be received back on the vessel on the next day. Dive plans, QGIS dive-projects, ROV and vessel navigation and dive data could be shared online prior and during the dives with the MARUM lab, which was setup for remote science participation prior to the cruise.

In Bremen, Wolfgang Bach (MARUM), Christian Borowski (MPI) and Yann Marcon (MARUM) were the scientists taking part at various times during the dives, providing critical decision support for fluid sampling, expert discussion and near realtime data processing (3D reconstruction).

Over the public internet, a maximum of 1540 client access connections was recorded on the MARUM based webserver which provided the public video stream. Although most replies from clients worldwide were very positive regarding stream quality, some replies showed broken links or streaming content errors on the web page during transmission. To overcome possible performance gaps of the used server system as a reason, installation of either a high capacity server or a rental of a dedicated commercial web-streaming service will be investigated for future applications.

During various dedicated live PR events located at different German museum institutions, a workshop at the federal ministry of education and research (Fona-Forum, BMBF) and a school project, realtime streaming and communication performance was very good and without errors, which allows us to confirm the proof of concept and technology. Finally, in the context of telepresence we want to pronounce that we are very grateful for the continuous and steady support and very close cooperation with the vessels electronics department, which was of critical importance to be able to run a successful and routine telepresence workflow during the entire cruise.

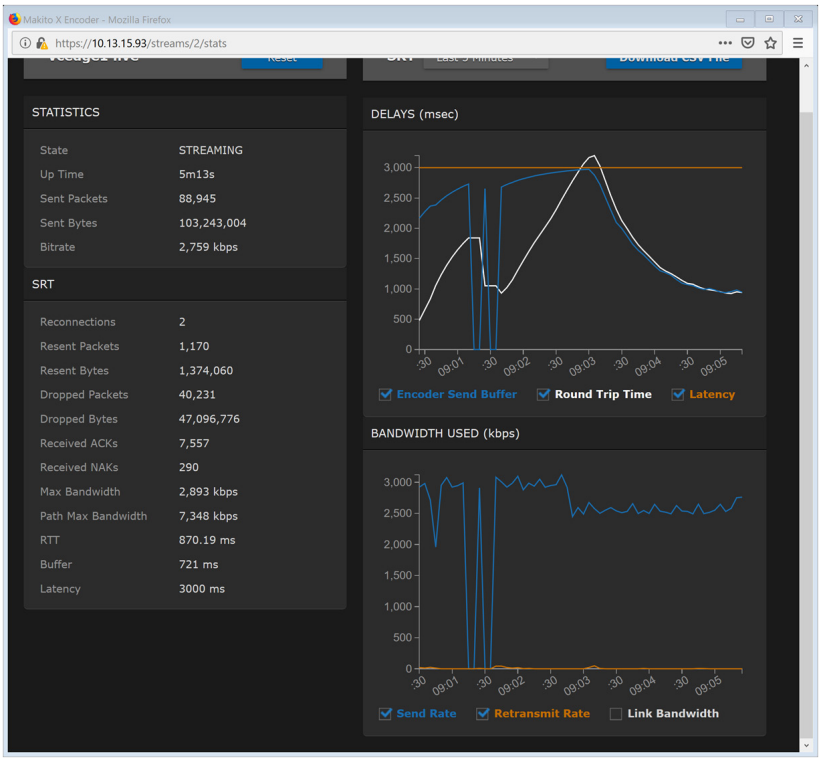

Fig. 7.2: Bandwidth statistics of outgoing stream SRT data of the Makito X encoder. In this screenshot, clearly visible is the limitation of a maximum bandwidth below 3 Mbit for a stable stream (after 09:03). Before, at 3 Mbit, the encoder send buffer reached the latency setting of 3 seconds, which resulted in transmission errors. A higher setting of the latency would allow higher bandwidth, but at the price of larger time delay. Since low latency transmission was an important goal, we kept latency setting at 3 secs max.

Data management

Post-cruise data archival will be hosted by the World Data Center PANGAEA Data Publisher for Earth & Environmental Science (www.pangaea.de), which is operated on a long-term base in cooperation by MARUM in Bremen and the AWI in Bremerhaven.

7.2 MARUM QUEST dive reports

Katrin Linse[1], Gerhard Bohrmann[2], Julia Sigwart[3], Anna Lichtschlag[4], Miriam Römer[2], Yoland Bosiger[5], Yiting Tseng[2], Paul Wintersteller[2], Crispin Little[6], Alexander Diehl[7], Marta Torres[8], Victoria Kürzinger[7], Martin Meschede[9], Thomas Pape[2], Maximilian Franke[10], Benedikt Geier[10], Sam Lewis Meyrick[5]

[1]BAS, Cambridge
[2]MARUM, Bremen
[3]QUB-QML, Portaferry
[4]NOC, Southampton
[5]BBC, Bristol
[6]SEE-UL, Leeds
[7]GeoB, Bremen
[8]CEOAS, Corvallis
[9]IGG-UG, Greifswald
[10]MPI, Bremen

Preliminary results

ROV Dive 444 (Station PS119_013_0)

Area:	East Scotia Ridge E2_South
Date:	Wednesday, April 24, 2019
Start bottom (UTC):	16:24
End bottom (UTC):	21:27
Bottom Time:	05:03
Start bottom (Lat/Long/Depth):	56°05.2844'S/30°19.1219'W/2611 m
End bottom (Lat/Long/Depth):	56°05.2804'S/30°19.1565'W/2579 m
Responsible scientist:	Katrin Linse

Original WP and depth based on ROV Isis USBL positions:

WP 1:	56° 05.316'S	30° 19.100'S	~2,619 m (Anemone Field)
WP 2:	56° 05.270'S	30° 19.148'S	~2,606 m (Dog's Head)
WP 3:	56° 05.350'S	30° 19.119'S	~2,646 m (Cindy's Castle)
WP 4:	56° 05.345'S	30° 19.088'S	~2,645 m (Crab City)
WP 5:	56° 05.281'S	30° 19.065'S	~2,612 m (Sepia)

Key results

The E2_South hydrothermal vent field, last mapped and visited by NERC ROV *Isis* during JC80 in 2012, was surveyed from its northern to southern edge to examine changes in hydrothermal activity and visually identify chimney structures. Key features visited were the black smokers "Dog's Head" and the diffuse flow areas "Anemone Field", "Cindy's Castle" and "Crab City" (Fig. 7.3). All five features were positively matched and significant changes were observed. The sites "Cindy's Castle" and "Crab City", previously hosting communities of *Gigantopelta chessoia* and *Kiwa tyleri* in visible diffuse flow and shimmering water localities, were barren and no or few living specimens were observed, suggesting a reduction of hydrothermal flow. The dense, wide spread populations of actinostolid anemones in "Anemone Field" have significantly reduced their range while *Kiwa* were still present on the basalts and in groups in the crack. This could also indicate a change in diffuse flow rate. "Dog's Head" is still smoking black and while some orifices appear to be at the same locations on the western side of the structure, a new black smoking orifice is active at the eastern side.

Technical description

Pre-dive the positions of the given waypoints (WP) did not match the structures on the micro-bathymetry map and we decided that not the map but the WP will be shifted. The initial WP based on ROV Isis USBL positions were shifted about 40 m to N near "Dog's Head" but almost

match “Cindy’s Castle”. During the dive visibility of the dive was impacted by the amount of black smoker originating particles in the water column. This hindered the spotting of white precipitates and bacterial mats on chimney structures to navigate from chimney to chimney. The ROV sonar was not working reliable and could not be used to spot chimney structures in the surrounding. We experienced problems with the ROV’s Doppler and USBL positioning system. The two systems did not only show their general drift, which can be minimized by Doppler resets, but also sudden jumps of the USBL position which out the ROV moving. This made position recognition in relation to the navigation map difficult.

Tab. 7.2: Samples and measurements

No	Instrument	UTC Start	UTC End	Position	Depth	Comment
13-1	Net-1	19:17	19:23	56°05.3514‘S 30°19.0975‘W	2,652 m	Collected 33x *Gigantopelta chessoia*, *Lepetodrilus* sp., 1x *Kiwa tyleri*

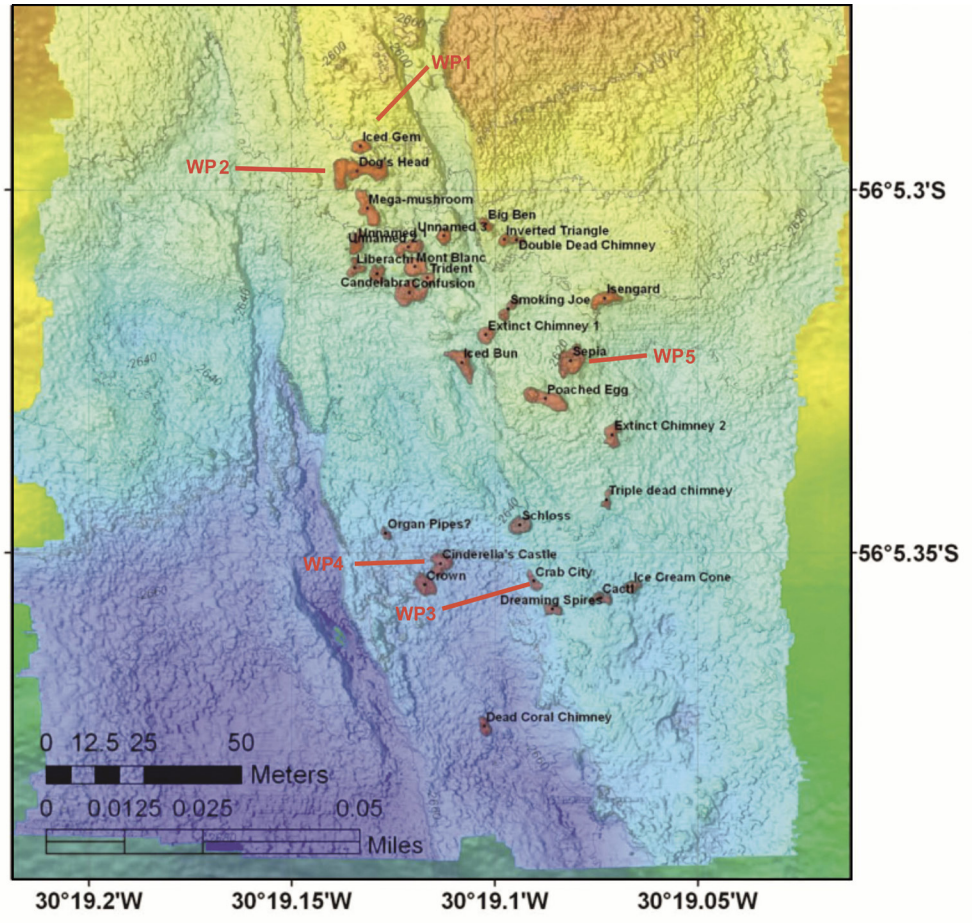

Fig. 7.3: Map of the area covered by QUEST Dive 444. Map taken from Tyler 2013, JC80 cruise report

Dive description

The dive was planned to start north of WP1, to the NE of the known black smoker “Dog’s Head”. On decent, about 200 m above the seafloor particles, including clearly visible flocculates, formed a dense, whitish-grey cloud in the water column, indicating the position of the neutrally buoyant plume. 40 m above the ground visibility dropped and particle density increased significantly. The ROV dropped next to a black smoking chimney which multiple overhanging balconies that looked unfamiliar. As the navigation map showed ROV QUEST about 40 m too far north of “Dog’s Head”, the ROV was first flown in a circle to recognize nearby structures, passing pillow basalts, before heading southwards towards the WP for “Dog’s Head” on the navigation map. QUEST was flying over hydrothermal active chimneys but none resembled the distinct “Dog’s head” (DH) structure (Fig. 7.4).

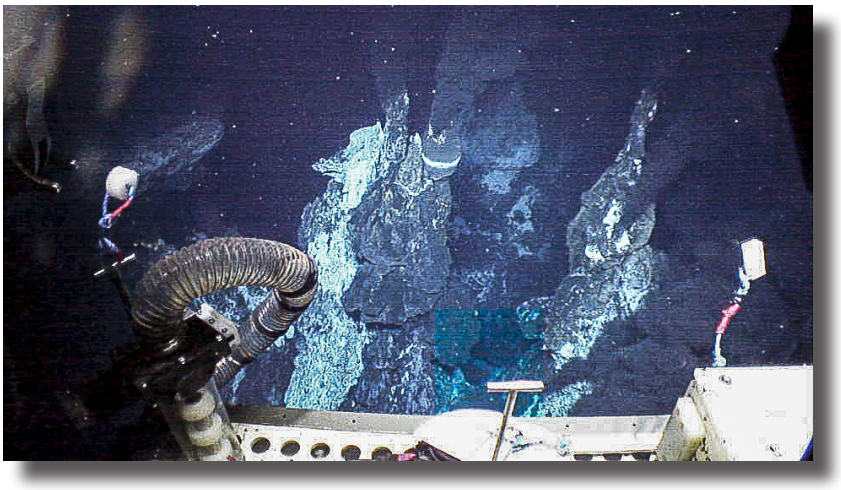

Fig.7.4: Dog’s Head in 2012; 2D © ChEsSO, NERC

After passing DH on the navigation map, the decision was taken to head eastwards to find the distinct scarp for navigational help and then to head south to WP3 (“Crab City”). On the eastward track, a white, flanging structure appeared that resembled the black smoking chimney “Sepia” (WP5) and was on closer view identified as “Sepia” but based on USBL positioning data the site reached is the feature identified as “Isengard” on maps from JC80. Based on this position, the dive continued southward and south-westward along the outer extend of the venting field until the scarp was encountered and the ROV dropped to the lower area. On passing a needle-like extinct chimney that reminded of “Dead Coral Chimney”, the ROV turned north, leaving the scarp on the starboard side /90° bearing, towards “Crab City”. A familiar looking basaltic formation was passed, which resembled “Crab City” but numbers of the yeti crab *Kiwa tyleri* had significantly dropped compared with 2012 (Figs. 7.5A and B). Behind this “Crab City”, a tall chimney structure raised up covered in whitish precipitate or bacterial mats, as well as yeti crabs and anemones. At this point the ROV’s sonar showed signals for chimneys to the east. Therefore, the ROV turned to explore these two structures as they were in the direction of “Cindy’s Castle” and “Crown”.

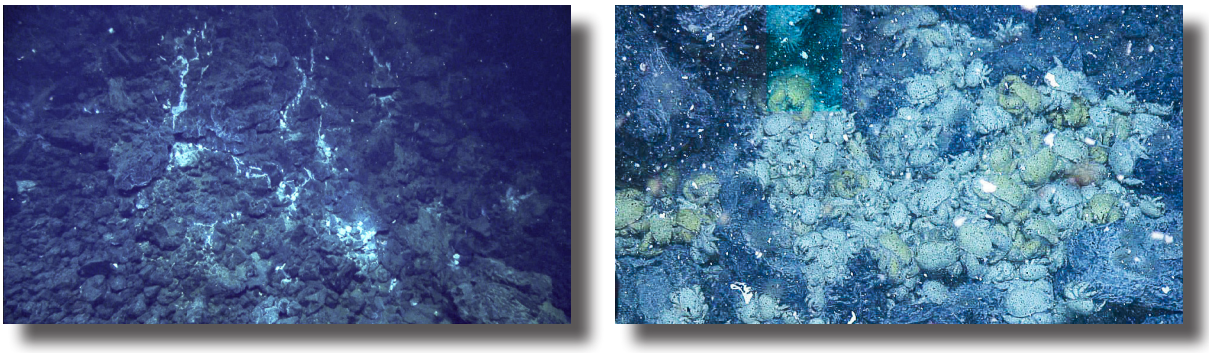

Fig. 7.5: A) "Crab City" in 2019; B) "Crab City" in 2012 © ChEsSO, NERC

WP4 "Cindy's Castle" was chosen for its distinct structure and its dense population of *Gigantopelta chessoia*, which had been observed in 2010 and 2012 (Fig. 7.6A). The structures detected in the sonar were positively identified as "Cindy's Castle" and "Crown", despite changes in their morphology. No bunches of *Gigantopelta chessoia* were observed on the turrets and balconies or even in the yard of "Cindy's Castle", only a few dead shells, while anemones present were in the same position as ones 7 years ago. After surrounding "Crown", these structures were left to head towards "Crab City", using a marker based on the original ROV Isis USBL position. On the way the tall chimney structure (an unnamed structure not mapped in JC80, approximately 15 m south of "Dreaming Spires") was passed again and a bunch of *Gigantopelta chessoia* with a few *Kiwa tyleri* seen on a balcony and sampled (Figs. 7.6A and B). After confirming that the earlier passed structure identified as "Crab City" matched the 2012 position for it, we headed NNW (315°) towards DH, using bearings taken from the ChEsSO JC80 map.

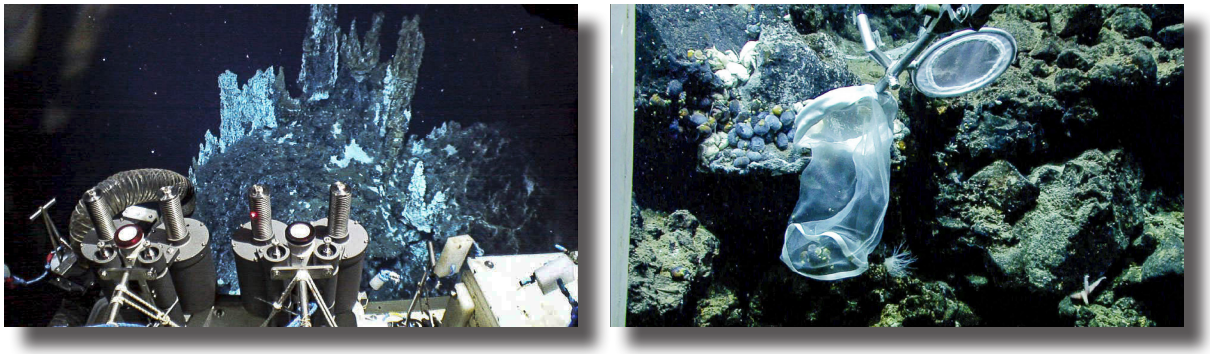

Fig.7.6: A) Chimney structure "Cindy's Castle" in 2010 © ChEsSO, NERC; B) Gigantopelta chessoia sampling

The ROV flew over unrecognized flange and chimney structures of which some were covered in white precipitates/bacterial mats or black smoking, that belong to the structure complex south of DH, including "Unnamed 3" of JC80 (at 19:52) and many previously unmapped structures. After passing this smoking area, QUEST flew over large sized pillow basalts with the occasional *Kiwa* but not covered in anemones. Initially an unstructured search was looking for DH until the decision to head north until an elongated pillow wall was hit. There the ROV was turned 180° and headed forward until reaching another wall. The ROV was turned again, 5 m set off to south and headed forward until a white flangy cone structure ("Iced Gem") appeared in the back of the Zeus camera. Heading towards it, a second white flangy cone appeared with black smoke behind. This setting resembled the western end of "Dog's Head"

and this prominent black smoker's identity was confirmed. Before rock and fluid sampling at DH could begin, problems with the ROV winch system ended the dive after almost 5 h bottom time and ROV QUEST was recovered back on deck after 12:30 h of operation.

ROV Dive 445 (Station PS119_017_0)

Area:	East Scotia Ridge E2, West (A. v. Humboldt field)
Date:	Saturday, April 27, 2019
Start bottom (UTC):	21:00
End bottom (UTC):	02:23, Sunday, April 28, 2019
Bottom Time:	05:03
Start bottom (Lat/Long/Depth):	56°04.6217'S/30°19.4137'W/2596 m
End bottom (Lat/Long/Depth):	56°04.6105'S/30°19.3704'W/2583 m
Responsible scientist:	Gerhard Bohrmann

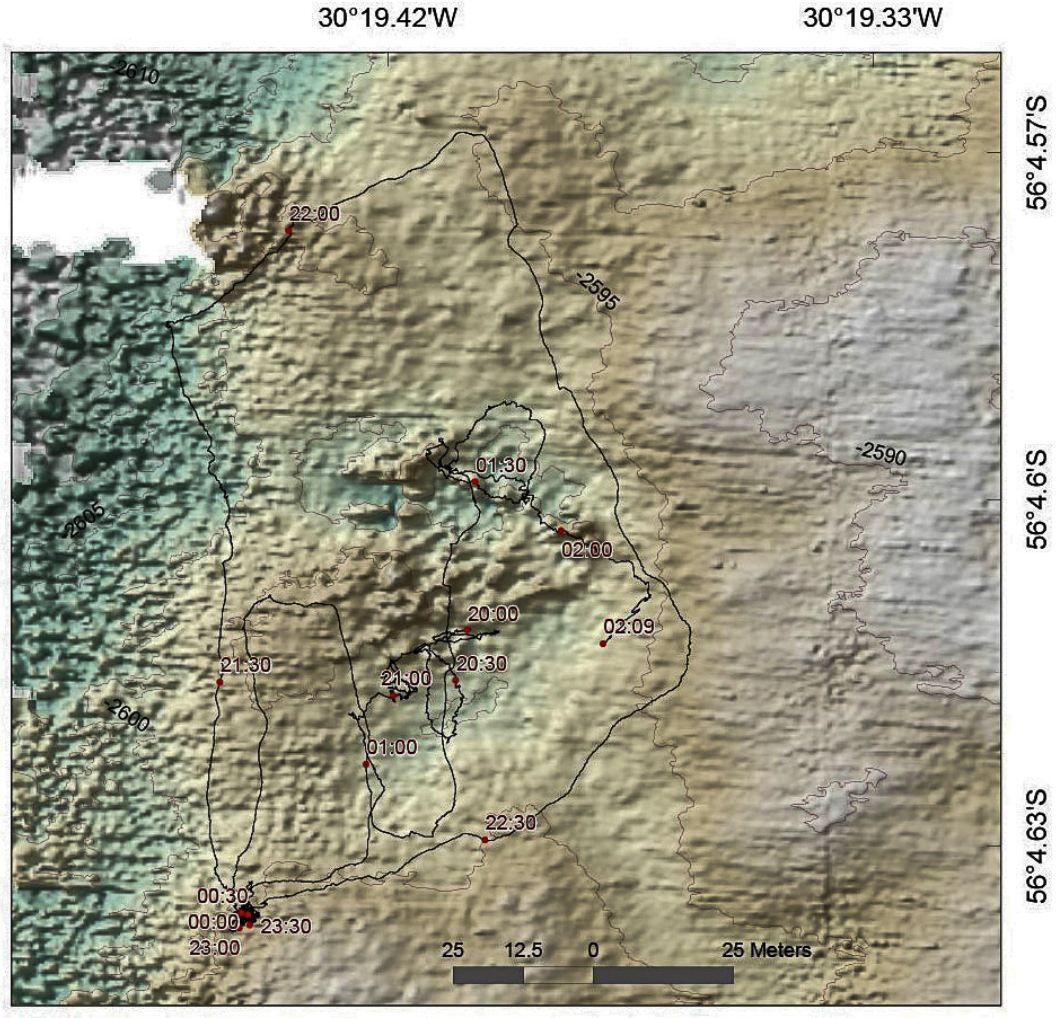

Fig. 7.7: Map of the area covered by QUEST ROV Dive 445

Key results

A new field (ca. 40 m in diameter) of low-temperature fluid outflow was discovered, containing many chimney structures in an area approximately 10 m deeper than the surrounding seafloor covered by black pillow basalt lava. Ca. 50 m southwest of the field an isolated fluid emission

site (30-53°C hot) was sampled. A sampled yellow precipitate from the outflow position was very friable and dominantly composed of amorphous silicate. The new field was named Alexander von Humboldt hydrothermal vent field.

Table 7.3: Samples and measurements during ROV dive 445

No	Instrument	UTC Start	Position	Depth m	Comment
17-1	Net	23:12	56°04.6430'S 30°19.4364'W	2591	Yellow chimney precipitate
17-2	IGT	23:42	56°04.6428'S 30°19.436'W	2591	IGT-1: 30°C
17-3	IGT	00:26	56°04.6105'S 30°19.4384'W	2591	IGT-3: 53°C

Dive description

ROV Dive 445 was planned in segment E2 of the East Scotia Ridge west of the area, where hydrothermal vent field have been documented. Several measurements in the water column e.g. CTD-Station (CTD-3; PS119_12-1) indicated hydrothermal activity at the bottom. Until this dive the area was unexplored. Beside the exploration of the area, precipitates and fluid samples were planned. The micro-bathymetry map (Fig. 7.7) derived from OFOBS deployment 3 (PS119_11-1) was not available during the dive. The map became available at the end of the cruise and the ROV dive track was plotted after the navigation correction. Some time marks and the location of sampling are shown (Fig. 7.7).

Fig. 7.8: Sediment-free pillow basalt

Fig. 7.9: Large single sponge attached to the magmatic rock at the seafloor.

ROV QUEST reached the seafloor at UTC 21:04. Well-developed pillow lava mounds were exposed at the seafloor during most of the dive time (Fig. 7.8). Single benthic organisms like sponges (Fig. 7.9) or corals are attached to the pillows. We dived 35 m in southern direction before we moved 20 m to the west. At 21:25 we already observed some yellowish precipitates. At 21:25 we explored the seafloor along a south/north transect until 21:52 and observed at 21:40 some chimney structures composed of dark brownish precipitates with some yellowish rims. The structures seemed not active, however, we have not taken a closer look, because of time constraints.

At 21:52 we changed then to a southwest/northeast direction until 22:12 and moved then in southeastern direction another 100 m (Fig. 7.7). The exploration showed only basaltic pillow lava at the seafloor, with more or less sediment in crotches between the pillows.

At 22:37 we reached a tubular pillow lava, which was split along the tube, and yellowish material was seen on the left side of the otherwise unweathered-looking pillow structure. A more detailed inspection showed an outflow of shimmering water from yellowish precipitates, which are covered by whitish flakes, probably representing microbial biomass (Fig. 7.10). At 23:12 we took a net-sample from this yellowish material which was relative friable. During the following fluid sampling by the IGT-sampler, we measured a temperature of ca. 30°C in the fluid outflow. We took several detailed images and recorded detail with the HD camera. A much stronger outflow of shimmering water was detected close-by and a second IGT-fluid sample was taken at that location (00:26). The measured temperature of ca. 53°C was some higher as at the previous outflow (Tab. 7.3).

Fig. 7.10: Fluid outflow at temperatures of 30°C measured by IGT sampler.

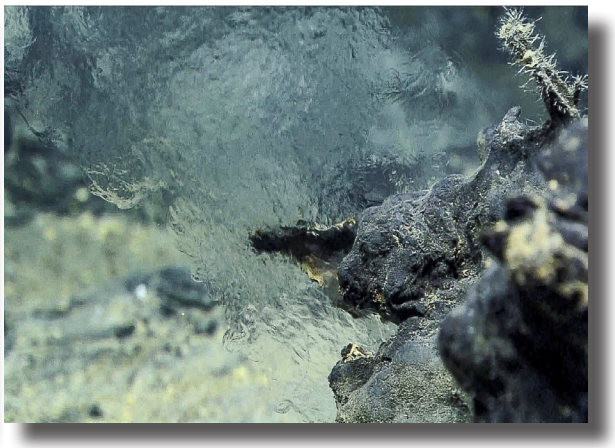

Fig. 7.11: Shimmering water flowing out in the neighborhood of volcanic rocks.

Further exploration of 50 m to the north, 15 m to the east and another 40 m to the south showed again the extensive coverage of the seafloor by pillow basalt. At 01:05 we started another track to the north and found a larger field of chimneys starting at 01:10 which continued until the end of the dive at 02:03 (Fig. 7.7). The field of chimneys is well outlined by the hilly micro-bathymetry, and has a diameter of ca. 40 m. No detailed examinations could be performed, however, based on the scattered distribution of the Hoff crabs, similar low-temperature outflows as measured before are expected in the area.

ROV Dive 446 (Station PS119_020-0)

Area:	East Scotia Ridge E2_South
Date:	Monday, April 29, 2019
Start bottom (UTC):	13:42
End bottom (UTC):	00:09 (Tuesday, April 30, 2019)
Bottom Time:	10:27
Start bottom (Lat/Long/Depth):	56°05.2769'S/30°19.1355'W/2571 m
End bottom (Lat/Long/Depth):	56°05.2769'S/30°19.1355'W/2571 m
Responsible scientist:	Julia Sigwart

Waypoints

WP1 (dropdown):	56° 05.316'S	30° 19.100'S	~2,619 m (Anemone Field)
WP 2:	56° 05.270'S	30° 19.148'S	~2,606 m (Dog's Head)
WP 3:	56° 05.347'S	30° 19.174'S	~2664 m (Confusion)
WP 4:	56° 05.300'S	30° 19.174'S	~2630 m (Mont Blanc)

Key results

This second dive on the E2_S hydrothermal vent field (last mapped and visited by NERC ROV *Isis* during JC80 in 2012) focused on surveying the ring of chimney structures in the northern part of the vent field.

Key features visited were the black smokers "Dog's Head" (also seen in Dive 444) the chimneys called "Schloss", and "Iced Bun" (Fig. 7.12). Faunal collections were made of all target species: *Gigantopelta*, *Kiwa*, and the vent peripheral taxa *Paulasterias* and *Cladorhiza*. Additional species were collected incidentally: sea spiders *Sericosura* spp., the gastropods *Provanna* sp. and *Lepetodrilus* sp. and a small hydrozoan *Candelabrum* living epibiotically on *Cladorhiza*. Temperature measurements in colonies of *Kiwa* and *Gigantopelta* confirmed visual observations of low temperature, diffuse flow environments. High temperature fluid samples were taken at two black smokers, "Iced Bun" and "Dog's Head" which will provide comparisons with earlier measurements of high temperature hydrothermal activity from 2012.

Technical description

The initial landing position in Anemone Field adjacent to Dog's Head was successfully found. Thereafter, issues with the Posidonia positioning system prevented the waypoints from being used during navigation on the seafloor; bathymetric map from JC80 was used to establish headings to attempt to follow the course set in the dive plan (Fig. 7.12).

Tab. 7. 4: Samples and measurements

No	Instrument	UTC Start	UTC End	Position	Depth m	Comment
20-1	Net 1	14:50	15:10	56°05.3279'S 30°19.1355'W	2641	Collected sponge *Cladorhiza* (n=1) and epibiotic *Candelabrum*
20-2	Net 2	15:34	15:59	56°05.3342'S 30°19.1026'W	2637	Collected *Kiwa* (n=3)
20-3	Temperature probe	16:13	16:23	56°05.3343'S 30°19.1024'W	2635	3.5-4.1°C at colony of *Gigantopelta*
20-4	Net 3	16:26	16:50	56°05.3325'S 30°19.1013'W	2635	Collected *Gigantopelta* (n=4) and epibiotic *Lepetodrilus* (n=5)
20-5	Net 4	17:45	17:51	56°05.3433'S 30°19.0849'W	2645	Collected dead *Kiwa*, pycnogonids (*Sericosura*, n=2) and sediment including *Provanna* (many)
20-6	Claw	17:52		56°05.3433'S 30°19.0837'W	2645	*Paulasterias* in biobox

No	Instrument	UTC Start	UTC End	Position	Depth m	Comment
20-7	Claw	19:26	19:28	56°05.3049‘S 30°19.1287‘W	2623	Rock sample 5R in box I
20-8	IGT	19:32	19:38	56°05.3050‘S 30°19.1287‘W	2618	Fluid sample 6F in IGT1
20-9	IGT	19:43	19:46	56°05.3047‘S 30°19.1292‘W	2618	Fluid sample 7F in IGT2
20-10	Temperature probe	19:54	19:58	56°05.3048‘S 30°19.1294‘W	2624	320°C in black smoker orifice
20-11	Scoop	20:35	20:44	56°05.3039’S 30°19.1267‘W	2624	Sediment sample 8R
20-12	Claw	21:08	21:11	56°05.3004‘S 30°19.1516‘W	2623	Rock sample 9R
20-13	IGT	23:09	23:11	56°05.2839‘S 30°19.1496‘W	2623	Fluid sample 10F in IGT3
20-14	IGT	23:25	23:27	56°05.2850‘S 30°19.1499‘W	2607	Fluid sample 11F in IGT4
20-15	Temperature probe	23:45		56°05.2864‘S 30°19.1487‘W	2583	343°C in black smoker orifice
20-16	Claw	23:55				Rock sample 12R

Dive description

The dive began at WP1, at Anemone Field to the North of Dog’s Head, and immediately progressed to WP2 Dog’s Head. Observations of this structure confirmed that (1) it is Dog’s Head as named in previous cruises (JC80 and earlier) and (2) it is the same structure observed at the start and the end of Dive 444. We examined the base of the structure looking for *Gigantopelta* colonies, observed several small groups but in positions that were not practical to collect by net.

Left Dog’s Head at *ca*. 14:27 UTC and moved in a heading approximately south over pillow basalt, lost bearings as positioning issues became apparent. Copious vent peripheral fauna including *Candelabrum* hydrozoans and *Cladorhiza* sponges (collected, Sample 1). At 15:31 arrived at a chimney structure identified as Schloss, with abundant very large *Kiwa* (Sample 2). The structure had a series of small pinnacle like pale chimneys colored white and yellow and copious diffuse flow (Fig. 7.13). We also collected part of a small colony of *Gigantopelta* and measured the temperature at the colony (Sample 3, Sample 4). At the same position the ROV CTD temperature showed 1.9°C. As the position did not allow collection of sufficient snails for sample target (n=20) the net was retained in the claw awaiting later sampling.

At 16:44 moving south-west to extinct chimney structures identified as Triple Dead Chimney (at 17:12) – this structure matched to the chimney seen in JC80 ISIS Dive 187 (Fig. 7.15). Continued west to next structure identified as Cacti. At this structure, stopped to collect *Paulasterias* where two seastars were observed feeding(?) on the remains of a large *Kiwa* (Fig. 7.14). The dead *Kiwa* and sediment were collected with the net also already containing *Gigatopelta* and the net secured (Sample 5) and one *Paulasterias* collected with the manipulator claw (Sample 6).

At 18:02 moved around Cacti to avoid umbilical entanglement, then (18:06) continued NNW toward Trident; did not find expected landmarks, as at the time we expected our position

to be much further north and attempted course correction more toward due North at 18:07. At this point, we were in a vent peripheral area with typical non-vent setting of pillow basalt with copious sediment between pillows and fauna including giant pycnogonid sea-spiders. Continued ENE at 18:28, then corrected course to return SW and came to Ice Cream Cone (18:34) slightly east of Cacti (18:43). Turned NW once again to attempt to follow planned dive path; we encountered a scarp structure at 18:53 and followed it N and encountered large chimneys at the top of the wall (19:00) with active black smoker identified as Iced Bun. Fluid and rock samples taken here (Samples 7-11). Maximum temperature recorded was 320 C. The first attempt to sample a piece of chimney (Sample 7) found very friable brittle rock. Second attempt to collect part of the chimney used the sediment scoop (Sample 11) to take fine black sediment from below the solid chimney orifice.

Leaving Iced Bun 20:48 at a heading of 315° toward Dog's Head. Several of the chimneys were observed to have yellow coloration in the sediment which could be barite as tentatively identified in diffuse flow area on Dive 445. A sample was taken for comparison (Sample 12).

Returned to Dog's Head at 21:36, and resumed attempt to find and collect larger colony of *Gigantopelta*. We successfully identified the face of Dog's Head that had a large *Gigantopelta* colony but found only small numbers of snails in inaccessible positions. Snail collection was aborted at 22:15 and the remaining dive time used to take fluid samples from black smoker orifices on Dog's Head (Samples 13-15) and a rock sample of the chimney (Sample 16). The maximum temperature recorded was 343°C.

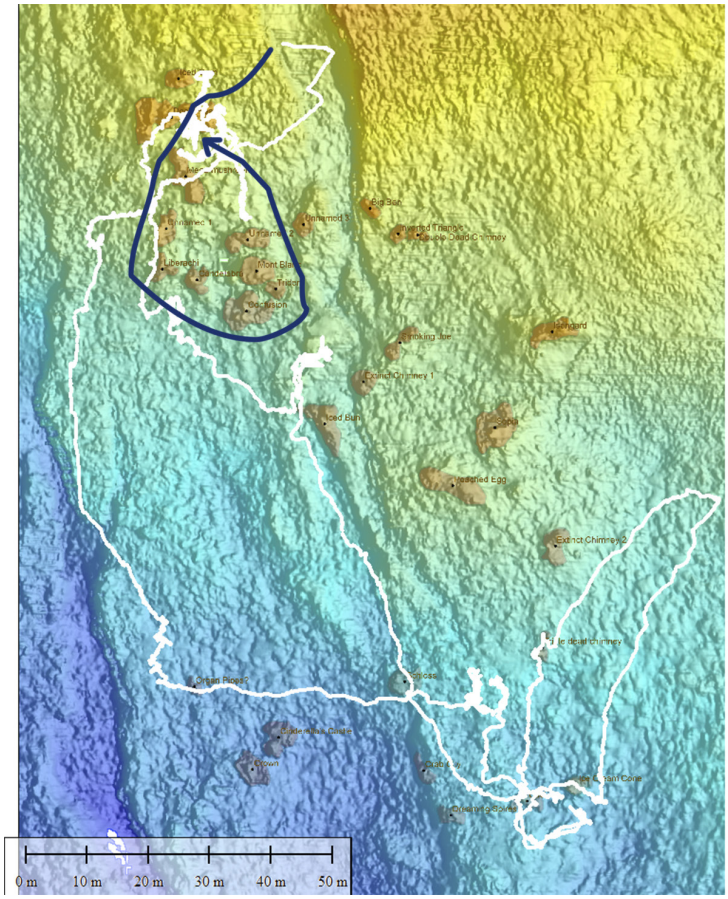

Fig. 7.12: Planned dive path, names and positions of major chimney structures. This does not correspond to the actual track from the dive.

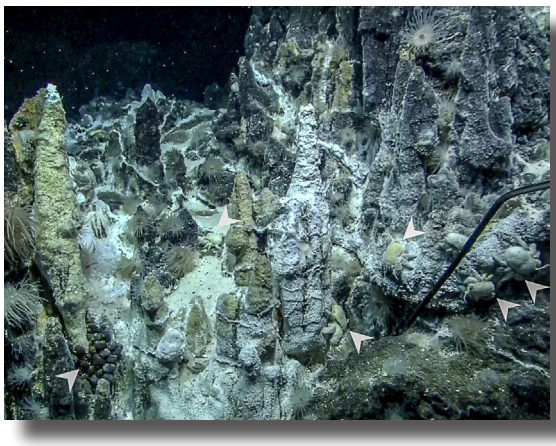

Fig. 7.13: Chimney structures at "Schloss". Arrowheads indicate Gigantopelta colony at lower left (Sample 4) and Kiwa crabs elsewhere. The temperature probe is visible in the foreground center right.

Fig. 7.14: Paulasterias tyleri feeding on the remains of Kiwa tyleri (claws visible at right). Two sea spiders (Sericosura spp.) are also visible on the sediment between and below the claws. (Sample 5 and Sample 6.)

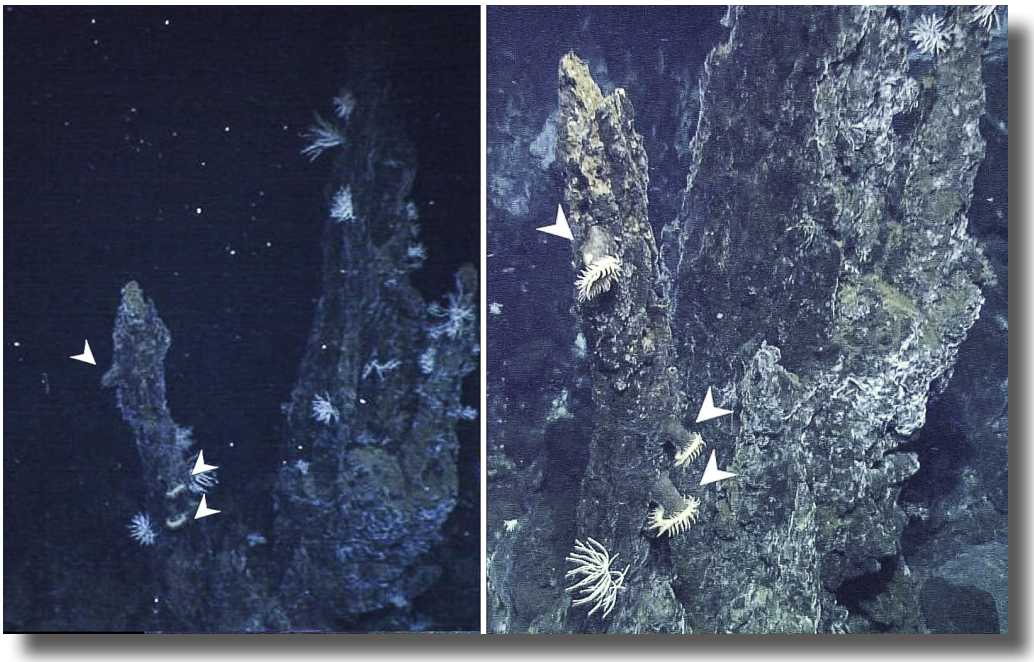

Fig. 7.15: Extinct chimney seen on JC80 (left, copyright NERC 2012) and on Dive 446 (right), identified as "Triple Dead Chimney" on maps from JC80. Arrowheads indicate anemones in same position 7 years later.

ROV Dive 447 (Station PS119_028_0)

Area:	Kemp Caldera
Date:	Tuesday, May 7, 2019
Start bottom (UTC):	12:40
End bottom (UTC):	00:29, Wednesday, May 8, 2019
Bottom Time:	11:49
Start bottom (Lat/Long/Depth):	59°41.6740'S/28°21.0965'W/1407 m
End bottom (Lat/Long/Depth):	59°41.6313'S/28°21.1271'W/1391 m
Responsible scientist:	Anna Lichtschlag

Waypoints: -> WPs are from previous cruise reports

WP1 (dropdown)	28°21.098'W	59°41.678'S	Great Wall
WP2	28°21.009'W	59°41.689'S	Toxic castle (PC position)
WP3	28°20.992'W	59°41.690'S	Winter Palace (PC)
WP4	28°21.692'W	59°41.588'S	Exploration WP4

Alternative waypoints from the high-resolution map provided by NOC

WP1.1	28°21.083'W	59°41.680'S	Great Wall
WP2.2	28°21.012'W	59°41.687'S	Toxic castle
WP3.3	28°20.955'W	59°41.697'S	Winter Palace

Key results

The ROV Dive 447 (PS119_Station 28) was dedicated to geological and geochemical sampling and the exploration of an unknown area in the Kemp caldera inner cone. During the dive we achieved the sampling of hydrothermal rocks, the collection of push cores and the sampling of hydrothermal fluids at the Kemp features "Great Wall", "Toxic Castle" and "Winter Palace". The final part of the dive was dedicated to the exploration of the area north of this very active zone and we opportunistically sampled living clams from a field that we discovered during the transit from "Winter Palace" to the north.

Technical description

Due to the drift of the ship during the ROV deployment, we started the dive about 700 m north of the first way point, reaching the target by flying about 200 m above the ground. During the dive we didn't experience any of the positioning problems as during the dives at E2. During the last part of the dive the manipulator arm was not always responding correctly; however, this did not interfere with any sampling activities. Also, there was an iceberg in the vicinity of the ship (about 2 miles away) and we kept an eye on the distance of the ROV and the ship to the iceberg.

Table 7.5: Samples and measurements

No	Instrument	UTC Start	UTC End	Latitude S	Longitude W	Depth	Comment
28-1	PC-9	13:36	13:54	59°41.67881'	28°21.09335'	1418.2	< 1/4 full
28-2	PC-10	13:44	13:51	59°41.67893'	28°21.09288'	1418.5	> 1/2 full

No	Instrument	UTC Start	UTC End	Latitude S	Longitude W	Depth	Comment
28-3	T-Stick	14:00	14:09	59°41.67912‘	28°21.09214‘	1418.1	5.75 °C; 1.75 °C background
28-4	PC-11	14:16	14:25	59°41.67841‘	28°21.09175‘	1418	1/3 full
28-5	Claw	14:38	14:40	59°41.67919‘	28°21.09273‘	1418.6	basalt GW into „I“
28-6	Claw	14:53	14:55	59°41.67806‘	28°21.09526‘	1416.7	great wall rock into „I“ + „K“
28-7	Claw	15:02	15:05	59°41.67830‘	28°21.09610‘	1416.3	sulfur „I“
28-8	IGT-1	15:20	15:29	59°41.67685‘	28°21.09480‘	1419.5	62.95 °C; 0.1 °C ambient
28-9	PC-1	16:34	16:35	59°41.68994‘	28°21.00788‘	1424.1	< 1/2 full
28-10	PC-2	16:37	16:37	59°41.68983‘	28°21.00800‘	1424.2	~ 1/3 full (very dusty)
28-11	Claw	16:44	16:47	59°41.68990‘	28°21.00850‘	1422.9	black chimney into „H“
28-12	PC-3	17:38	17:39	59°41.68568‘	28°21.01370‘	1422.7	sediments in front of a small mound
28-13	PC-4	17:40	17:42	59°41.68532‘	28°21.01488‘	1423.5	next to PC-3 (right hand side)
28-14	PC-12	17:43	17:44	59°41.68498‘	28°21.01586‘	1422.1	next to PC-4 (right hand side)
28-15	T-Stick	17:50	17:51	59°41.68517‘	28°21.01543‘	1422.6	55.4 °C
28-16	IGT-3	18:47	18:48	59°41.68582‘	28°21.01379‘	1422.7	230 °C
28-17	IGT-4	19:02	19:04	59°41.68546‘	28°21.01492‘	1422.8	190 °C
28-18	Blue + red handle scoop	19:50	19:54	59°41.68508‘	28°21.01406‘	1423.1	scoop of sulphur + dark minerals
28-19	PC-5	08:27	21:29	59°41.69247‘	28°20.98073‘	1426.7	probably only partly recovered, most red fell out
28-20	PC-6	21:32	21:33	59°41.69235‘	28°20.98004‘	1426.7	most sediment fell out
28-21	T-Stick	21:42	21:43	59°41.69233‘	28°20.98155‘	1426.7	11-6 °C
28-22	T-Stick	21:44	21:45	59°41.69227‘	28°20.98105‘	1426.7	6-1 °C
28-23	T-Stick	21:52	21:54	59°41.69210‘	28°20.98219‘	1425.6	TS: 100 °C
28-24	T-Stick	22:04	22:06	59°41.69142‘	28°20.99475‘	1424.6	TS: ~ 105 °C
28-25	Net blue	22:59	23:25	59°41.66439‘	28°21.05474‘	1419.6	taking living clams
28-26	T-Stick	23:28	23:36	59°41.66450‘	28°21.05500‘	1419.6	temperature in clam field 4.2 °C

Dive description

During the descent, turbid water was already visible, and was constantly present during

the descent to the seafloor. QUEST arrived at the seafloor in sight of the Great Wall (i.e. an approximately 1 m high wall-like structure formed of brittle, bright yellow and white sulphur where fluids are precipitating along a seafloor fissure in the basalt and can be followed for at least 10s of meters along the seafloor). The Great Wall itself had areas that were covered with limpets and anemones attached to the blocks of basalt lying on the seafloor next to the Great Wall fissure.

The first task of the dive was to sample at Great Wall (WP1, Fig. 7.16). Push cores were taken approximately 2 m away from it, where the sediment was covered with a white (unidentified) material (Fig. 7.16). As the sediments here were not well consolidated, several attempts had to be made to recover three intact sediment cores (PC-9, -10, -11, up to 22 cm length). Sediments recovered from here had a distinctive layering with a white layer in between 2 black layers. The temperature within the sediment was about 4 °C higher than the bottom water temperature. Next, a piece of basalt was broken off from a large basalt block next to the push core location. From the Great Wall itself, we sampled pieces of older material (grey) and fresh precipitates (shiny white) close to where diffuse fluids (shimmering water) were flowing out of the Great Wall structure. One of the more diffuse fluid outflows were sampled with an IGT sampler and the ROV left for the next target (WP2).

At the next target, “Toxic Castle” (WP2), many very active smokers were present and we discovered a flange (Fig. 7.16), from below which white smoke was rising and that had black small chimneys growing in its vicinity. PCs (no 1 and 2) were sampled on the slope of this complex. Fluid sampling from the flange was attempted, but it was aborted as it was too difficult to hold the ROV motionless in the water column. Hence we sampled one of the black chimney structures and moved about 10 m to the west, where we had previously seen a very active white smoker. Here we sampled 3 more PC cores (nos. 3, 4, 12) that recovered up to 18 cm sediment. The temperature of the sediment measured with the T-lance was up to 55 °C in ca 20 cm sediment depth. Unfortunately, the outflow of the big white smoker was again not in reach of the ROV manipulator arm, hence the same fluids were sampled twice with the ITG samplers from smaller smokers in the close by vicinity (Fig. 7.16). At the same spot we also found liquid sulfur flowing out of the rock, forming droplets and changing colour from red to yellow while cooling down (Fig. 7.16). As the rock was very crumbly when trying to sample with the manipulator arm, pieces of rocks, including some sulfur droplets, were scooped up with the sediment scoop.

The next way point (Winter Palace, WP3) was more difficult to locate. The terrain was very rough with ridges and troughs. Some dead shrimp and a dead fish was discovered in the troughs. Push coring was attempted in one of the troughs and the resultant hole in the ground showed black sediments (and a living polychaete). Here, and also in the next trough, pushcoring was not successful as the sediment was too unconsolidated for sampling. Another IGT sampling was tried at Winter Palace as well, but aborted.

Afterwards we moved towards the northwest (WP4) to reach the area that had not yet been surveyed by previous expeditions. When crossing a sediment patch with living clams, as visible by the siphons sticking out of the sediment (Fig. 7.16), we used a small net to collect living specimens. Afterwards we continued to the northwest, discovering additional stretches of the Great Wall. An increasing amount of sponges were present after Great Wall ended. Here, the terrain was rougher, consisting of black basalts. At 00:16 the dive stopped as the weather conditions were getting worse.

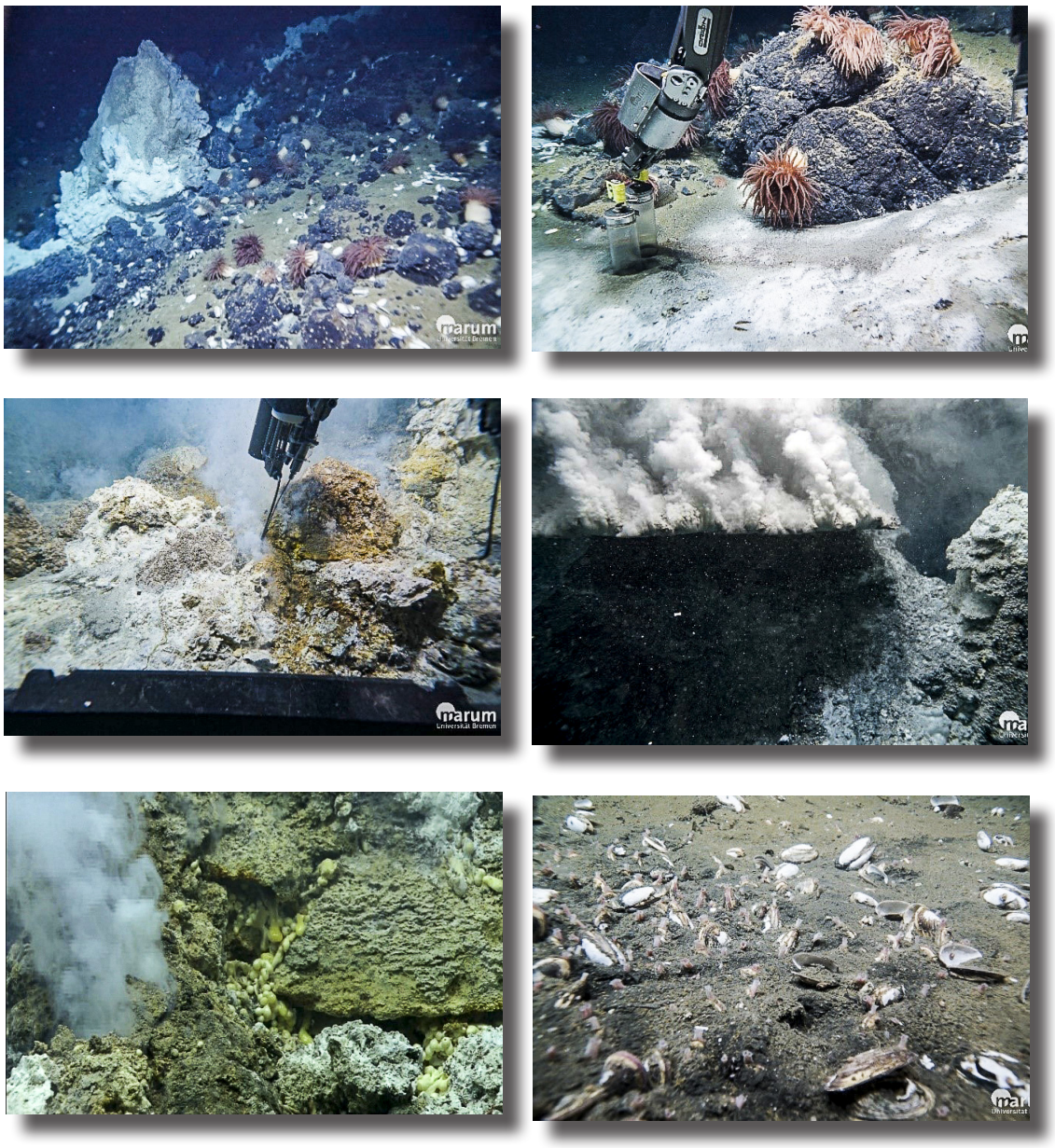

Fig. 7.16: Upper left: Great Wall with basalt blocks on which anemones lived (red); Upper right: push coring on a sediment patch close to Great Wall; Middle left: fluid sampling with the IGT sampler at Toxic Castle; Middle right: flange expelling white smoke at Toxic Castle; Lower left: newly formed sulphur droplets flowing out of a crack at Toxic castle; lower right: living clams on a sediment patch North of Great Wall.

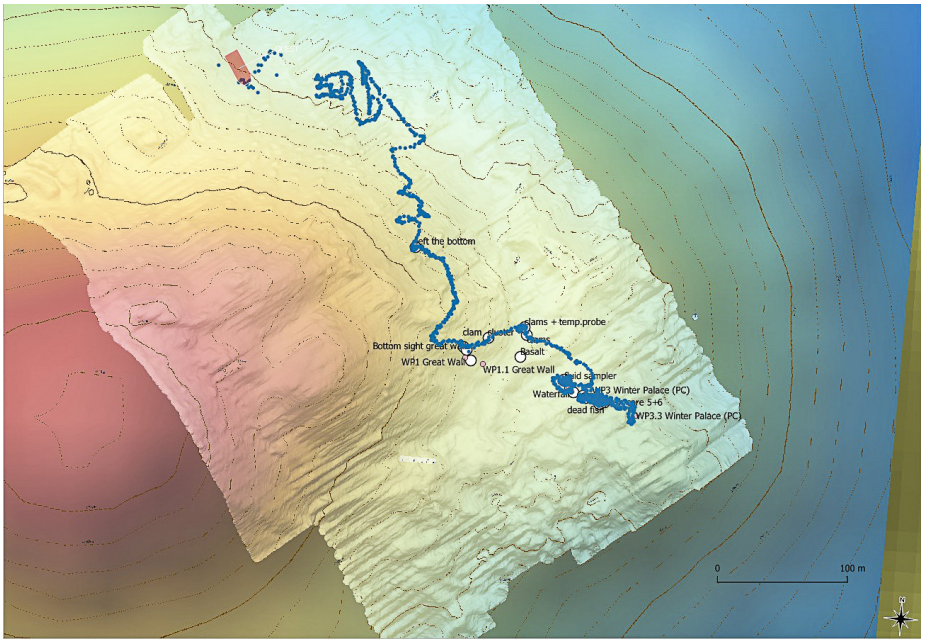

Fig. 7.17: Dive Track from Dive 447 at Kemp Caldera

ROV Dive 448 (Station PS119_033_0)

Area:	Kemp Caldera, resurgent cone
Date:	Saturday, May 11, 2019
Start bottom (UTC):	12:02
End bottom (UTC):	15:00
Bottom Time:	02:58
Start bottom (Lat/Long/Depth):	59°42.0211'S/28°21.2502'W/1463 m
End bottom (Lat/Long/Depth):	59°41.6919'S/28°20.9804'W/1425 m
Responsible scientist:	Katrin Linse

Waypoints

WP 1:	59°42.024'S	28°21.233'W ~1487 m, Clam Road
WP 2:	59°41.664'S	28°21.054'W ~1420 m, Clams Dive 447
WP 3:	59°41.594'S	28°21.005'W ~1453 m, OFOBS4 sonar anomaly 1
WP 4:	59°41.596'S	28°21.032'W ~1450 m, OFOBS4 sonar anomaly 2
WP 5:	59°41.593'S	28°21.057'W ~1442 m, OFOBS4 sonar anomaly 3

Key results

Arriving at location WP1 "Clam Road", no living vesicomyid clams were encountered, only a low number of dead shells were seen. After a brief search track up the mount and back down to almost WP1, the search was called off and the dive progressed towards WP2. On the top of the mount, a shimmering water and bacterial mat field was discovered next to an extinct chimney. Just before WP2, in a field of clams living burrowed in sediment, two pushcores were successfully taken before clams were collected with a large net and placed into the biobox. Time constraints permitted T-lance measurements at the clam site as well as fluid sampling at white smokers or the investigation of the OFOBS4 sonar anomalies.

Technical description

The decent through the water column was uneventful and MARUM QUEST dropped down directly on the WP. Initially a white line of dead clamshells was investigated to find living ones between them. The dive progressed in an uphill search pattern of horizontal lines before stepping up at the edge of the line of view. After 1 hour, the search was abandoned and MARUM QUEST flew in ~20 m above ground from WP1 to WP2.

Tab. 7.6: Samples and measurements

No	Instrument	UTC Start	UTC End	Position	Depth m	Comment
33-1	PC3	14:04	14:09	59°41.6683'S 28°21.0547'W	1427	~3/4 full push core
33-2	PC6	14:06	14:07	59°41.6685'S 28°21.0526'W	1427	~1/2 full push core
33-3 Net, red, large		14:14	14:32	59°41.6685'S 28°21.0541'W	1427	4x large net scooped through clam field. Net ~2/3 full of sediment, almost too large to be fitted into biobox.
33-4	Temperature probe	14:37		59°41.6726'S/ 28°21.0446'W	1423	TL 0.3°C

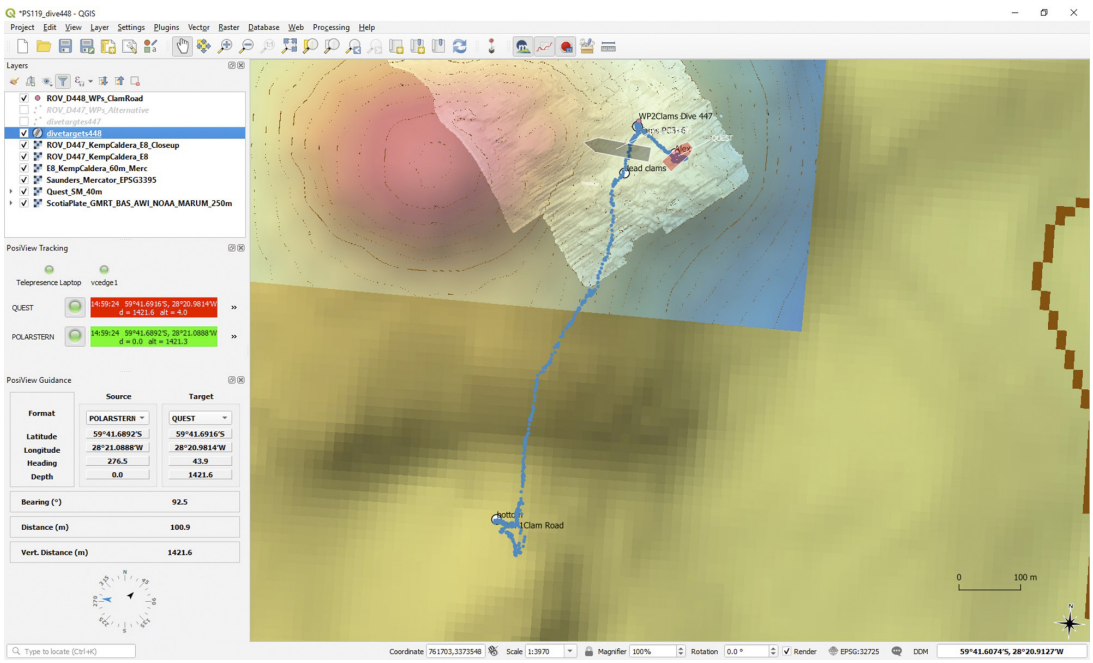

Fig. 7.18: Map of the area covered by QUEST Dive 448. Screen shot of navigation computer

Dive description

MARUM QUEST entered the water at 10:48 UTC to start dive 448. After 78 min descending through the water column, passing naturally bouyant plumes around 1100 m and 1300 m depth, the seafloor was visible in 1475 m depth. Occasional empty vescomyid clam shells were seen on the seafloor (Fig. 7.19A) and along an uphill running line. Initially Quest followed this clam line uphill until it faded out. The density of clam shells was not comparable to the number of clams encounter on Calm Road in 2010 (Fig. 7.19B). At that point a horizontal line survey was followed, stepping up by 3 m and following the line until the top of Ash Mount was reached.

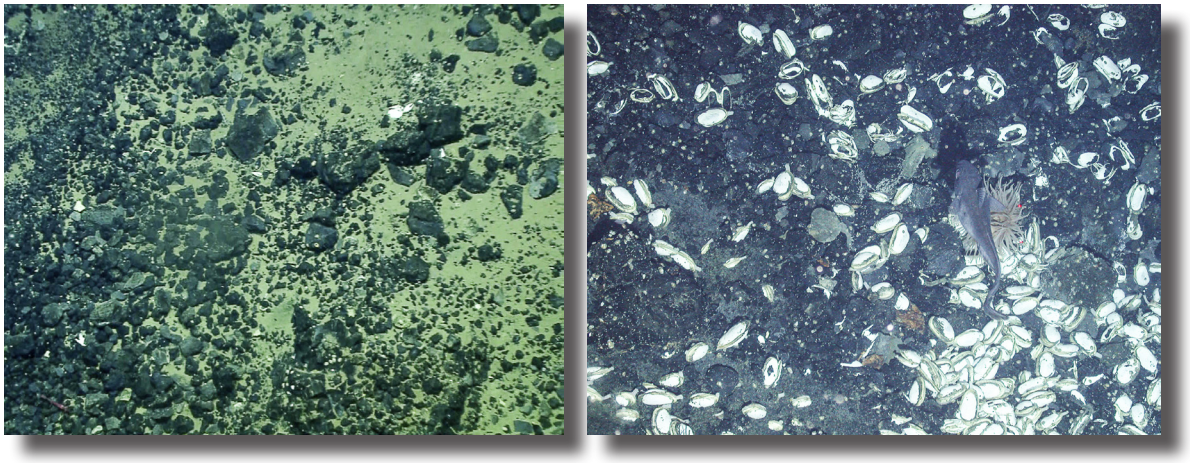

Fig. 7.19: A) Clam Road in 2019; B) Clam Road in 2010, © ChEsSO, NERC

On the top of Ash Mount a wide area of shimmering water and bacterial mats was encountered that was not observed in the mount top in 2010. Hydrothermal activity associated sea spiders of the genus *Sericosura*, *S. bamberi*, the limpet *Lepetodrilus concentricus* and a cocculinid limpet dominated the area in huge numbers (Fig. 7.20A). Their densities per square meter were roughly estimated by using the 20 cm wide laser pointers as a reference and counting visible sea spiders or limpets in a 10 cm by 10 cm or 1 cm x 1 cm quadrat. The cocculinid limpet had an estimate of 600 individuals per square meter, the sea spider an estimate of 940 individuals per square meter and the lepetodrilid limpet an estimate of 58.000 individuals per square meter.

Investigating the top of Ash Mount further, areas of rusty colored sediment (Fig. 7.20B) as well as of a large extinct chimney were seen which appeared larger that the extinct chimney structure seen on Ash Mount during ROV Isis dive 147 in 2010. From the top of the mount, the ROV descended back towards WP1 to locate free-living clams. After 1 h bottom time, the search abandoned and the transit to WP2 started. As WP2 was ~700 m away, the ROV flew in about 18-20 m above the seafloor until coming close to the waypoint and dropping closer to the seafloor.

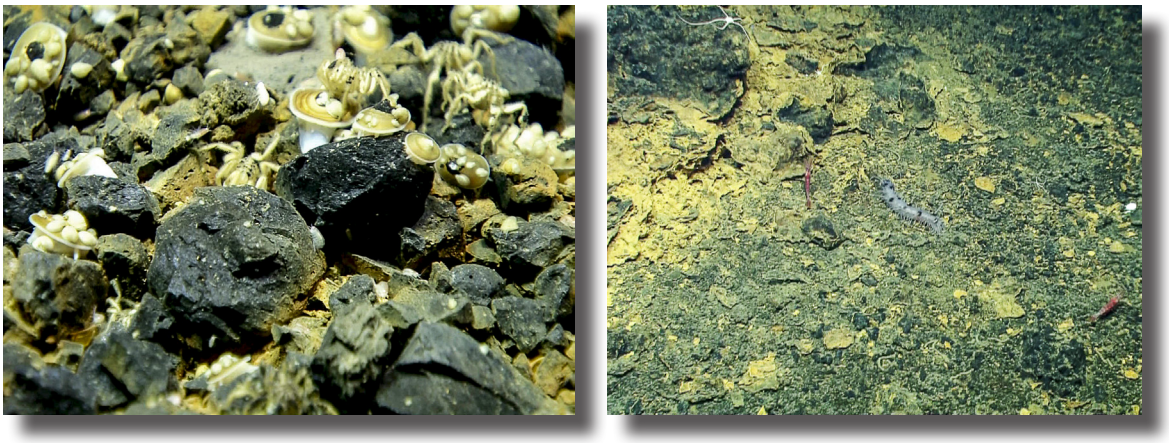

Fig. 7.20: Top of Ash Mount A) Close up of shimmering water area; B) Rusty looking substrate, 3D © ChEsSO, NERC

On approach to WP2, patches of wite precipitate and sediment came into view. When dead clam shells were seen lying on top of the sediment, the ROV stopped and set down for sampling after a patch of living clams was observed burrowed in the sediment. The first sampling events were push coring to analyze sediment layering, composition and geochemistry. Push cores 3 and 6 were taken in parallel within the living clam patch (Fig. 7.21A) and successfully recovered. For the clams sampling the large net (it handle had been shortened to fit into the bio box) was used and scooped through the sediment (Fig. 7.21B). Between each sampling, the net was shaken in the water to remove fine sediment. Sampling ended after four successful scoops. On trying to place the ¾ full net into the bio box, we had to note that a full net of this larger size does not fit into the bio box. As the draw was too full to fit the full net, the manipulator had to grab the bottom end of the net to shake sediment and clams out. The arm pushed onto the full bag, potentially breaking clams. After the net was placed in the bio box, a short look at the T-lance showed that the ambient temperature on top of the sediment was 0.3°.

Fig. 7.21: A) Push core sampling; B) Net sampling of living, burrowing clams

The ROV then moved to a position of a white smoking chimney at 59°41.690'S, 28°20.988'W, which was given to the PSO during the dive, about 70 m away on heading 120°. After passing an area of precipitated sediment and arriving in an area with white chimney structures and white smoke, a short search started to find the source of the white smoke for IGT fluid sampling. As the weather on the surface was deteriorating, the dive had to end before a white smoking

chimney was found. MARUM QUEST left the seafloor at 14:59 UTC, giving the dive about 3 hours bottom time. At 16:13 UTC MARUM QUEST was safely back on deck of *Polarstern.*

ROV Dive 449 (Station PS119_042_0)

Area:	Kemp caldera, flare site
Date:	Tuesday, May 14, 2019
Start bottom (UTC):	16:30
End bottom (UTC):	01:40, Wednesday, May 15, 2019
Bottom Time:	09:10
Start bottom (Lat/Long/Depth):	59°40.5615'S/28°21.4059'W/1138 m
End bottom (Lat/Long/Depth):	59°40.6102'S/ 28°21.5183'W/1162,3m
Responsible scientist:	Miriam Römer

Waypoints

WP 1:	59°40.563'S	28°21.407'W	Flare site 1
WP 2:	59°40.545'S	28°21.398'W	CTD anomaly
WP 3:	59°40.622'S	28°21.426'W	OFOBS smoke and ORP

Key results

The source of gas bubbles detected with the ship's echosounder could not be localized, although the first half of the dive was used to map the water column for bubbles with the ROV mounted forward looking sonar. The second part of the dive was spent to find vent sites at the seafloor, which in contrast to the bubble emission search was very successful. A black smoker was found, where two fluid samples and two chimneys where taken. Along a ridge crest, numerous signs of fluid escape were observed with large microbial mats. Here, two pushcorers were successfully sampled. Finally, an extent vent field with several large chimney structures was found. However, none of the chimneys was actively smoking, but shimmering water and white coatings on some of the chimneys indicated that activity has not entirely ceased, is intermittent or at least the chimneys were not since a long time inactive. A high-resolution photomosaic of one of the chimneys was taken. At the end of the dive fluids were sampled and the temperature measurement indicated with almost 200 °C that the emitting fluids are very hot although not releasing dark smoke.

Technical description

The technical performance during this ROV dive was good. No problems with the navigation. Two times in the first part of the dive, the ROV pilots had problems to keep track and altitude above seafloor, which led to some delay of the water column mapping.

Tab. 7.7: Samples and measurements

No.	Instrument	UTC Start	UTC End	Position	Depth	Comment
42-1	IGT-1	21:19	21:23	59°40.5538'S 28°21.4672'W	1129	231 °C
42-2	Rock	21:31	21:37	59°40.5538'S 28°21.4672'W	1129	Old chimney next to vent

No.	Instrument	UTC Start	UTC End	Position	Depth	Comment
42-3	Rock	21:46	21:50	59°40.5551‘S 28°21.4669‘W	1130	Black with white coating chimney
42-4	IGT-3	21:50	22:02	59°40.5551‘S 28°21.4669‘W	1130	229°C
42-5	PC-2	23:04	23:10	59°40.6125‘S 28°21.4362‘W	1167	Sampled ~10 cm
42-6	PC-8	23:08	23:08	59°40.6125‘S 28°21.4362‘W	1167	Lost sediment during recovery
42-7	PC-10	23:12	23:13	59°40.6125‘S 28°21.4362‘W	1167	Sampled ~10 cm
42-8	High-T-Lance	23:17	23:21	59°40.6125‘S 28°21.4362‘W	1167	8.7 °C, 15.5 °C
42-9	IGT-4	00:40	00:52	59°40.6102‘S 28°21.5162‘W	1163.5	shimmering water, T not measureable
42-10	High-T-Lance	01:14	01:25	59°40.6102‘S 28°21.5162‘W	1163.5	198.25 °C

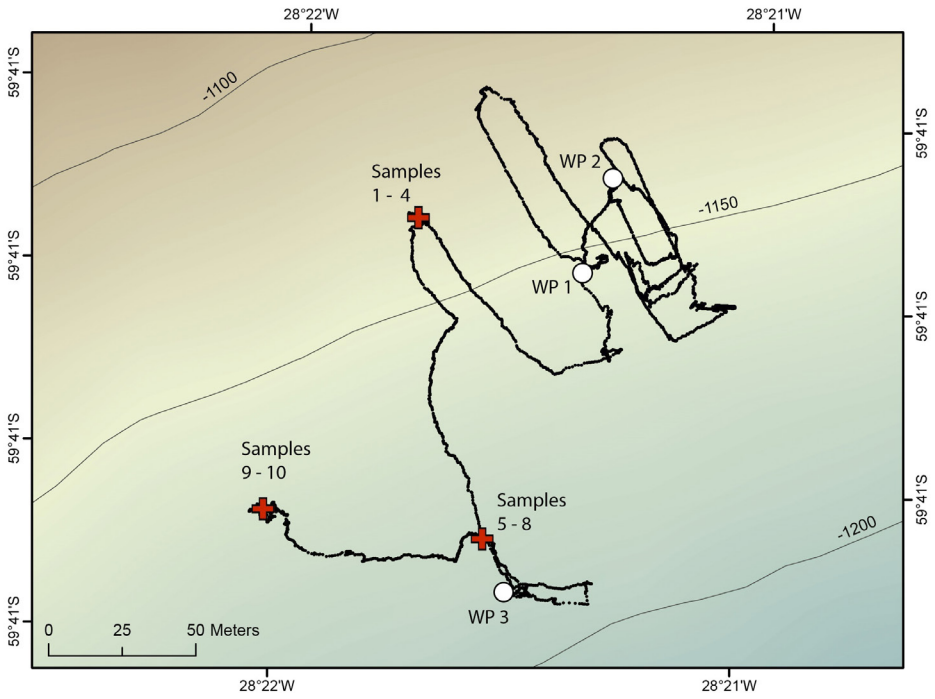

Fig. 7.22: Map of the area covered by QUEST Dive 449 (black line is the track of the ROV). The dive started at WP1 and ended after sampling of no. 9 and 10. Red crosses show the three different sampling locations

Dive description

At 15:00 UTC weather conditions were good enough and it was decided to conduct the dive. At 15:20 UTC the ROV was in water and arrived at the seafloor at 16:30 UTC as planned at waypoint (WP) 1. The objective for the first part of the dive was to find and locate the source of the flare that was recorded by the ship's echosounder, which is presumably related to an active vent area or other pronounced seafloor features that release fluids into the water column. WPs 1 and 2 are placed within the area of the flare footprint and mark locations of prior detected anomalies in water chemistry using the MAPR sensors. A visual inspection of the area around WP 1 and the following flight to WP 2 did reveal several seafloor structures that were interpreted to be chimneys and smaller conduits. Some showed very bright yellow colored rims and edges, which could be microbial mat or sulfidic precipitates. Several appearing inactive chimneys were seen, having brown to red rusty colors. Some structures also had fluffy white mats covered on the rocks, which are probably microbial mats and indicative for active diffuse fluid flow. Also, some areas with shimmering water clearly indicate active fluid emissions. However, the source of gas bubbles or an active smoker system could not be detected.

Therefore, it was decided at 17:15 UTC to use the forward looking sonar installed at the ROV upper top part, in which gas bubbles would appear as strong reflectors leading to the emission source. The ROV went up to an altitude of 15 m and a 360° turn in 4 steps allowed for a round view of about 20 m in radius around WP 2. The only anomalies seen were small dots, which we interpreted as fish, as also many fish were recognized visually in this area. In order to cover the footprint area of the flare, the ROV moved in a grid of ~50 m length in several parallel lines with a distance of ~10 m. The height was increased to 20 m. The water column mapping was performed until 20:30 UTC, unfortunately without successfully finding a sonar anomaly that would lead to a bubble emission site. Only very small continuous anomalies were seen, which most probably were produced by fish. Larger anomalies piercing from the seafloor were also seen in the sonar, but represented chimney structures. Nevertheless, some of these structures were visually proven if the chimneys show emission activity. As before, the seafloor structures showed fluid emission activity in form of shimmering waters and/or bacterial mats, but none of the chimneys was actively smoking. Due to some technical issues with the mapping in 20 m altitude, only 3 and a half transect lines of the mapping were conducted until it was decided to finish the approach finding gas bubbles with the forward looking sonar.

After a shift change of the scientist in the container, the following part of the dive was spent close to the seafloor searching for emission sites visually. The ROV was moved along a parallel track to the prior mapped ones and after ~50 meters without indications of venting, a seafloor structure was found that had a small but actively venting chimney on top (Fig. 7.23a). The smoke was slightly black, however still very transparent, especially close to the outlet. The chimney was broken off for sampling, however, fell out of the claw and down to the seafloor. Unfortunately, this part was not reachable for sampling, so that this chimney had to be left at the seafloor. A fluid sample was taken in the orifice of the broken off chimney (Fig. 7.23b). Temperatures were measured at 231°C. As the broken off chimney could not be sampled, another older chimney lying next to the orifice was taken (Fig. 7.23c). Finally, another fluid emission site was seen about a meter aside of the structure. Small dark appearing but white coated chimneys are found here and one of these was sampled (Fig. 7.23d). Afterwards, a second fluid sample was taken here and temperatures revealed 229 °C.

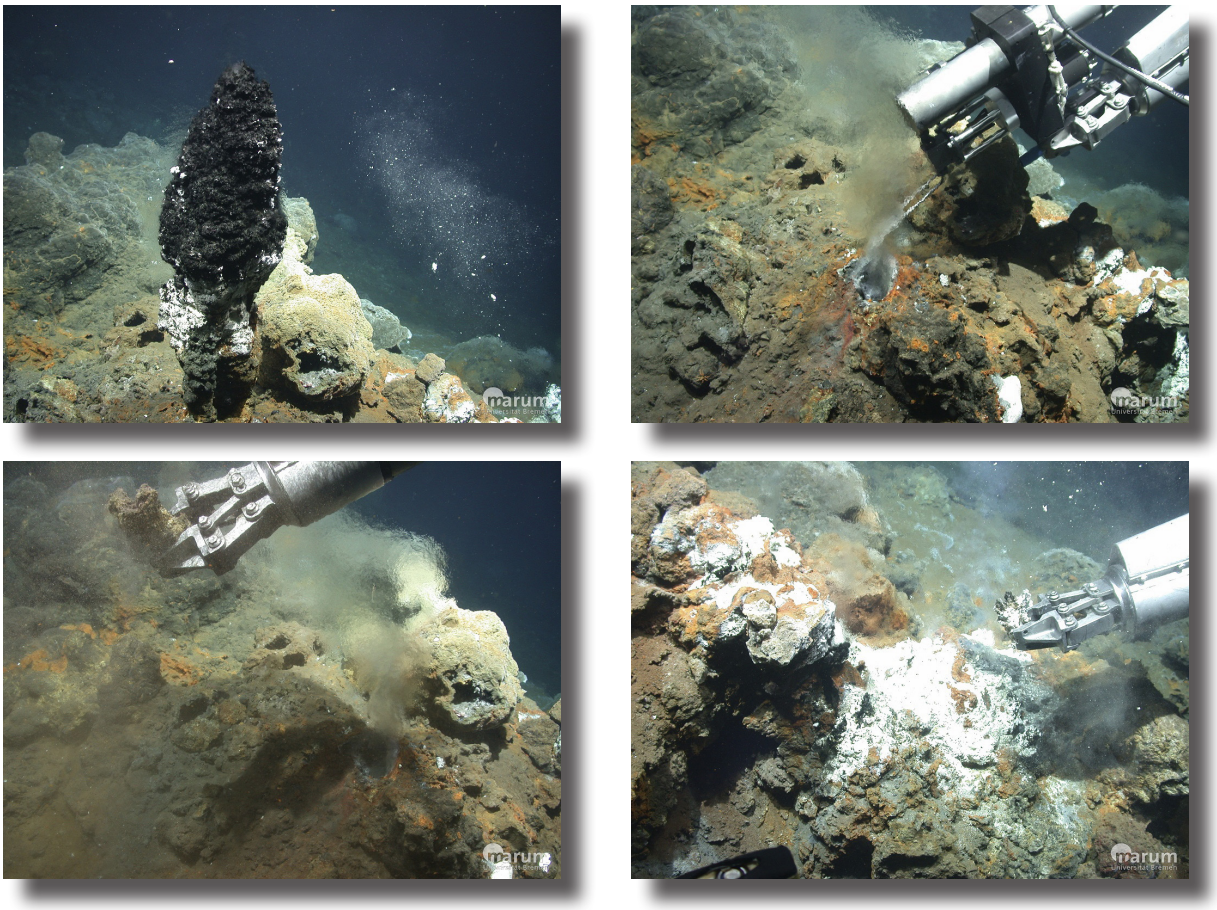

Fig. 7.23: Seafloor images taken at the first sampling location. a) smoking chimney with black and white staining before sampling. b) Fluid orifice after breaking off the chimney visible in 2a. The first IGT- sample was taken and the temperature probe revealed fluids of 231 °C. c) Old appearing loose chimney close to the orifice sampled with the manipulator. d) Second rock sample at another fluid release less than a meter next to the first one. After rock sampling the fluids were taken as well and temperatures revealed 229 °C.

Next objective of this dive was moving to WP 3, which is about 130 m in southern direction. On the way, rocks covered by white filaments were observed and 10 m before reaching WP 3 a ridge with built-ups and white microbial mats along its crest were passed. After 30 minutes, WP 3 was reached and investigated. The seafloor is very steep and sediment covered. White stains were seen, which appears to be microbial mat material that slided down from the crest area where large microbial mats have been seen. The ROV was moved up again to the crest and one of the larger microbial mats was chosen as next sampling location for pushcoring (Fig. 7.24a). Two pushcorers should be sampled. As one failed, as sediments fall out before storing back, a third pushcorer was successfully taken (Fig. 7.24b). The high-temperature lance was used to measure the surface sediments close to the sampling site within the microbial mat and revealed 8.7 °C and 15.25 °C.

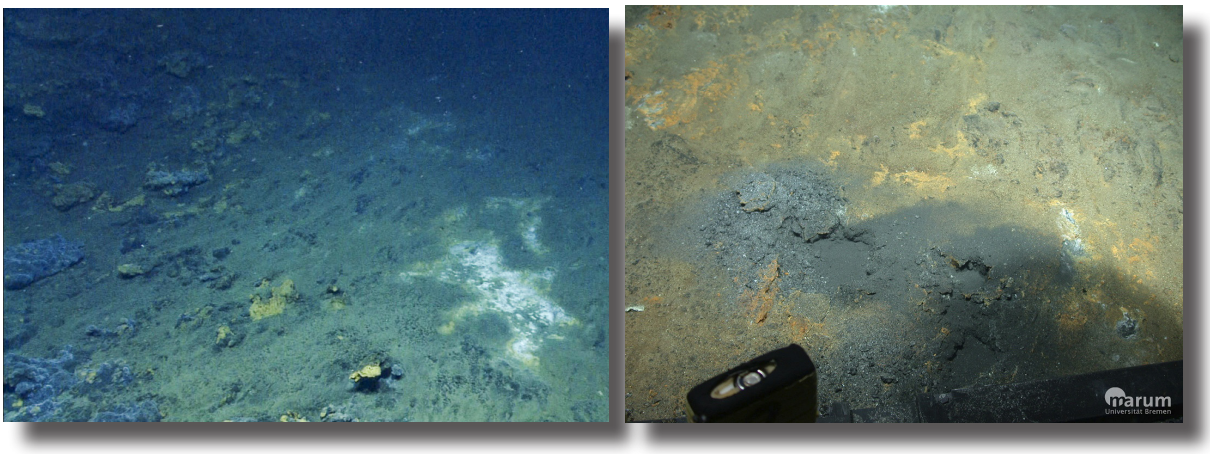

Fig. 7.24: Seafloor images from the second sampling location. a) White mat surrounded with yellow color chosen for pushcorer sampling. b) Three pushcorers were taken within the white patch. Sediments in PC-8 were fallen out during sampling.

The last part of the dive was spent to explore the seafloor following the ridge crest along which numerous vent-related areas were found by built-ups, microbial mats and shimmering water. After another half an hour moving slowly westwards, a large field of several high chimney structures was detected. None of the chimneys was seen to be actively smoking, however, more turbit appearing water was passed when approaching this site. One impressive chimney structure was chosen for detailed investigations (Fig. 7.25). A high-resolution photomosaic was taken carefully for about 25 minutes. Some shimmering water flows were observed coming from the foot of the structure. A fluid sample was taken in there and temperatures measured afterwards with the high-temperature probe (as the fluid sampler sensor did not work properly), which revealed 198.25 °C. In the last minutes, a chimney should be sampled with the manipulator, but due to unstable positioning it failed and the dive had to be finished.

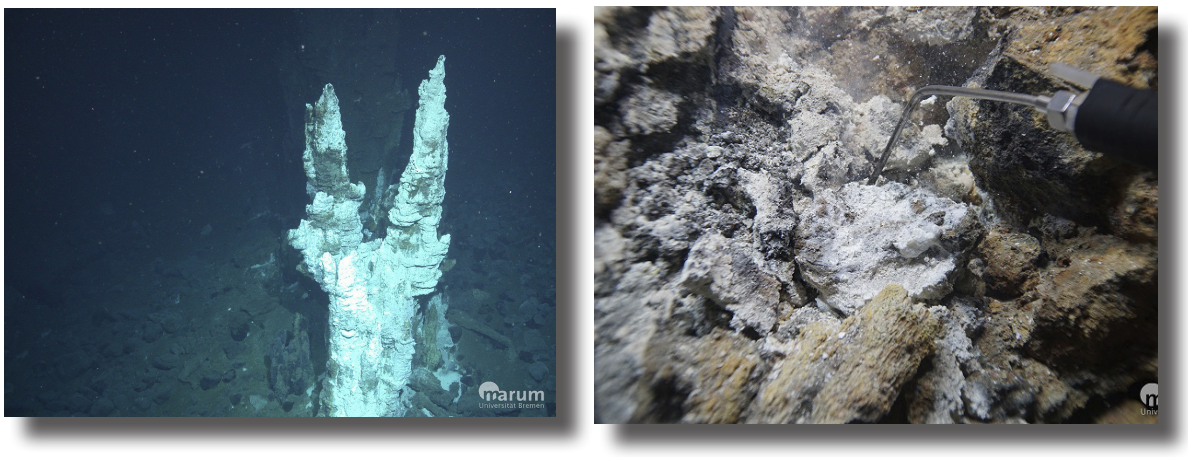

Fig. 7.25: Seafloor images from the third sampling location. An extent vent field was discovered with several huge chimney structures. a) A high-resolution photomosaic was taken at this mostly white coated chimney. b) A fluid sample was taken at the foot of the same chimney, which has been measured to be almost 200 °C in temperature.

ROV Dive 450 (Station PS119_047_0)

Area:	East Scotia Ridge E2, South
Date:	Saturday, May 18, 2019
Start bottom (UTC):	12:48
End bottom (UTC):	19:46
Bottom Time:	06:58
Start bottom (Lat/Long/Depth):	56°05.2723'S/30°19.1451'W/2590 m
End bottom (Lat/Long/Depth):	56°05.3424'S/30°19.0962'W/2643 m
Responsible scientist:	Yoland Bosiger

Waypoints

WP1	30°19.139'W	56°05.271'S Anemone Field (2600 m)
WP2	30°19.155'W	56°05.284'S Dog's Head (2601 m)
WP3	30°19.131'W	59°05.304'S Unknown black smoker (2621 m)
WP4	30°19.132'W	56°05.334'S Liberachi (2636 m)

Key results

The fourth dive on the E2_S hydrothermal vent field focused on filming the Hoff crab, *Kiwa tyleri* and the surrounding hydrothermal vents for the BBC series Frozen Planet II. Key features visited were the black smokers "Dogs Head", the diffuse flow area "Anemone Field" and the extinct chimneys of "Cindy's Castle" and "Dreaming Spires".

Technical Description

Our waypoints were taken from the ROV QUEST'S USBL positions on previous ROV dives during this cruise (primarily dive 444 and 446). The positions matched very well and we were able to find WP1-3 without issue. While the intention was to land on "Liberachi" as WP4 it is likely that we travelled over this waypoint to arrive on "Cindy's Castle" and "Dreaming Spires" instead. As these locations were equally interesting for filming we made the decision to remain at these locations as our final waypoint. Visibility during the dive was good although currents at "Anemone Field" and "Cindy's Castle" made filming steady shots challenging at times. We also experienced some problems with the ROV QUEST'S thrusters upon reaching "Cindy's Castle" but all in all the ROV dive was completed without incident.

Tab. 7.8: Samples and measurements

No	Instrument	UTC Start	UTC End	Position	Depth	Comment
47-1	Net	19:06	19:13	30°19.087'W 56°05.343'S	2641.1	Collected 5 x *Kiwa tyleri*

Dive description

The dive began at WP1, known as "Anemone Fields". The site was characterized by a large number of *Kiwa tyleri* in the diffuse flow. The BBC filmed shots at this location both to introduce the crabs as characters and to reveal large numbers. Shots attempted are below and those successfully captured are indicated with an *.

Introduction to crab

- Wide shot descending from the blackness to the sea floor with one Hoff crab in wide shot. *
- Medium arrival to Hoff crab.
- Close up static shot of Hoff crab. *
- Wide and medium tilt down onto crab from the black. *
- Medium shot single crab with some shimmer to introduce the possibility of the vent.

Groups of crabs

- Medium and close up static lots of Hoff crabs. *
- Medium shot pan across group of Hoff crabs. *
- Reveal lots of Hoff crabs: focus in on one Hoff crab and then slow pull out to reveal large numbers of Hoff crabs in wide. *
- Tracking shots to reveal lots of Hoff crabs. *

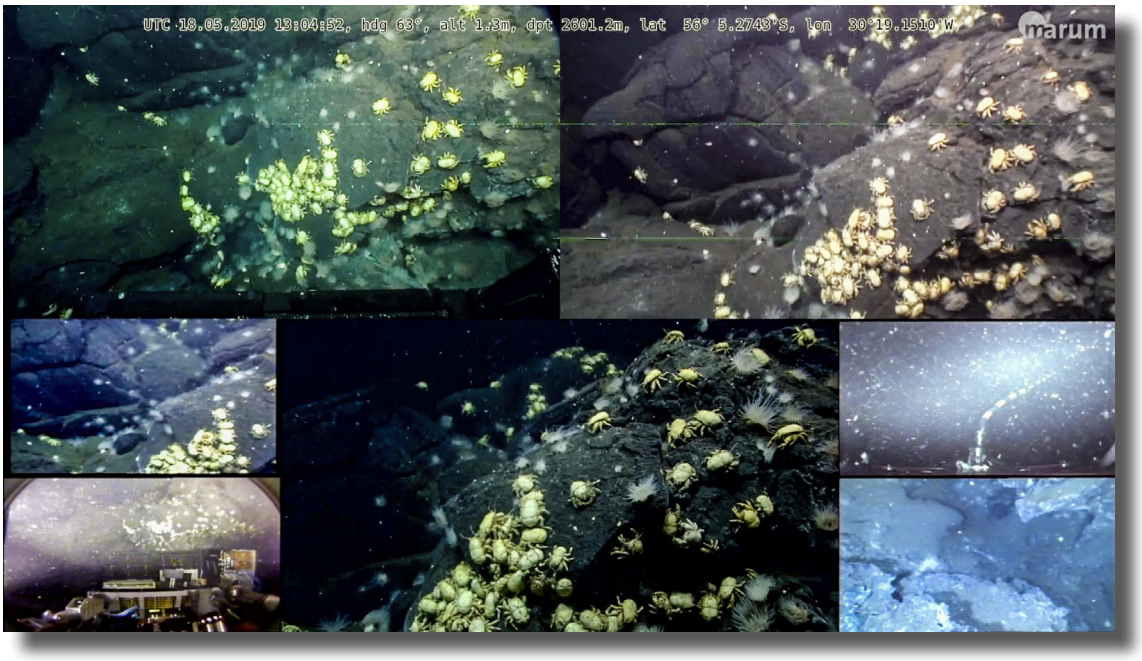

Fig. 7.26: The Hoff crab, Kiwa tyleri in large numbers at "Anemone Fields"

After 95 minutes filming, the ROV QUEST travelled 5 m in distance to the black smoking chimneys of "Dogs Head". The goal at this location was to film general views and establishing shots of the chimneys as well as any *Kiwa tyleri* that could be seen on the chimneys. Shots attempted are below and those successfully captured are indicated with an *. The team spent a total of 112 minutes filming at "Dogs Head" before moving to WP4.

Introduction to chimneys

- Wide and medium static views of "Dogs Head" from afar with multiple chimneys. *
- Forward tracking shot arriving from the open sea to the chimneys straight on. *
- Shot of black smoke filling frame. *

- Move down from black smoke to chimney with smoke. *
- Wide and medium move around the chimney at top of “Dogs Head” - circular movement. *
- Vertical climb shot moving up the chimneys/ vertical shot going down chimneys.
- Close up static views of a chimney with smoke.

Crab on chimneys

- Wide/ mid shot of a crab on a chimney. *
- Tracking shot going up over a Hoff crab.
- Hoff Crab in frame and wait until it exits frame.
- Closer shot of Hoff crab feeding.

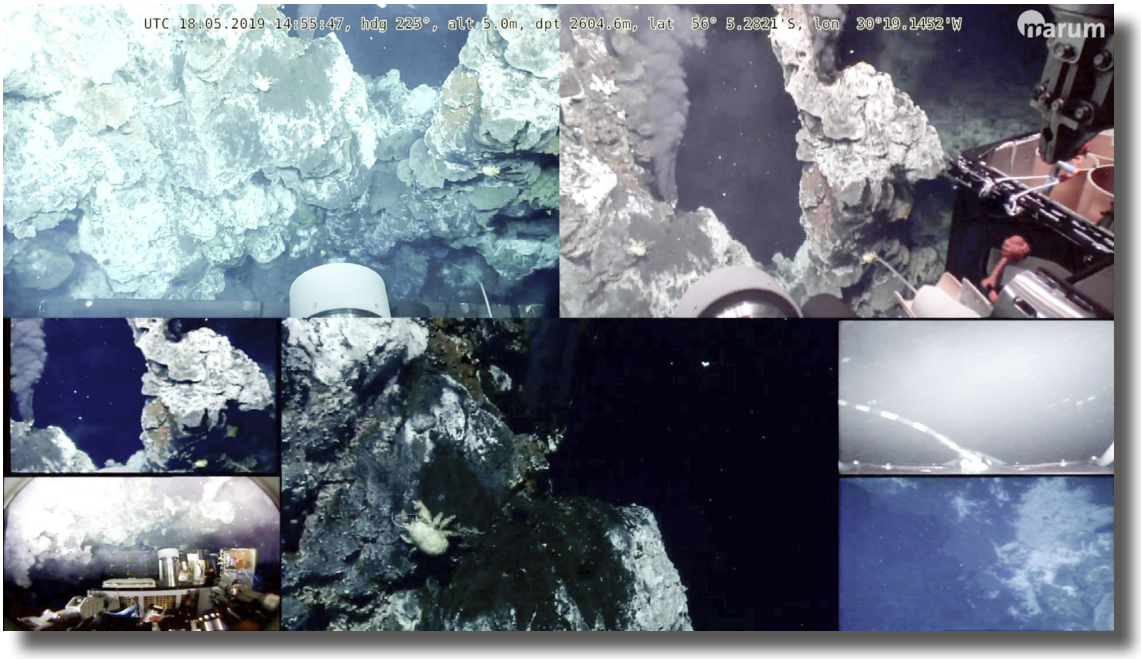

Fig. 7.27: The Hoff crab, Kiwa tyleri at the black smoking chimneys of “Dogs Head”

QUEST ROV travelled for South following filming at “Dogs Head” and arrived at the black smoker described as WP3. The ROV spent 15 minutes travelling and covered a total distance of 120 m before coming upon a chimney that the scientists on board knew to be “Cindy’s Castle”. We discussed whether we might have passed our waypoint but decided to film “Cindy’s Castle” before moving on. We were able to capture a sideways tracking shot around the structure that may also be used for scientific mosaic projects. After 26 minutes at “Cindy’s Castle“, we moved on to find WP4.

After another 7 minutes travelling, the ROV QUEST came across a structure that scientists believed to be “Dreaming Spires”. Given that a storm was threatening to cut our dive short we decided to remain and film at this location rather than the site thought to be “Liberachi”. We filmed some establishing shots of the extinct chimney and quickly focused on filming the crabs in large numbers on the chimney slope. Almost immediately we noticed two crabs arguing with each other but unfortunately we couldn’t position the ROV to see it clearly because of a large structure blocking any landing spot. We instead focused on getting close up and medium shots of individual crabs on the chimneys where a landing could be made whilst still trying to pick up some shots of the Kiwa tyleri fighting. Shots attempted are below and those successfully

captured are indicated with an *. The team spent 57 min at this location before moving to the next site.

Establishers of chimney

- Wide move around the liberachi area (circular). *
- Wide and medium statics of liberachi scene. *
- Wide move up and descend down this scene. *
- Medium move around one of these chimneys with crabs on it (circular).

Crab and feeding

- Medium shot of a number of Hoff crabs with shimmer moving across them. *
- Medium shots of Hoff crabs feeding, picking bits off their claws.
- Close up shots of Hoff crabs feeding, picking bits off their claws.
- Medium shot sideways pan across Hoff crabs. *
- Wide/ Medium/ Close up static lots of Hoff crabs. *
- Medium of a single Hoff crab in shimmer feeding.
- Details of a fight situation between two Hoff crabs. *

Introduce travel up a chimney

- Wide/ mid shot of a crab on a chimney. *
- Tracking shot going up over a Hoff crab.*
- Hoff crab in frame and wait until it exits frame.

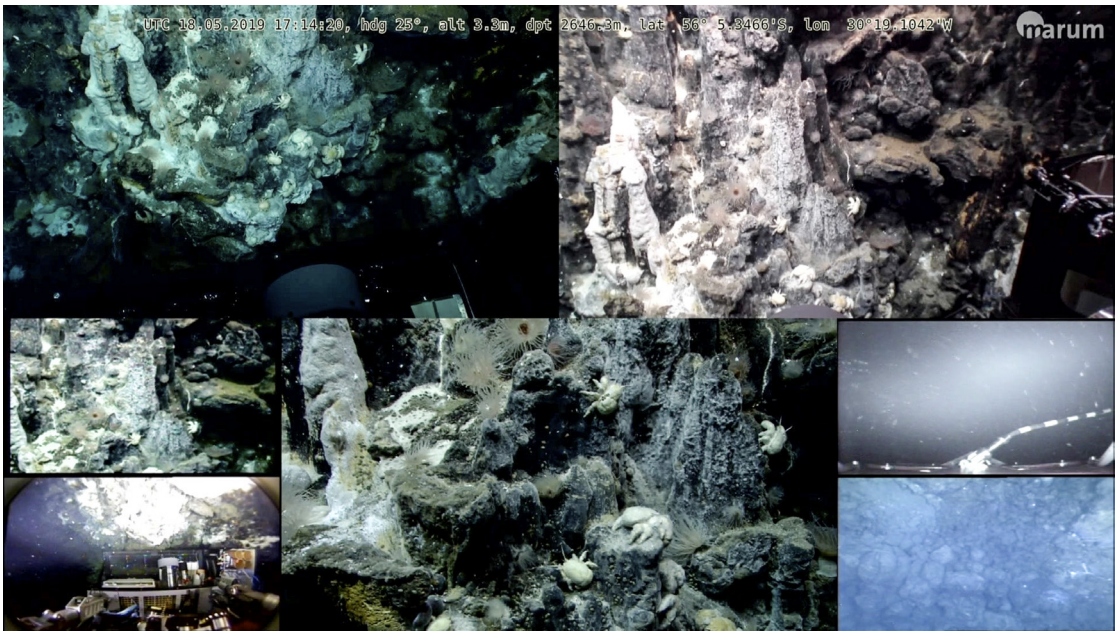

*Fig. 7.28: Filming the extinct chimney known as "Dreaming Spires". The goal was then to find an extinct chimney with Kiwa tyleri near to the top. Luckily we found a site just off the side of "Dreaming Spires" which was exactly what we were looking for. Shots attempted are below and those successfully captured are indicated with an *. The team spent 67 minutes at this site and also sampled 5 Kiwa tyleri with a net once filming was completed for scientific purposes.*

Variety of shots

- Shots moving up and down the chimney over Hoff crabs. *
- Close ups of crabs on the chimney structure near to the top. *
- Departure shots of the chimney. *
- Large groups of Hoff crabs. *

Our final site was conducted at the base of the extinct chimney and there we tried to film a female Kiwa tyleri. We spent 31 minutes at this site before the dive had to be terminated as a result of weather. Shots attempted are below and those successfully captured are indicated with a *

Females

- Wide and medium shots of the Hoff crab female *
- Tilt up from rocks to reveal a Hoff crab female
- Vertical arrival at Hoff crab female using ROV *
- Medium and wide static shots of a number of Hoff crab females.
- Medium sideways pan across number of female Hoff crabs.
- Slow pull out shots *

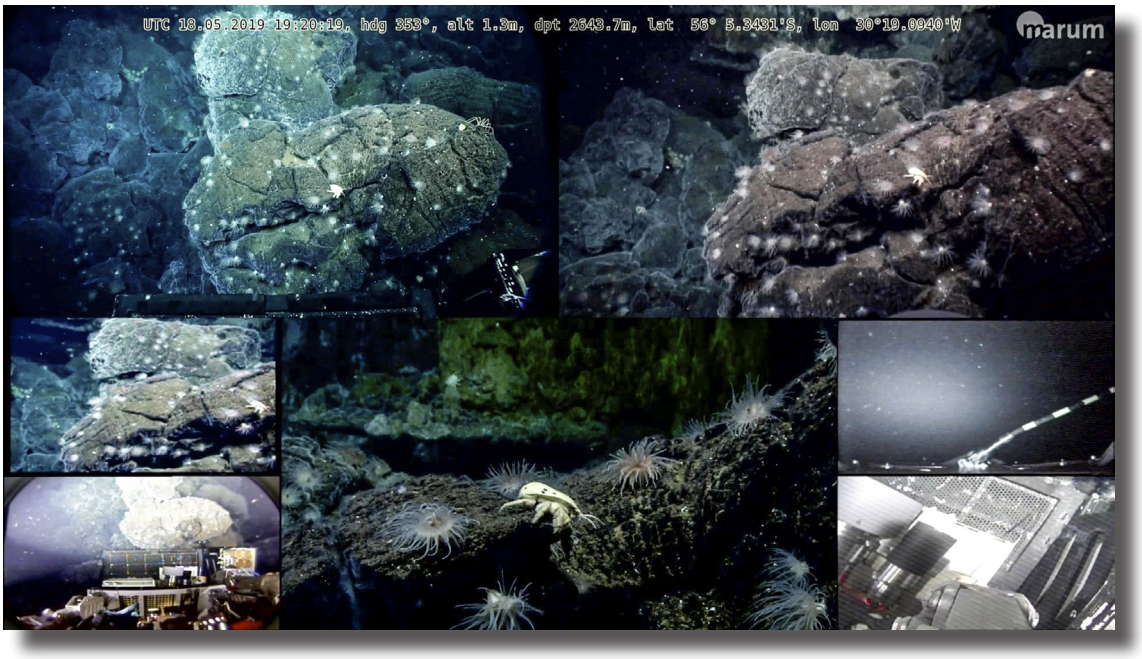

Fig. 7.29: Pillow lava with female off the extinct chimney site

Data management

All data archival will be published by the World Data Center PANGAEA Data Publisher for Earth & Environmental Science (www.pangaea.de).

8. HYDROTHERMAL FLUIDS & PRECIPITATES

Alexander Diehl[1], Samuel Pereira[1] Male Köster[2],
Wolfgang Bach[3] (not on board)

[1]GeoB, Bremen
[2]AWI, Bremerhaven
[3]MARUM, Bremen

Grant-No. AWI_PS119_00

Objectives

Due to weather conditions, hydrothermal systems in the South Sandwich Arc (SSA) and the East Scotia Ridge (ESR) back-arc spreading-systems remain to be poorly investigated compared to active vents of the well investigated Mariana Arc or Tonga-Kermadec Arc and their respective back-arcs. At the ESR traces of hydrothermal systems cooling active volcanic centers have been found at the ridge segments E2 and E9 (German et al., 2000). In the year 2010 these segments were revisited and investigated by ROV operations. Several vent areas were discovered and sampled (James et al., 2014; Hawkes et al., 2013; Cole et al., 2014). Two vent fields were discovered at the northern portion of the ESR (the E2 segment) and the southernmost part of the ESR (the E9 segment), respectively. Furthermore, active vents were investigated in the Kemp Caldera, a volcanic edifice within the southern part of the SSA.

In this cruise we want to investigate hydrothermal fluids from known hydrothermal vents and explore new hydrothermal areas associated with the ESR as well as within the SSA. One aim is to re-sample vents that were discovered in 2010 and compare the fluids expelled today with the fluids analyzed nine years ago. These investigations will show if changes have occurred to these hydrothermal vents within the last decade. Further, we put effort in analyzing volatile species (H_2, CH_4, CO_2) that help us to infer the subsurface fluid-rock reactions and various influences on hydrothermal vent fluid compositions (phase separation or influx of volcanic volatiles). Our goal is to retrieve samples from back-arc and arc hosted hydrothermal vents and to study the differences between these two geologic environments. We are especially interested in the different character of back-arc-hosted and arc-hosted hydrothermal fluids and we focus on the influence of volcanic degassing to the vent sites hosted in the different geological settings. For this purpose, we use isobaric gas-tight hydrothermal fluid samplers (IGT; Seewald et al., 2001). In the northernmost and southernmost parts of the SSA the ESR back-arc spreading center and the SSA intersect. In these regions vent sites from these very different geologic environments can be effectively studied in close proximity.

Work at sea

Isobaric gas-tight (IGT) fluid samplers (Fig. 8.1 A-B) were provided through collaboration with Prof. Dr. Jill McDermott, Lehigh University, USA. This device is made of titanium and is developed to sample hydrothermal fluids up to temperatures of at least 400 °C and pressures of up to at least 450 bars. A thermocouple attached to the sample inlet allows real-time readings of temperature during the sample procedure. The IGT fluid sampler maintains the sample at *in-situ* pressure during recovery of the sampler and sample withdrawal in the laboratory. This enables subsampling without degassing of the fluid in the sample chamber and is an important

feature for high quality quantification of dissolved volatiles in hydrothermal fluids. A detailed description of the IGT sampler can be found in Seewald et al. (2001).

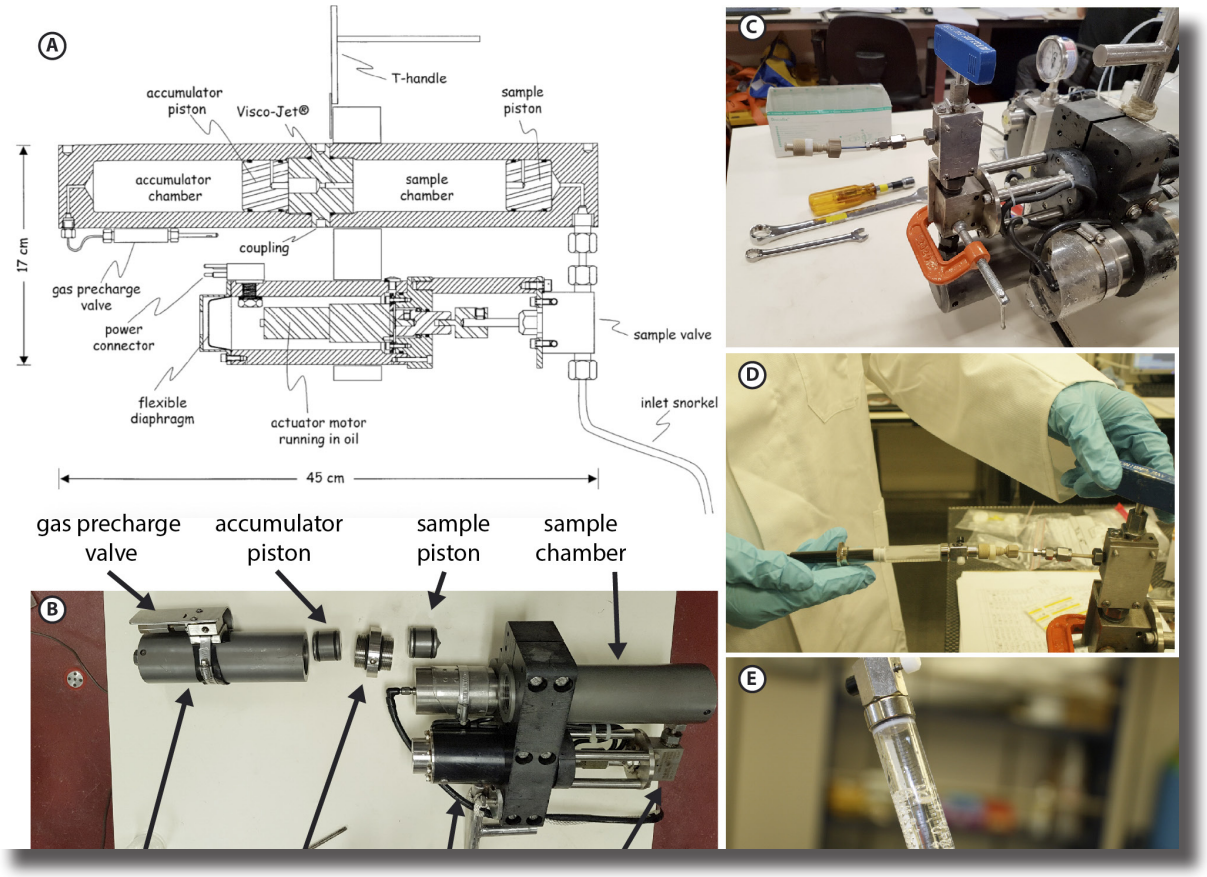

Fig. 8.1: Collage illustrating the handling of IGT samplers. A: Construction scheme of an IGT sampler (from Seewald et al., 2001). B: Photograph of an IGT sampler. C: Setup of the sample draw procedure. D: Drawing of a sample into a gas tight syringe. E: Degassing of a subsample upon application of under-pressure.

During pre-dive preparations the samplers are assembled and the accumulator-side and sample-side pistons are inserted to the corresponding positions. The snorkel, the thermocouples and the non-contact serial communication are tested for functionality. The sample chamber and the dead volume of the snorkel is filled with background seawater from the area. The sample valve is prime-closed with a current of 400 mA. The accumulator chamber is pre-charged using compressed nitrogen and a pressure of about 10 % of the seafloor pressure. The pre-pressure damps the inflow of the hydrothermal fluid and helps to avoid entrainment of seawater during the sampling. Finally, the samplers are attached to ROV Quest and the communication (via inductively coupled link; ICL) is tested in the final setup on the vehicle prior to each dive. During the dive sampling of hydrothermal fluids is accompanied by monitoring of the temperature at the sampler's inlet. When the snorkel is positioned in the hydrothermal orifice and the vehicle has a stable position, the temperature is monitored to find the optimal position to fire the sampler (Fig. 8.2) and the sample valve is opened. The high in-situ pressure exceeds the pressure in the accumulator chamber, so both pistons are pushed back and the pre-filled seawater from the sample chamber travels into the accumulator chamber while the sample chamber is filled with the hydrothermal fluid. The sample valve is open for 90 seconds and closes automatically.

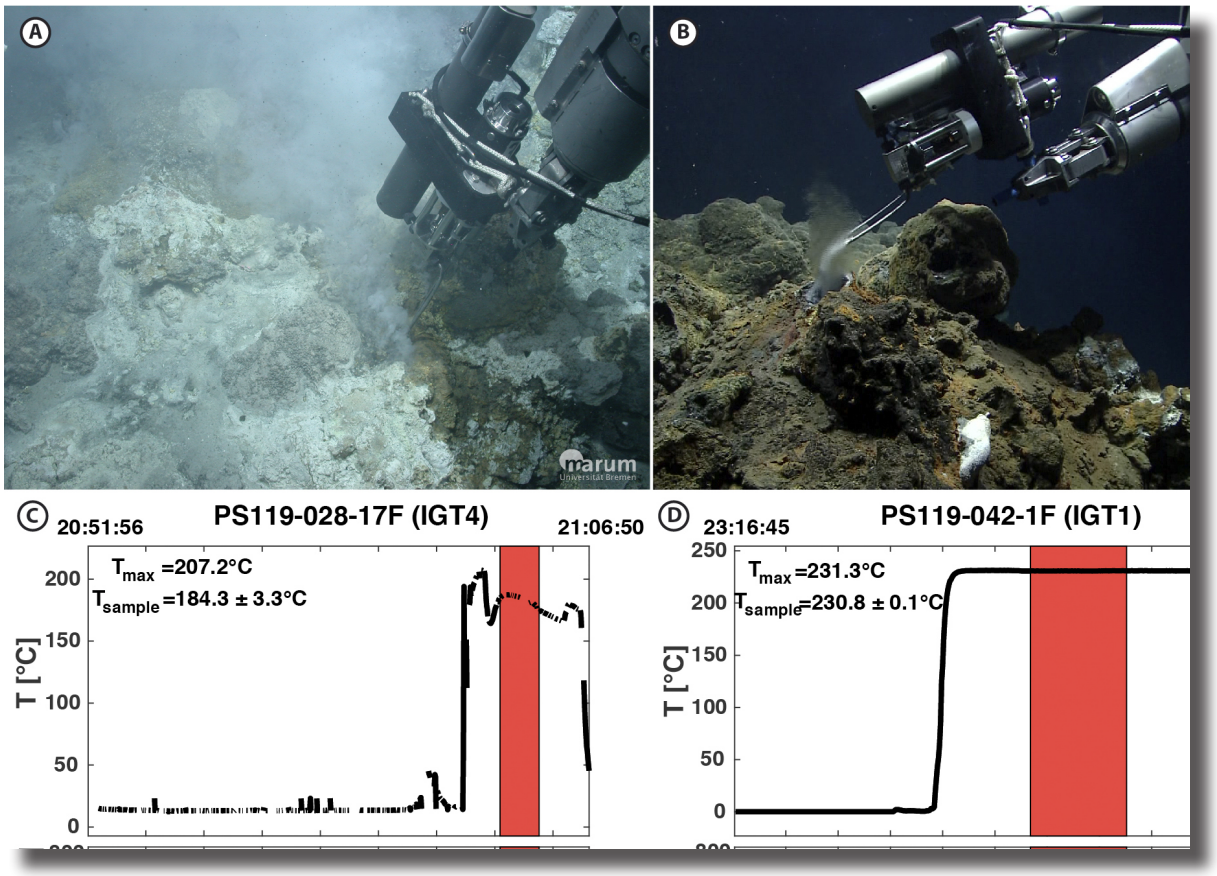

Fig. 8.2: Photographs of sampling sites and corresponding temperature logs. A-B: Fluid sampling at Kemp Caldera (left: Toxic Castle; right: newly discovered vent at the inner part of the Caldera Rim). Photographs: ®MARUM QUEST. C-D: IGT temperature logs during the sampling procedure. The I/t log shows the motor current of the actuator motor (when the current increases the valve opens or closes). The sampling period is marked in red.

After recovery, the samplers are thoroughly rinsed with freshwater and brought into the laboratory. Here, the thermocouple and snorkel are replaced by a second sampling valve (Fig. 8.1C) that follows the sampler's main valve. A high-pressure liquid chromatography pump (HPLC) is attached to the pre-charge valve and the accumulator chamber is pressurized with a pressure exceeding the *in-situ* pressure of the hydrothermal fluid. The sampler's main valve is opened and the fluid can be drawn using the second valve following the sampler's main valve. The hydrothermal fluid is then pushed into a gas-tight syringe where it is pressure released (Fig. 8.1D-E).

Hydrothermal fluid samples were used for onboard analytics of dissolved volatiles (H_2, CH_4) as well as pH and Fe concentration. Concentrations of H_2 and CH_4 were determined by gas chromatography within 24 h after each dive. Sample volumes between 1 and 1.5 mL of hydrothermal fluid were transferred from the IGT samplers into gas-tight syringes. The dissolved volatiles were extracted by a headspace extraction. One mL of pure nitrogen is brought in contact with the hydrothermal fluid in the syringe. An under-pressure is created by pulling down the stamp of the syringe. This way volatiles are extracted from the liquid into the headspace (*cf*. Henry's law). The nitrogen gas, enriched with dissolved volatiles from the hydrothermal fluid, then is injected into the gas chromatograph. The procedure is repeated until the detector signal becomes neglectable compared to the signal of the prior injections and in this way a nearly complete removal of dissolved volatiles from the liquid fraction is achieved. The gas chromatograph used was an 7820A Agilent. The GC was equipped with

a packed Molsieve 60/80 column (Sigma-Aldrich, St. Louis, MO) and was operated with N_2 as carrier gas at 90 °C. H_2 was quantified using a thermal conductivity detector, whereas CH_4 was quantified with a flame ionization detector. The device was calibrated with reference gases of 253 mol-ppm H_2 and 120 mol-ppm CH_4 in a daily fashion. For each sample multiple measurements (usually three) with different aliquots were conducted. The precision was better than 5 % for all samples. The pH value was measured with a “seven2go” pH electrode from Mettler Toledo instantly after removing the sample from the gas-tight syringe to minimize the effect of degassing. The electrode was calibrated with 4-point calibrations using reference solutions of pH 2, 4, 7 and 11 on a daily basis. The dissolved Fe concentration was determined photometrically by the sediment geochemistry group. For details on the analytic technique confer “Chapter 12 Sediment Geochemistry”.

After the onboard analytics were completed, various aliquots were collected for shore-based analyses. Three aliquots of 5 ml were prepared for determination of DIC concentration. The aliquots were injected into pre-weighted He-filled and subsequently evacuated glass serum vials to prevent atmospheric CO_2 contamination. Samples were transferred from gas-tight syringes through the vial’s septa. The vials were stored upside down to seal the septa by the fluid and prevent diffusive gas loss. The determination of CO_2 will be done following the method of Reeves et al. (2011). Several aliquots for determination of H_2S were drawn. Sulfide will be quantified with a gravimetric and a photometric approach: We have transferred 15 ml of fluid into 25 ml evacuated glass-serum vials and acidified these samples with 3 ml of 25 wt. % phosphoric acid. Then nitrogen was used to flush out H_2S into a wash-flask filled with silver nitrate solution. The H_2S quantitatively precipitates as AgS. The precipitates were then filtered on cellulose acetate and polycarbonate filters. The pre-weighed filters will be dried and weighed to calculate the H_2S concentration from the weight of the AgS precipitates. Furthermore 0.1 ml fluid was mixed with 0.9 ml of 11.4 mM zinc-acetate solution and 1.5 ml of fluid was mixed with 0.5 ml of 47.4 mM zinc-acetate solution. This way photometric measurements are prepared for the determination of H_2S concentration in different concentration ranges. Aliquots for inductively coupled plasma optical emission spectroscopy (ICP-OES) analyses comprised of 10 ml of fluid that were filtrated through 0.45 μm filters and acidified with 200 μl of concentrated nitric acid. Further 10 ml of aliquot for analyses of anions by ion chromatography (IC) were filtrated through 0.45 μm filters and not acidified. 2 ml of untreated sample were stored away for Sr isotope analyses. 5 ml were given away to the chemosynthesis group for analyses of P-species. Aliquots of 10 ml for trace metal and iron isotope analyses were filtered through a 0.2 µm polyethersulfone filter, acidified with concentrated double distilled hydrochloric acid and stored at ~4 °C. The remaining fluid was untreated and filled in PE bottles as archive samples. A list of the fluid samples and the results of on-board analytics is found in Table 8.1.

Tab. 8.1: List of IGT fluid samples

Sample ID	Date/ Time	Location	Tmax [°C]	pH	H2 [µM]	CH4 [µM]	Fe [µM]	Comments
PS119-017-3F	28.04.2019 0:35	**E2- West**	53,4	6,2	0,66	1,59	12,1	(new discovered diffuse vent site with intensively altered host rocks)
PS119-020-7F	29.04.2019 19:45	**E2- South**	320	3,3	59,5	48,9	610	(vigorously venting black smoker chimney, (T from T-lance due to poor IGT communication)
PS119-020-10F	29.04.2019 23:09	**E2- South Dogs Head**	344	3,2	36,0	25,6	898	vigorously venting black smoker chimney, extremely particle-rich (T from T-lance due to poor IGT communication)

Sample ID	Date/ Time	Location	Tmax [°C]	pH	H2 [µM]	CH4 [µM]	Fe [µM]	Comments
PS119-028-8F	07.05.2019 15:20	**Kemp Caldera Great Wall**	63,1	5,4	0,98	15,7	5	diffuse outflow of clear fluids at great wall
PS119-028-17F	07.05.2019 19:03	**Kemp Caldera Toxic Castle**	207,2	5,7	13,7	2,15	-	mound with white smokers and liquid native sulfur, valve clogged by native sulfur (approx. 2ml of sample)
PS119-042-1F	14.05.2019 21:19	**Kemp Caldera Northern Rim**	231,3	2,3	1,0	2,96	1820	beehive chimney venting clear fluids with only some black particles. After breaking vigorously venting clear fluids
PS119-042-4F	14.05.2019 22:02	**Kemp Caldera Northern Rim**	229,4	-	-	-	bdl.	orifice next to 042-1F (mostly seawater temperature not representative)
PS119-042-9F	15.05.2019 00:49	**Kemp Caldera Northern Rim**	198,5	5,5	0,05	1,6	11,9	diffuse vent at the base of a large chimney with clear fluids emanating. Temp from T-lance

Specimen of volcanic rocks and hydrothermal precipitates were collected by ROV Quest, either using a shovel, a scoop-net or by grab (Fig. 8.3). The rocks were dried in the laboratory and subsequently described, photographed and investigated with a hand-lens. Macroscopic mineral identification was done using a typical 10x magnification lens. In total 13 specimen were recovered and processed. The igneous samples range from pristine volcanic rocks with different degrees of vesicularity and phenocrystal contents, up to glassy material representing the composition of a magmatic melt. Hydrothermal precipitates range from Fe-sulfide-rich and Zn-sulfide-rich aggregates at the E2 segment to native-sulfur dominated precipitates at Kemp Caldera. Sulfate crystals (barite or anhydrite) are found in all locations. A sample list with *in-situ* and *ex-situ* photographs and short descriptions can be found in Table 8.2.

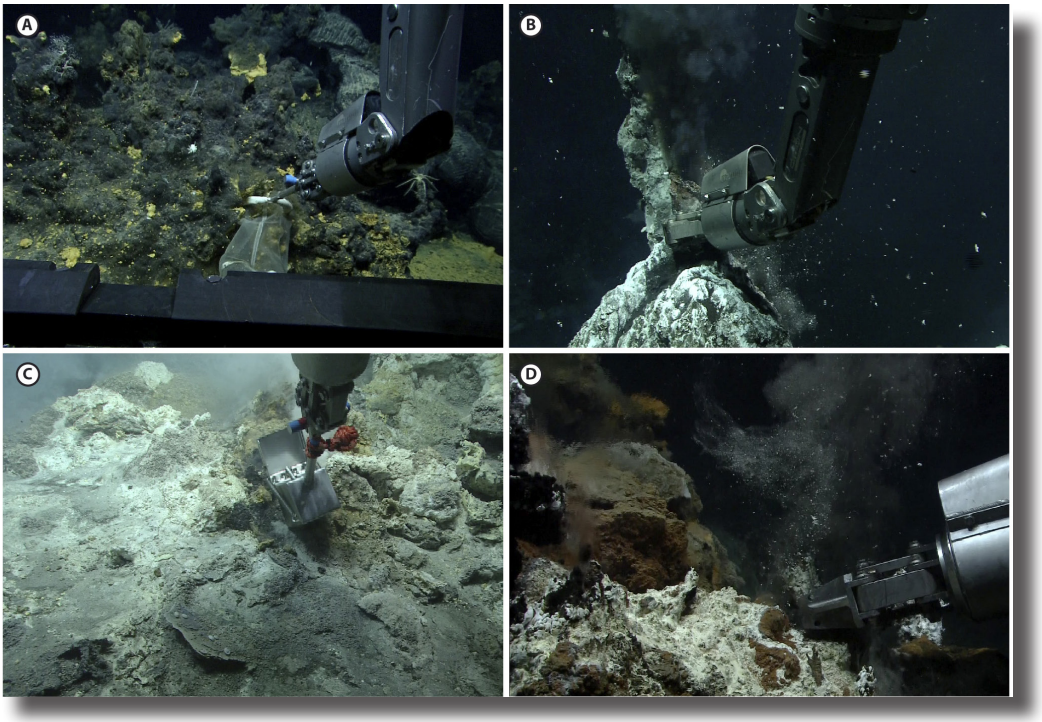

Fig. 8.3: Collection of rock samples by different means. A: Scoop sample of very fragile altered rocks at E2-West. B: Grab of a vigorously venting chimney at E2-South. C: Shovel sample of native sulfur precipitates next to a white smoker vent at Toxic Castle, Kemp Caldera. D: Grab of a small chimney fragment of an actively venting orifice at the northern rim of Kemp Caldera. All photos ®MARUM QUEST.

Tab. 8.2: List of rock samples recovered with ROV Quest

Sample ID	Date/ Time	Location	Description
PS119-017-1R	27.04.10 23:12	**E2-West**	highly vesicular and fragile white rock with black crusts. -> intensively altered lava (advanced argillic alteration) with manganese crusts
PS119-020-4B	29.04.19 17:52	**E2-South**	three handspecimen (1 altered rock and 2 chimney pieces) inadvertantly sampled with the net during biological sampling
PS119-020-5R	29.04.19 19:27	**E2-South**	small crumbles of an actively venting chimney sampled for fluids. Sphalerite-rich, abundant sulfate, traces of an inner conduit (cpy).
PS119-020-9R	29.04.19 21:09	**E2-South**	Sphalerite-rich and sulfate-rich largely intact chimney specimen of a flange structure. Transect from white crusts (silica) to an inner conduit made of sphalerite and sulfate.
PS119-020-12R	29.04.19 23:55	**E2-South**	Large piece of a Fe-sulfide-rich and sulfate-rich actively venting orifice. Abundant chalcopyrite disseminated in the interior.
PS119-028-5R	07.05.19 14:38	**Kemp Caldera Cone**	small piece of an aphyric and sparsely vesicled black basaltic rock with crusts of native sulfur
PS119-028-6R	07.05.19 14:53	**Kemp Caldera Cone**	one larger and 3 small pieces of a sparsely plagioclase phyric basaltic rock with sparse vesicles and traces of native sulfur. Surface extensively altered to pale grey. Several mm thick layers of Fe-oxihydroxides
PS119-028-7R	07.05.19 15:03	**Kemp Caldera Cone**	one larger piece and crumbles of yellow-orangish crystalline native sulfur with varying crystal sizes. Rims are oxidized to white color. Small fragments of black particles (presumably sulfides)
PS119-028-11R	07.05.19 16:45	**Kemp Caldera Cone**	1 small piece and crumbles of a black-colored chimney structure growing at the edge of a flange. Contains abundant bornite (colors of peacock ore) and traces of sulfate and native sulfur.
PS119-028-18R	07.05.19 19:52	**Kemp Caldera Cone**	Scoop sample of a mound crust. Abundant globular drops of solidified liquid native sulfur. Abundant sulfate crystals (probably anhydrite) and Fe-oxihydroxides. Crust has a brecciated character with different fragments entrained.
PS119-033-3B	11.05.19 14:14	**Kemp Caldera Cone**	Rocks entrained in a bionet sample of clams. Fragments of grey porphyritic rocks and black glassy material. Traces of white precipitates and fragments of clamp shells.
PS119-042-2R	14.05.19 21:37	**Kemp Caldera Northern Rim**	Chimney debris from next to an active oricifice. One larger piece and crumbles of a Sphalerite-rich specimen with traces of Cu-sulfides (presumably bornite) and abundant sulfate in the inner conduit.
PS119-042-3R	14.05.19 21:50	**Kemp Caldera Northern Rim**	One small specimen of actively venting orifice. Mineralogy similar to sample 042-2R. Additional traces of Fe-Sulfides and abundant white crusts (silica and microbial mats?) at the rim.

Preliminary (expected) results

Our investigations on the E2 segment will provide information about the long-term development of the hydrothermal systems at E2-South. We have seen dramatic changes in some orifices like “Cindys Castle”, where formerly active vents became inactive. Our measured hydrothermal fluid temperatures of 320 °C and 344 °C compare well to the temperature data of hydrothermal fluids sampled in 2010 (James et al., 2014), which were between 331 °C and 351 °C for E2 high-temperature black smoker chimneys. Furthermore, our pH values of 3.2 and 3.3 are only slightly higher than pH values published in James et al. 2014. They measured pH values between 2.9 and 3.14. Our measured Fe concentrations of 610 µM and 898 µM are slightly lower than the range of 728 – 1350 µM presented by James et al. (2014). Our comparably lower temperatures and Fe concentrations in combination with the higher pH values are likely a consequence of a higher dilution of our samples with seawater. These preliminary results suggest that the conditions in the root-zone of the hydrothermal systems in the E2-south area have not undergone dramatic changes during the last decade. However, we are keen to see the shore-based analyses and compare the fluid chemistry data with the data of our British colleagues. Our chimney samples from the E2-South area are typical for this kind of high temperature hydrothermal environment and are dominated by Zn-sulfides and Fe-sulfides and contain varying amounts of sulfate and Cu-sulfides (chalcopyrite) in the center of the chimneys. The mineralogical composition of the samples will be also compared with the data of James et al. (2014).

In the new discovered E2-West diffuse venting site we recovered a 50 °C fluid with a pH of 6.2 and a fairly high CH4 concentration of 1.6 µM. This fluid compositions appears especially interesting in the combination with the recovered rock sample: The scientists on board had lively discussions during the cruise about if this rock is composed of barite or if this rock is an altered volcanic rock composed of mainly silica. If latter is the case this rock suggests hydrothermal alteration under acidic conditions which seems contradictive to the high pH value measured for this fluid. A mineralogical study will be carried out at the Department of Geosciences, University of Bremen and provide the answer to this question.

Our second research area, Kemp Caldera, is dominated by either vigorously venting white-smoker fluids, high temperature vigorously venting clear fluids or diffuse vents. We have successfully recovered one high temperature clear fluid with the lowest pH value of 2.3 measured during this cruise. The temperature of this fluid was 231 °C and the fluid has the highest Fe concentration of 1,820 µM measured during the cruise. The hydrothermal precipitates at Kemp Caldera are clearly dominated by mineralization of native sulfur. This type of mineralization and hydrothermal fluids with low pH values suggest that the input of volcanic SO2 affects the hydrothermal fluids. The appearance of liquid native sulfur at Toxic Castle underlines that influx of volcanic volatiles affects the hydrothermal vents. Unfortunately, our sampling of hydrothermal fluids at Toxic Castle failed due to clogging of the samplers by liquid sulfur that solidified upon entrainment into the sampler. Apart from native sulfur we recovered an entirely black chimney that seem to consist almost entirely of high-grade Cu-sulfide (bornite). Acidic fluids have a high potential to mobilize metals from basement rocks and the high Fe concentration found at Kemp Caldera and the deposition of the Cu-rich mineralization might be also a consequence of inflowing magmatic volatiles. Our observations are in concordance with the flat REE pattern for diffuse hydrothermal fluids presented by Cole et al. (2014). These flat REE pattern are typical for acidic conditions in hydrothermal environments affected by volcanic degassing of SO2. The fluid samples recovered in the Kemp Caldera during our cruise are scarce but promising and will comprehend previous findings of our British colleagues. The planned chemical analyses will shed light on the character of the hydrothermal fluids in the ESR and the SSA.

Data management

The rock & fluid samples will be stored and processed at the Department of Geosciences of the University of Bremen. All data collected and generated by this project will be made publicly available via the World Data Center PANGAEA Data Publisher for Earth & Environmental Science (www.pangaea.de).

References

Cole CS, James RH, Conelly DP, Hathorne EC (2014) Rare earth elements as indicators of hydrothermal processes within the East Scotia subduction zone system. Geochimica et cosmochimica acta, 140, 20-38.

German CR, Livermore RA, Baker ET, Bruguier NI, Connelly DP, Cunningham AP, Morris P, Rouse IP, Statham PJ, Tyler PA (2000) Hydrothermal plumes above the East Scotia Ridge: an isolated high-latitude back-arc spreading centre. Earth and Planetary Science Letters, 184, 241-250.

Hawkes JA, Conelly DP, Gledhill M, Achterberg EP (2013) The stabilization and transportation of dissolved iron from high temperature hydrothermal vent systems. Earth and planetary science letters, 375, 280-290.

James HJ, Green DRH, Stock MJ, Alker BJ, Banerjee NR, Cole C, German CR, Huvenne VAI, Powell AM, Conelly DP (2014) Composition of hydrothermal fluids and mineralogy of associated chimney material on the East Scotia Ridge bac-arc spreading centre. Geochimica et cosmochimica acta, 140, 20-38.

Seewald JS, Doherty KW, Hammar TR, Liberatore SP (2001) A new gas-tight isobarc sampler for hydrothermal fluids. Deep-sea research I, 49, 189-196.

Reeves EP, Seewald JS, Saccocia P, Bach W, Craddock PR, Shanks WC, Sylva SP, Walsh E, Pichler T, Rosner M (2011) Geochemistry of hydrothermal fluids from the PACMANUS, Northeast Pual and Vienna Woods hydrothermal fields, Manus Basin, Papua New Guinea. Geochimica et cosmochimica acta, 75(4),1088-1123.

9. MAPR DEPLOYMENTS

Miriam Römer[1], Yi-Ting Tseng[2], Ines Vejzovic[1], Victoria Kürzinger[1], Stefanie Gaide[1], Nontje Rücker[1], Sharon Walker[3] (not on board)

[1]GeoB, Bremen
[2]MARUM, Bremen
[3]NOAA, Seattle

Grant-No. AWI_PS119_00

Objectives

Hydrothermal fluids discharged from venting sites rise buoyantly and expand by incorporation of seawater. The rising hydrothermal plume eventually reaches a neutral buoyancy layer, where it spreads laterally and is carried away by ocean currents. Such plumes or effluent layers have distinctive hydrographic, optical and chemical characteristics, and can be located by tracing respective anomalies in the water column. For this purpose we used two self-contained miniature autonomous plume recorders (MAPRs) built by the Pacific Marine Environmental Laboratory (PMEL), Seattle. Each MAPR contains the following probes: 1) a pressure gauge with a range of 0-400 bars to record the water depth; 2) a thermistor with a resolution of 0.001°C mounted in a titanium probe; 3) a light back scattering sensor (LBSS, or “nephelometer”) that senses scattered light from a small volume within centimeters of the sensor window; and 4) an oxidation-reduction potential (ORP) sensor that responds to reduced hydrothermal chemicals in the water column. ORP detects hydrothermal discharge of all temperatures, including low-temperature diffuse venting as well as higher-temperature but particle-poor sources. It responds immediately, with decreasing potential values (E(mV)), to the presence of nanomolar concentrations of reduced hydrothermal chemicals such as Fe^{+2}, HS^{-}, H_2 that are out of equilibrium with the oxidizing ocean (Walker et al., 2007). These chemicals rapidly oxidize or metabolize in close proximity to their seafloor source.

Work at sea

During PS119 the MAPRs were mounted onto the ROV, attached to the OFOBS and to the CTD (Fig. 9.1). On the ROV and the OFOBS, one MAPR was installed in the lower part of the frame, in areas were the sensors could be placed well exposed to the water column. During all CTD casts, a MAPR was installed within the frame of the rosette, from which two bottles were taken off and the sensors again were well exposed to the water flowing through. A second MAPR was installed for most CTD casts in addition at the wire above the rosette. The distance between rosette and MAPS was in most areas 50 m, except in the WOW area a smaller distance of 20 m was chosen due to the expected low rising fluids.

In total, 37 deployments were successfully conducted during PS119, 3 further stations were cancelled before deployment and at one station the data was not recorded due to a programming mistake (Table 9.1). 16 CTD casts, 9 OFOBS deployments and 7 ROV dives were equipped with MAPRs. With 18 and 13 deployments, most deployments were conducted in the Kemp Caldera and E2, respectively. Only one record was taken in South Georgia, one in the Forearc, two in E5 and four in the WOW area (Fig. 9.2).

The MAPR performance was very good, besides the first four deployments of the MAPR with the ID 49, which showed erroneous data in the ORP sensor. After changing the sensor batteries, the error did not occur anymore. Most of the data of these four deployments can be still used and only some part of the data is not usable due to data quality affected by the erroneous behavior.

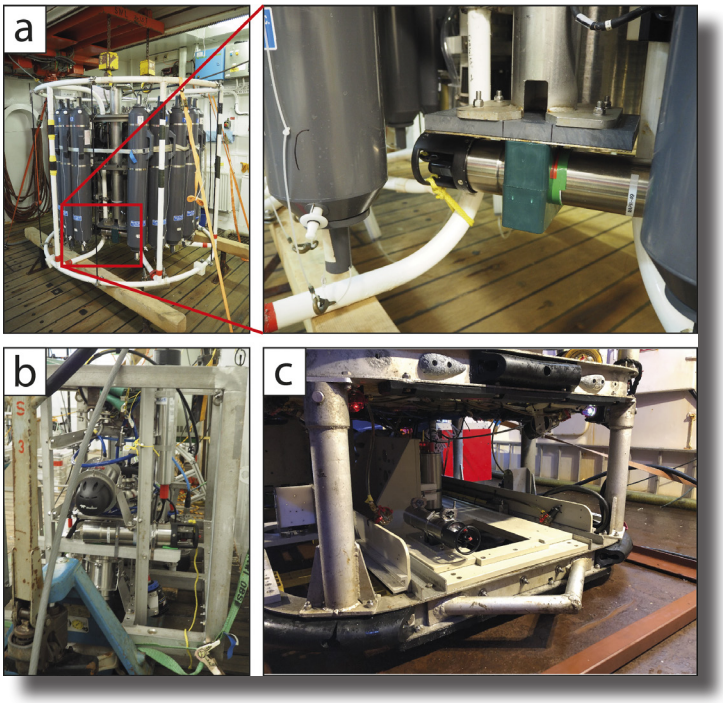

Fig. 9.1: Pictures illustrating the MAPR installations at three different devices: a) within the CTD rosette, b) at the lower front of the OFOBS, c) at the lower back of the ROV

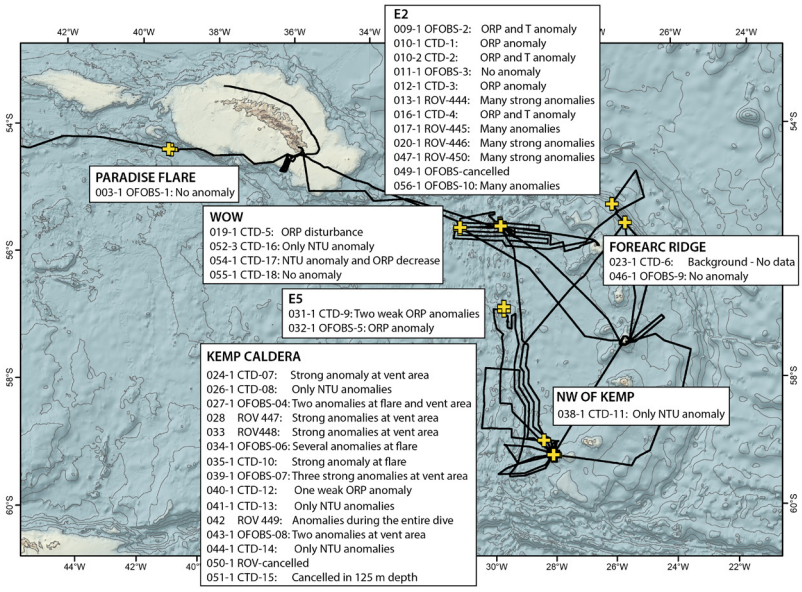

Fig. 9.2: Overview map of all MAPR deployments during PS119 including a short comment of their preliminary results

Preliminary (expected) results

MAPRs were deployed in five different work areas for the purpose of either detecting new vent areas or mapping and characterizing known vent areas:

South Georgia

At a known gas seep site found in 2017 during *Meteor* cruise M134, called Paradise flare, the first OFOBS deployment was conducted including the first MAPR record. The sensors did not show any anomaly in all sensors. As USBL positioning failed during this deployment, one explanation is that the site was missed or the other explanation, that it is not expected to detect an ORP or nephelometer signal at pure methane bubble emissions. Temperatures of seep sites might be slightly elevated, however only measurable in very close proximity to the emission site.

E2

MAPR were installed at four CTDs, three OFOBS deployments and four ROV dives conducted at E2. Except OFOBS-03, which was cancelled shortly after reaching the seafloor, all deployments revealed anomalies in the sensors of the MAPR.

The area most investigated was in the southern sector of E2, which was known for numerous active black smokers. ROV dive 444 was investigating several of these smokers and the respective MAPR plot is shown in Fig. 9.3a. The new discovered and investigated area found in the western sector of E2 was surveyed during ROV dive 445. No active black smokers were found, but extinct chimneys and build-ups with yellowish material that were accompanied with clear fluid escape indicated by shimmering water were seen several times. The MAPR data acquired during this dive (Fig. 9.3b) indicates less intense ORP but in the same places at least similar high temperature anomalies as seen in E2 south.

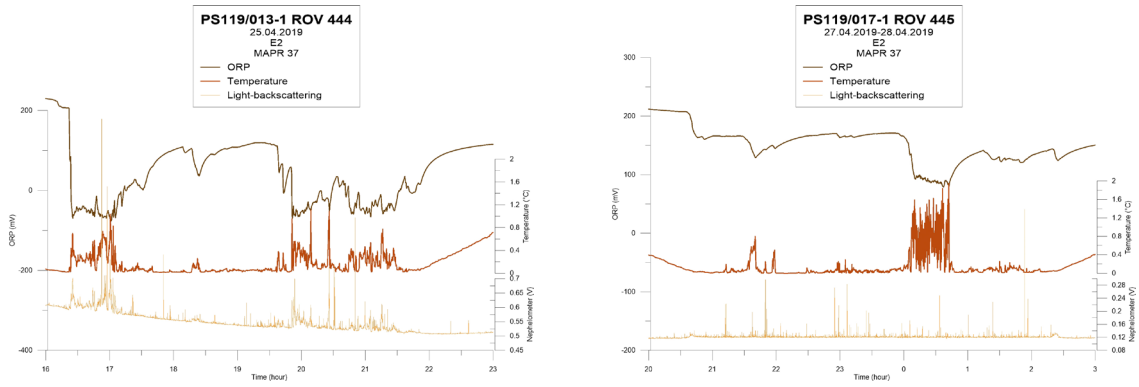

Fig. 9.3: MAPR data acquired during two ROV dives in a) E2 south and b) E2 west. ORP reactions are much higher in E2 south, and nephelometer anomalies only occurred in E2 south. However, temperature anomalies are in the same range detected in E2 west.

WOW

The WOW area located west of E2 has been investigated due to the finding of a water column anomaly visible in the ships mounted Parasound echosounder. MAPRs have been mounted on 4 CTDs, at all of them with a MAPR installed in the frame and in 3 of the four deployments in addition with a second MAPR about 20 m above the CTD at the wire. Two deployments showed a very weak anomaly in the ORP sensor during the downcasts and the two deployments

directly positioned into the suspicious echosounder anomaly indicated a slight increase in the nephelometer close to the bottom. However, no undoubting prove for fluid escape can be presented.

E5

In E5, no hydrothermal venting was known yet and stations conducted in this segment had an exploratory character. CTD-9 and an OFOBS-5, both equipped with MAPRs, were deployed in an area where hydrothermal activity was suspected to be most probably, at the most uplifted part in the central rift axis. In both deployments, two relatively weak but apparent anomalies in the ORP sensor were detected, suggesting a source of hydrothermal fluids in the area, but not sourcing at the seafloor exactly where the deployments have been conducted. More mapping would have been needed to locate the source of hydrothermal activities and investigate them.

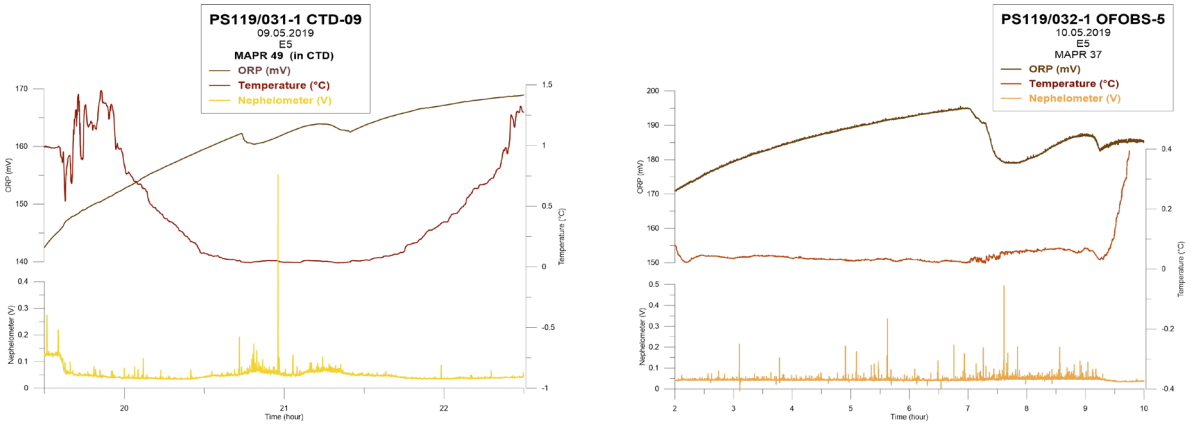

Fig. 9.4: MAPR data acquired during a) a CTD cast and b) an OFOBS deployment at E5. Small anomalies of the ORP signal were detected in both indicating the presence of hydrothermal fluid source(s) close but not exactly at the deployment sites.

Forearc

In the forearc area, dredging suggested possible serpentinization, which could cause methane production and hence fluid seep sites. During PS119, special focus was on finding seep sites in the forearc, where also during *Polarstern* cruise ANT-XXIX/4 (PS81) a potential seep site (*Polarstern* Seep) was detected with the hydroacoustic systems. During this cruise *Polarstern* Seep was detected again as well as three further similar anomalies located at a ridge structure, at which these earlier dredge findings indicate serpentenization. OFOBS-9 was deployed at the most intense appearing anomaly to investigate the seafloor and record the MAPR signals during the tow. However, any anomaly could prove the existence of seeping fluids from the seafloor.

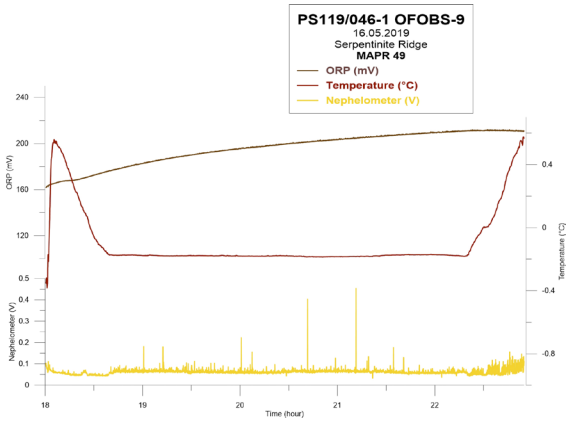

Fig. 9.5: MAPR data acquired at the Forearc, where a plume-like anomaly was detected using hydroacoustic systems. All three sensors of the MAPR show typical background data lacking anomalies.

Kemp Caldera

In total, 7 CTDs were deployed within the Kemp Caldera, Two of these CTDs were deployed at known fluid emission sites, one at the flare site at the inner rim of the caldera and one in the vent area at the cone in the center of the caldera. The other CTDs were taken in other areas within the caldera without evidence of fluid seepage. Finally, one CTD was deployed about 5 km outside the Caldera as a reference.

In addition, 4 OFOBS-deployments and 3 ROV dives equipped with a MAPR were conducted at the Kemp Caldera.

All deployments at the vent area were characterized by very strong anomalies in all sensors. Fig. 9.6a shows a CTD cast within the vent area illustrating the strong reactions close to the seafloor. Those deployments at the flare site were also accompanied by anomalies in all sensors, but less intense when compared to the vent area. A CTD cast conducted at the flare site is given in Fig. 9.6b for comparison. Please note the different scales on the y-axis, especially for the nephelometer the values are an order of magnitude higher in the vent area. Also different is the height of the recognized plume, as both MAPR are similarly affected in the vent area, although the second MAPR is installed 50 m above the CTD. In contrast, the MAPR installed 50 m above at the wire at the flare site did not recognize any anomaly.

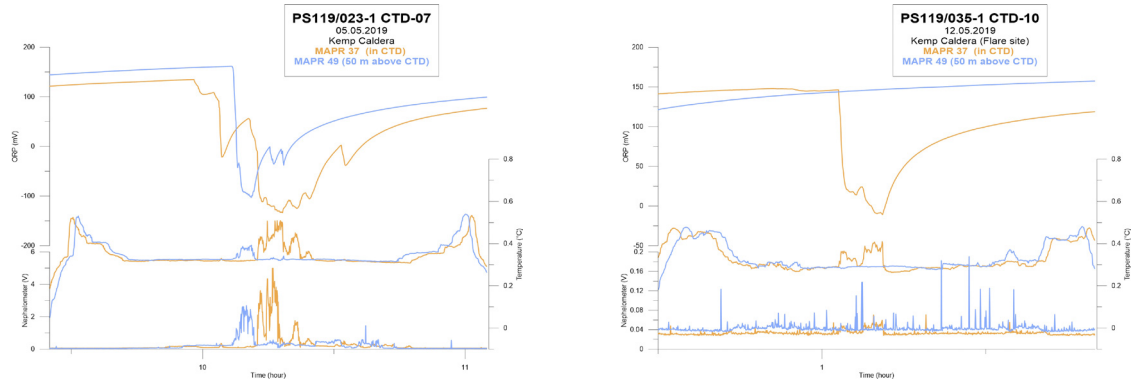

Fig. 9.6: MAPR plots for two CTD casts deployed in the Kemp Caldera

Tab. 9.1: Deployment list of both MAPRs during PS119 including preliminary observations

Event	ID	Station no. PS119_	Area	Device	Height	Comment
1	37	003-1	South Georgia	OFOBS-1	in frame	No anomaly
2	49					Cancelled ROV dive
3	49	009-1	E2	OFOBS-2	in frame	Anomaly in ORP
4	37	010-1 and -2	E2	CTD-1 and -2	in frame	Anomaly in ORP in CTD-1 and -2 and temperature peak at CTD-2
5	49	010-1 and -2	E2	CTD-1 and -2	50 m	Anomaly in ORP in CTD-2
6	37	011-1	E2	OFOBS-3	in frame	Dive was aborted after short time, no anomaly
7	49	012-1	E2	CTD-3	in frame	Anomaly in ORP
8	37	012-1	E2	CTD-3	50 m	Anomaly in ORP
9	37	013-1	E2	ROV-444	in frame	Many anomalies in all sensors above active vent fields

Event	ID	Station no. PS119_	Area	Device	Height	Comment
10	37	016-1	E2	CTD-4	50 m	Two anomalies in ORP and one with temperature peak
11	49	016-1	E2	CTD-4	in frame	ORP not usable, but temperature peak and also nephelometer
12	37	017-1	E2	ROV-445	in frame	Anomalies in ORP and temperature close to new vent fields
13	37	019-1	WOW	CTD-5	in frame	No anomaly, but disturbed curve
14	49	019-1	WOW	CTD-5	20 m	No anomaly
15	37	020-1	E2	ROV-446	in frame	Many anomalies in all sensors above active vent fields
16	49	023-1	Forearc	CTD-6	in frame	Wrong programming - no data
17	37	024-1	Kemp Caldera	CTD-7	in frame	Strong anomalies in all sensors
18	49	024-1	Kemp Caldera	CTD-7	50 m	Strong anomalies in all sensors
19	37	026-1	Kemp Caldera	CTD-8	in frame	In both downcast and upcast an anomaly in nephelometer
20	37	027-1	Kemp Caldera	OFOBS-4	in frame	Two anomalies in ORP, both with T increase and the second also in nephelometer
21	49	028-1	Kemp Caldera	ROV-447	in frame	Anomalies in all sensors during the entire dive
22	49	031-1	E5	CTD-9	in frame	Two small anomalies in down and upcast in the water column, in ORP and also increase in nephelometer
23	37	032-1	E5	OFOBS-5	in frame	Two anomalies in ORP, temperature slightly increased
24	37	033-1	Kemp Caldera	ROV-448	in frame	Many anomalies during the second part of the dive
25	49	034-1	Kemp Caldera	OFOBS-6	in frame	Numerous anomalies in all sensors during the entire deployment
26	37	035-1	Kemp Caldera	CTD-10	in frame	Anomaly at the lowermost point, visible in all sensors
27	49	035-1	Kemp Caldera	CTD-10	50 m	No anomaly
28	37	038-1	Kemp Caldera	CTD-11	in frame	No anomaly
29	49	039-1	Kemp Caldera	OFOBS-7	in frame	Three strong anomalies visible in all sensors
30	37	040-1	Kemp Caldera	CTD-12	in frame	One weak anomaly in ORP, slightly visible also in nephelometer during downcast, minor kink during upcast
31	37	041-1	Kemp Caldera	CTD-13	in frame	Two anomalies in nephelometer, both during downcast and upcast at same depth. No anomalies in ORP and temperature
32	49	042-1	Kemp Caldera	ROV-449	in frame	Anomalies in all sensors during the entire dive
33	37	043-1	Kemp Caldera	OFOBS-8	in frame	Two anomalies in all sensors
34	49	044-1	Kemp Caldera	CTD-14	in frame	Two anomalies in nephelometer, both during downcast and upcast at same depth. No anomalies in ORP and temperature
35	49	046-1	Forearc	OFOBS-9	in frame	No anomalies

Event	ID	Station no. PS119_	Area	Device	Height	Comment
36	37	047-1	E2	ROV-450	in frame	Anomalies in all sensors during the entire dive
37	37	049-1	E2	OFOBS-10	in frame	Cancelled before deployment into water
38	49	050-1	Kemp Caldera	ROV-451	in frame	Cancelled before deployment into water
39	37	051-1	Kemp Caldera	CTD-15	in frame	Cancelled after 125 m water depth reached
40	49	052-3	WOW	CTD-16	20 m	Only slight increase in light scattering close to bottom
41	37	052-3	WOW	CTD-16	in frame	Only slight increase in light scattering close to bottom
42	49	054-1	WOW	CTD-17	in frame	Only slight increase in nephelometer
43	37	054-1	WOW	CTD-17	20 m	Weak anomaly in ORP during downcast, slight increase in nephalometer
44	49	055-1	WOW	CTD-18	in frame	No anomaly
45	37	056-1	E2	OFOBS-11	in frame	Several anomalies in all sensors crossing the vent area

Data management

The raw data files (.datx) were processed and georeferenced using the USBL positioning (when available) for geographical plots in ArcGIS. Graphical plots were produced in addition using Golden software Grapher. The raw data files converted to excel tables as well as the summarizing table (Table 9.1) will be made publicly available via the World Data Center PANGAEA Data Publisher for Earth & Environmental Science (www.pangaea.de).

References

Walker SL, Baker ET, Resing JA, Nakamura K, McLain PD (2007) A new tool for detecting hydrothermal plumes: an ORP Sensor for the PMEL MAPR. Eos Trans, AGU88 (52). Fall Meet. Suppl., Abstract V21D-0753.

10. SEDIMENT CORES

Anna Lichtschlag[1], Maximilian Franke[2], Benedikt Geier[2]; Marcello Arevalo-Gonzales[3], Pascal Daub[3], Chris Jones[4], Adrian Höfken[3], Crispin Little[5], Norbert Lensch[3]

[1]NOCS, Southampton
[2]MPI, Bremen
[3]AWI, Bremerhaven
[4]OkState, Stillwater
[5]SEE-UL, Leeds

Grant-No. AWI_PS119_00

Objectives

During PS119 sediment cores were collected with a gravity corer (GC), a piston corer (PC), a multi corer (MUC) and with push cores (PUC) deployed by the ROV. Our target areas were South Georgia, the South Sandwich Islands and the Kemp Caldera. Locations for sampling were selected based on different objectives explained in the chapters 11-13, with the main focus on collecting solid phase material, fluids and gases to study sedimentological, geochemical, geomagnetic and physical properties, and micropaleontological parameters of the sediments from the different areas. The gear types and the length of the coring devices were chosen based on lithological information derived from sediment acoustic profiles provided by the echosounding system. A total of 20 gravity corer, 3 piston corer, 13 multi corer (MUC) deployments were performed and 11 push cores (PUC) were recovered successful.

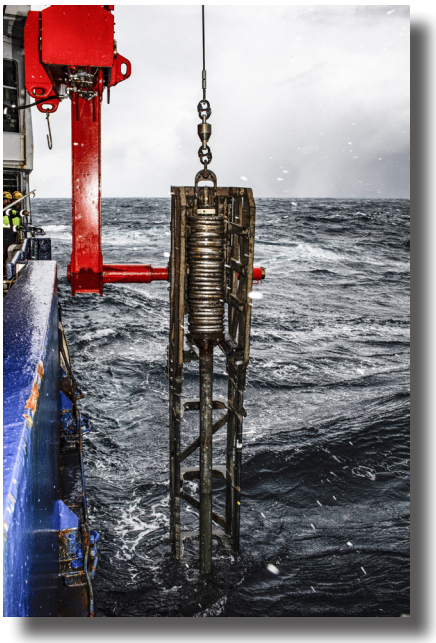

Fig. 10.1: Deployment of the gravity corer (photo: Holger von Neuhoff)

Work at sea

Gravity Corer

The gravity corer (Fig. 10.1) was fitted with core barrels of either 3 or 5 m length, which also were combined to longer cores, a head weight of about 1.5 tons and a core catcher. Core liners were composed of opaque PVC-tubes cut to length and with a diameter of 125 mm. The gravity corer was deployed along the starboard side of the vessel and was lowered with a rope speed of 1.5 m/s to the seafloor. Contact with the seafloor was monitored via the cable tension and after seafloor contact the corer was pulled out with a speed of 0.2 m/s and a heave velocity was 1.2 m/s.

On board or in the wet lab, the gravity cores were cut into 1-m long sections and sealed at both ends with endcaps. The sections were either stored away or split open horizontally. After splitting, photos were taken of the working and archive halves and both halves were covered with cling film. The working halves were immediately transported to a cold room to subsample

for geochemistry, mineralogy and microbiology (chapter 12 and 13). A first sedimentological description was done on the archive halves of the cores and the color of the sediments was determined using the Munsell Soil Color Chart. The lithology was visualized with the help of the STRATER 5.3.873 software. Afterwards the archive halves were warmed to room temperature and then logged for their sediment properties (chapter 11). Both halves were stored in D-tubes and labeled.

Piston Corer

The piston corer has core barrels of 5 m length that have been attached to each other to collect longer sediment cores. The piston corer was lowered with a rope speed of 1.0 m/s, lowered to 0.2 m/s before contact and heaved with 0.5 m/s. Core liners were composed of opaque PVC-tubes cut to length and 90 mm diameter. Upon recovery the piston cores were treated similarly as the gravity cores, except that the split core sections were not stored in D-tubes, but in transparent foil that was sealed at both ends with a heat sealer.

Multicorer

The multi corer (Fig. 10.2) was fitted with 12 transparent core liners with a diameter of 67 mm and a length of 60 cm. The multi corer was lowered to the seafloor with a rope speed of 1.2 m/s and the speed at bottom contact varied in between 0.4 and 0.9 m/s depending on the sediment type. Contact with the seafloor was monitored via the cable tension. The device was then pulled out with a speed of 0.1 m/s. Heave velocity was 0.5 m/s. After recovery the multicores were capped with rubber bungs at both sides, the length of the recovered sediment was measured and they were photographed and distributed.

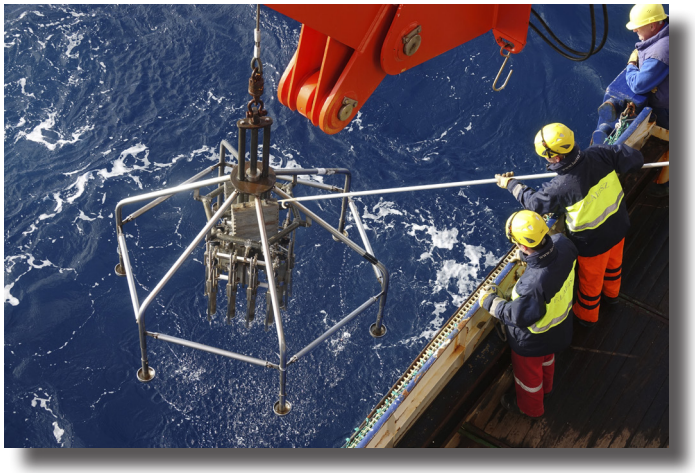

Fig. 10.2: Recovery of the multi corer (photo: Allan Derrien)

Push Cores

Push cores (Fig. 10.3: 70 mm diameter, ca. 30 cm length) were taken with the help of the ROV manipulator arm during 3 ROV dives at Kemp Caldera. After the ROV recovery the push cores were subsampled on deck as they had a strong sulfidic smell.

Fig. 10.3: Push core sampling in a clam bed at the Kemp Calera (photo: MARUM)

Preliminary results

Gravity Cores

Altogether, the gravity corer was deployed 20 times, 18 of the deployments were successful and in between 1.6 m and 9.4 m of sediments were recovered (Table 10.1). 12 of the cores were split and analyzed in detail for pore water sand solid phase geochemistry (AWI/BPS/NOC) and the remaining cores were stored away for sedimentological and micropaleontological work at AWI (AG Gerhard Kuhn), after measuring the physical properties. The sediment descriptions of the archive halves of the cores showed that the sediments differed substantially in between the different target areas. The cores close to South Georgia had a green-grey color, were more homogenous, some of them showed degassing structures and they smelled of sulfide. Closer to the hydrothermal areas the background sediments often consisted of layers of soft, beige-brown diatomaceous ooze and slightly darker and stiffer mud and the upper sediment layers were of more-red brown color. Coarse, dark layers were found in the sediment (Fig. 10.4), that could potentially be ash layers, glacially transported rocks or turbidities, which will be determined in more detailed on shore. Occasionally, the black layers had (red or transparent) volcanic glass particles interspersed. Dropstones of different size (mm- to cm-scale) were frequently found in the sediments. Slightly different sediments were collected from the Kemp Caldera, where thick layers of unconsolidated diatomaceous ooze of black, green, white and grey color was only occasionally interspersed with dark brown sandy sediments. A more detailed sediment description and the sediment logs can be found in Appendix 5.

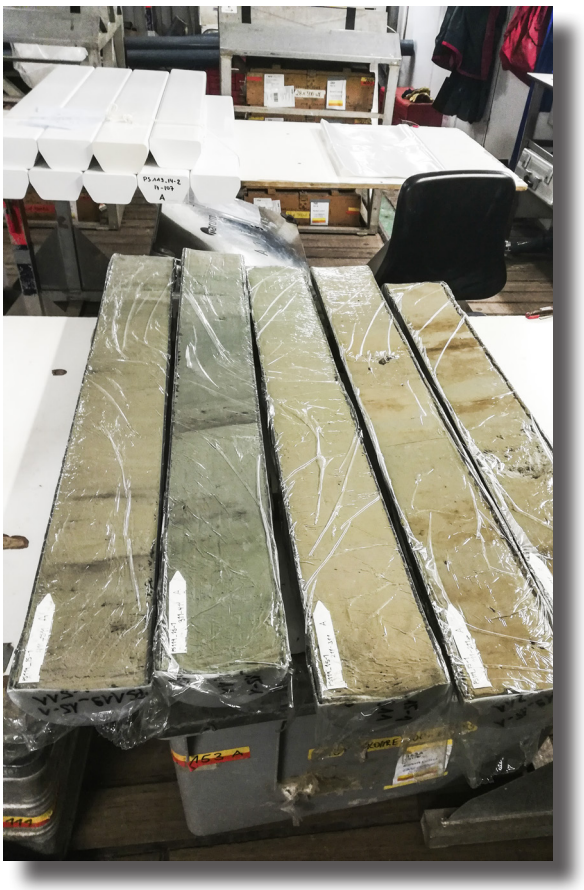

Fig. 10.4: Archive halves of a gravity core taken at the South Sandwich Islands (PS119_25_1/GC 14). (photo: Anna Lichtschlag)

Tab. 10.1: List and gravity cores details (SK: Sabine Kasten (AWI), GK: Gerhard Kuhn (AWI), NR: Natasha Riedinger (BPS), AL: Anna Lichtschlag (NOC))

Station	GC-no.	Location	Water depth [m]	Total length [cm]	No. of sections	Section length [cm]	Measure-ment
PS119_001-2	GC-01	SW of South Georgia	3620	389	4	0-90 90-189 189-289 289-389	GK
PS119_002-1	GC-02	SW of South Georgia	3524	653	7	0-53 53-152 152-252 252-353 353-453 453-553 553-653	GK
PS119_004-1	GC-03	Drygalski Fjord	225	empty	empty	empty	empty
PS119_004-2	GC-04	Drygalski Fjord	225	471	5	0-85 85-185 185-287 287-387 387-487	SK
PS119_005-1	GC-05	Drygalski Trough	290	822	9	0-33 33-133 133-232 232-332 332-436 436-536 536-636 636-736 736-822	GK
PS119_006-1	GC-06	Drygalski Trough	287	840	9	0-50 50-150 150-250 250-350 350-451 451-552 552-640 640-740 740-840	GK
PS119_007-1	GC-07	Drygalski Trough	323	940	10	0-49 49-149 149-248 248-348 348-448 448-548 548-648 648-740 740-840 840-940	GK
PS119_008-1	GC-08	Drygalski Trough	291	442	5	50-140 140-242 242-342 342-442 112-542	GK

Station	GC-no.	Location	Water depth [m]	Total length [cm]	No. of sections	Section length [cm]	Measure-ment
PS119_014-2	GC-09	ESR - East of E2	2776	506	5	17-107 107-206 206-306 306-406 406-506	NR
PS119_0015-1	GC-10	ESR - East of E2	3034	511	5	25-111 111-211 211-311 311-411 411-511	NR
PS119_018-2	GC-11	ESR - E2	3266	814	9	0-35 35-125 125-224 224-324 324-414 414-514 514-614 614-714	NR
PS119_0021-1	GC-12	ESR - E2 West	3363	309	3	22-109 109-209 209-309	NR
PS119_0022-1	GC-13	ESR - E2 West	3342	670	7	0-610	NR
PS119_0025-1	GC-14	ESR - E9	2899	231	3	0-37 37-131 131-231	NR
PS119_029-1	GC-15	ESR - E9	2631	3450	5	0 -50 50-150 150-250 250-350 350-450	NR
PS119_036-2	GC-16	Kemp Caldera	1619	159	2	0-66 66-159	AL
PS119_048-2	GC-17	ESR - E2	2909	empty	empty	empty	empty
PS119_052-1	GC-18	ESR - E2 West (WOW)	3355	500	5	12-100 100-200 200-300 300-400 400-500	NR
PS119_057-1	GC-19	ESR - E2 West (WOW)	3329	796	8	10-111 111-210 210-310 310-410 410-496 496-596 596-696 696-796	NR

Station	GC-no.	Location	Water depth [m]	Total length [cm]	No. of sections	Section length [cm]	Measure-ment
PS119_058-1	GC-20	Drygalski Trough	283	865	9	0-66 66-160 166-266 266-366 366-466 466-566- 566-666 666-765 765-865	SK

Piston Corer

The Piston corer was deployed 3 times (during one deployment the corer was bent, but the sediments were still recovered) and sediment cores in between 2.3 and 11.7 m were recovered. All piston cores were subsampled on board and occasionally also the trigger core was processed. The recovered sediments were similar as those from the gravity cores and sediment description can also be found in the Appendix.

Tab. 10.2: List and section length of piston cores (NR: Natasha Riedinger (BPS), AL: Anna Lichtschlag, (NOCS))

Station	PC-no	Location	Water depth [m]	total length [cm]	No. of sections	Section length [cm]	Measure-ment
PS119_030-1	PC-01	ESR - E9	2895	1173	13	0-59 TC 0-76 76-176 176-277 277-377 377-477 477-577 577-676 676-775 775-875 875-974 974-1073 1073-1173	NR
PS119_037-1	PC-02	ESR - E8	2637	867	10	TC 0-63 0-74 74-174 174-274 274-374 3774-469 449-568 568-667 667-767 767-867	NR
PS119_045-1	PC-03	Kemp Caldera	1610	230	4	TC 0-40 0-30 30-130 130-230	AL (core bend)

Multi corer

The multi corer was deployed 13 times and during each deployment sediments were recovered. Mostly all 12 cores were full and longest cores were recovered from the Kemp caldera (47 cm, Fig. 10.5). Multi cores were distributed as shown in Table 10.3. In general the sediment surface of the cores was intact and had a in between 2 mm and 3 cm fresh diatom layer on top, followed by red, brown or grey layers of ooze and mud. A more detailed sediment description can be found in Table 10.3.

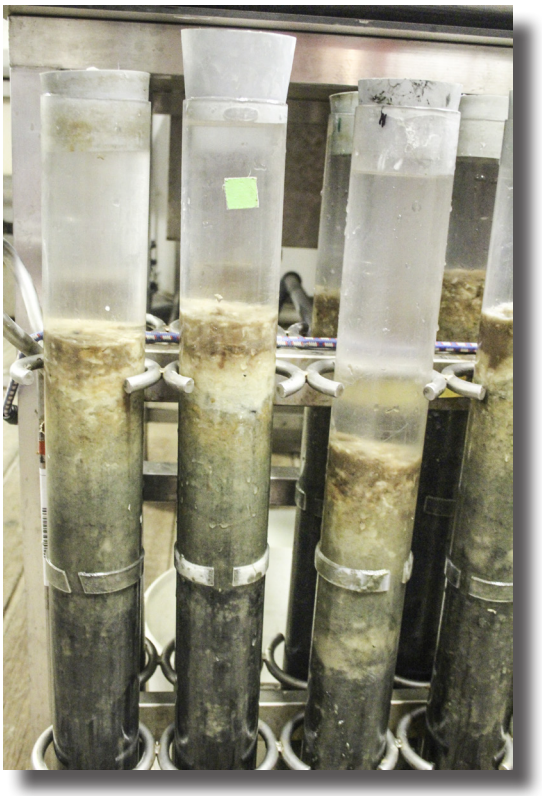

Fig. 10.5: Multicores collected from the Kemp Caldera consisted mainly of diatomaceous ooze of different color (photo: Anna Lichtschlag).

Tab. 10.3: List of multi cores collected during PS119, including sediment description and the measurements that will be performed (NR: Natasha Riedinger (BPS), TP: Thomas Pape (MARUM), KL: Katrin Linse(BAS, GK: Gerhard Kuhn (AWI), AH: Adrian Höfken (AWI), AL: Anna Lichtschlag (NOC), GB: Gerhard Bohrmann (MARUM)). The number depicts the number of cores per measurement.

Station	MUC no.	Location	Water depth [m]	Measurements*	Sediment description
PS119_001-1	MUC-01	SW of South Georgia	3621	NR: 3, TP: 1, KL: 3, GK: 3, AH: 1, AL: 1	# diatom mud, no changes in grain size visible throughout the core # first cm very fluffy, light brown # below light brown # below 17 cm beige-greenish until the end # interrupted by a layer at 28-34 cm with darker brown smears

Station	MUC no.	Location	Water depth [m]	Measurements*	Sediment description
PS119_007-2	MUC-02	Drygalski Trough	318	NR: 3, TP: 1, KL: 3, GK: 3, AL: 1	# diatom mud, no changes in grain size visible throughout the core # first cm very fluffy light brown # below light brown # below 6 cm black smears (until end of core) # below 24 cm some cores had lighter layers (without black smears) #in the first 10 cm Polychaeta burrows (and one Polychaeta)
PS119_014-1	MUC-03	ESR - East of E2	2763	NR: 3, TP: 1, KL: 3, GK: 3, AH: 1, AL: 1	# very fluffy white surface, ca 2-3 mm # 0-19 cm red-brown sediment, getting successively darker, one slightly darker red layer at 9-11 cm # 19-25cm dark brown-red layer # below beige # when slicing the core beige lumps (cm-size, silicate?) visible in the lower part of the core
PS119_015-2	MUC-04	ESR - East of E2	3034	NR: 3, TP: 1, KL: 4, GK: 3, AH: 1	# very fluffy white surface, ca 2-3 mm # 0-10 cm red-brown sediment color, many cracks developing in this layer # 10-24 cm greyish-green # 24-31 cm reddish layer # 31 cm to the end greyish layer
PS119_018-1	MUC-05	ESR - E2	3258	NR: 3, TP: 1, KL: 4, GK: 3, AH: 1	# a bit of fluff on the surface, but not as extensive as in previous cores # 0-9 cm reddish-brown, again cracks developing in this layer in several cores # 9 cm to end beige brown with dark brown-reddish layers at 9-11 cm, 18-20 cm and 30-32 cm # in some of the longer cores a little bit of a beige layer at the bottom
PS119_022-1	MUC-06	ESR - E2 West	3342	NR: 3, TP: 1, KL: 3, GK: 3, AH: 1, AL: 1	# white fluffy diatom layer (2 mm) # 0-14 cm reddish brown, gradually becoming more greyish, some cores had cracks at 5-7 cm # 14 cm to end grey

Station	MUC no.	Location	Water depth [m]	Measurements*	Sediment description
PS119_025-2	MUC-07	ESR - E9	2897	NR: 3, TP: 1, KL: 4, GK: 3, AH: 1	# no fluffy layer on top # brown-red color full length, no obvious lamination or layers in the top of the cores # bottom 5 cm have several paler layers 1-2 cm thick with diffuse boundaries, some mottling in base, also laminations of dark brown layers ca 5 mm thick, maybe clay?
PS119_029-2	MUC-08	ESR - E9	2631	NR: 3, TP: 1, KL: 3, GK: 3, AH: 1, AL: 1	# only little fluff on top # below homogenous red-brown # below 21-23 cm again more mottled # little darker brown below 30 cm
PS119_036-1	MUC-09	Kemp Caldera	1618	AL: 4, TP: 1, KL: 2, GK: 2, AH: 1, GB: 2	# 0-2 cm very fluffy beige layer, some white 0.5 cm blobs on top, at the bottom of the layer red 1/2 cm red blobs # 2-4 cm white fluff, at bottom some iron-oxide red clumps # 4-10 cm thick beige layer, still very fluffy # 10-18 cm brown-grey mottled, fluffy but compacted layer # 18-20 cm medium, white dense „cotton-like“ structure # 20-33 cm dark grey/white/ black mottled layer # 33 cm to end very black layer
PS119_037-2	MUC-10	ESR - E8	2639	NR: 3, TP: 1, KL: 4, GK: 3, AH: 1	# only very little fluff on top # 0-8 cm red brown # 8-21 cm medium grey layer # 21-31 cm potentially a bit more red here again # 31 cm - end dark grey layer
PS119_048-1	MUC-11	ESR - E2	2909	NR: 2, KL2	# some fluffy layer on top # upper 6 cm light brown, very homogeneous # 6-26 cm sharp boundary, below medium to dark grey, increasingly getting darker appearing black at the bottom, increasingly getting sandy, with white sprinkles (volcanic glass?)
PS119_052-2	MUC-12	ESR - E2 West (WOW)	3359	NR: 3, TP: 1, KL: 4, GK: 3, AH: 1	# thick fluffy layer of up to 3 cm on top, occasionally mixed into the sediment # 3 cm to end brown homogeneous brown layer, getting gradually from more red to more grey-brown

Station	MUC no.	Location	Water depth [m]	Measurements*	Sediment description
PS119_053-1	MUC-13	ESR - E2 West (WOW)	3321	NR: 4, TP: 1, KL: 3, GK: 3, AH: 1	# 2-3 mm thick, white fluffy layer on top of the sediment # 0-7 cm reddish brown sediments # 7-11cm transitional zone to more grey # 11 cm to end homogeneous grey sediment

Push Cores

Eleven push cores were collected during 3 ROV dives at the Kemp Caldera. Targets were sediments close to i) the active sites Great Wall and Toxic Castle, ii) a clam field close to the inner cone and iii) a sediment patch at a hydrothermally active site at the northern rim. All collected sediments had a strong sulfidic smell, were coarse grained and were either entirely black or had a black and white layering. For further details see Table 10.4.

Tab. 10.4: List of push cores collected during PS119, including the measurements that will be performed on the description of the sediment. Push cores were only taken at the Kemp Caldera. Methane and porosity will be measured by Thomas Pape (MARUM); pore water and solid phase will be measured by Anna Lichtschlag (NOC).

Dive	Station	PUC no	Location	Length [cm]	Measurement	Comment
447	PS119_28_1	PUC 9	Great Wall	14.5	lost during transplantation	
447	PS119_28_2	PUC10	Great Wall	22	Pore water, solid phase	# white fluffy on top # 1-2 cm grey layer # 2-4 cm black layer # below white
447	PS119_28-4	PUC11	Great Wall	12 to 15	Methane and porosity	sloping surface
447	PS119_28-9	PUC1	Toxic Castle, slope		Empty	
447	PS119_28-10	PUC2	Toxic Castle, slope		Empty	
447	PS119_28_12	PUC3	Toxic Castle	18	Pore water, solid phase	# 0-4 cm grey layer # 4-6 cm grey/white layer # 6 to end black/brown
447	PS119_28_13	PUC4	Toxic Castle	13-17	lost during transplant	sloping surface , sampled bulk, 1/2 frozen 1/2 cold, strong sulfidic smell
447	PS119_28_14	PUC12	Toxic Castle	10/12.5	Methane/Porosity	sloping surface
447	PS119_28_19	PUC5	Great Wall	9.5-15		sloping surface
447	PS119_28_20	PUC6	Great Wall	2 cm in quiver	not used	not used

Dive	Station	PUC no	Location	Length [cm]	Measurement	Comment
448	PS119_33_1	PUC6	Clam field	13	Pore water, solid phase	# lots of animals (amphipods) on top + 1 clam, sulfidic smell # no white fluff on top # 0 - 4 (5) cm: brown layer, # 4 (5) cm to 11 cm: more whitish grey #11-13 cm brownish layer at bottom (looks like different grain size?)
448	PS119_33_2	PUC3	Clam field	14	Methane/Porosity	
449	PS119_42_5	PUC2	orange/ white spot on slope	8	Pore water	# pitch black with bits of orange lumps on top # very sloping surface, so the first layer is mainly 0-1 cm # 2-3 cm black, yellow bits, very coarse, # 3-4 cm very coarse, yellow bits # 4-5 cm very coarse # 5-6 cm very coarse # 6-7 cm very coarse
449	PS119_42_6	PUC8			empty	Empty
449	PS119_42_7	PUC10	orange/ white spot on slope	6	Methane/Porosity	pitch black with big orange lump on top, soft, frozen severalty

Data management

The data management of the results that will be produced from any of these sediment cores will be described in the specific sections of this report (*cf*. chapters 11 and 12).

11. MULTI-SENSOR CORE LOGGING

Adrian Höfken[1], Marcello Arevalo-Gonzales[1], [1]AWI, Bremerhaven
Pascal Daub[1], Norbert Lensch[1]

Grant-No. AWI_PS119_00

Objectives

During *Polarstern* Cruise PS119 on board, non-destructive physical properties logging was carried out on all acquired gravity and piston cores. Core logging was done on both unopened and split sediment cores. The measurements were used as a first reference basis for core descriptions, the refinement of sampling strategies and for the evaluation of the coring site.

The measured parameters included:

-magnetic volume susceptibility κ
-wet bulk density ρ *
-p-wave velocity v_p * *measured on unopened cores only

Magnetic Volume Susceptibility Measurements

The magnetic volume susceptibility κ is a quantity that describes the magnetic response of a material to the magnetic field applied. It is defined as the dimensionless ratio of the samples magnetization B and the strength of the applied magnetizing field H:

$$\kappa = B \cdot (\mu_0 \cdot \mu_r \cdot H)^{-1}$$

with μ_0 and μ_r being the absolute and the relative permeabilities.

The magnetic susceptibility values for marine sediments may vary in a wide range depending on the sediments' mineralogical composition and the porosity. In case of purely diamagnetic mineral content such as carbonates or pure silica/opal susceptibility values as low as -15×10^{-6} may be measured. On the other side volcano-clastic material rich in (titano-) magnetite may lead to susceptibility values above 10.000×10^{-6}. Due to the weak magnetic response of dia- and paramagnetic minerals to the overall magnetization the main factor influencing the magnetic susceptibility of marine sediments is the content of ferrimagnetic minerals such as lithogenic or authigenic magnetite. Changes of ferrimagnetic mineral content therefore often allow the characterization and correlation of marine sediment records based on the susceptibility logs. Afar from this, low magnetic susceptibility values may indicate diagenetic processes affecting specifically iron oxide minerals in the sediments.

The down-core magnetic susceptibility is measured with the Multi-Sensor Core Loggers susceptibility meter based on a *Bartington M.S.2C* susceptibility meter and a corresponding 140 mm loop sensor. This sensor has a wide measurement characteristic which results in averaging of the susceptibility values over a down core distance of ca. 8 cm. Abrupt changes

of the susceptibility therefore appear to be smoothed out and thin layers may not be properly resolved. This may lead to underestimation of local magnetic susceptibility values. A positive side effect of this large sensor characteristic is that the magnetic susceptibility values are virtually unaffected by section-end artifacts from the liners plastic end caps. Therefore, satisfying processing may be achieved by simply removing the end cap thickness from the final core logs. This way gaps in the down core data may be avoided and a continuous down-core composite log can be generated.

Wet Bulk Density Measurements

The bulk density ρ is a characteristic quantity of marine sediments that describes the ratio of the bulk mass and the specific volume according to:

$$\rho = V^{-1} \sum_{i=1}^{n} \rho_i V_i$$

with ρ being the bulk density, V being the total volume, ρ_i being the density of the i-th component and V_i being the corresponding volume of the i-th component.

It is affected by both the relative proportion of material with varying densities (e.g. water with ca. 1 g/cm^3 or quartz grains with ca. 2.65 g/cm^3) within the sediments as well as the specific density ρ_i of the mineral grains themselves. Due to the large difference between the specific density of the pore water and the solid phase the bulk density is heavily affected by variations of the sediments' fractional porosity which may indirectly act as a grain size indicator. Only in extreme cases the bulk density indicates changes of the sediments' mineralogical composition. It is therefore a relative unambiguous parameter that may be used to discriminate between different sediment lithologies and often allows first insights into the sedimentation history.

The wet bulk density is indirectly determined using calibrated measurements of gamma ray attenuation within the sediments. For this purpose the Multi-Sensor Core Logger is equipped with an enclosed ^{137}Cs gamma radiation source (activity of ca. 326 MBq at the time of use) on one side of the sediment core and a NaI based scintillation detector on the opposing side. The sensor has a relatively narrow sensor characteristic of less than 2 cm which effectively means that virtually no averaging over multiple samples occurs. Therefore, density changes within ranges of 1 cm may be resolved by the core logging data. For calibration an aluminum bar with stepwise increasing thickness submerged in a water filled piece of a sediment core liner was used.

P-Wave Velocity Measurements

Similar to the bulk density the p-wave velocity v_p is a physical property that is characteristic to the sediments composition. It is mainly affected by the materials mechanical properties (bulk modulus M_b and shear modulus M_s) as well as the materials density ρ according to:

$$v_p = \sqrt{\frac{M_b M_s}{\rho}}$$

In the absence of gas bubbles the fluid phase (pore water) is usually the constituent with by far the lowest p-wave velocity value (ca. 1500 m/s depending on the temperature). Therefore the p-wave value is highly dependent on the sediments porosity. Analogous to the wet bulk density

the p-wave velocity log may therefore be used to discriminate between different sediment units and varying sedimentation regimes.

The sediments p-wave velocity is determined by the p-wave travel time through the sediment core and the core diameter derived from the caliper measurements. For this purpose the Multi-Sensor Core Logger is equipped with two, spring-loaded, cylindrical transducers that are acoustically coupled to the sediment through the sediment cores liner. The emitting transducer sends out acoustic signals of 230 kHz frequency at a repetition rate of 200 Hz. The *GEOTEK* software automatically detects the first motion and picks the corresponding travel time. Due to the potentially complex velocity profile of the sediments it is difficult to estimate the down core resolution of the p-wave measurements but in general resolutions below the loggers step size (in this case 1 cm) may be expected. In order to generate reliable values, the system needs to be corrected for the p-wave travel time within the transducers and the liner (travel time offset). For this purpose, a dummy core filled with demineralized water was measured before and after each sediment core. Given the known travel time in demineralized water at the known temperature the travel time offset of the system can be determined and subtracted from the measured raw data during the data processing. The p-wave velocity measurement is heavily affected by partial or complete loss of proper acoustic coupling between the transducers and the sediment. Unfortunately, such bad acoustic coupling is unavoidable around the end caps of each core section and may also occur at locations with rough liner surfaces. Out of this reason gaps of ca. 10 cm in the p-wave velocity log along the cores section boundaries need to be tolerated.

Work at sea

A single *GEOTEK* Multi-Sensor Core Logging System (AWI MSCL #25) as a table top version was used during *Polarstern* cruise PS119 and the previous *Polarstern* cruise PS118. All measurements were accompanied by temperature measurements of a reference piece in order to correct the temperature dependant parameters during the preliminary on board data processing. In the case of unopened cores also the core diameter was measured in order to correct density and p-wave travel time data for the sediment core thickness. The system uses a stepper motor driven pushing mechanism and an optical sensor for precise positioning. All measurements were carried out with a 1 cm down core step size and all core sections were measured in a single process without adding spacers between each section. Edge effects at the end cap positions of each section were removed from the data during processing. The Multi-Sensor Core Logging setup is displayed in Fig. 11.1.

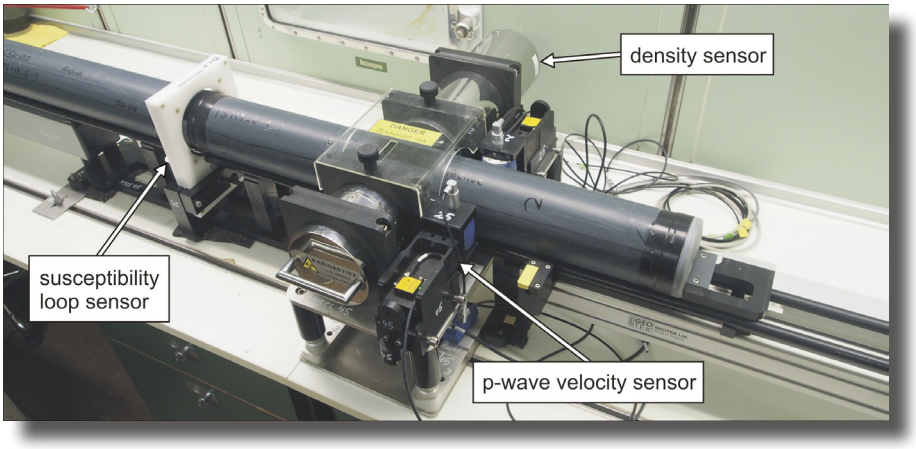

Fig. 11.1: Multi-Sensor Core Logging System during onboard operation during PS119

Measurements of all three physical parameters (magnetic susceptibility, bulk density and p-wave velocity) have been carried out on the seven sediment cores that have not been opened directly on board. The remaining 15 sediment cores were directly opened for geochemical sampling. Due to the core loggers' geometry and structural limitations only the magnetic susceptibility could be measured on these sediment cores. All 20 gravity cores had an outer diameter of 12.5 cm while the three piston cores were of a smaller diameter of 9 cm. The core logging data was corrected for this change of calliper during the preliminary on board data processing but revision and final reprocessing should be applied post cruise to allow reliable and accurate absolute susceptibility values.

Tab. 11.1: Overview of the Multi-Sensor Logger configuration, measurement parameters and calibration values.

Magnetic Susceptibility susceptibility meter: Bartington M.S.2C Magnetic Susceptibility Meter loop sensor diameter: 14 mm (for GC, PC and TC) count time: 10 sec frequency: 565 Hz
Bulk Density gamma ray source: enclosed ^{137}Cs source activity: 326 MBq source energy: 0.662 MeV aperture diameter: 5 mm (for GC, PC and TC) count time: 10 sec calibration coefficients: A=-0.0002 B=-0.0572 C=10.076 detector type: titanium doped NaI scintillation crystal and photomultiplier tube hand held radiation detector/monitor: Gamma-Scout (serial number: 037892)
P-Wave Velocity transducer type: static rolling transducers calibration: 12.5 cm liner filled with demineralized water before and after each core repetition rate: 200 Hz number of samples per measurement: 2000 core diameter measurement: dual laser distance sensor
Temperature type: bimetal temperature probe measurement: equilibrated reference piece
Fractional Porosity density estimates: 2.65 g/cm^3 for solid phase (quartz), 1.026 g/cm^3 for pore water

The calibration of the density measurements was only carried out once before the first sediment core was logged on April, 22. The calibration constants were applied to all the following 7 sediment cores that have been logged during the following two days. After this initial period no more density measurements were carried out until the end of the cruise. The change of the radiation source' activity during these two days of density measurements negligible compared to the impact of other uncontrollable factors, such as the proper alignment of the calibration piece. In all cases that involved p-wave velocity measurements a calibration core filled with demineralized water was measured before and after each sediment core. These measurements allow drift correction, recalibration and error assessment during post cruise data revision and reprocessing. All calibration constants and system parameters are listed in Table 11.1.

Preliminary results

Core logging was successfully carried out on all 25 gravity-, piston- and corresponding trigger cores. The sediment cores may be grouped into 9 coring sites and cover a broad range of different geologic settings. This diversity is also indicated by the core logging data. All sediment cores show complex down core density (where available) and magnetic susceptibility profiles that may not easily be interpreted thoroughly without additional sedimentological examination and further in depth analysis. Most sediment cores have a high mean magnetic susceptibility in the range of 1000 x 10^{-6} to 3000 x 10^{-6} which may be indicative for a significant influx of lithogenic particles of volcanic origin rich in (titano-) magnetite to the sediments. Due to the high impact of magnetite on the total magnetic susceptibility even small changes and local fluctuations of material influx may change the down core susceptibility profiles entirely. This explains why only few cores from nearby sites may be correlated with each other.

Core-Logging Data of the Drygalski Fjord / Drygalski Trough

High variability is also to be expected in close proximity of terrigenous sediment source areas such as within the Drygalski Fjord and the Drygalski Trough. In fact, the six unopened sediment cores acquired from the Drygalski Fjord and the Drygalski Trough show very diverse core logs and are not correlatable based on the logging data alone. A characteristic feature of two of the cores from the Drygalski Trough (PS119_6-1 and PS119_8-1) is the high concentration of methane that caused intensive degassing during the warming up. The degassing heavily affected the p-wave velocity measurements and finally resulted in the complete loss of p-wave data of the corresponding cores. Judging from the core logging data methane degassing occurred at a depth of ca. 3.5 m at site PS119_6-1 and at ca. 1.2 m at site PS119_8-1. Furthermore, the susceptibility profile of PS119_6-1 shows a gradual decrease of magnetic mineral content while the corresponding density profile does not follow this trend. In general the magnetic susceptibility for most of the cores from the Drygalski Fjord and Drygalski Trough indicate an almost linear relation of magnetic susceptibility and density which indicates that the material responsible for the density changes such as lithogenic particles is also the carrier of the magnetic signal (see Fig. 11.2). An increase of the relative volume of these particles (larger grainsizes and correspondingly lower porosity) would lead to a proportional increase of both magnetic susceptibility and density. The divergence of magnetic susceptibility and density in core PS119_6-1 therefore implies that the magnetic minerals in these lithogenic particles have been altered by diagnosis processes. Suspiciously no such extensive alteration is indicated by the core log data of PS119_8-1 which also showed methane degassing but this may at least partly be attributed to the fact that this core is significantly shorter.

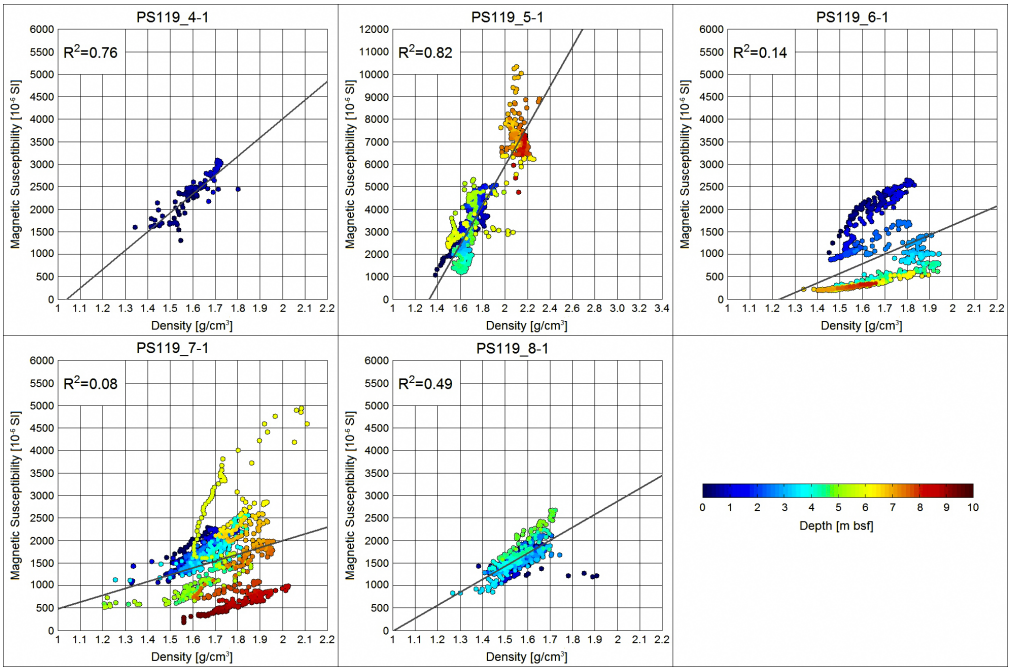

Fig. 11.2: Crossplots of magnetic susceptibility and density measurements of sediment cores from the Drygalski Fjord and Drygalski Trough. The color indicates the depth within the sediments.

Core-Logging Data of East Scotia Ridge Segment E2

All cores from the East Scotia Ridge have been opened and therefore only susceptibility values are available for these cores. In general, the down core susceptibility profiles of the cores from the East Scotia Ridge appear to show lower variability than those of the cores from the Drygalski Fjord and Trough area but still hardly any of the cores may easily be correlated with each other (see Fig. 11.3). The only exceptions are the two cores PS119_14-2 and PS119_15-1 from a site east of E2 (core PS119_22-1 and PS119_57-1 originate from the same coring site).

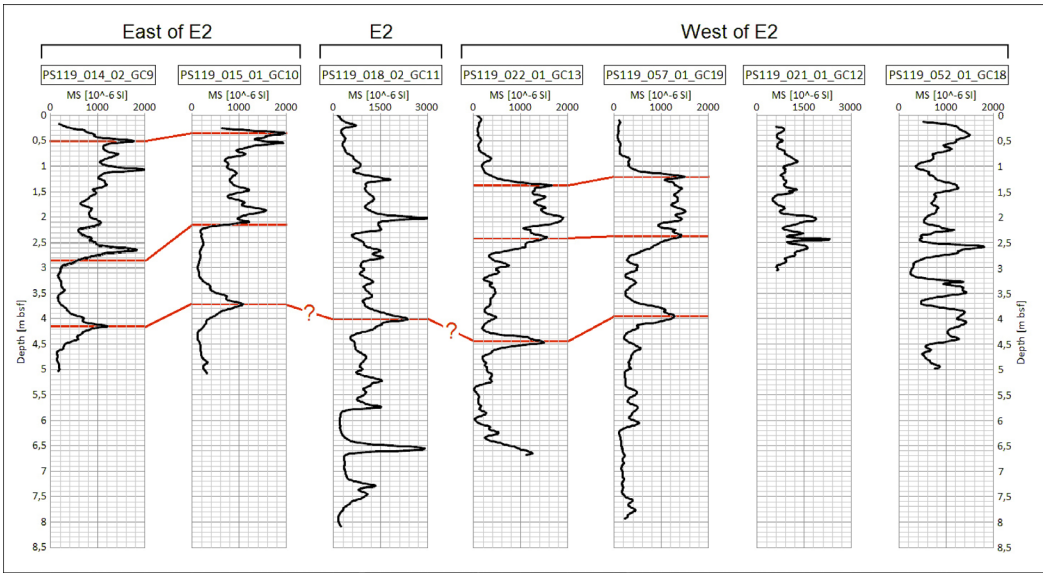

Fig. 11.3: Down core susceptibility profiles from the coring sites at E2. The red lines indicate potential marker horizons that may be correlated.

The correlation of these two sites indicates a slightly higher sediment influx at site PS119_14-2. Both cores have low magnetic susceptibility values (ca. 200 x 10^{-6}) at depths below 2.5 to 3.0 m with exception of a prominent broad peak at around 4.0 m depth. This pattern correlates with the dissolved iron measurements and may indicate diagenetic overprinting in form of iron oxide depletion. The susceptibility logs of the other cores from East Scotia Ridge Segment E2 show complex profiles that do not allow further interpretation without additional information.

Core-Logging Data of East Scotia Ridge Segment E8 and E9

In comparison to the cores from East Scotia Ridge Segment E2 the magnetic susceptibility values of the cores from East Scotia Ridge Segments E8 and E9 are elevated (mean values of ca. 2000 x 10^{-6} to 3500 x 10^{-6} at E8 and E9 compared to ca. 500 x 10^{-6} to 800 x 10^{-6}). This suggests that either the influx of magnetic material such as volcanogenic particles is greater in this region or the magnetic record is less diluted by weak magnetic minerals than at the sites at E2. Two gravity cores were recovered at a site near East Scotia Ridge Segment E9. Since only 2.3 m of sediments could be recovered at site PS119_25-1 a piston core (PS119_30-1) was deployed at the same location which resulted in the recovery of 11.7 m of sediment. The corresponding down core susceptibility profile indicates several relatively homogenous layers of 1.0 to 1.5 m thickness that show a gradual down core increase of magnetic susceptibility. The two most recognizable of these layers appear at depths of 1.0 to 2.5 m and 3.8 to 5.0 m. Such susceptibility patterns may be indicative for mass transport and sorted re-deposition processes. The piston core PS119-37-1 recovered at a site near E8 had a length of 8.7 m and shows a relatively continuous down core susceptibility profile with one exception towards the lower end below 7.9 m where very high susceptibility values of up to 13000 x 10^{-6} have been measured. Such high susceptibility values can only be explained with a high content of magnetite in the sediments.

Core-Logging Data of the Kemp Caldera

A single gravity and one piston core were recovered in the Kemp Caldera but both cores are of short length (PS119_36-2 with 1.6 m sediment recovery and PS119_45-1 with 2.3 m sediment recovery). Although both cores originate from the same site the susceptibility logs do not show similarities which suggests that the sediments in this area are laterally highly heterogeneous. Both cores have in common, that the mean magnetic susceptibility is relatively low (ca. 800 x 10^{-6}).

Data management

Data was provided onboard in form of processed core logs. Multi-Sensor Core Logs of all gravity, piston and corresponding trigger cores are available in Appendix A.6. All raw data and the corresponding calibration data will be provided to the AWI for final reprocessing and data revision. After revision and reprocessing all data will be archived and published by the World Data Center PANGAEA Data Publisher for Earth & Environmental Science (www.pangaea.de).

12. SEDIMENT GEOCHEMISTRY

Natascha Riedinger[1], Male Köster[2], Anna Lichtschlag[3], Christopher Jones[1], Marta Torres[4]

[1]OkState, Stillwater
[2]AWI, Bremerhaven
[3]NOCS, Southampton
[4]CEOAS, Corvallis

Grant-No. AWI_PS119_00

Objectives

In accordance with the overall expedition objectives to investigate hydrothermal vent and cold seep systems near South Georgia and the South Sandwich Islands, the main goals of the biogeochemistry group were three-fold: 1) to study the iron cycle in the methanic zone near South Georgia; 2) to fully characterize the impact of hydrothermal fluid and diagenetic metal oxide alteration on the trace metal cycle (including its isotopic composition) at the East Scotia Ridge, the back arc, and on the Scotia plate; and 3) to investigate the hydrothermally driven sulfur and metal cycle at Kemp Caldera. In addition to these 3 main tasks, we also collected samples from the sediment surface for diatom incubation experiments (R. Robinson, pers. comm.).

Iron cycling in the methanic zone of South Georgia

The investigation of iron cycling in the methanic zone was the main objective of previous expeditions to the South Georgia region. Our efforts during expedition PS119 were limited to the collection of two gravity cores in the Drygalski Fjord area, aimed at obtaining sediments deeper than was previously achieved. Here the methane is biogenic in origin (Gepraegs et al., 2016), and ongoing AWI investigations are targeting the role of iron in carbon cycling, particularly the potential for iron-mediated anaerobic methane oxidation (Fe-AOM) (S. Kasten, pers. comm.).

Impact of hydrothermal fluid and diagenetic metal oxide alteration on the trace metal cycle

The study of biogeochemical cycles, and the reconstruction of paleoceanographic conditions rely heavily on trace metals proxies preserved in the sediment record (e.g., Tribovillard et al., 2006, and references therein). Reconstructions of paleo-environmental conditions require an understanding of the processes that can cause changes in trace metal elemental and isotopic distributions from their original input signal through diagenesis and preservation in the sediment record (e.g., Calvert and Pedersen, 1993; Algeo and Rowe, 2012). Missing in previous studies in the Antarctic region is the consideration of the role that hydrothermal/volcanogenic sources have on the primary trace metal input to the surface sediment, which is particularly important since this region is surrounded by spreading ridges, some of which are known to be currently active (e.g., Bohrmann, et al., 1999; German et al., 2000). Dissolved metals sourced through hydrothermal fluids can fractionate isotopically, form precipitates in the water column, and/or be scavenged by particles settling on the seafloor, mainly by adsorption onto iron-colloids (e.g., Crocket, 1990; Sander and Koschinsky, 2011; Yücel et al., 2011; Hawkes et al., 2014). Metals in the solid phase also constitute a significant trace metal input term, as sulfide precipitates have been observed to travel over long distances (Yücel et al., 2011), likely impacting sedimentary

environments distal to the hydrothermal source. Following deposition, diagenetic processes result in metal accumulation in the solid phase through formation of new authigenic phases, or metal release to the water column (Fig. 12.1).

Here we aim to identify metal cycling in sediments proximal to, and impacted by, hydrothermal vents, and to distinguish primary hydrothermal deposits from sediments that have been re-oxidized by fluids circulating within the crust. To address these objectives, we will analyze sediment and associated pore fluids from piston (PC), gravity (GC) and multicorer (MUC) core samples recovered at various distances from the hydrothermal input. The hydrothermally sourced metals and their diagenetic transformations will be characterized using a matrix of geochemical tracers that include strontium isotopes, noble metals, rare earth elements (REE), and redox-sensitive elements and their isotopes (including Mo, U, Fe). These analyses will be complemented with incubation experiments of MUC samples to characterize trace metal cycling over time and identify microbial communities that may be responsible for biogeochemical changes.

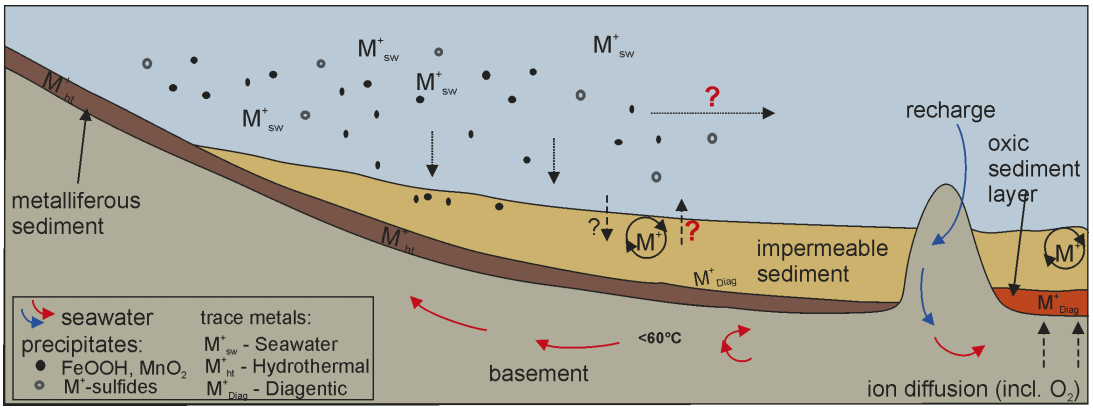

Fig. 12.1: Schematic sketch showing the general circulation pattern of fluids through the crust and release from the vent impacting the cycling of metals at a hydrothermal vent system and adjacent deposits. M represents vent associated metals (modified after Wheat et al., 2002; German et al., 2016).

Sulphide and metal cycling at the Kemp Caldera

At the Kemp Caldera the aim is to identify the geochemical cycles in the sediments deposited in closer proximity to the hydrothermally active sites, with a focus on the metal and the sulfur cycle. We want to understand if there is diffuse fluid flow through the near-vent hydrothermal sediments and how far this influences the geochemistry of the sediments after their deposition. In addition, we want to test if the sediments can be used as a record for different phases of activity, with potentially different hydrothermal fluid chemistry. This will be done by comparing results in pore water and solid phase geochemistry with results from a previous expedition (*JC42*) with a focus on the sulfur, carbon and metal cycles. It is important to understand these processes as metalliferous sediments are increasingly used as vectors to identify hydrothermal deposits, although the diagenetic processes after their deposition are not well understood. To achieve our goals, targeted push cores were collected in different areas of the Kemp Caldera with the ROV Quest, and in longer sediment cores were collected (1 PC, 1 GC, 1 MUC) in the deepest part of the caldera.

Work at sea

The location of cores collected for biogeochemical investigations is listed in Table 12.1. We use a similar approach to processing samples retrieved for each of the objectives listed above. Sediment cores from MUC and push core (PUC) samplers were processed immediately after

recovery. Parallel cores from the MUC were separately sampled for 1) supernatant bottom water, pore water and co-located solid phase analyses; 2) microbiology; and 3) measurement of ^{210}Pb for sedimentation rate estimates. Few, selected cores were additionally sampled for incubation experiments. Samples for pore water extraction were sliced, placed into 50 ml centrifuge tubes, and immediately transferred to the cold room (~4°C). In the cases where headspace was observed in the centrifuge tubes (sample slices < 2cm), the sample was flushed with argon to avoid oxidation. The solid phase remaining in the centrifuge tube was sealed under argon and frozen for total acid digestions to be conducted shore-based. Samples, collected for microbiology, were sliced using sterilized spatulas and immediately frozen at -80°C in sterile whirl-pack bags. For ^{210}Pb analyses, samples were taken every centimeter and stored at 4°C. Samples for incubation experiments were stored at 4°C in an argon atmosphere. PUC samples were sliced, placed on centrifuge tubes and processed in an analogous fashion to the MUC samples described above. Retrieved GC and PC were cut open and the working half was transferred into the cold room at a temperature of approximately 4°C for pore-water and solid phase sampling. Pore water samples were taken in intervals of 20 to 30 cm, and co-located solid phase samples were collected with 10 mL cut-off syringes. All solid phase samples will be stored frozen at -20°C for further analyses. Samples taken for microbiology at selected intervals were stored at -80°C.

Pore water was extracted from the sediment using Rhizons (average pore size of 0.15 µm; Seeberg-Elverfeldt et al., 2005); either directly from the GC and PC working halves or from sealed centrifuge tubes in the case of MUC and PUC samples. To avoid any dilution or oxidation during the pore-water sampling by Rhizons, the first mL of the freshly extracted pore water was discarded. Dissolved iron was immediately analyzed on-board for all samples except those from Kemp Caldera, and alkalinity was analyzed for all samples. Dissolved iron (Fe^{2+}) was detected photometrically (DR Lange HACH 2800 photometer) at a wavelength of 565 nm. An aliquot of 1 mL of the extracted pore water was pre-treated with 50 µL of ascorbic acid and then added to 50 µL Ferrospectral solution to complex dissolved Fe for colorimetric measurement. In case of high concentrations of Fe^{2+} (>1 mg L^{-1}) the samples were diluted with oxygen-free artificial seawater. Alkalinity was determined on a 1 mL aliquot of sample by titration with 10 or 50 mM HCl. The pH measurements were performed using a Mettler Toledo micro-electrode. The samples were titrated with a digital burette to a pH of approximately 3.9 and both titration volume and final pH were recorded. The alkalinity was calculated using a modified equation from Grasshoff et al. (1999).

Pore water aliquots for shore based analyses of trace metal (1-4 mL), major element (1-1.8 mL), nutrients (1 mL), dissolved inorganic carbon (DIC) and its stable carbon isotopes (δ^{13}C-DIC) (1-2 mL), chloride, sulphate and hydrogen sulphide (1-4 mL), oxygen and hydrogen isotopes (2 mL), and iron isotopes (3-10 mL) were taken based on pore water availability and stored accordingly (Table 12.1).

All solid phase samples were stored in argon-flushed, sealed aluminum bags for the determination of minor and major element content, selected metal isotope composition, iron speciation and their isotopic composition, total organic/inorganic carbon and total sulphur contents (Table 12.1). About 5 samples were taken from 3 selected parallel MUC cores (see Table 12.1) for incubation experiments, sealed under argon in aluminum bags and stored at ~4°C.

Samples collected for diatom cultures (Table 12.2) were taken from the uppermost sediment material in MUC cores and kept in centrifuge tubes with enough bottom seawater to avoid desiccation of the material. Samples were stored at ~4°C.

Preliminary (expected) results

Results from the shipboard analyses are shown in Figs. 12.2 and 12.3. The alkalinity concentrations indicate low alteration of organic material in the sediment (Fig. 12.2). The

plotted dissolved iron data illustrate the large impact of iron cycling in these sediments where dissolved ferrous iron is present in sediment sequences as large as 8 meters (Fig. 12.3).

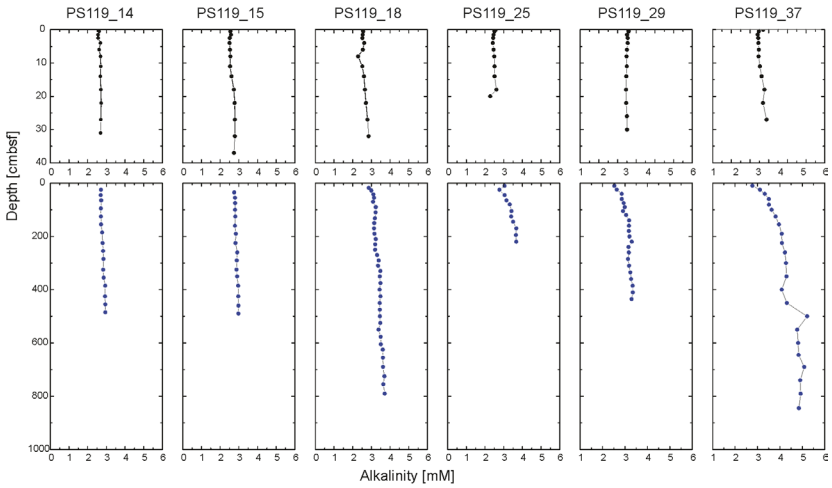

Fig. 12.2: Alkalinity concentration in multicorer sample (black filled circles) and gravity core samples (blue filled circles) as well as piston core samples (Site PS119_37-1) from selected sites.

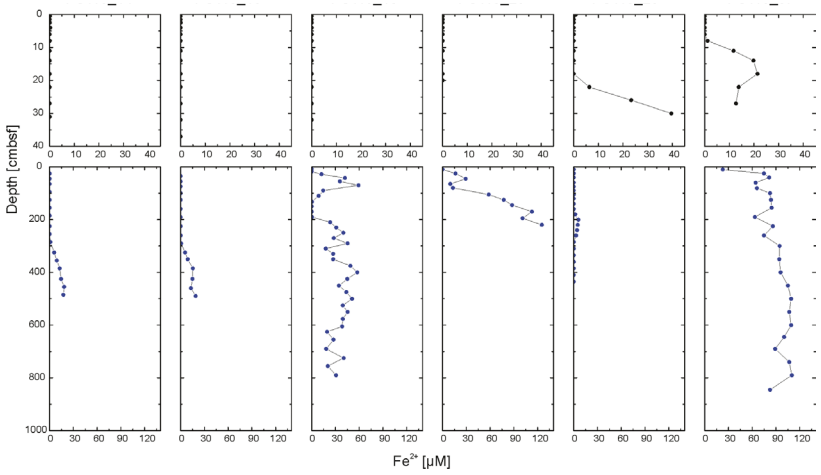

Fig. 12.3: Dissolved ferrous iron (Fe^{2+}) concentration in multicorer sample (black filled circles; note different scale) and gravity core samples (blue filled circles) as well as piston core samples (Site PS119_37-1) from selected sites.

Further shore-based analyses of fluids and solid phase samples in the context of our proposed multi-element approach will provide unique constraints on the contribution of metal-rich vent fluids to metal recycling in subsurface environments. Metals such as Fe, U and Mo are frequently applied for paleo redox reconstructions (Lyons et al., 2009, and references therein); therefore, identifying the impact of hydrothermal vents systems on these metals is crucial for its application as redox proxy at sites in vicinity to hydrothermal sources. The incubation experiments and associated microbiological analysis will further clarify the processes controlling trace metal cycles near hydrothermal systems allowing a greater understanding for their application as redox proxies.

Sediments undergo early diagenetic alteration during burial that can lead to the release of metals into the pore water and potentially back to the water column. Therefore, fingerprinting the trace metal inventory in the hydrothermal vent system and adjacent sediments will help us to understand the activity and survival of microbial communities in these extreme environments, the impact of trace metals on benthic macro fauna, and the availability and necessity of bio-essential trace metals to the subsurface biosphere.

Tab. 12.1: Investigated sites where geochemical samples were taken during this cruise with parameters to be analyzed on board and aliquots of samples stored and conserved.

Station PS119_	Device	Trace Metals	Nutrients	Major elements	Cl-,SO4/HS-	DIC/ d13C	O/H isotopes	Fe isotopes	Sed. Frozen	Microbio.	Sed. ^{210}Pb	Incubations
1-1	MUC	BPS	CEOAS	CEOAS	-	CEOAS	-	-	BPS	CEOAS/ BPS	-	BPS
4-2	GC	-	AWI	AWI	AWI	AWI	-	AWI	AWI	AWI	-	-
7-2	MUC	BPS	CEOAS	CEOAS	-	CEOAS	-	AWI	BPS/ AWI	CEOAS/ BPS	-	BPS
10-2	CTD	BPS	-	-	-	-	-	-	-	-	-	-
14-1	MUC	BPS	CEOAS	CEOAS	-	CEOAS	BPS	-	BPS	CEOAS/ BPS	-	BPS
14-2	GC	BPS	CEOAS	CEOAS	-	CEOAS	BPS	AWI	BPS/ AWI	CEOAS/ BPS	-	-
15-1	GC	BPS	CEOAS	CEOAS	-	CEOAS	BPS	-	BPS	CEOAS/ BPS	-	-
15-2	MUC	BPS	CEOAS	CEOAS	-	CEOAS	BPS	-	BPS	CEOAS/ BPS		BPS
17-1	ROV	BPS	-	-	-	-	-	AWI	-	-	-	-
19-1	CTD	BPS	-	BPS	-	-	-	-	-	-	-	-
18-1	MUC	BPS	CEOAS	CEOAS	-	CEOAS	BPS	-	BPS	CEOAS/ BPS	BPS	-
18-2	GC	BPS	CEOAS	CEOAS	-	CEOAS	BPS	-	BPS	CEOAS/ BPS	-	-
21-1	GC	BPS	CEOAS	CEOAS	-	CEOAS	BPS	-	BPS	CEOAS/ BPS	-	-
20-7F	ROV	BPS	-	-	-	-	-	AWI	-	-	-	-
20-10F	ROV	BPS	-	-	-	-	-	AWI	-	-	-	-
22-2	MUC	BPS	CEOAS	CEOAS	-	CEOAS	BPS	-	BPS	CEOAS/ BPS	BPS	-
22-1	GC	BPS	CEOAS	CEOAS	-	CEOAS	BPS	-	BPS	CEOAS/ BPS	-	-
24-1	CTD	BPS	-	BPS	-	CEOAS	BPS	-	BPS	CEOAS/ BPS	-	-
25-1	GC	BPS	CEOAS	CEOAS	-	CEOAS	BPS	AWI	BPS/ AWI	CEOAS/ BPS	-	-
25-2	MUC	BPS	CEOAS	CEOAS	-	CEOAS	BPS	-	BPS	CEOAS/ BPS	BPS	-
29-2	MUC	BPS	CEOAS	CEOAS	-	CEOAS	BPS	-	BPS	CEOAS/ BPS	BPS	-
29-1	GC	BPS	CEOAS	CEOAS	-	CEOAS	BPS	AWI	BPS/ AWI	CEOAS/ BPS	-	-
30-1	PC	BPS	CEOAS	CEOAS	-	CEOAS	BPS	AWI	BPS/ AWI	CEOAS/ BPS	-	-
33-1	ROV	NOC	NOC	NOC	NOC	NOC	-	-	NOC	-	-	-
36-1	MUC	NOC	NOC	NOC	NOC	NOC	-	-	NOC	-	-	-
36-2	GC	NOC	NOC	NOC	NOC	NOC	-	-	NOC	-	-	-
37-1	PC	BPS	CEOAS	CEOAS	-	CEOAS	BPS	AWI	BPS/ AWI	CEOAS/ BPS	-	-

Station PS119_	Device	Trace Metals	Nutrients	Major elements	Cl-,SO4/HS-	DIC/d13C	O/H isotopes	Fe isotopes	Sed. Frozen	Microbio.	Sed. ^{210}Pb	Incubations
37-2	MUC	BPS	CEOAS	CEOAS	-	CEOAS	BPS	-	BPS	CEOAS/BPS	BPS	-
42-1	ROV	NOC	NOC	NOC	NOC	NOC	-	-	NOC	-	-	-
45-1	PC	NOC/BPS	NOC	NOC	NOC	NOC	-	AWI	NOC/BPS/AWI	BPS	-	-
48-1	MUC	BPS	CEOAS	CEOAS	-	CEOAS	BPS	-	BPS	CEOAS/BPS	-	-
52-1	GC	BPS	CEOAS	CEOAS	-	CEOAS	BPS	-	BPS	CEOAS/BPS	BPS	-
52-2	MUC	BPS	CEOAS	CEOAS	-	CEOAS	BPS	-	BPS	CEOAS/BPS	BPS	-
52-3	CTD	BPS	-	BPS	-	-	-	-	-	-	-	-
53-1	MUC	BPS	CEOAS	CEOAS	-	CEOAS	BPS	AWI	BPS/AWI	CEOAS/BPS	BPS	-
57-1	GC	BPS	CEOAS	CEOAS	-	CEOAS	BPS	AWI	BPS/AWI	CEOAS/BPS	BPS	-
58-1	GC	BPS	AWI	AWI/CEOAS	AWI	CEOAS	-	AWI	AWI/BPS	AWI	-	-

Tab. 12.1: Sampling sites and sample numbers for diatom incubation experiments

Core	Depth	Number of samples	ID number
PS119_14-1	BW	3	49
PS119_5-2	BW	2	78
PS119_18-1	BW	4	109
PS119_18-1	0-1 cm	2	110
PS119_18-1	1-2 cm	1	111
PS119_22-2	BW	3	188
PS119_22-2	0-1 cm	1	189
PS119_25-2	BW	2	253
PS119_25-2	0-1 cm	1	254
PS119_29-2	BW	1	264
PS119_29-2	0-1 cm	1	265
PS119_36-1	BW	2	KC
PS119_36-1	mixed depths	1	KC
PS119_37-2	BW	3	346
PS119_37-2	0-1 cm	1	347

Data management

The geochemical data sets generated during the cruise and in course of the proposed project, as well as contextual details of laboratory methods, will be careful documented in lab books and Microsoft Excel spreadsheets. All raw data will be kept intact and archived separately from processed data for data transparency. Data will be available online and freely accessible

through the World Data Center PANGAEA Data Publisher for Earth & Environmental Science (www.pangaea.de), a member of the ICSU World Data System. Data dissemination will be noted in the publications within the Materials and Methods section to inform the scientific community of the data availability and accessibility.

References

Algeo TJ, Rowe H (2012) Paleoceanographic applications of trace-metal concentration data. Chemical Geology, 324, 6-18.

Bohrmann G, Chin C, Petersen S, Sahling H, Schwarz-Schampera U, Greinert J, Lammers S, Rehder G, Daehlmann A, Wallmann K, Dijkstra S (1999) Hydrothermal activity at Hook Ridge in the central Bransfield basin, Antarctica. Geo-Marine Letters, 18, 277-284.

Calvert SE, Pedersen TF (1993) Geochemistry of recent oxic and anoxic marine sediments: implications for the geological record. Marine Geology, 113, 67-88.

Crocket JH (1990) Noble metals in seafloor hydrothermal mineralization from the Juan de Fuca and Mid-Atlantic ridges; a fractionation of gold from platinum metals in hydrothermal fields. The Canadian Mineralogist, 28, 639-648.

Geprägs P, Torres ME, Mau S, Kasten S, Römer M, Bohrmann G (2016) Carbon cycling fed by methane seepage at the shallow Cumberland Bay, South Georgia, sub-Antarctic. *Geochemistry, Geophysics, Geosystems*, *17*(4), pp.1401-1418.

German CR, Livermore RA, Baker ET, Bruguier NI, Connelly DP, Cunningham AP, Morris P, Rouse IP, Statham PJ, Tyler PA (2000) Hydrothermal plumes above the East Scotia Ridge: an isolated high-latitude back-arc spreading centre. Earth and Planetary Science Letters, 184, 241-250.

German CR, Casciotti KA, Dutay JC, Heimbürger LE, Jenkins WJ, Mills RA, Obata H, Schlitzer R, Tagliabue A, Turner DR, Whitby H (2016) Hydrothermal impacts on trace element and isotope ocean biogeochemistry. Phil. Trans. R. Soc. A, 374, 20160035.

Grasshoff K, Kremling K, Ehrhardt, M (eds) (1999) Methods of seawater analysis, 3rd edition. Wiley-VCH, Weinheim, New York.

Hawkes JA, Connelly DP, Rijkenberg MJ, Achterberg EP (2014) The importance of shallow hydrothermal island arc systems in ocean biogeochemistry. Geophysical Research Letters, 41, 942-947.

Lyons TW, Anbar AD, Severmann S, Scott C, Gill BC (2009) Tracking euxinia in the ancient ocean: A multiproxy perspective and Proterozoic case study. Annual Review in Earth and Planetary Sciences 37, 507-534.

Sander SG, Koschinsky A (2011) Metal flux from hydrothermal vents increased by organic complexation. Nature Geoscience, 4, 145.

Seeberg-Elverfeldt J, Schlüter M, Feseker T, and Kölling M (2005) Rhizon sampling of porewaters near the sediment-water interface of aquatic systems. Limnology and Oceanography, Methods 3, 361-371.

Tribovillard N, Algeo TJ, Lyons TW, Riboulleau A (2006) Trace metals as paleoredox and paleoproductivity proxies: an update. Chemical Geology, 232, 12-32.

Wheat CG, Mottl MJ, Rudnicki M (2002) Trace element and REE composition of a low-temperature ridge-flank hydrothermal spring. Geochimica et Cosmochimica Acta, 66, 3693-3705.

Yücel M, Gartman A, Chan CS, Luther III GW (2011) Hydrothermal vents as a kinetically stable source of iron-sulphide-bearing nanoparticles to the ocean. Nature Geoscience, 4, 367.

13. METHANE DISTRIBUTIONS IN SEDIMENTS AND IN THE WATER COLUMN

Thomas Pape[1], Janice Malnati[1], Yiting Tseng[1], Marta Torres[2]

[1]MARUM, Bremen
[2]CEOAS, Corvallis

Grant-No. AWI_PS119_00

Objectives

- identification of relative methane enrichments in sediments indicative for methane upward migration from the deep subsurface
- characterization spatial distributions of methane enrichments in the water column in order to localize injections of methane-rich fluids from hydrothermal sources
- preparation of gas samples for the determination of stable carbon and hydrogen isotope compositions in the home lab

Work at sea

Methods

For analysis of methane dissolved in pore water, a modified headspace technique after Kvenvolden and McDonald (1986) was used. 3 ml of bulk sediment retrieved with the gravity corer (GC), the multicorer (MUC), and ROV-handled push cores were transferred to 20 ml glass vials prefilled with 5 ml NaOH, thereby creating a headspace volume of 12 ml. For gravity cores in rigid PVC liners, samples were taken from the segment cuts (1 m vertical resolution, 'rapid sampling'). From some gravity cores additional samples were collected after cores have been split lengthwise and opened work halves were accessible for high-resolution (20–30 cm intervals) sampling ('later sampling'). Cores obtained with the multicorer or with push cores during ROV dives were sampled in 1 or 2 cm intervals. In total samples from 17 GCs, 12 MUCs, 4 push cores, and 3 piston cores were collected. Methane concentrations in the headspace samples were determined by gas chromatography (Pape et al., 2010). Reported concentrations are *ex-situ* concentrations uncorrected for sediment porosity and Bunsen coefficient.

For analysis of dissolved methane in the water column, water samples were collected by filling water from the Niskin bottles through air-free silicone tubes into two 140 ml plastic syringes immediately after recovery of the CTD-rosette system on deck. The syringes, that were outfitted with a gas tight valve each, were flushed and filled with 100 ml of seawater without any air bubbles. A headspace was generated in each syringe by drawing 40 ml of methane-free air (called 'Zero Air') into the syringe. Syringes were shaken vigorously for more than 1.5 minutes to allow for equilibration between the water phase and the headspace gas.

Methane concentrations in the headspace gas were measured immediately on board using a Greenhouse Gas Analyzer (GGA; Los Gatos Research) provided by the, College of Earth, Ocean and Atmospheric Sciences, Oregon State University. In order to minimize the risk of water injection into the GGA instrument chamber the 40 ml headspace gas from both syringes

were transferred to a 140 ml plastic syringe via a Luer Lock adapter, and the combined gas volume of 80 ml was injected in one step. This injection was followed by immediate injection of 60 ml of commercially available methane-free synthetic air ('Zero Air') that is needed to reach the required gas volume of 140 ml in the GGA measurement cell.

During PS119, methane concentrations were determined in 22 water samples each from 15 CTD/rosette stations (except stations CTD-01, -02, and -15). Because methane enrichments in the water column, e.g. in deep-water plumes, were often found to be spatially associated with turbid water masses, methane concentrations and beam transmissions are shown in combined figures.

Preliminary results

Dissolved methane in pore water

Methane concentrations in most sediment cores investigated during PS119 for methane distributions were in the lower µM-range. Exceptions were gravity cores GC-04 from the Drygalski Fjord, GC-06 and GC-20 from the Drygalski Trough, as well as push cores ROV-447, PC-11 and ROV-448, PC-03 from the Kemp Caldera. Those cores showed relative methane enrichments in shallow sediments diagnostic for methane upward migration from the deeper subsurface.

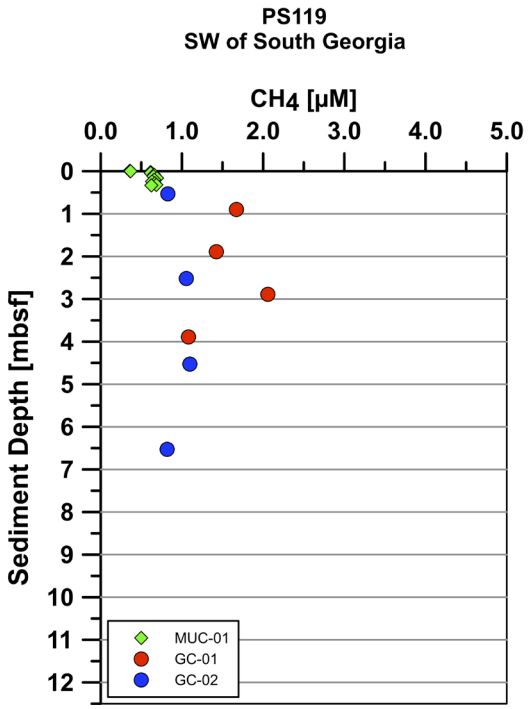

Fig. 13.1: Dissolved CH_4 in sediments SW of South Georgia

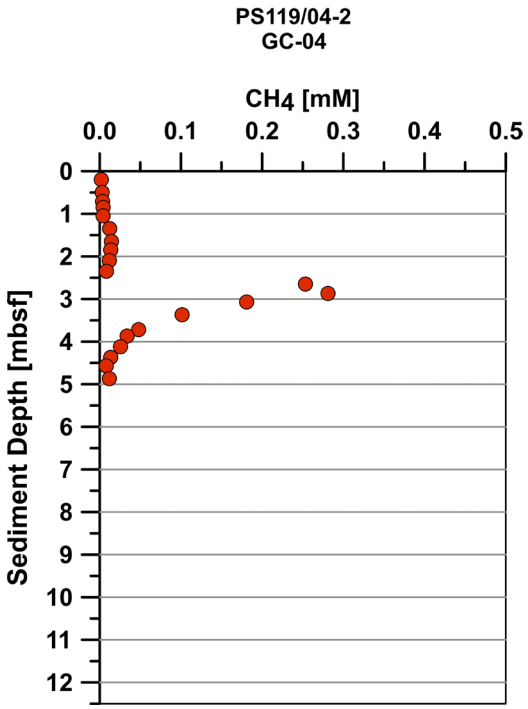

Fig. 13.2: Dissolved CH_4 in sediments at station GC-04 in the Drygalski Fjord

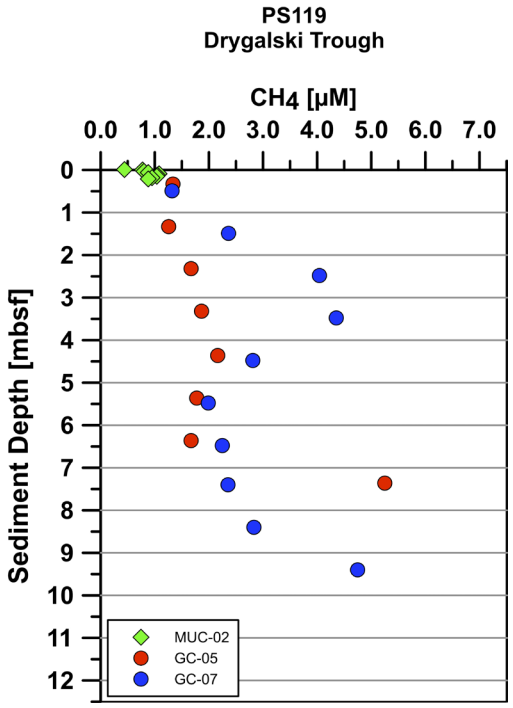

Fig. 13.3: Dissolved CH_4 in relatively methane-poor sediments in the Drygalski Trough

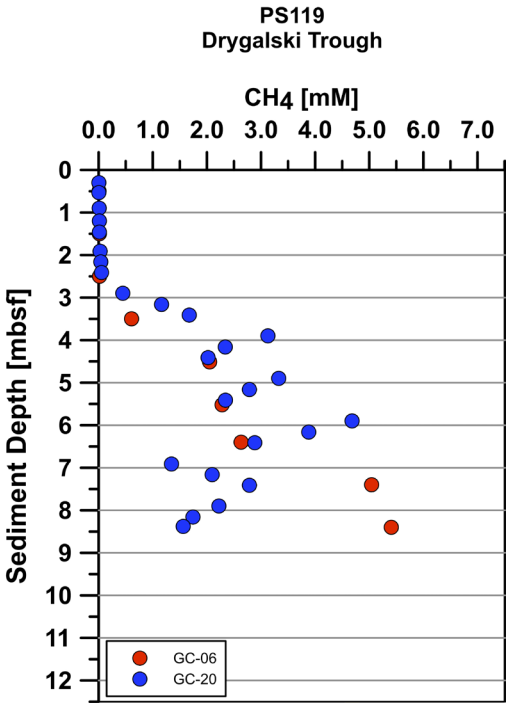

Fig. 13.4: Dissolved CH_4 in relatively methane-rich sediments in the Drygalski Trough

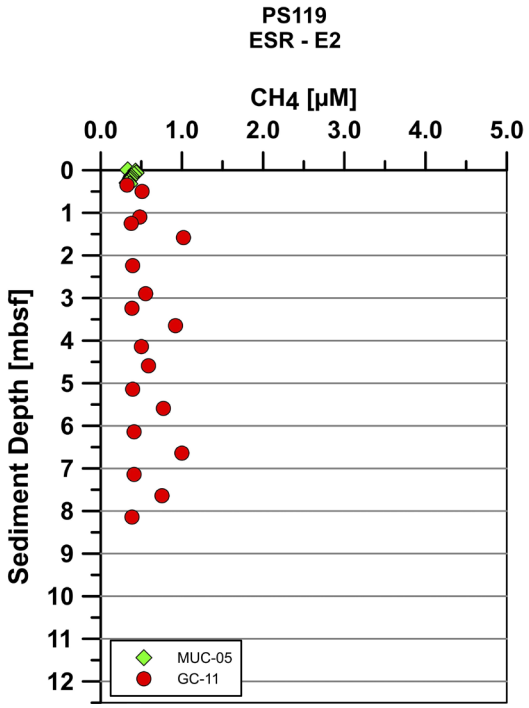

Fig. 13.5: Dissolved CH_4 in sediments at site E2

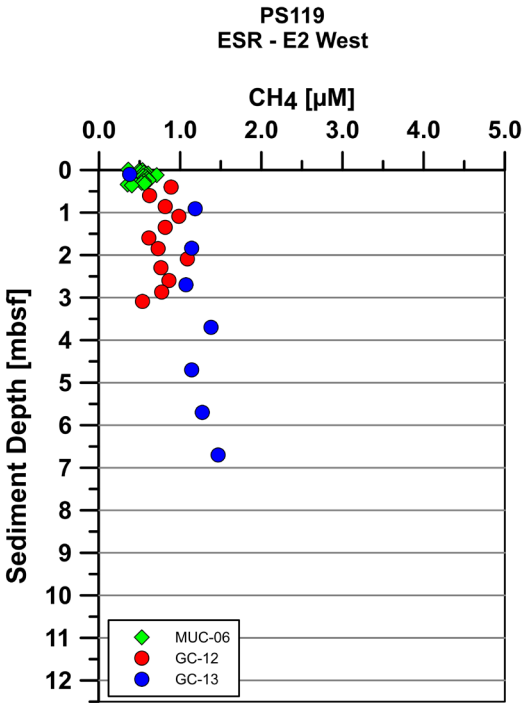

Fig. 13.6: Dissolved CH_4 in sediments at site E2 West

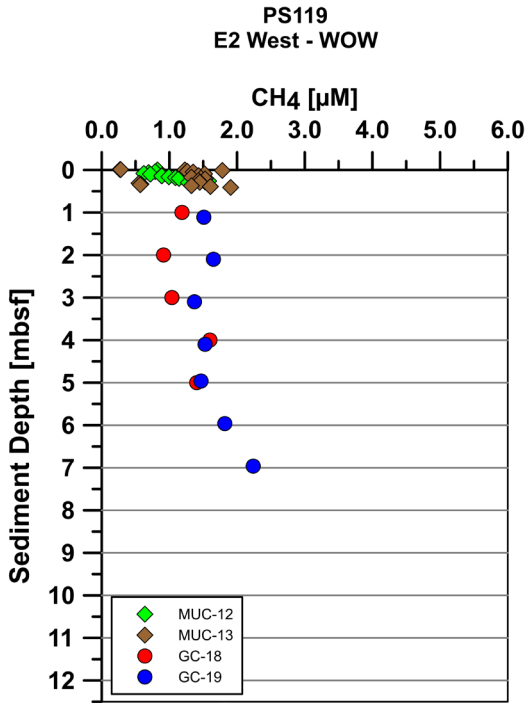

Fig. 13.7: Dissolved CH_4 in sediments at site E2 West (WOW)

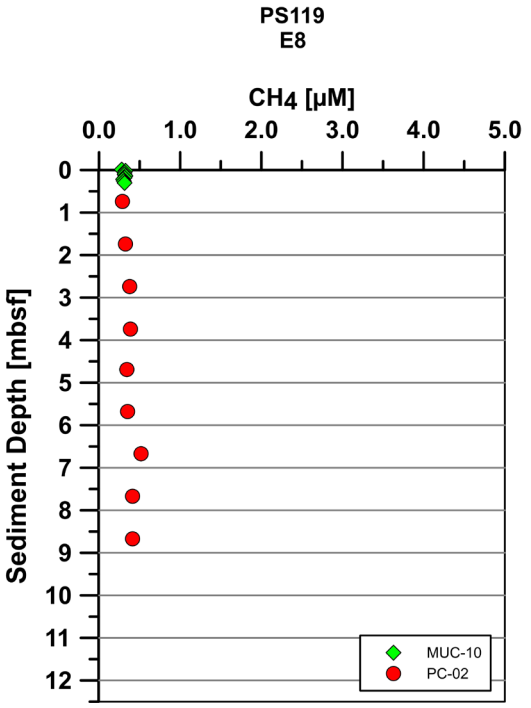

Fig. 13.8: Dissolved CH_4 in sediments at site E8

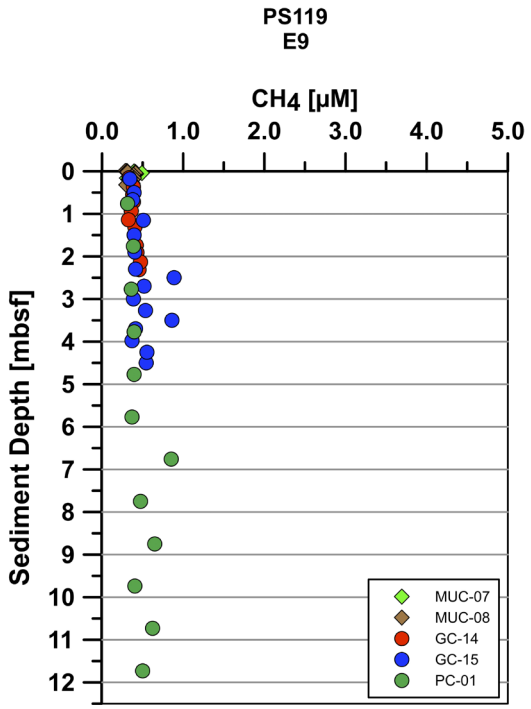

Fig. 13.9: Dissolved CH_4 in sediments at site E9

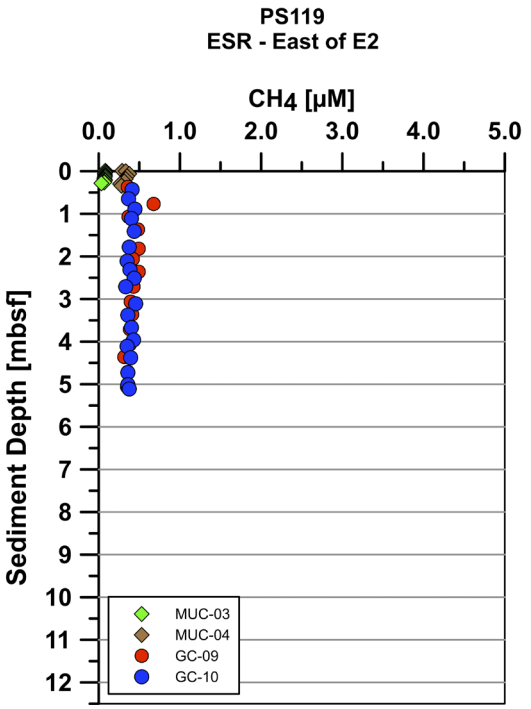

Fig. 13.10: Dissolved CH_4 in sediments at site East of E2

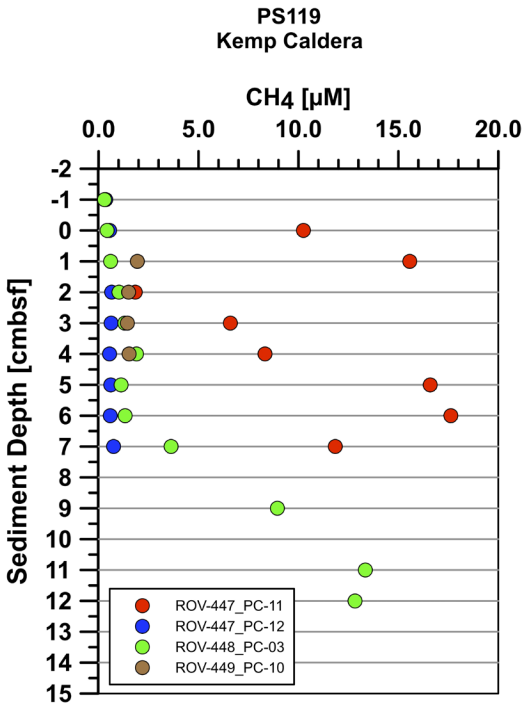

Fig. 13.11: Dissolved CH_4 in push cores from the Kemp Caldera

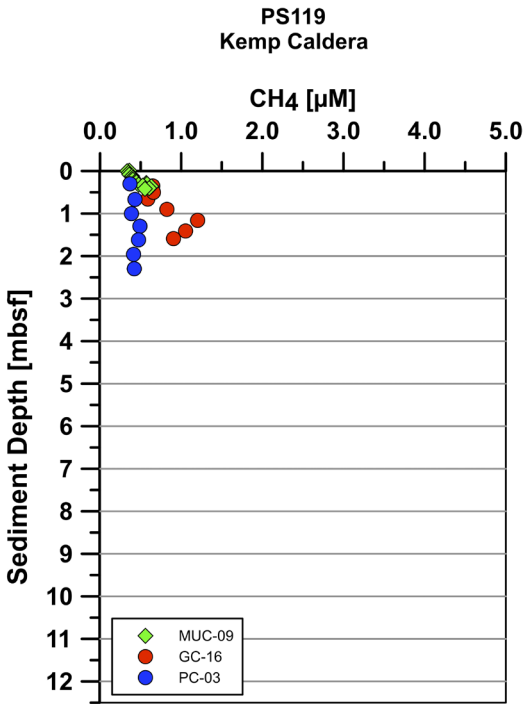

Fig. 13.12: Dissolved CH_4 in the multi core, gravity core and piston core from the Kemp Caldera

Dissolved methane in the water column

During PS119, slight relative methane enrichments associated with decreases in beam transmission, were observed in near-bottom waters and close to the surface at all stations investigated. In addition, relative methane enrichments several hundreds of meters above sea floor were observed at 'ESR-E2 West' and in the Kemp Caldera. Those methane enrichments were correlated with significant decreases in beam transmission as well and, thus, believed to indicate significant methane injections into the water column driven by hydrothermal activity.

East Scotia Ridge - E2

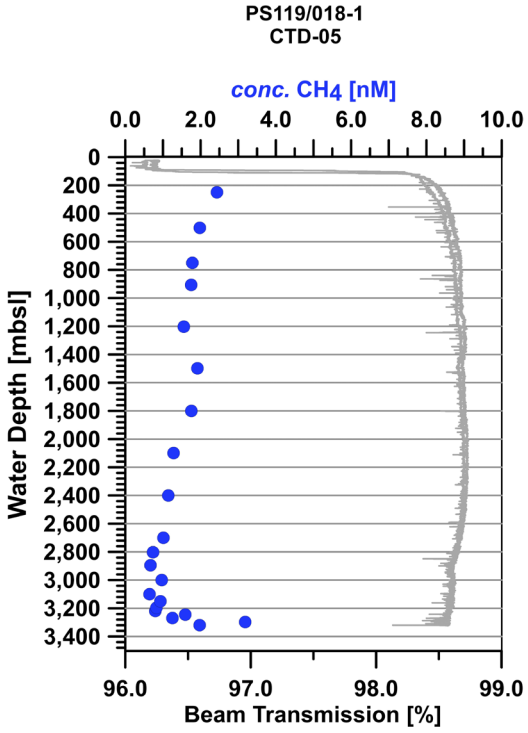

Fig. 13.13: Dissolved CH_4 and beam transmission at station CTD-05

ESR - E2 West

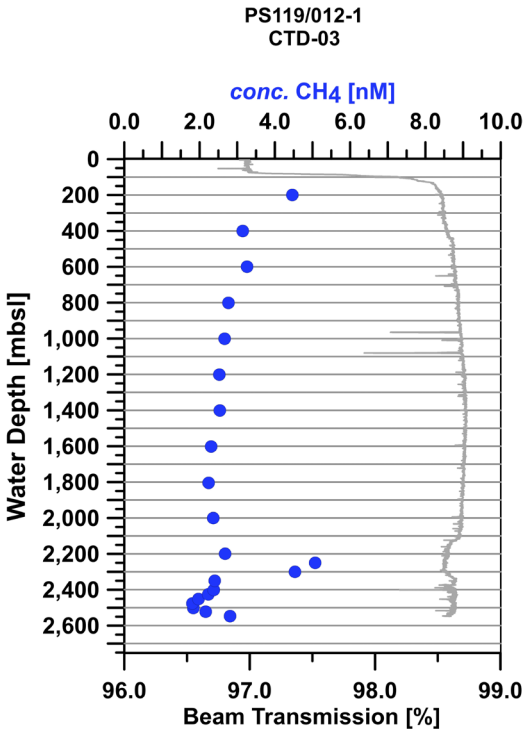

Fig. 13.14: Dissolved CH_4 and beam transmission at station CTD-03

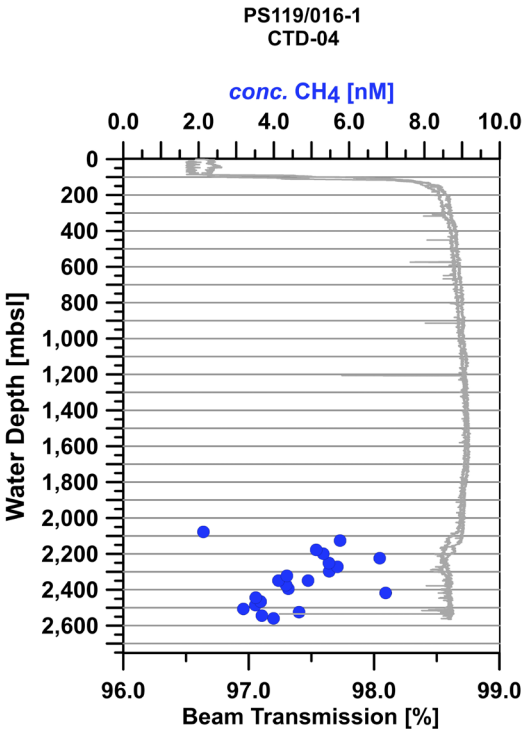

Fig. 13.15: Dissolved CH_4 and beam transmission at station CTD-04

ESR – E2 West (WOW)

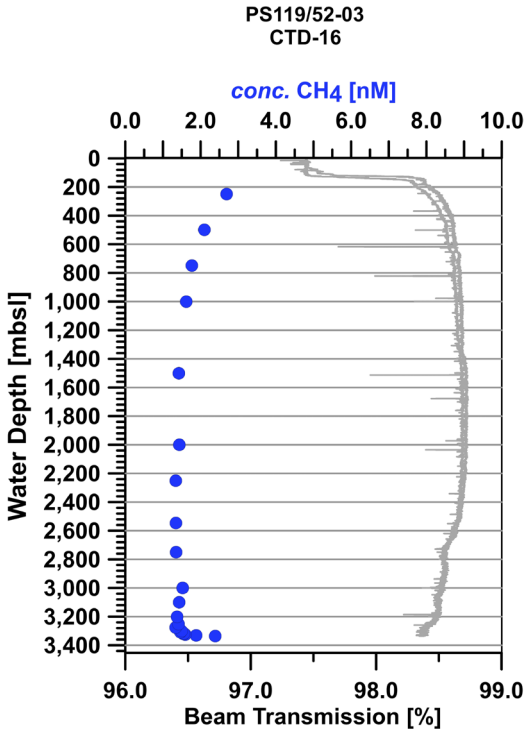

Fig. 13.16: Dissolved CH_4 and beam transmission at station CTD-16

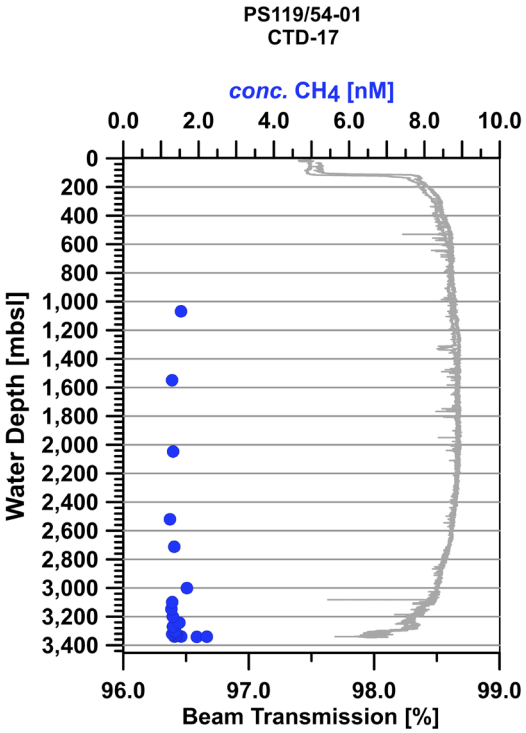

Fig. 13.17: Dissolved CH_4 and beam transmission at station CTD-17

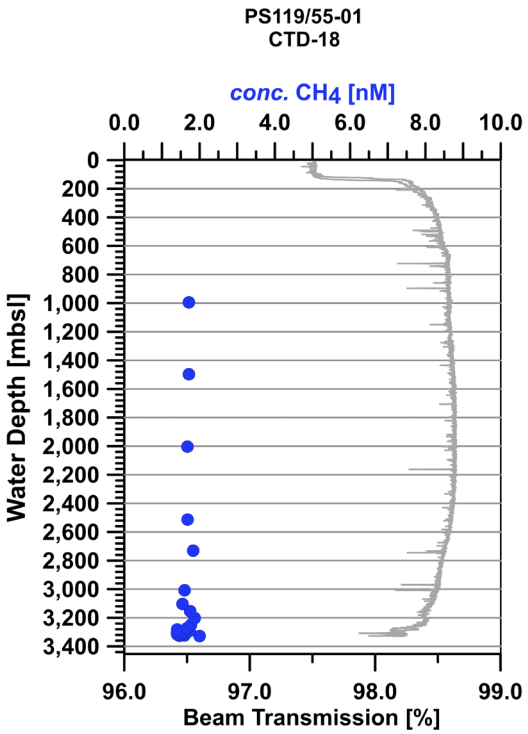

Fig. 13.18: Dissolved CH_4 and beam transmission at station CTD-18

ESR – E5

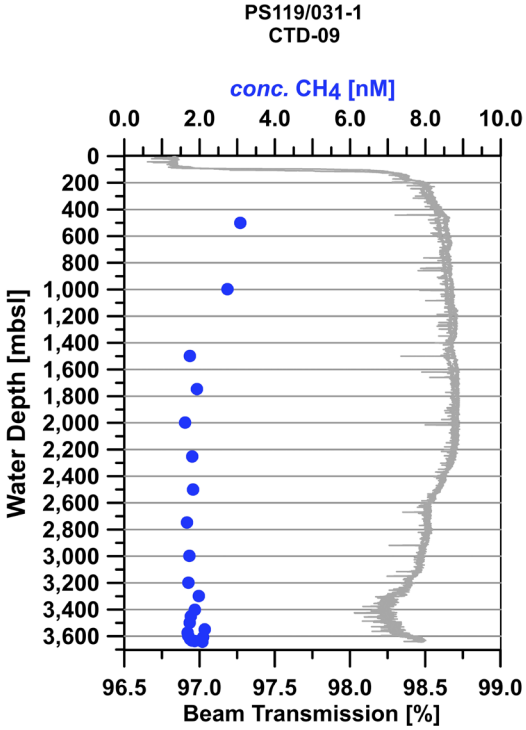

Fig. 13.19: Dissolved CH_4 and beam transmission at station CTD-09

ESR – E8

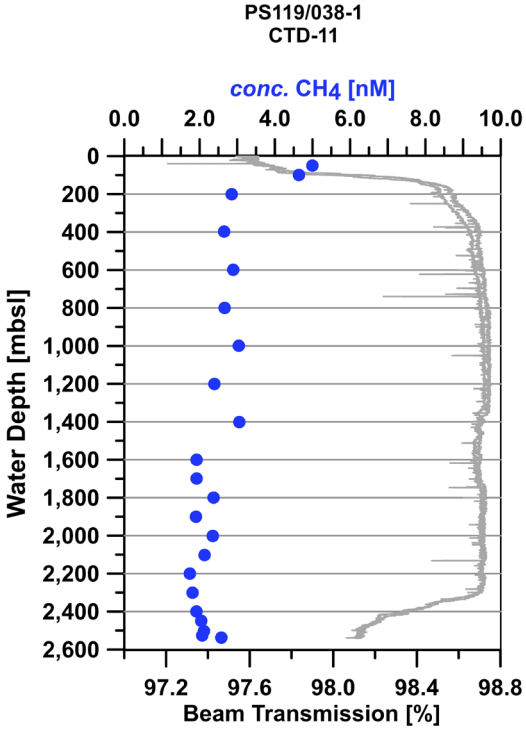

Fig. 13.20: Dissolved CH_4 and beam transmission at station CTD-11

Kemp Caldera

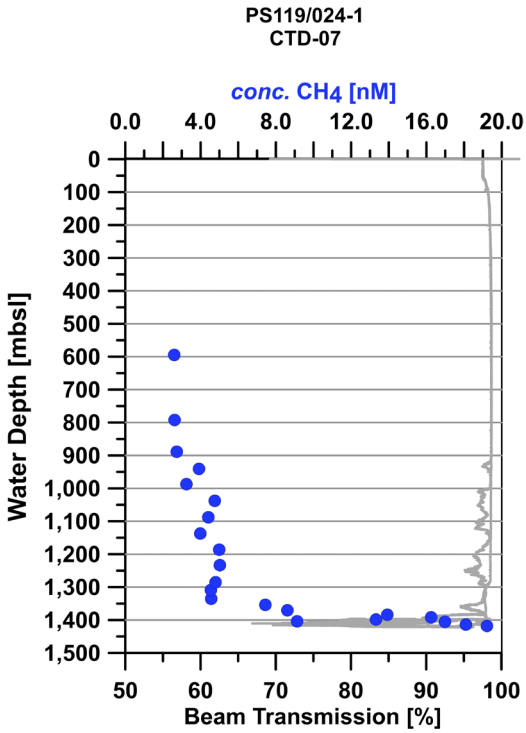

Fig. 13.21: Dissolved CH_4 and beam transmission at station CTD-07

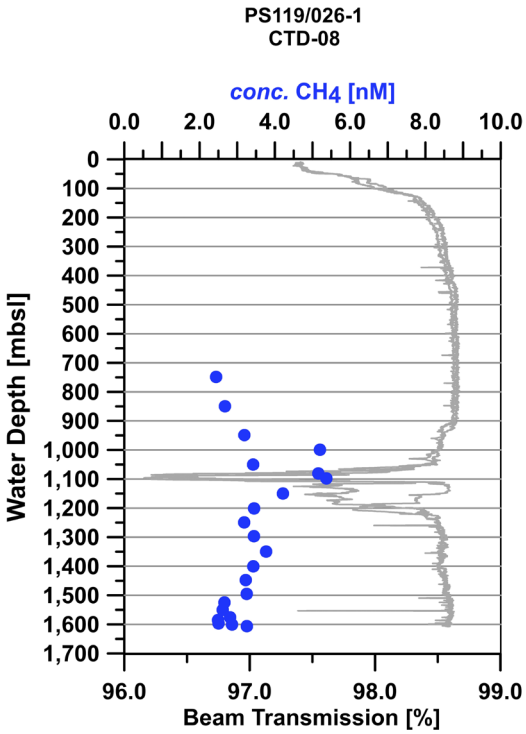

Fig. 13.22: Dissolved CH_4 and beam transmission at station CTD-08

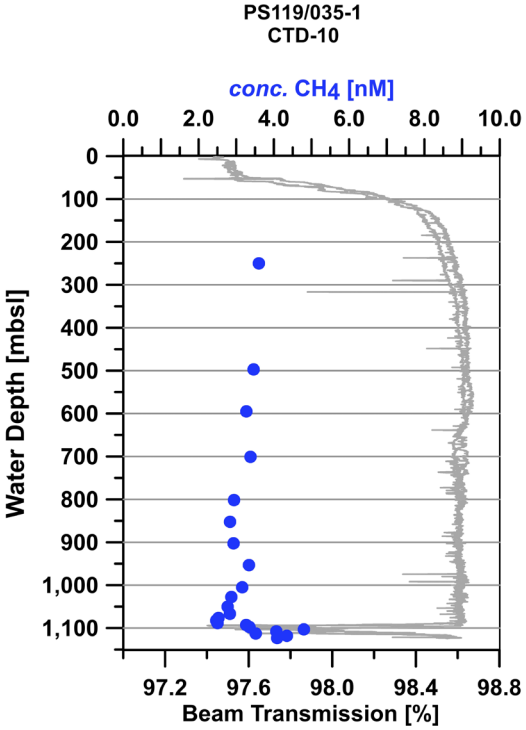

Fig. 13.23: Dissolved CH_4 and beam transmission at station CTD-10

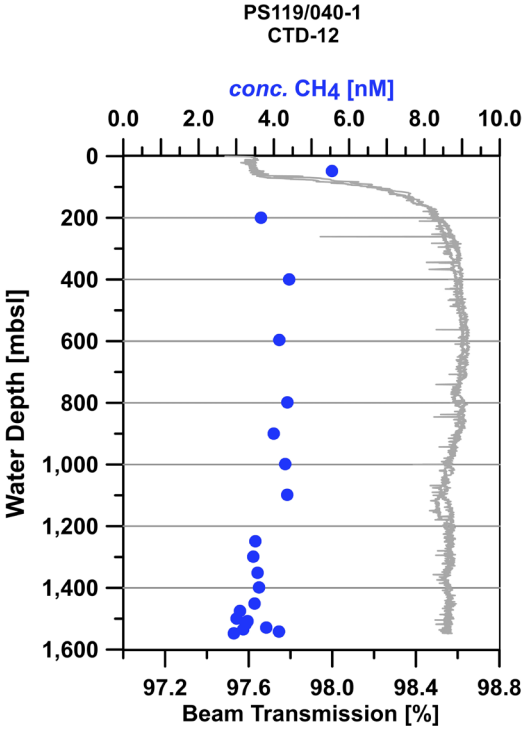

Fig. 13.24: Dissolved CH_4 and beam transmission at station CTD-12

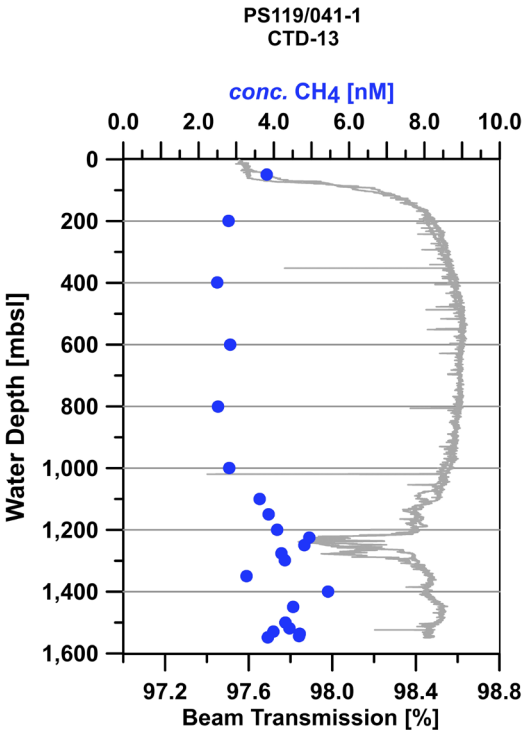

Fig. 13.25: Dissolved CH_4 and beam transmission at station CTD-13

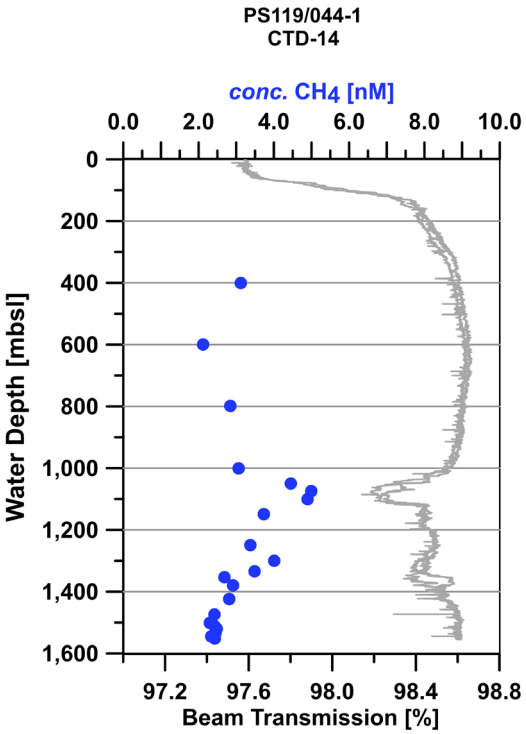

Fig. 13.26: Dissolved CH_4 and beam transmission at station CTD-14

South Sandwich forearc

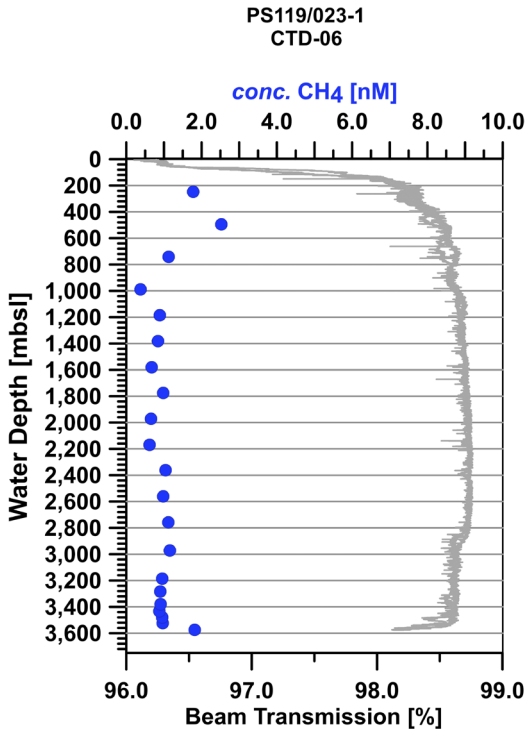

Fig. 13.27: Dissolved CH_4 and beam transmission at station CTD-06

Data management

All data collected and generated by this project will be made publicly available via the World Data Center PANGAEA Data Publisher for Earth & Environmental Science (www.pangaea.de).

References

Kvenvolden KA, McDonald TJ (1986) Organic geochemistry on the Joides Resolution: An assay, Technical Note. Ocean Drilling Program, Texas A&M Univ, College Station, Tex., p. 147.

Pape T, Bahr A, Rethemeyer J, Kessler JD, Sahling H, Hinrichs KU, Klapp SA, Reeburgh WS, Bohrmann G (2010) Molecular and isotopic partitioning of low-molecular weight hydrocarbons during migration and gas hydrate precipitation in deposits of a high-flux seepage site. Chem. Geol. 269, 350-363. doi:10.1016/j.chemgeo.2009.10.009.

14. BIODIVERSITY AND ECOLOGY OF MACRO- AND MEGABENTHIC SPECIES IN THE EAST SCOTIA RIDGE AND SOUTH SANDWICH ISLAND CHAIN HYDROTHERMAL ECOSYSTEMS

Katrin Linse[1], Julia Sigwart[2]

[1]BAS, Cambridge

[2]QUB-QML, Portaferry

Grant-No. AWI_PS119_00

Outline

The first active chemosynthetic ecosystems south of the Polar front were discovered in 2009 on the East Scotia Ridge (ESR) by the NERC ChEsSo consortium (Chemosynthetic Ecosystems) (Rogers et al., 2012). To date, only the communities in vent fields at E2 and E9 have been characterized (Rogers et al., 2012; Marsh et al., 2012, 2013) (Fig. 14.1A). The ecosystem and assemblages at the Kemp Caldera differ from those of the ESR and are currently under description (Linse et al., in review) (Fig. 14.1B). The assessments of the microbial structure in the plumes and water columns around the three vent sites showed differences in community assemblage and diversity (Zwirglmaier et al., unpublished ChEsSO results). The ecosystems at the other sites (Adventure Crater, Quest Caldera) have not yet been investigated in detail and little is known of their faunal and chemical characteristics.

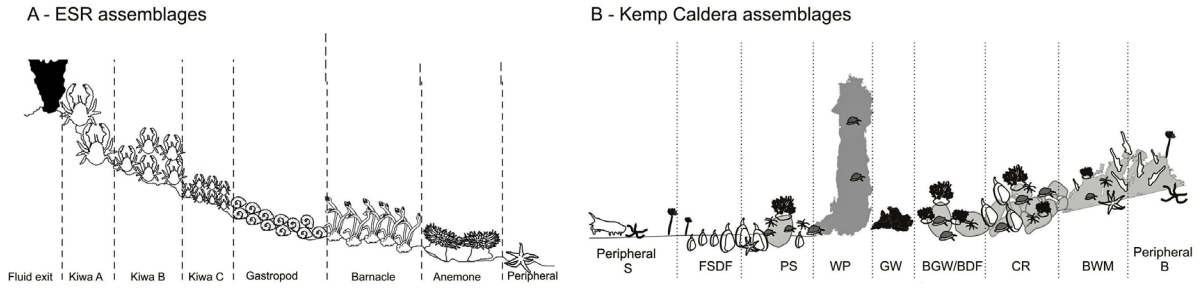

Fig. 14.1: Faunal vent assemblages A) at ESR, after [28], B) in Kemp Caldera, Linse et al., in review

The ESR vent sites E2 and E9 in 2,400 – 2,600 m depth are characterized by pillow basalts, sheet lavas and black smoking chimneys of 351-383°C. The vent fluid composition, whilst variable between E2 and E9, is similar to other basalt hosted vent sites (James et al., 2014). While E2 is defined by numerous active and extinct chimneys and spatially limited diffuse flow fields, E9 has more distinct chimneys surrounded by extended diffuse flow fields. Dominant species defining the local microzonation are the yeti crab *Kiwa tyleri,* the gastropod *Gigantopelta chessoia*, the stalked barnacles *Neolepas scotianensis*, and an actinostylid anemone. Further species primarily using chemosynthetic or mixed food sources and present at both sites are the gastropods *Lepetodrilus* sp. and *Provanna cooki*., the sea spiders *Sericosura* spp. and the starfish *Paulasterias tyleri*. Survey work at E2 in 2012 updated the initial faunal list and confirmed the presence of all species listed at both sites. The vent sites discovered so far in the

Kemp Caldera at 1,500 m depth are associated with a resurgent cone. The vents themselves are characterized by white smoking chimneys of 103-212°C (Rogers, 2010), and wide ranging diffuse flow areas at basalt and sediment areas. The vent fluid composition is distinctly different from the nearby E9 site, being high in hydrogen sulphide and iron, with evidence for an input of magmatic gas Cole et al,. 2014; Hawkes et al., 2014). Dominant megafauna are an in- and epibenthic living, large vesicomyid clam, the limpets *Lepetodrilus* sp. and cocculinid sp., the seaspiders *Sericosura* spp., as well as actinostylid anemones. The presence of *N. scotianensis* and the predator *P. tyleri*, are rare.

The back-arc sites on the ESR segments E2 and E9, 440 km apart, represent a globally unique biogeographic vent province with a specialized SO chemosynthetic fauna (e.g. Rogers et al., 2012; Thatje et al., 2015; Chen et al., 2015; Arango & Linse, 2015). Biological and geochemical analyses of these ESR sites have shown certain differences in the composition of the faunal assemblages and chemical characteristics of the environments at ESR (Marsh et al., 2012; James et al., 2014). In contrast, the Kemp Caldera vent fauna composition, separated by only 90 km from E9, is characterized by the absence of key species from ESR (E2 and E9), the dominance of species absent at ESR, and differences in abundances of those species that do overlap. The ESR community forms distinct assemblages and micro-zonations (Marsh et al., 2012) (Fig. 14.1A) as does the Kemp Caldera community (Fig. 14.1B). Initial food web analysis of the ESR sites confirms the dependence of the dominant megafauna on bacterial chemosynthesis, as well as regional differences in the bacterial and isotopic compositions of the vent fluids and in megafaunal species (Reid et al., 2013; Zwirglmaier et al., 2014), while for the Kemp Caldera no information is yet available on the food web structure. The levels of (dis) similarity in species composition and food web structure between the megafaunal communities of the ESR sites (E2, E9) and the Kemp Caldera as well as the other hydrothermal site in the area (e.g. Quest Caldera, Adventure Crater) have not been studied. Genetic connectivity between the ESR sites E2 and E9 and between ESR and Kemp Caldera in the indirect developers *K. tyleri*, *G. chessoia*, *Lepetodrilus* sp. and *N. scotianesis* is shown by COI haplotype and/or microsatellite studies (Chen et al., 2015; Roterman et al,. 2016) and supports the presence of oceanographic currents for larval transport between sites. The study on *Lepetodrilus* sp. also showed a high level of differentiation in COI and microsatellites between the ESR and Kemp Caldera indicating a different, nearby source population for the caldera. These analyses indicated that the ESR and Kemp limpet populations might be adapted to different hydrothermal fluid chemistries, which could prevent colonization and/or reproduction in a vent habitat with different geochemistry.

On this and prior cruises, opportunistic sampling from deployments of a Multicorer (MUC) on the shelf of South Georgia and the bathyal of the eastern Scotia Sea enabled us to collect cores for studies on the quantitative biodiversity of benthic macro- and meiofauna in methane-enriched or hydrothermally influenced sediments as well as for the analysis on the presence of microplastics. Comparable biodiversity data on macro- and meiobenthic fauna collected by MUC in the Southern Ocean from the shelf to the deep-sea basins are available through the publications of Glover et al. (2008), and more specifically for the Icefjord Trough, South Georgia by Bell et al. (2016) and Woulds et al (2019). The latter noted that the cores came from an area with methane emissions but that the fauna resembled known Southern Ocean taxa. Additional comparative samples, which yet need to be analyzed for biodiversity and microplastics were collected on the shelf of South Georgia in 2017 (Linse & Hogg, 2017 in Bohrmann et al., 2017) and in the Prince Gustav Channel, eastern Antarctic Peninsula in 2018 (Linse, 2018) (Fig. 14.2). In recent years, the problems of marine plastic debris and its negative impacts on wildlife and the environment came to the focus of marine environmentalists. Microplastic fragments were discovered in oceanic gyres and shallow water sediments, but the majority of microplastics are thought to sink to the deep ocean seafloor (Woodall et al., 2014). Records on plastic debris in the Southern Ocean is limited to a few publications on visible pieces, washed ashore, seen at

sea or impacting wildlife. Microplastic records from deep-water Southern Ocean sediments are however still absent (Waller et al., 2017).

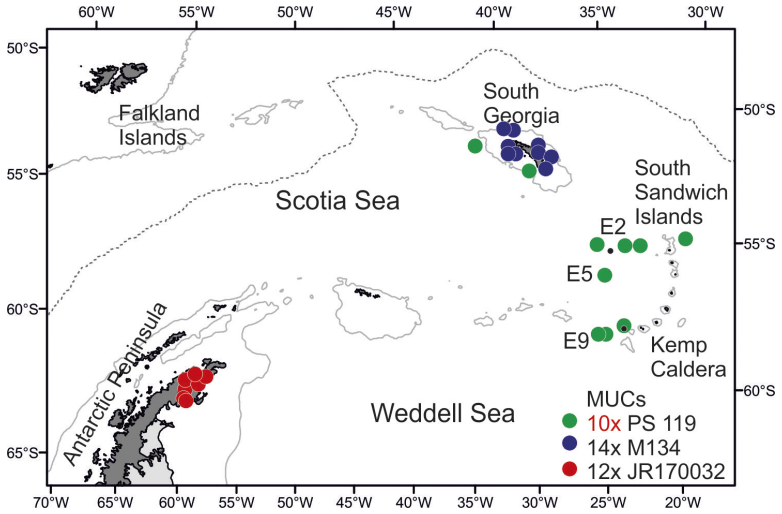

Fig. 14.2: Locations of MUC deployments during the expeditions PS119, M134 and JR17003a

Objectives

Objective 1: Documentation of the vent faunal communities and their microdistributions in terms of species richness, community composition and abundance using ROV video and specimen sampling.

The zonations of the epibenthic megafaunal communities at E2 and Kemp have been visually defined (Fig. 14.1), but have not been sampled previously in a coherent way (combining geochemistry and biology). In collaboration with the Bohrmann group, additional characteristics of the fine-scale physical environment will be derived from the bathymetry data (e.g. slope, Benthic Positioning index) or from other sensor data (e.g. temperature, salinity). Key locations might be imaged through videomosaicing, to obtain information at the highest spatial scale for detailed habitat mapping and predictive habitat modelling.

Objective 2: Phylogenetic and population genetic analyses in verified, selected direct and indirect developing species

For biological analyses specimens will be collected per site and location. Taxonomic validity checks will be done by morphological and molecular (barcoding) techniques. For connectivity studies between back-arc and island arc vent sites we will analyze the fine-scale molecular population structure of selected direct (dd) and indirect (id) developing species collected from different microdistribution zones within our sites. The two main study sites E2 and Kemp Caldera share some chemosynthetic species, *Lepetodrilus* sp., *N. scotianensis* (both id), *Sericosura bamberi*, *S. curva*, and *S. dimorpha* (all dd), while others like *K. tyleri*, *G. chessoia,* the vesicomyid clam (all id) or *Provanna cooki* (dd) occur only at one type of vent setting. We will assess the molecular population structure of selected species (e.g. *Lepetodrilus*) using COI mtDNA and microsatellite markers.

Objective 3: Comparison of macrofaunal biodiversity and community structure at hydrothermally influenced sites in the eastern Scotia Sea with sites on the shelf of South Georgia and in the Prince Gustave Channel, eastern Antarctic Peninsula.

Objective 4: Detection of microplastics at different sites of South Georgia and the eastern Scotia with varying anthropogenic presence.

Work at sea

Objective 1: The ROV dive videos, frame grabs and notes written during the dives were logged, saved and reviewed, and are reported in the Chapter 7 of this expedition report for each individual dive.

For Objectives 2 we required physical specimens to be collected by ROV. ROV MARUM QUEST sample collections for macro-and megafauna took place at the ridge segment E2 and in the Kemp Caldera.

On arrival on deck, the collected specimens were removed from the ROV's sampling boxes and nets, and distributed for further analysis. The sediment remaining in the sampling nets were collected and fixed in ethanol for later sorting, picking out for small sized-macrofauna in the home laboratory.

Objective 2: The benthic specimens for genetic and genomic analyses were fixed in ethanol, or frozen at -20°C and -80°C. A checklist of the physical specimens collected for objectives 2 are available in the appendix with indication which specimens will be used for which type of further analyses.

The 12-core MUC, consisting of twelve 7.5 cm diameter tubes, was one of the main pieces of equipment to help answer the geochemical and geological objectives of the PS119 project proposal. On arrival on deck, all tubes were photographed to record sediment height, layering and color by our geological colleagues (references to overall MUC report with core photos etc). After tubes were taken for analyses of pore water, methane, solid phase, sediment layering description, Fe isotope and magnetic analyses, the remaining tubes were available for macrofauna, and microplastic analyses. A total of 40 7.5 cm tube samples were taken. Each tube was sliced at 0-2 cm and 2-5 cm layers using a core extruder, resulting in at least two individual samples (Table 14.1). Samples for microplastics were frozen in plastic ziplock bags at -20°C, and samples for macrofauna analysis were sieved through a 300 µm sieve in ambient temperature of 2-5°C, initially fixed in 96% ethanol at -20°C for at least 48 h and later stored at +4°C. No samples were sorted on board. For location and depth information please refer to the overall station list in the appendix.

Tab. 14.1: Distribution of core tubes and depth layers for macrofaunal and microplastic analysis

MUC-number	PS119_ Station	Macrofauna 0-2 cm	Macrofauna 2-5 cm	Microplastics 0-2 cm	Microplatics 2-5 cm
MUC-1	1-1	2	2	1	1
MUC-2	7-2	2	2	1	1
MUC-3	14-2	2	2	1	1
MUC-4	15-2	3	3	1	1
MUC-5	18-1	2	2	1	1
MUC-6	22-1	2	2	1	1
MUC-7	25-2	2	2	2	2
MUC-8	29-2	2	2	1	1
MUC-9	36-1	-	-	2	2
MUC-10	37-2	2	2	2	2
MUC-11	48-1	-	-	2	-
MUC-12	52-2	2	2	2	2
MUC-13	53-1	-	-	2	2

Preliminary (expected) results

Objective 1: Three hydrothermally active areas have been investigated by ROV QUEST, the areas E2_S and E2_W on the East Scotia Ridge segment E2, and the Kemp Caldera on the southern end of the volcanic island arc.

The initial analysis of the ROV dive footage (video and stills) from the E2_S hydrothermally active field around the black smoker Dog's Head showed significant changes in the macro- and megafaunal assemblage compositions and densities when compared to footage of the expeditions JC42 and JC80 in 2010 and 2012. In the area named "Anemone Field" in 2010 for the abundance of actinostolid anemones on a wide ranging basalt boulder field with diffuse flow, only a small area with anemones on basalts were observed. The yeti crab *Kiwa tyleri* was observed – like in the past – as singletons walking over boulders or in groups in crack between boulders where also shimmering waters were seen. One component of this faunal assemblage, the stalked barnacle *Neolepas scotiaensis* has almost disappeared. While in 2010 representatives of the species' short-stalked, robust type had been observed in dense clusters (Buckeridge et al., 2013) only single specimens with very short stalks were seen. The appearance of black smoker "Dog's Head" has changed as well. On its eastern end, a black smoking orifice has opened and many flanging balconies have been built. The dense population of *Gigantopelta chessoia* has disappeared. Over all the number of observed macro- and megafaunal specimens, e.g. of *Kiwa tyleri*, *G. chessoia*, *Provanna cooki* and *Lepetodrilus* sp., have dropped. The dense populations of *Kiwa tyleri* in "Crab City" and of *Gigantopelta chessoia* in "Cindy's Castle" have disappeared.

The area E2_W, a hydrothermal active area geochemically located during JC80, was visually examined by ROV for the first time during dive 445. The area was characterized by non-smoking, tall chimney structures, which still showed areas of shimmering water. Occasional *Kiwa tyleri* were seen on the chimneys as well as in the basalt boulder fields around the chimney structures. At three locations of basalts with shimmering water the decapod shrimp *Eualus amandae* was seen, that had not been seen in obviously hydrothermally active habitats before.

In the Kemp Caldera, the observed changes were in the distributional shift of some biotopes locations. Charismatic structures like "Great Wall", "Toxic Castle" and "Winter Palace" were looking similar to 2010, still with white smoking chimneys and shimmering water. A faunal change was the increased density of lepetodrilid limpets on the white smoking chimneys. On the north-eastern flank of a side cone to the south of the resurgent cone, the population of the free-living ecotype of *Laubiericoncha puertodesadoi* was not found, despite moving up in a survey pattern to the top of the cone to the area "Ash Mount". On top of "Ash Mount" a field of shimmering water and bacterial mats was seen, which had a dense assemblage of lepetodrilid and cocculinid limpets, *Sericosura* seaspiders and amphipods.

Back in the home institutes, we will robustly compare this expeditions *in-situ* images from the hydrothermally active areas of E2-S and Kemp Caldera with those taken during JC42 and JC80 in 2010 and 2012 respectively, assess the differences and describe the changes in peer-reviewed publications.

Objective 2: During the ROV QUEST dives, specimens, apart from those of the species selected for respirometer studies (*Gigantopelta chessoia* and *Laubiericoncha puertodeseartoi*), were collected very specifically in low numbers, e.g. for *Paulasterias tyleri* and *Kiwa tyleri*, or opportunistically with rock and precipitate samples, e.g. the limpets *Lepetodrilus* sp and cocculinid sp., and *Provanna cooki*. The specimens of all taxa collected will be tissue sampled for DNA extraction and COI barcode gene analysis to investigate if the current specimens originate from the pool of known haplotypes (Roterman et al., 2016). For *Lepetodrilus* sp, as morpho-molecular analyses will be carried out to investigate if the specimens collected during PS119 fall within the morphometric and molecular data collected during JC42 and JC80 in 2010 and 2012.

Objective 3: On return of the macrofaunal samples to the UK, the macrofaunal samples will initially be sorted to 16 higher taxa and later will be sorted visually into morphospecies, critically compared between stations for species overlaps and species-station matrixes for multivariate statistical analyses created in order to find out if significant differences between stations and areas are present. It is planned to publish the abundance and assemblage composition data in collaboration with the geochemists to study the influence of the abiotic factors on the macrofauna. The biodiversity data will be compared with complementary data collected during M134 and JR 17003a.

Objective 4: The collected dataset of frozen MUC tube samples from several sites will provide a unique dataset of sediment cores for the analysis of microplastics in the Southern Ocean. The samples will be compared with MUC samples collected for microplastics analyses on the shelves of South Georgia and the eastern Antarctic Peninsula (Fig. 14.2).

Data management

Metadata of the ROV deployments will be deposited in the World Data Center PANGAEA Data Publisher for Earth & Environmental Science (www.pangaea.de). Biological samples for macro- and megafauna studies will be housed at BAS and Queen's University Belfast's Portaferry Marine Lab. Taxonomic information (molecular barcode sequences, georeferenced location records, *in-situ* images) will be published in the relevant international databases, e.g. Genbank, OBIS and Deep-sea Imagery database. Specimens collected will be submitted to natural history museums (e.g. London, Frankfurt) on publication of related data. Community analysis and ecological raw data will be submitted to the Polar Data Centre housed in BAS for long-term storage.

References

Arango CP, Linse K (2015) New *Sericosura* (Pycnogonida: Ammotheidae) from deep-sea hydrothermal vents in the Southern Ocean. Zootaxa, 3995, 037-050.

Bell, JB, Aquilina, A, Woulds, C, Glover AG, Little, CTS, Reid WDK, Hepburn, LE, Newton, J, Mills, RA (2016) Geochemistry, faunal composition and trophic structure in reducing sediments on the southwest South Georgia margin. Royal Society Open Science, 3, 160284.

Buckeridge J, Linse K, Jackson J (2013) Vulcanolepas scotiaensis sp. nov., a new deep-sea scalpelliform barnacle (Eolepadidae: Neolepadinae) from hydrothermal vents in the Scotia Sea, Antarctica. Zootaxa 3745, 551-568.

Chen C, Linse K, Roterman CN, Copley JT, Rogers AD (2015) A new Genus of large hydrothermal vent-endemic gastropod (Neomphalina: Peltospiridae) with two new species showing evidence of recent demographic expansion. Zoological Journal of the Linnean Society, 175, 319-335.

Cole CS, James RH, Connelly DP, Hathorne EC (2014) Geochim et Cosmochim Acta, 140, 20-38.

Glover, AG, Smith, CR, Mincks, SL, Sumida, PYG, Thurber, AR (2008) Macrofaunal abundance and composition on the West Antarctic Peninsula continental shelf: Evidence for a sediment "food bank" and similarities to deep-sea habitats. Deep-Sea Research Part II: Topical Studies in Oceanography, 55(22-23), 2491–2501.

Hawkes JA, Connelly DP, Rijkenberg MJA, Achterberg (2014) The importance of shallow hydrothermal island arc systems in ocean biogeochemistry. Geophysical Research Letter, 41, 942-947.

James RA, Green DRH, Stock MJ, Alker BJ, Banerjee NR, Cole C, German CR, Huvenne WAI, Powell AM, Connelly DP (2014) Composition of hydrothermal fluids and mineralogy of associated chimney material on the East Scotia Ridge back-arc spreading centre. Geochim Cosmochim Actca, 139, 47-71.

Linse, K (2018) JR17003a cruise report. www.bodc.ac.uk

Linse, K, Hogg, O. (2017) Chapter 12. Biology - Biological and Environmental Collections from Multicorer Samples in the South Georgia's Shelf Troughs In: eds: in Bohrmann et al., R/V METEOR CRUISE REPORT M134. Berichte aus dem MARUM und dem Fachbereich Geowissenschaften der Universität Bremen. 136-145

Linse K, Copley J, Connelly DP, Larter RD, Pearce DA, Polunin NVC, Rogers AD, Chen C, Clarke AC, Glover AG, Graham AGC, Huvenne VAI, Marsh L, Reid WDK, Roterman CN, Sweeting CJ, Zwirglmaier K, Tyler PA (in review). The fauna of the upper bathyal hydrothermal vents of the Kemp Caldera (South Sandwich Arc, Antarctica). RSOS

Marsh L, Copley J, Huvenne V, Linse K, Reid WDK, Rogers A, Sweeting CJ, Tyler P (2012) Microdistribution of faunal assemblages at deep-sea hydrothermal vents in the Southern Ocean PLoSOne, 7, e48348 doi:10.1371/journal.pone.0048348.

Marsh L, Copley JT, Huvenne VAI, Tyler PA (2013) Getting the bigger picture: Using precision Remotely Operated Vehicle (ROV) videography to acquire high-definition mosaic images of newly discovered hydrothermal vents in the Southern Ocean. Deep-Sea Research II, 92, 124-135.

Reid WDK, Sweeting CJ, Wigham BD, Zwirglmaier K, Hawkes JA, McGill RAR, Linse K, Polunin NVC (2013) Spatial differences in East Scotia Ridge hydrothermal vent food webs: influences of chemistry, microbiology and predation on trophodynamics. PLoSOne, 9 (6), e65553.

Rogers AD (2010) Cruise report JC042 www.bodc.ac.uk.

Rogers AD, Tyler PA, Connelly DP, Copley JT, R. James R, Larter RD, Linse K, Mills RA, et al (2012) The discovery of new deep-sea hydrothermal vent communities in the Southern Ocean and implications for biogeography. PLoS Biology, 10(1), e1001234. doi:10.1371/journal.pbio.1001234.

Roterman CN, Copley JT, Linse K, Tyler PA, Rogers AD (2016) Connectivity in the cold: the comparative population genetics of vent-endemic fauna in the Scotia Sea, Southern Ocean. Molecular Ecology, 25, 1073-1088.

Thatje S, Marsh L, Roterman CN, Mavrigordate MN, Linse K (2015) Adaptations to hydrothermal vent life in Kiwa tyleri, a new species of yeti crab from the East Scotia Ridge, Antarctica. PLoS One 10(6): e0127621.doi:10.1371/journal.pone.017621.

Waller, C, Griffiths, HJG, Hughes, K, Waluda, C, Thorpe, S, Alamo, I, Moreno, B, Pacherres, C (2017) Microplastics in the Antarctic marine system: An emerging area of research. Science of the Total Environment 568, 220-227.

Woodall, LC, Sanchez-Vidal, A, Canals, M, Paterson, GLJ, Coppock, R, Sleight, V, Antonio Calafat, A, Rogers, AD, Narayanaswamy, BE, Thompson, RC (2014) The deep sea is a major sink for microplastic debris. Royal Society Open Science, 1, 140317.

Woulds, C, Bell, JB, Glover AG, Bouillon S, Brown LB. (2019) Carbon processing by the benthic ecosystem and benthic C fixation in methane-rich sediments on the South Georgia margin. Antarctic Science 31, 59-68.

Zwirglmaier K, Reid W, Heywood J, Sweeting C, Wigham B, Polunin N, Hawkes J, Connelly D, Pearce D, Linse K (2014) Diversity of epibiotic bacteria and trophic ecology a new species of Kiwaidae (Decapoda, Anomura) at two hydrothermal vent fields on the East Scotia Ridge, Antarctica, exhibit high regional differences. Microbiology Open doi: 10.1002/mbo3.227.

15. EXPERIMENTAL PHYSIOLOGY OF DEEP-SEA ANIMALS

Julia Sigwart[1], Katrin Linse[2]
Chong Chen[1] (not on board)

[1]QUB-QML Portaferry
[2]BAS, Cambridge

Grant-No. AWI_PS119_00

Objectives

Physiological traits are the foundation of an organism's success in a dynamic environment; the ability to metabolize oxygen can determine an animal species' fitness, spatial distribution, and its capacity to adapt to changing conditions. Our research aims during PS119 were to measure routine metabolism (oxygen uptake) in molluscs from hydrothermally influenced environments. Both of our target animals host chemoautotrophic endosymbionts. The two target species occur in high abundance at study sites important to this cruise: the hydrothermal vent gastropod *Gigantopelta chessoia*, at E2, and the chemosymbiotic bivalve *Laubiericoncha puertodeseadoi* in Kemp Caldera.

Our previous work on other vent gastropods, in the Indian Ocean, showed that responses to temperature differed between species with different anatomical mechanisms to host the symbiotic microbes on which the gastropods depend for food. In the Indian Ocean, the scaly-foot snail, *Chrysomallon squamiferum* hosts microbes in a specialized internal organ, and is more tolerant of temperature change than another gastropod *Alviniconcha* that hosts microbes in its gill (Sigwart & Chen, 2018). At the East Scotia Ridge, the gastropod *Gigantopelta chessoia* also hosts microbes in a specialized internal organ and we predicted that its physiological response to temperature would be similar to *Chrysomallon.*

Chemosymbiotic bivalves in the subfamily Pliocardiinae, commonly referred to as vesicomyids, are known from chemoautotrophic ecosystems including vents and seeps worldwide. *Laubiericoncha puertodeseadoi* is the only living chemosymbiotic vesicomyid known from the Southern Ocean. The oxygen metabolism has been described for six species in the group, from *ex-situ* and *in-situ* experiments in the Atlantic and Pacific (Decker et al., 2012). This provides useful context to compare the physiology of these Southern Ocean vesicomyids.

For these two study systems, our objectives were to use *ex-situ* closed chamber respirometry to measure routine oxygen uptake rates, and use infrared sensors to measure ventilation of the pericardium to record heartrate.

Work at sea

We collected specimens with nets deployed on ROV MARUM QUEST. Specimens of *Gigantopelta chessoia* were collected on two dives at E2, and *Laubiericoncha puertodeseadoi* on two further dives in Kemp Caldera (Table 15.1). Animals were held in seawater aquaria in three temperature-controlled containers on board set at temperatures of 2°C, 10°C, and 20°C.

Experiments were conducted using continuous-recording fibre-optic probes (Ocean Optics, Dunedin, USA) that record oxygen saturation at 1 second intervals on a dedicated computer.

Six probes were available; thus five experimental animals and one control (seawater only) could be measured simultaneously (Fig. 15.1). Standard protocols for closed-chamber respirometry were applied (Carey et al., 2013). An animal subject is placed into a sealed chamber fitted with a fibre-optic probe. Chambers are placed into a water bath that is maintained at constant temperature. As the chamber is sealed, the animal has a fixed amount of oxygen available, which decreases during the experiment (Fig. 15.2). The rate of decline (mg O_2 / time / animal mass) is an effective proxy for routine metabolism. Heart rate was measured from 8 specimens of *Laubiericoncha puertodeseadoi* using infrared sensors glued to the shell above the pericardium following the methods of Gurr et al. (2018) (Fig. 15.3).

Tab. 15.1: Summary data for respirometry experiments on board PS119

Species	QUEST Dive	Sample number	Date of dive	Temperature (number of trials)			Dates of experiments
				2 °C	10°C	20°C	
Gigantopelta chessoia	444	PS119_13 sample 1	24.04.2019		6	12	26-30/4/2019
	446	PS119_20 sample 4	29.04.2019		5		30/4/2019
Laubiericoncha puertodeseadoi	447	PS119_28 sample 25	07.05.2019	7	7		8-9/5/2019
	448	PS119_33 sample 3	11.05.2019	20	13		12-15/5/2019

Preliminary (expected) results

Initial analysis of the data while on board, and observations of captive animals, indicate that the physiological responses of *Gigantopelta chessoia* differ from the proposed hypothesis. The animals responded to warmer temperatures (20 °C) with depressed metabolic rates and increased mortality. For ectothermic animals, metabolic rate is expected to track temperature changes, increasing with warming environment, unless the animal is beyond its natural thermal tolerance. In the analogous system in the Indian Ocean, *Chrysomallon squamiferum* has very similar (but convergent) anatomical adaptations to the vent environment shared with *Gigantopelta chessoia*; however, while *Chrysomallon* is tolerant of a wide thermal range, *Gigantopelta* is intolerant of elevated temperatures.

Initial extraction of heart beat recordings for *Laubiericoncha puertodeseadoi* found a heartrate of 12-18 bpm, compared to ~23 bpm for intertidal bivalves (Gurr et al. 2018).

During the cruise, 89 experimental trials were successfully completed by Sigwart and Linse. Data analysis requires precise and accurate measurements of animal mass, which will be completed from preserved specimens.

Data management

Data produced in this project include the original recordings for oxygen saturation in respirometry experiments and heart rate. These will be archived following Queen's University Belfast data management policies. Resulting metadata, rates extracted from each experimental trial and vetted by quality checks, will be included in resulting publications.

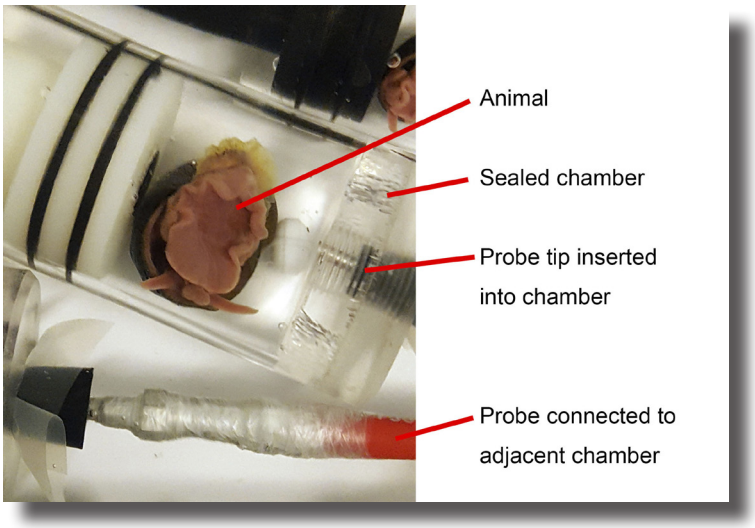

Fig. 15.1: Photograph of experimental set up for measuring respiration rate. An individual of the gastropod Gigantopelta chessoia in a sealed chamber fitted with a fibre optic oxygen probe.

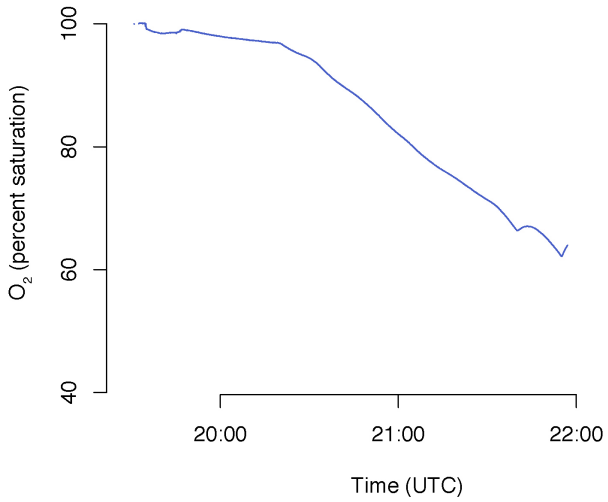

Fig. 15.2: Example recording of decreasing oxygen in a closed-chamber respirometry experiment by the gastropod Gigantopelta chessoia. Decline from normoxic conditions (100%) to ~50% of available oxygen over the course of approximately 2.5 hours at 10°C.

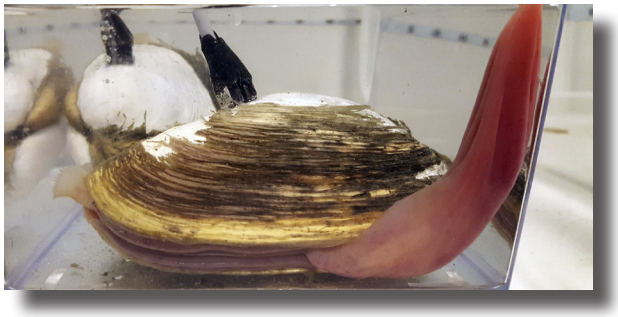

Fig. 15.3: Photograph of experimental set up for measuring heart rate. An individual of the bivalve Laubiericoncha puertodeseadoi with heartbeat sensor glued to the shell (black sensor housing connected to grey-coated wire). A second clam is visible to the rear. The main animal has its siphon (left) and foot (right, pink) extended.

References

Carey N, Sigwart JD, Richards JG (2013) Economies of scaling: more evidence that allometry ofmetabolismis linked to activity, metabolic rate and habitat. Journal of experimental marine biology and ecology, 439, 7–14.

Decker C, Caprais J-C, Khripounoff A, Olu K (2012) First respiration estimates of cold-seep vesicomyid bivalves from in situ total oxygen uptake measurements. Comptes rendus biologies, 335, 261–270

Gurr SJ, Goleskia J, Limab FP, Seabrab R, Goblera CJ, Volkenborna N (2018) Cardiac responses of the bay scallop Argopecten irradians to diel-cycling hypoxia. Journal of experimental marine biology and ecology, 500, 18–29.

Sigwart JD, Chen C (2018) Comparative Oxygen Consumption of Gastropod Holobionts from Deep-Sea Hydrothermal Vents in the Indian Ocean. Biological bulletin, 235.

16. ANIMAL ADAPTATION TO THE HYDROTHERMAL VENT ENVIRONMENT

Crispin Little[1], Adrian Glover[2] (not on board), Magdalena Georgieva[2] (not on board), Ana Riesgo[2] (not on board), Richard Herrington[2] (not on board), Jon Copley[3] (not on board)

[1]SEE-UL, Leeds
[2]NHM, London
[3]NOCS, Southampton

Grant-No. AWI_PS119_00

Outline

To understand how the evolution of metazoans has proceeded in some of Earth's most remarkable environments, the NERCUK-funded project aims to unravel the animal colonization of hydrothermal vents across deep-time and modern-day perspectives. As part of this, we are exploring the phenotypic and genetic processes involved in recent and ongoing metazoan colonization of vents. Hydrothermal vents are challenging for colonization because of their characteristically unstable temperature regimes and high toxicity; however, metazoans that can overcome these challenges reap the rewards of abundant biological production at these sites. To determine if we can witness vent adaptation occurring in species that can live both at vents but also in non-vent settings, we are using a genomic approach - we will compare gene expression, adaptive variation, and the microbiomes of near-vent (peripheral) and non-vent populations of target taxa in a variety of vent localities. For these taxa we will firstly examine the surfaces/tissues of animals for microbial associations. Any potential symbionts will be identified through microscopy and the sequencing of microbiomes. We will then proceed to sequence transcriptomes for individuals from each collected species to assess gene expression, and we will also obtain single nucleotide polymorphisms (SNPs) from all individuals through the application of a ddRADseq protocol. We hope that this work will reveal whether, and what, particular adaptations are required in order to colonize vent environments, and thus shed insights into the fundamental biological processes that occur during evolutionary colonization of hydrothermal vent environments. Ultimately, this research will help us to test our overall project hypothesis that hydrothermal vents have acted as continuous incubators of evolutionary novelty, where metazoans from diverse taxonomic lineages have recurrently adapted to the steep temperature and chemical gradients to benefit from the bounty of hydrothermal vent environments.

In the Scotia Sea area our target taxa are those that occur at the periphery of the hydrothermal vent sites, these being the worm tube *Sclerolinum* (Annelida: Siboglinidae), the carnivorous sponge *Cladorhiza* sp. (Porifera: Cladorhizidae) and the starfish *Paulasterias tyleri* (Echinodermata: Paulasteriidae) (see Fig. 16.1). *Sclerolinum* is an ideal taxon for this work because the various known populations of just one species, *S. contortum*, can be found living at vents, methane seeps and organic falls (Georgieva et al., 2015), and we can thus assess whether populations living at vents have particular adaptations to that environment. For this work, we already have some specimens of this species from sedimented vents in the Southern Ocean (Bransfield Strait), vents and seeps in the Arctic, as well as seep populations from the Gulf of Mexico. *Cladorhiza* sp. has been observed to be living very close to the vents at E2, East Scotia Ridge

(Rogers et al., 2012). Other species in this genus have adapted to a chemosynthetic mode of life by developing a symbiotic relationship with methanotrophs at seeps off Barbados, and we want to know whether the E2 cladorhizid may be making similar adaptations.

Objectives

The objectives of the project are to sample using the QUEST ROV up to four specimens of *Sclerolinum* sp., *Cladorhiza* sp. and *Paulasterias tyleri* from each of the hydrothermal vent sites studied during the cruise. For each collected individual a protocol will be followed that will result in a subsample of tissues fixed in RNAlater and frozen at -80°C for subsequent analysis in the laboratories of the Natural History Museum, London.

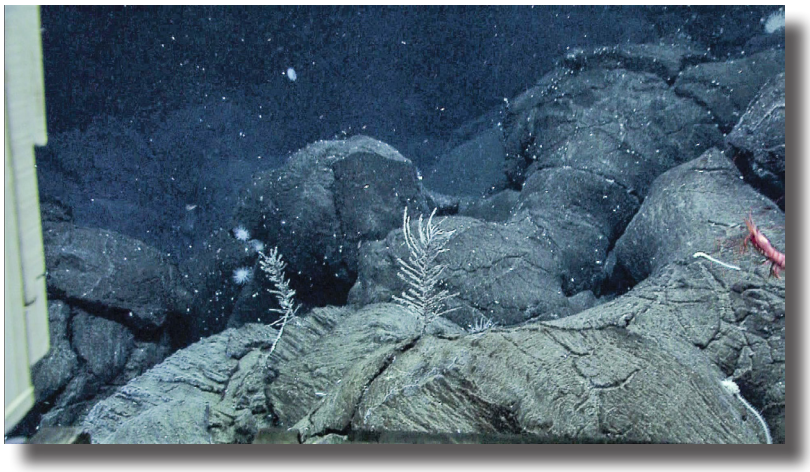

Fig. 16.1: ROV Zeus camera image of Cladorhiza sp. specimens attached to pillow lavas, E2. The collected specimen is the larger one in the center of the image.

Fig. 16.2: ROV Zeus camera image of two Paulasterias tyleri specimens feeding on a large dead Kiwa tyleri, E2. The collected specimen is the smaller of the two.

Work at sea

A small number of specimens was collected from the hydrothermal vents in the working area (Table 16.1). All specimens were subsequently fixed in RNAlater and placed in the MPI -80 °C freezer. The single *Cladorhiza* sp. specimen was collected using a net from an off-vent location in an ambient temperature of 0.15 °C (QUEST ROV CTD) or 0.05 °C (MAPR) (Fig. 16.1). The single *Paulasterias tyleri* specimen was collected using the ROV manipulator claw in an ambient temperature of 0.017 °C (QUEST ROV CTD) or 0.005 °C (MAPR). This specimen was the smaller one of two found feeding on a large dead *Kiwa tyleri* specimen on base of the vent chimney later identified as 'Cacti' from the JC80 cruise maps for E2S (Fig. 16.2). The *Sclerolinum* sp. tubes were obtained from sieved sediments from two clam beds (*Laubiericoncha puertodeseadoi* – see chapters 14, 15 and 17) in the Kemp Caldera resurgent cone vent area, at stations PS119/028-25 and PS119/033-3. The ambient temperature at station PS119/028-25 was 0.32 °C (QUEST ROV CTD) or 0.33 °C (MAPR) and the sediment temperature was 4.2 °C (QUEST HighTemp sensor). The ambient temperature at station PS119/033-3 was 0.44 °C (both QUEST ROV CTD and MAPR). The majority, or possibly all, of the tubes collected were fragmentary, and subsequent on-board investigation using a binocular microscope did not identify any living worm specimens within them. However, the dark color of many of the tubes may be obscuring any living tissue. Some of the collected *Sclerolinum* sp. tubes were incorporated into yellow colored precipitates (Fig. 16.3), with the appearance of fluid conduits. A similar phenomenon has been recorded previously from Kemp Caldera (Georgieva et al., 2015).

Tab. 16.1: Samples obtained for genetic analysis

Taxon	Vent site	Number of individual specimens	Number of subsamples
Paulasterias tyleri	E2_S	1	4
Cladorhiza sp.	E2_S	1	6
Sclerolinum sp.	Kemp Caldera	Ca. 150 tubes	

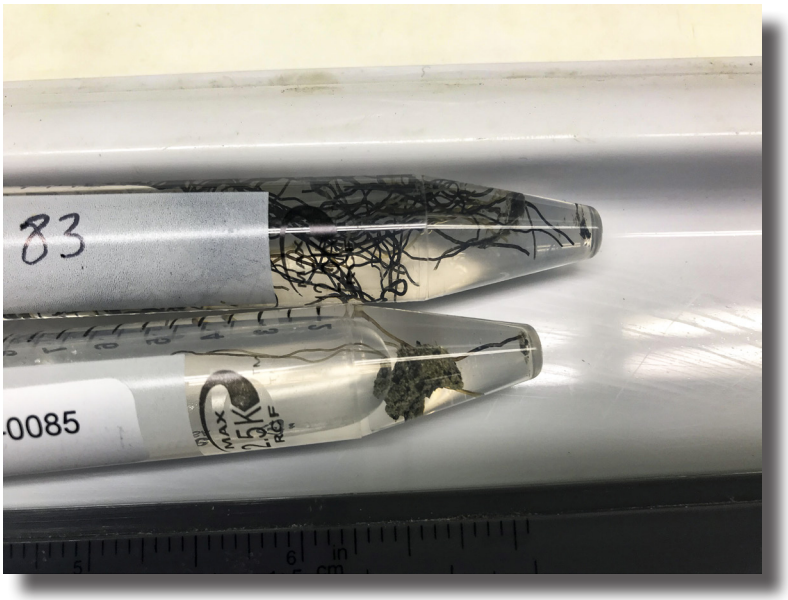

Fig. 16.3: Photograph of Sclerolium sp. worm tubes collected from station PS119/028-25, Kemp Caldera. The tubes in the left vial are incorporated into sulphur-rich precipitates.

Preliminary (expected) results

None as yet.

Data management

The sequencing output, transcriptome and SNP alignment data from the collected material will be included in the data plan for the Natural Environment Research Council (UK) grant NE/R000670/1, led by the Natural History Museum, UK.

References

Georgieva MN, Wiklund H, Bell JB, Eilertsen MH, Mills RA, Little CTS, Glover AG (2015) A chemosynthetic weed: the tubeworm *Sclerolinum contortum* is a bipolar, cosmopolitan species. BMC Evolutionary Biology, 15, doi:10.1186/s12862-015-0559-y.

Rogers AD, Tyler PA, Connelly DP, Copley JT, R. James R, Larter RD, Linse K, Mills RA, et al (2012) The discovery of new deep-sea hydrothermal vent communities in the Southern Ocean and implications for biogeography. PLoS Biology, 10(1), e1001234. doi:10.1371/journal.pbio.1001234.

17. MOLECULAR ANALYSIS OF THE INTERACTIONS BETWEEN DEEP-SEA BIVALVES AND THEIR CHEMOSYNTHETIC, SYMBIOTIC BACTERIA

Maximilian Franke[1], Benedikt Geier[1], Christian Borowski[1] Nicole Dubilier[1] (not on board)

[1]MPI, Bremen

Grant-No. AWI_PS119_00

Objectives

The chemosynthetic fauna along the South Sandwich Arc presents a globally unique community that is distinct from vent and seep communities for instance, found at hydrothermal systems along the Mid-Atlantic Ridge (Rogers et al., 2012). So far, the only bivalves with chemosynthetic symbionts that have been found along the South Sandwich Arc are Vesicomyid clams. We aim to explore the hydrothermal systems along the South Sandwich Arc for another chemosynthetic bivalve of the subfamily Bathymodiolinae. Bathymodiolin mussels thrive at hydrothermal vents and cold seeps for example along the Mid Atlantic Ridge, dominating the chemosynthetic fauna in terms their biomass.

Vesicomyid clams rely on their intracellular, sulfur-oxidizing (SOX) bacteria to provide them with nutrition through the fixation of carbon via the oxidation of reduced sulfur compounds from the vent fluids (e.g. H_2S). Their symbiotic SOX are passed along the germline to the next generation (vertical transmission), resulting in increased co-speciation between host and symbionts and lower genetic diversity between the symbiont genomes. In contrast, *Bathymodiolus* mussels take up their symbionts anew in each generation from the environment. This allowed for a high evolutionary versatility of host-symbiont associations within the Bathymodiolinae subfamily, for example different types of symbionts, such as methane (MOX) and sulphur oxidizers (SOX). Finding Bathymodiolin mussels would advance our understanding of their biogeography and possibly reveal new species or microbial symbionts with novel metabolic pathways, adapted to the local environments.

Work at sea

In addition to monitoring the ROV dives, the on board work was comprised of sample processing, fixation and adequate storage until analyses in the respective laboratories. Upon recovery, the animals were directly dissected into gills (the symbiotic organ that harbors most of the symbiotic bacteria), mantle, foot and digestive system. The shells were also kept and stored for potential isotopic analyses to determine the animals‘ food sources.

Dissected tissues were preserved in various fixatives for different omics, microscopic and isotopic analyses and stored at +4°C, -20°C or -80°C.

Preliminary (expected) results

Although, sites in the Kemp Caldera showed increased levels of methane, which could have provided a potential energy source for MOX symbionts, we did not find Bathymodiolin mussels. This could indicate a biogeographic barrier towards the polar front or suboptimal environmental conditions for Bathymodiolin mussels to thrive at hydrothermal vents along the South Sandwich Arc.

Instead, we sampled Vesicomyid clams from the Kemp Caldera for which we anticipate a close phylogenetic relationship of the symbiotic bacteria to other SOX symbionts of Vesicomyid clams. The samples, which we preserved for a well-rounded molecular analysis of host and symbionts will be stored at the MPI in Bremen.

Fig. 17.1: The figure shows a bed of Vesicomyid clams, found in the Kemp Caldera (left panel) and a close-up (right panel) of an individual with an extended siphon, covered with small limpets and snails.

Data management

All data collected and generated by this project will be made publicly available via the World Data Center PANGAEA Data Publisher for Earth & Environmental Science (www.pangaea.de). Our data will also be accessible from public databases such as NCBI, EBI or image repositories such as figshare at latest with publication.

References

Rogers AD,…,Zwirglmaier K (2012) The Discovery of New Deep-Sea Hydrothermal Vent Communities in the Southern Ocean and Implications for Biogeography. PLoS Biology, 10, 1-17.

18. LARGE WHALE DISTRIBUTION AROUND SOUTH GEORGIA AND THE SOUTH SANDWICH ISLANDS IN THE POST-WHALING ERA

Helena Herr[1] (not on board), Sacha Viquerat[1], Tina Kesselring[1], Chintara Krieger[1], Michael Gischler[2], Carsten Zillgen[2], Roland Richter[2], Victor Santos[2]

[1]CeNak, Hamburg
[2]HeliService, Emden

Grant-No. AWI_PS119_00

Objectives

The Scotia Sea has long been known as one of the most productive and biologically rich regions of the Southern Ocean (El-Sayed & Weber, 1982). Historical exploration of the Scotia Arc area was largely driven by top predator exploitation (sealing and whaling) endeavours. Whaling histories show extensive catches of large baleen whales, particularly blue (*Balaenoptera musculus*), fin (*B. physalus*) and humpback whales (*Megaptera novaeangliae*) from the Scotia Sea region, with catches centered in the waters around South Georgia (Tønnessen & Johnsen, 1982). Over 2 million large whales were killed during the times of commercial whaling in the Southern Ocean (1904 – 1986) (Clapham & Baker, 2002). Today, there is little information about the recovery status, abundance and distribution of large whale populations formerly using these waters as feeding habitat (Leaper & Miller, 2011).

The Scotia Sea region has rarely been surveyed for whales and very few records are available for areas beyond the established Antarctic tourism destination of South Georgia. The results of our studies at PS119 will provide important information on the occurrence of cetaceans in this area and will contribute information on the recovery status, abundance and distribution of large whale populations, in particular of fin whales in a historically heavily exploited area of the Southern Ocean.

Work at sea

We recorded cetacean sightings using a modified distance sampling methodology during crow's nest surveys and helicopter surveys (Scheidat et al., 2011; Williams et al. 2015; Viquerat & Herr 2017; Herr et al., 2019). In addition, opportunistic sighting data were collected when conduction of line transect distance sampling was impossible.

Survey flights were conducted following the line-transect distance sampling (Buckland et al., 2007) methodology for marine mammals, collecting sighting and environmental information along designed track lines (Scheidat et al., 2011, Williams et al. 2015, Herr et al., 2019). Track lines were designed *ad-hoc* shortly before each survey flight, adapting the design to the ship's position, the prevalent weather conditions, and the ship's schedule. Due to helicopter specifications, the total length of planned track lines was limited to app. 120 nm per flight. Track lines were laid out in rectangular shape around *Polarstern*. During the latter half of the cruise, adverse weather conditions with severe icing threats limited the operational radius to the vicinity of the ship (i.e. not further away than 10 nautical miles at any given point in time). The data recorder seated in the front recorded all cetacean sightings made by the observers using

dedicated survey software (Hiby & Lovell, 1998). Two side observers recorded the species, group size and the distance to the track line of all cetacean groups encountered on effort.

Surveys from the crow's nest were conducted whenever helicopter surveys were not possible and survey requirements were met (i.e. ship's speed > 7 knots and feasible weather conditions). All observations were made from the crow's nest platform of *Polarstern* at an altitude of app. 29 m asl. Two observers were positioned outside on the platform and scanned the area around the trackline for cetaceans by naked eye and, in case of a cetacean sighting, used binoculars to measure distance to the sighting and to determine the species. A third person inside the cabin acted as data recorder, relaying radio transmitted sighting information into a dedicated survey software (Hiby & Lovell, 1998).

Opportunistic sighting data were collected as a last resort when neither dedicated method was feasible. Most observations were collected from the bridge, providing shelter from the weather and a moderate view ahead and to the sides of the ship. Additional information was gathered from fellow cruise participants, who provided information on cetacean sightings that were not available to the dedicated bridge observers. Sightings were classified as certain and uncertain, based on photographic evidence and weather conditions. We recorded the group size of each cetacean group and used the timestamp to associate each sighting with a geographical position provided by the ship GPS.

Preliminary results

Dedicated distance sampling surveys

We systematically covered a total of 888 km on effort during helicopter surveys and 189.94 km during crow's nest surveys using dedicated distance sampling survey methods (Buckland et al., 2007; Hedley & Buckland, 2004; Scheidat et al., 2011). A total of 8 groups of fin whales comprising 12 individuals were recorded during helicopter surveys and 3 groups with 6 individuals during Crow's Nest surveys (Table 18.1, Fig. 18.1, Fig. 18.2).

Tab. 18.1: Summary of sightings and effort from helicopter and crow's nest surveys conducted during PS119. Platform indicates the survey platform; L: indicates the total length of transect in kilometers that was observed on effort; Species: marks the type of observation recorded (Minke whale indicates either B. acutorostrata or B. bonaerensis); G gives the number of groups recorded on effort; I indicates the number of individuals recorded on effort; gs indicates the average group size as individuals per group; nL indicates the encounter rate of groups per km on effort.

Platform	L [km]	Species	G	I	gs [ind / grp]	nL [grps / km]
Helicopter	887.57	unidentified blow	4	4	1	0.0045
		B. physalus	8	12	1.5	0.0090
		M. novaeangliae	4	6	1.5	0.0045
		unidentified large whale	2	2	1	0.0023
Crow's Nest	189.94	unidentified blow	17	21	1.2	0.0895
		B. physalus	3	6	2	0.0158
		Minke whale	1	1	1	0.0053
		M. novaeangliae	33	43	1.3	0.1737
		unidentified large whale	1	1	1	0.0053

Neither helicopter nor crow's nest surveys yielded enough fin whale group sightings to estimate a detection function; however, the addition of previous datasets will provide enough samples

for detection function estimation. Long stretches of bad weather limited survey activities substantially and effort from both platforms was spatially constrained to the vicinity of the ship. The overall sighting numbers were low, neither dedicated distance sampling data set allows robust abundance and density estimates for the area. Once data collected during this cruise is pooled with previous expeditions (Herr et al., 2018a–f; Scheidat & Herr, 2018; Scheidat et al., 2018a; b), a subsequent additive modelling analysis stage will be able to produce a distribution map providing robust density estimates for fin whales in the area (Viquerat & Herr, 2017; Herr et al., 2019).

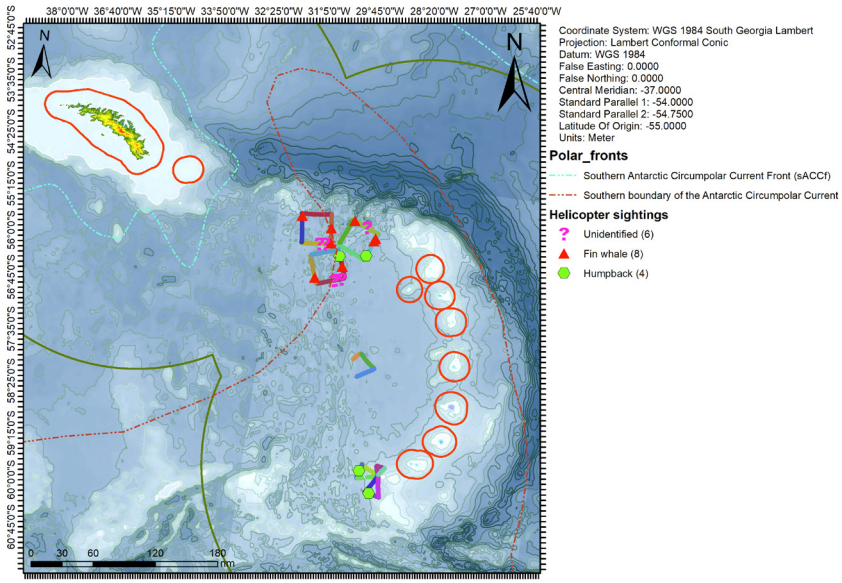

Fig. 18.1: Summary of helicopter surveys during PS119. Colored lines indicate individual 'on effort' stretches, symbols indicate cetacean sightings while on effort. Red triangles indicate fin whales, the target species in this project. The dashed red line indicates the southern boundary of the ACC, which forms a loop further in the south.

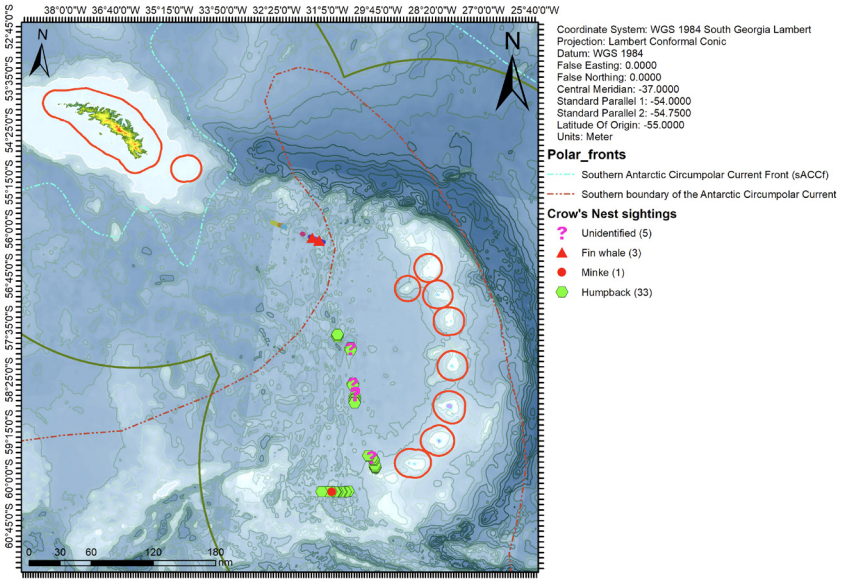

Fig. 18.2: Summary of crow's nest surveys during PS119. Solid lines indicate on effort stretches (individual transects are colour-coded), symbols indicate cetacean sightings while on effort. Red triangles indicate fin whales, the target species in this project. The dashed red line indicates the southern boundary of the ACC, which forms a loop further in the south.

Opportunistic Sightings

In light of adverse weather conditions, we collected incidental sightings events when off effort for as long as daytime permitted mostly from the bridge of *Polarstern* (see Fig. 18.3). A total of 9 groups of fin whales comprising of 16 individuals were recorded, with an additional 4 groups with 10 individuals that were grouped as either fin or sei whale. Given the challenging weather situation during opportunistic sighting efforts, the two species can be hard to identify from the ship with certainty. A total of 24 groups of humpback whales were recorded, comprising of 57 animals.

During PS119, we recorded 5 different baleen species (Fin, Humpback, Sei, Minke and Southern right whale) and 2 dolphin species, Commerson's dolphin (*Cephalorhynchus commersonii*) and Hourglass Dolphin (*Lagenorhynchus cruciger*). An additional 11 groups of unspecified blows (likely large whales) were also noted (Table 18.2).

Tab. 18.2: Preliminary summary of opportunistic survey effort for cetaceans. 'Fin or Sei whale' include cetacean group sightings that could not be attributed to either species. 'Minke whale' are animals that could be either *B. bonaerensis* or *B. acutorostrata*.

Species	Groups	Individuals
Fin whale (*Balaenoptera physalus*)	9	16
Sei whale (*Balaenoptera borealis*)	5	7
Fin or Sei whale	4	10
Humpback whale (*Megaptera novaeangliae*)	24	57
Unidentified blows	11	18
Minke whale (*B. bonaerensis / B. acutorostrata*)	4	5
Southern Right Whale (*Eubalaena australis*)	1	1
Commerson's dolphin (*Cephalorhynchus commersonii*)	1	5
Hourglass dolphin (*Lagenorhynchus cruciger*)	1	3
Total	**60**	**122**

Location data and auxiliary data from ship devices (such as *in-situ* measurements of depth) were not yet available in sufficient spatiotemporal resolution for all records, but will be associated with each sighting upon the end of the voyage. In the light of lacking dedicated survey coverage these data represent a valuable source of information for a sparsely studied region within the Scotia Sea and may be used in habitat suitability models (for example Ainley et al., 2012; Gregr et al., 2014; Smith et al., 2012).

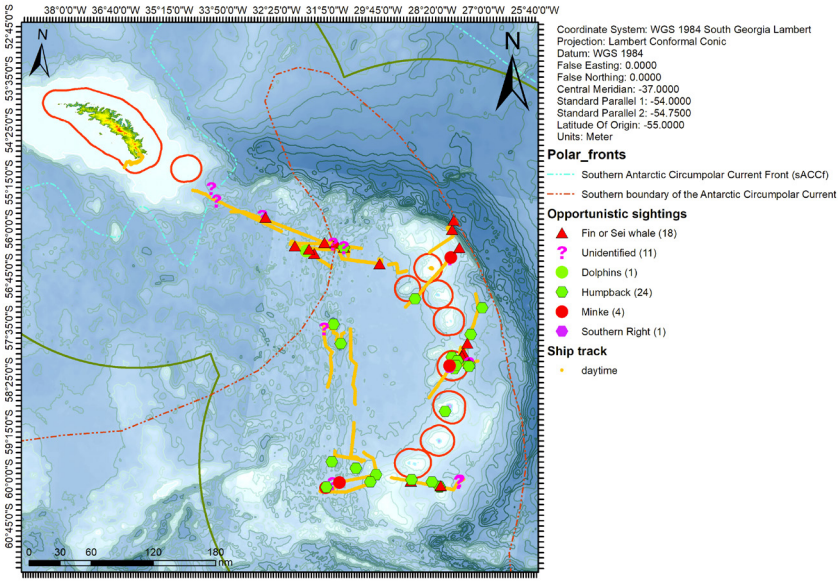

Fig. 18.3: Summary of opportunistic sightings during PS119. Solid lines indicate daylight time, symbols indicate cetacean sightings / species groups. Red triangles indicate Fin whales or Sei whales (for details see text). The dashed red line indicates the southern boundary of the ACC, the dashed light blue line indicates the Southern Antarctic Circumpolar Current Front.

Data management

Upon publication or after 3 years by the latest, all data will be made available on the World Data Center PANGAEA Data Publisher for Earth & Environmental Science (www.pangaea.de) and GBIF (http://www.gbif.org, Global Biodiversity Information Facility) / ANTABIF (http://www.biodiversity.aq). All images suitable for Photo Identification will be submitted to happywhale.com.

References

Ainley DG, Jongsomjit D, Ballard G, Thiele D, Fraser WR & Tynan CT (2012) Modeling the relationship of Antarctic minke whales to major ocean boundaries. Polar Biology, *35*(2), 281–290.

Buckland ST, Anderson DR, Burnham KP, Laake J, Borchers DL & Thomas L (2007) Advanced distance sampling. In Advanced distance sampling (p. 416). New York, NY: Oxford University Press.

Clapham PJ & Baker CS (2002) Modern whaling. In Perrin WF, Würsig B & Thewissen JGM (Eds.), Encyclopedia of marine mammals (pp. 1328–1332). New York, NY: Academic Press.

El-Sayed SZ & Weber LH (1982) Spatial and temporal variations in phytoplankton biomass and primary productivity in the southwest Atlantic and the Scotia Sea. Polar Biology, *1*, 83–90.

Gregr EJ, Baumgartner MF, Laidre L & Palacios DM (2014) Marine mammal habitat models come of age: The emergence of ecological and management relevance. Endangered Species Research, *22*(3), 205–212. doi:10.3354/esr00476

Hedley SL & Buckland ST (2004) Spatial models for line transect sampling. Journal of Agricultural, Biological, and Environmental Statistics, 9(2), 181–199. doi:10.1198/1085711043578

Herr H, Lehnert LS & Siebert U (2018a) Aerial cetacean survey Southern Ocean 2010/2011. PANGAEA Retrieved from https://doi.pangaea.de/10.1594/PANGAEA894934

Herr H, Lehnert LS, & Siebert U (2018b) Aerial cetacean survey Southern Ocean 2011/2012. PANGAEA Retrieved from https://doi.pangaea.de/10.1594/PANGAEA894924

Herr H, Lehnert LS & Siebert U (2018c) Ship based cetacean survey Southern Ocean 2010/2011. PANGAEA Retrieved from https://doi.pangaea.de/10.1594/PANGAEA894910

Herr H, Lehnert LS & Siebert U (2018d) Ship based cetacean survey Southern Ocean 2011/2012. PANGAEA Retrieved from https://doi.pangaea.de/10.1594/PANGAEA894909

Herr H, Viquerat S & Siebert U (2018e) Aerial cetacean survey Southern Ocean 2014/2015. PANGAEA Retrieved from https://doi.pangaea.de/10.1594/PANGAEA894938

Herr H, Viquerat S & Siebert U (2018f) Ship based cetacean survey Southern Ocean 2014/2015. PANGAEA Retrieved from https://doi.pangaea.de/10.1594/PANGAEA894873

Herr H, Viquerat S, Kelly N, Hermann K, Linn K, Lehnert S, Williams R & Siebert U (2019) Aerial surveys for Antarctic minke whales (Balaenoptera bonaerensis) reveal sea ice dependent distribution patterns. Ecology and Evolution, (March), 1–19. doi:10.1002/ece3.5149

Hiby L & Lovell P (1998) Using aircraft in tandem formation to estimate abundance of harbour porpoise. Biometrics, 54, 1280–1289.

Leaper R & Miller C (2011) Management of Antarctic baleen whales amid past exploitation, current threats and complex marine eco-systems. Antarctic Science, (23), 503–529.

Scheidat M, Friedlaender A, Kock KH, Lehnert L, Boebel O, Roberts J & Williams R (2011) Cetacean surveys in the Southern Ocean using icebreaker-supported helicopters. Polar Biology, 34(10), 1513–1522. doi:10.1007/s00300-011-1010-5

Scheidat M & Herr H (2018) Aerial cetacean survey Southern Ocean 2006/2007. PANGAEA doi:10.1594/PANGAEA894937

Scheidat M, Herr H & Siebert U (2018a) Aerial cetacean survey Southern Ocean 2008/2009. PANGAEA Retrieved from https://doi.pangaea.de/10.1594/PANGAEA894936

Scheidat M, Herr H & Siebert U (2018b) Ship based cetacean survey Southern Ocean 2008/2009. PANGAEA Retrieved from https://doi.pangaea.de/10.1594/PANGAEA894911

Smith JN, Grantham HS, Gales N, Double MC, Noad MJ & Paton D (2012) Identification of humpback whale breeding and calving habitat in the Great Barrier Reef. Marine Ecology Progress Series, 447(Harwood 2001), 259–272. doi:10.3354/meps09462

Tønnessen JN & Johnsen AO (1982) The history of modern whaling. Los Angeles: University of California Press.

Viquerat S & Herr H (2017) Mid-summer abundance estimates of fin whales *Balaenoptera physalus* around the South Orkney Islands and Elephant Island. Endangered Species Research, 32, 515–524. doi:10.3354/esr00832

Williams R, Kelly N, Boebel O, Friedlaender AS, Herr H, Kock K-H, Lehnert LS, Maksym T, Roberts J, Scheidat, M, Siebert U & Brierley AS (2015) Counting whales in a challenging, changing environment. Scientific Reports, 4(1), 4170. doi:10.1038/srep04170

19. INVESTIGATION OF ACTIVE VOLCANIC PROCESSES

Nicole Richter[1,2], Allan Derrien[2], Martin Meschede[3], Phil Leat[4] (not on board)

[1]GFZ, Potsdam
[2]OVPF-IPGP, Paris
[3]IGG-UG, Greifswald
[4]BAS, Cambridge

Grant-No. AWI_PS119_00

Objectives

The active volcanoes of the South Sandwich Islands remain some of the few spots on Earth that we know almost nothing about. None of them are equipped with ground-based instruments and therefore monitoring relies fully on satellite data and rare visits. A very recent study by Gray (2018) suggests that Mount Michael on Saunders Island holds a persistent (and not recurrent as previously thought) lava lake since at least 1995, suggesting the existence of a well-developed shallow plumbing system within the volcanic edifice. Permanent lava lakes are a particularly rare volcanic feature with only a few worldwide that are verified as active at any one time. This highlights the importance of closely studying these phenomena wherever they occur. Both of this makes Mount Michael a unique target to study lava lake activity and volcanic processes within an open conduit that is connected to the uppermost part of a subsurface volcanic plumbing system.

The scientific objectives of the volcano-related project during the PS119 expedition were to map in unprecedented detail the surface geomorphology of the active Mount Michael Volcano, which is characterized by the presence of a permanent active lava lake within its summit crater. We were aiming at generating high-resolution and high-quality digital elevation models of both Saunders and Zavodovski Islands by acquiring photogrammetric data using drones and applying the Structure-from-Motion method. This data are of utmost importance in order to be able to further process, investigate and correctly interpret our radar satellite observations that have the advantage of not being affected by the almost persistent cloud coverage in the area and that have been routinely acquired since February 2017. No overnight field campaigns were planned. At Mount Michael, and potentially at Mount Curry, we were aiming for the collection of gas and rock samples, and the investigation of the eruptive activity of the volcanos, including observations of lava lake activity within the summit crater of Mount Michael. In the following the overall aims of the SSIVOLC (reduced CAT2 proposal) are listed, bold are the parts that we were able to realize while all other points could not be achieved due to the weather conditions and limited ship time:

Complete **photogrammetric survey (drone-based) of Saunders** and Zavodovski Islands → **DEM**

- Footage of active lava lake
- IR footage of lava lake (IR camera)
- MultiGAS measurements of gas plume (ground- and/or drone-based)
- **UV Camera observations (from *Polarstern*)**
- Collection of 25 kg of mafic lava rock samples

The collected data will be further analyzed. We are particularly interested in studying the effect of extreme climatic conditions and magmatic activity on the landscape genesis, edifice evolution, and edifice stability.

Work at sea

In preparation of a land-based mission on Saunders Island, the SSIVOLC team (together with the BBC team who were planning to accompany the field trip) held a number of meetings, equipment checks, and trainings, which are listed in Table 19.1. Furthermore, mission planning included the preparation of paths and maps for the drone surveys, a zodiac reconnaissance cruise of two *Polarstern* crew members on May 3, 2019, and the presentation of the mission and state of planning to all scientists on board the cruise.

Tab. 19.1: Activities in preparation of a land-based mission on Saunders Island

What	Who	Why	When
Meetings	Chief Scientist, Captain, Zodiac drivers, BBC team, SSIVOLC team	Mission planning	April 17, 2019
	Weather team Captain Helicopter team Wale team PI SSIVOLC	Weather meetings	daily
Equipment checks		Survival suits and zodiacs	April 24/25, 2019
		Medical kit First aid kit	April 30, 2019
		Survival bags bivouac	May 2, 2019
		Survival bags personal	May 2, 2019
		UV Camera Test	April 14, 2019
		Food	May 1, 2019
		Tents	April 24, 2019
Trainings	Drone pilots	Launching/Landing *Polarstern* Helipad	April 20, 2019
	Doctor	First aid training	April 30, 2019
	Heli-Team, SSIVOLC-Team	Helicopter rescue training for emergency situations	May 2, 2019
	Captain, Gerhard Bohrmann, BBC, SSIVOLC	Communication plan and training	April 17, 2019

In addition, the PI of SSIVOLC kept track of and reported on all earthquake activity in the wider South Sandwich Island region during the entire PS119 research cruise. A list of earthquakes that occurred in the area of interest and during the time of investigation is given in Fig. 19.1.

GFZ Helmholtz-Zentrum Potsdam

GEOFON

GEOFON Program

Helmholtz-Zentrum Potsdam Deutsches GeoForschungsZentrum

Mission | Earthquake Info | Waveform Access | Software | Contribute | Contact | Home

This real-time bulletin is a product of the GEOFON Extended Virtual Network (GEVN) and credit belongs to all involved institutions!

Disclaimer: Unless revised by a geophysicist, automatically determined earthquake locations may be erroneous!

This bulletin is customizable and also available as RSS news feed.

Output restricted to latitude range from 62.00°S to 56.00°S, to longitude range from 45.00°W to 20.00°W and to dates from 2019-04-01 to 2019-05-29.
[Customize] [Remove]

New search FAQ

Earlier events — No newer events

Origin Time UTC	Mag	Latitude degrees	Longitude degrees	Depth km	A	M	Flinn-Engdahl Region Name
2019-05-27 23:29:34	5.7	56.35°S	27.77°W	130	C	MT	South Sandwich Islands Region
2019-05-19 11:48:33	5.2	60.67°S	26.78°W	10	M		South Sandwich Islands Region
2019-04-25 11:42:49	5.0	57.85°S	24.84°W	55	C		South Sandwich Islands Region
2019-04-24 04:41:30	4.6	58.44°S	30.43°W	63	A		South Sandwich Islands Region
2019-04-22 14:49:08	**6.0**	56.33°S	27.58°W	101	C	MT	South Sandwich Islands Region
2019-04-16 16:59:17	5.4	58.76°S	23.50°W	10	C		South Sandwich Islands Region
2019-04-09 17:53:59	**6.5**	58.64°S	25.38°W	34	C	MT	South Sandwich Islands Region
2019-04-05 16:14:18	**6.4**	56.03°S	27.93°W	65	C	MT	South Sandwich Islands Region

Earlier events — No newer events

© Helmholtz-Zentrum Potsdam Deutsches GeoForschungsZentrum GFZ

HELMHOLTZ SPITZENFORSCHUNG FÜR GROSSE HERAUSFORDERUNGEN

Fig. 19.1: Earthquakes that occurred in the South Sandwich Island Region during PS119 (as of May 29, 2019).

Mapping of Saunders Island

On two separate days (May 17, 2019 and May 22, 2019), we realized 24 drone flights in total in order to complete the mapping survey of Saunders Island. All flights were launched from *Polarstern*, which was circling around the island. A land-based mission was not possible due to time constraints and conflicts with concurrent projects on board, and unfortunate weather conditions. Each flight took 12-15 minutes, and delivered aerial stereo-photography data covering an area of ~2 square kilometers. The UAS were operated at an elevation of up to 1,100 m above sea level. The UASs were not flying more than 3 km away from their launch base, providing for a sufficient margin for manual and failsafe procedures. The operator put the UASs in GNSS-assisted mode in addition to auto-stabilization settings. In addition to the optical cameras, two drone flights were equipped with a mini FLIR camera, measuring the temperature. On May 17, 2019, the SO_2 flux of the gas plume that was emitted from the summit crater of Mount Michael was measured using a UV camera (cf. Fig. 19.3). Results are not yet available.

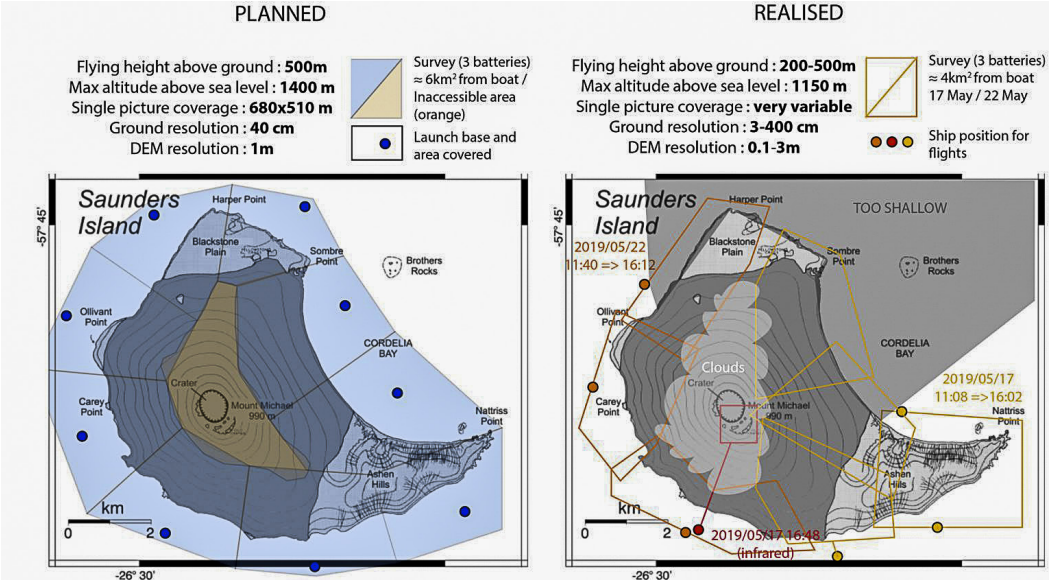

Fig. 19.2: Comparison of the planned and realized drone-based mapping of Saunders Island. All flights were launched from Polarstern.

Fig. 19.3: UV camera test on board Polarstern

Preliminary (expected) results

The photogrammetric mapping of Saunders Island was the major aim of this project. So far, the best topographical maps that exist of Saunders Island are data that were acquired by the BAS mapping unit. These feature contour interval of 200 m, and any DEMs that show closer contour intervals are interpolated from existing data (personal communication with Phil Leat). The mapping during PS119 was done using drones that were launched from *Polarstern* circulating the island of interest.

Two scientists/operators were needed full time for the drone-based survey. During surveys the drone was set on GPS-flight and the camera was set on automatic modes. Pre-planned paths and maps for the drone surveys had been previously prepared.

Fig. 19.4 shows the resulting digital elevation model in 2.6 m spatial resolution, while Fig. 19.5 exemplifies a FLIR infrared measurement showing that the rim of the side crater at Mount Michael's summit is significantly warmer than its surrounding.

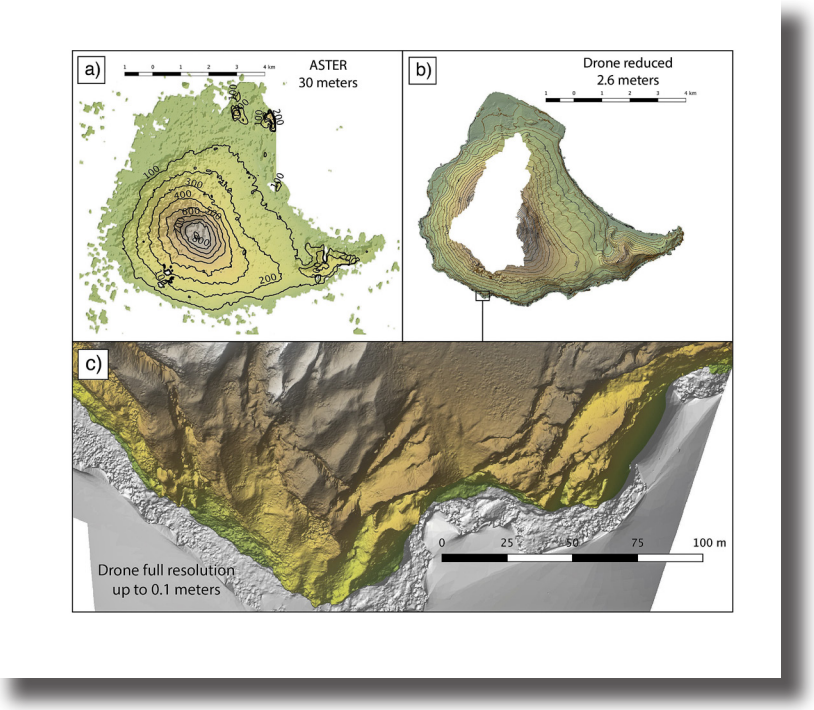

Fig. 19.4: Comparison of the preexisting ASTER DEM (in 30 m spatial resolution) (a) and the SSIVOLC DEM (in 2.6 m spatial resolution) that has been processed from the photogrammetric data collected during the PS119 cruise (b). Further processing will allow the generation of topographic data of locally up to 10 cm spatial resolution as exemplified in (c).

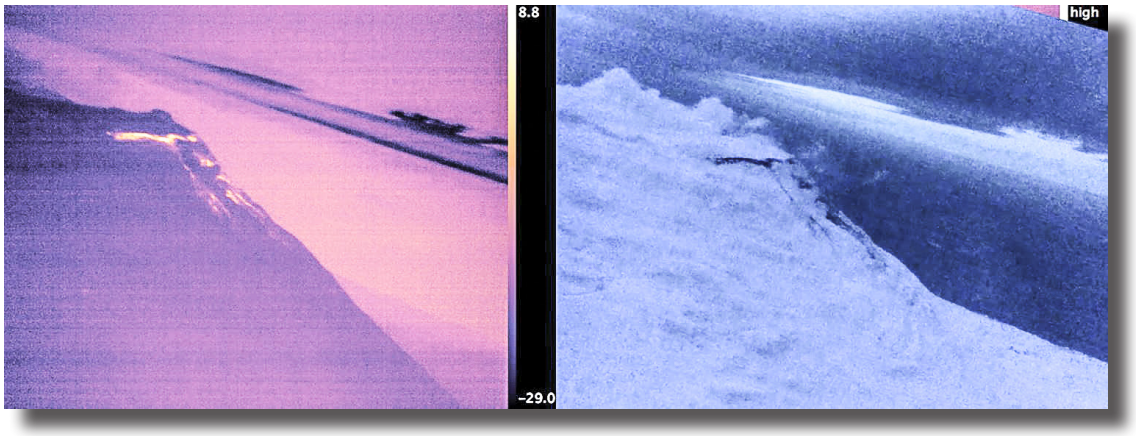

Fig. 19.5: FLIR infrared measurement (left) and photograph (right) showing that the rim of the side crater at Mount Michael's summit is significantly warmer than its surrounding

Data management

The scientists of the SSIVOLC project during PS119 agreed to publish processed data and data products via the World Data Center PANGAEA Data Publisher for Earth & Environmental Science (www.pangaea.de), a repository that is operated as an open access library aimed at archiving, publishing and distributing georeferenced data from earth system research (https://pangaea.de/about/). PANGAEA guarantees long-term availability of its content through a commitment of the hosting institutions, i.e. the Alfred Wegener Institute, Helmholtz Center for Polar and Marine Research (AWI) and the Center for Marine Environmental Sciences, University of Bremen (MARUM).

References

Derrien, Allan; Richter, Nicole; Meschede, Martin; Walter, Thomas (2019): Optical DSLR camera- and UAV footage of the remote Mount Michael Volcano, Saunders Island (South Sandwich Islands), acquired in May 2019. GFZ Data Services. http://doi.org/10.5880/GFZ.2.1.2019.003

Gray D (2018) Remote Sensing of Mt. Michael volcano to determine the presence of a permanent lava lake. Research dissertation submitted for the MSc Environmental Mapping at University College London. 70 pp.

20. PUBLIC OUTREACH

Holger von Neuhoff[1], Stephanie von Neuhoff[1] [1]IMMH, Hamburg

Grant-No. AWI_PS119_00

250 years after Alexander von Humboldt's birth, we are experiencing fundamental changes in all areas of our life today. Humboldt postulated the "web of life" in which man is an organism among many. All life is interconnected: not the human – as generally believed – stands above the system of earth, but is a part of this interconnectedness among the organisms. Reflection by science promotes knowledge and sustainability. Humboldt created the so-called "nature painting" in which the connections for each person were vividly outlined on paper.

What are our requirements in today's world? Our world, which at first glance has become smaller due to the acceleration of the information flows, but also requires new orientation maps to cope with the huge data streams. In keeping with Humboldt's idea, we are in search of a new "digital nature painting" that takes every human being on a journey into the future.

The authors Stephanie and Holger von Neuhoff see themselves in the classical sense as chroniclers and observers of today's modern research work, which is carried out by *Polarstern* in the polar regions. A work, that under difficult climatic conditions can redefine all possibilities of measurements through our current technology and make them accessible to the public.

It is a journey with the winter storms and the data streams that we want to understand in science. Also an expedition, in which we have searched for further partners who will take up and continue the dialogue on land.

1. Google was won as a partner for the companionship of the expedition. During the cruise, a lively and deep exchange took place with the leaders of "Google Arts and Culture" in order to present the results on the same platform in July 2019. The BMBF is partner of the presentation. The work on land and at sea as well as the preparations can be classified as very successful so far.

2. With the curators of the "Humboldt Lab", which is part of the "Humboldt-Forum" in the Berlin Castle we also build a strong partnership. It is planned to present results of the expedition in their opening exhibition.

3. A book in the context of the three research cruises to South Georgia and the South Sandwich Islands (2013, 2016, 2019) of chief scientist Gerhard Bohrmann will be published in 2020.

4. As a coordinated PR-action, a blog was produced for the HANSA magazine during the cruise.

5. The SHZ newspaper group was supplied and will continue to produce further, larger articles about the expedition after the cruise.

6. Articles and smaller online appearances have been realized or are in progress.

7. Under the motto “school as a research vessel” an educational programme was developed with the district school Hamburg-Wilhelmsburg, for which among other things a Live-Talk via the telepresence was realized.

8. For the “Long Night of the Museums” in Hamburg, a Live-Talk was organized in the International Maritime Museum in Hamburg to present marine research work to a wider public.

We would like to thank all our supporters who, in the spirit of Humboldt, want to strengthen and understand the “web of life” with their knowledge and work:

Real hope for our future begins with comprehension and science.

Work at sea

Over 4,000 photographs, a huge amount of 360°-pictures, video-material, extended interviews with scientists and crew-members, short and long written texts, a lot of conceptual work to bring the data in an attractive form, web-work for the online-presentations, deep dialogues with project partners on land.

21. BBC NATURAL HISTORY UNIT

Yoland Bosiger[1], Sam Meyrick[1] [1]BBC, Bristol

Grant-No. AWI_PS119_00

Aims of BBC filming

The BBC Studios Natural History Unit were invited aboard *Polarstern* PS119 Sandwich Venting II Cruise with the aim of attaining footage for the series "Frozen Planet II" which is due to broadcast in Autumn 2021. This 6-part series showcases the 'cold regions' of our planet from Arctic and Antarctic to tundra and high mountains. The series will capture extraordinary new behaviour and surprising new landscapes while also highlight the fragility of these habitats and how they are changing. The filming on this cruise has four main aims detailed below. They contribute directly to the Antarctic Episode of Frozen Planet II.

1. To film the extraordinary story of a newly discovered species of Hoff crab, Kiwa tyleri, which makes its home around the deep hydrothermal vents off the South Sandwich Islands.

2. To film the spectacular aerial scenery of the South Sandwich Islands, primarily Saunders Island and Zavodovski Island. Our goal was to film the mountains, volcanic activity and surrounding wildlife both by deploying onto the islands alongside scientist, Nicole Richter and from the *Polarstern* itself.

3. To capture a story about penguins battling as they try to take refuge on an iceberg, scrambling out of Earth's roughest ocean.

4. To film making of footage of the science and research being conducted onboard the Pola*rstern*.

Personnel & equipment involved

Yoland Bosiger is a former research biologist who has worked for the BBC Natural History Unit for 5 years as an Assistant Producer / Researcher for wildlife films. Sam Meyrick has 7 years of experience in filming for high-end natural history programs and joined the BBC Natural History Unit as a cameraman appointed to film solely for Frozen Planet II. They brought with them an array of filming equipment with which to document the expedition including: RED Dragon camera for studio filming, DJI Inspire II and Mavic drones for filming the aerial perspective, and small cameras like the Sony Z90 making of camera and GoPro systems for covering timelapse. In order to capture the Hoff Crab story, the BBC team used the MARUM ROV QUEST which is capable of reaching depths of 4,000 m and was operated by a team of eight highly qualified ROV pilots and technicians.

Filming achieved

The team was able to achieve a number of goals during the expedition which are detailed below.

Fig. 21.1: Left: Director Yoland Bosiger and Cameraman Sam Meyrick flying their drone. Right: The MARUM ROV QUEST being deployed. Photo courtesy of Holger von Neuhoff.

Hoff Crabs

On the May 18, the BBC team conducted a dedicated filming dive at E2 on the East Scotia Ridge. The ROV spent six hours on the sea floor filming Hoff crabs, *Kiwa tyleri* at a variety of locations including “Dogs Head” and “Anemone Field” and the extinct chimneys of “Dreaming Spires”. During the dive the BBC was able to film the Hoff crabs behaviour around the vents as well as in large numbers of Hoff crabs at “Anemone field”. While the dive was cut short due to bad weather, the dive was a success and the BBC was able to attempt the majority of the shots that they set out to achieve. The BBC was also to access opportunistic filming material during the science dives conducted on board the vessel.

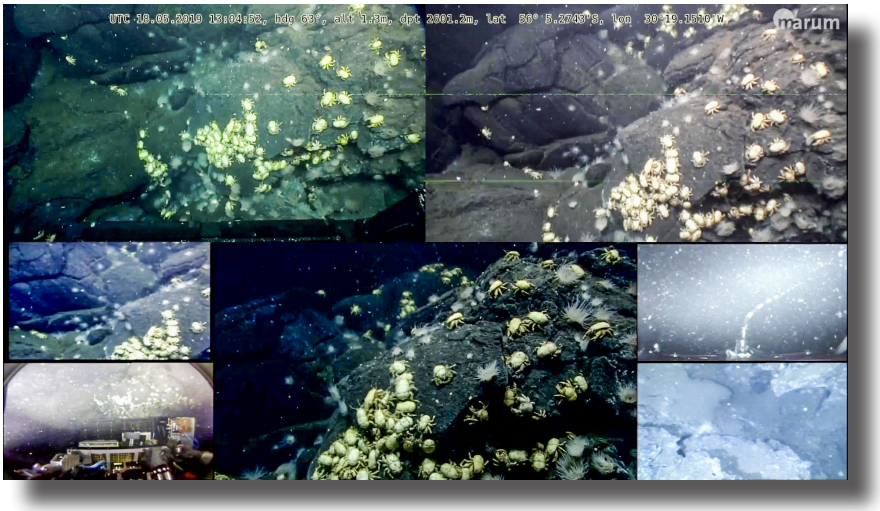

Fig. 21.2: Pilots screen showing the Hoff crab, Kiwa tyleri in large numbers at “Anemone Field”

The South Sandwich Islands

The BBC team was able to film Saunders Island with its drones on two occasions and was able to capture stunning imagery of the islands barren and hostile landscape. The BBC conducted 10 drone flights around the island and focused specifically on ‘arrival shots’ to introduce the islands within the Antarctic program. While the weather was not always suitable for drone flying (the drone can only fly in winds less than 20 knots) the team was particularly fortunate to get one afternoon of clear skies and low wind to capture beautiful imagery of Mt Michael Volcano. The team was still able to satisfy the filming requirements by deploying the drone directly from the *Polarstern* as a landing on the Island was not possible due to weather.

Fig. 21.3: Saunders Island from the drone

Penguins on Icebergs

There were two opportunities during the cruise where we encountered penguins on icebergs and the BBC was able to attempt filming on both occasions. While high winds and waves made filming this scene very challenging, the BBC was able to capture preliminary imagery which will be incredibly useful for this story.

Fig. 21.4: Left: Penguins on an iceberg. Photo courtesy of Alan Derrien. Right: Director Yoland Bosiger and Cameraman Sam Meyrick flying their drone.

Making of

Making of filming consisted of a number of interviews with key personnel and actuality of scientific operations. Interviews were carried out with Gerhard Bohrmann, Moritz Langhinrichs, Katrin Linse, Miriam Römer, Volker Ratmeyer and weather expert Harald Rentsch. These interviews focused on various aspects of the expedition and documented some of the goals, highlights and challenges faced when working on an expedition vessel in the Southern Ocean. Scientific work filmed included deployment of the ROV QUEST, deployment of the CTD, OFOBS and various sediment cores including the piston and gravity corer. The team also filmed the processing of samples, mapping and OFOBS camera feed. This footage will form part of short digital pieces and making of material to be broadcast alongside the final series.

22. ANNOTATED STATION LIST AND ACTION LOG FOR SEAFLOOR NAVIGATION

				Time (UTC)				Begin / on seafloor			End / off seafloor				
Date	St.	Instrument	Location		on	off		Latitude	Longitude	Water	Latitude	Longitude	Water	Core length/ Penetration/ Recovery	
2019	PS119/			Begin	seafloor	seafloor	End	S	W	depth (m)	S	W	depth (m)	Remarks	
2019-04-20	001-1	MUC-01	SW of S. Georgia	13:11	14:29		16:00	54°42.8442	39°32.4560	3621				12 x 35 cm	
2019-04-20	001-2	GC-01	SW of S. Georgia	16:03	17:21		19:08	54°42.8777	39°32.4607	3620				13 m/8 m/3.89 m	
2019-04-20	002-1	GC-02	SW of S. Georgia	19:35	20:32		22:42	54°42.214‘	39°36.746‘	3524				10 m/9 m/6.53 m	*
2019-04-21	003-1	OFOBS-01	Paradise Flare	09:16	12:01	13:07	13:21	54°56.524‘	36°14.812‘	174	54°56.328‘	36°16.020‘			*
2019-04-21	004-1	GC-03	Drygalski Fjord	16:44	16:52		17:30	54°48.873‘	36°00.656‘	225				10 m/bended at 2 m	*
2019-04-21	004-2	GC-04	Drygalski Fjord	17:31	17:44		17:59	54°48.874‘	36°00.647‘	225				5 m/6 m/4.71 m	*
2019-04-22	005-1	GC-05	Drygalski Trough	12:15	12:45		14:02	54°59.135‘	36°13.885‘	290				10 m/10 m/8.22 m	*
2019-04-22	006-1	GC-06	Drygalski Trough	15:00	15:17		16:40	54°55.514‘	35°59.702‘	287				13 m/10 m/8.40 m	*
2019-04-22	007-1	GC-07	Drygalski Trough	17:31	17:42		18:13	54°54.163‘	35°56.692‘	323				13 m/11 m/9.40 m	*
2019-04-22	007-2	MUC-02	Drygalski Trough	18:13	18:22		19:29	54°54.152‘	35°56.662‘	318				11 x 29 cm	*
2019-04-22	008-1	GC-08	Drygalski Trough	20:12	20:29		21:06	54°51.727‘	35°54.361‘	291				5 m/~6 m/4.42 m	*
2019-04-23	009-1	OFOBS-02	ESR - E2 West	20:37	22:50	01:11	02:00	56°03.9115	30°19.4109	2683	56°05.8985	30°19.3007	2383	no video footage	
2019-04-24	010-1	CTD-01	ESR - E2 West	02:43	03:52		04:48	56°04.5944	30°19.4017	2529				Altimeter did not worked, repaired after tool was recovered; 22 sample bottles	
2019-04-24	010-2	CTD-02	ESR - E2 West	06:17	07:45	08:30	10:11	56°04.3901	30°19.4460	2506	56°04.1451	30°19.1197	2561	Yo-Yo CTD, 22 sample bottles	
2019-04-24	011-1	OFOBS-03	ESR - E2 West	17:34	19:01	19:07	19:31	56°02.600‘	30°20.424‘	2710	56°02.641‘	30°20.397‘	2710	Saw seafloor but sonar failed	*
2019-04-24	012-1	CTD-03	ESR - E2 West	21:05	22:55	01:34	03:30	56°03.2021	30°20.4140	2697	56°04.6634	30°19.0128	2548	Yo-Yo CTD, 21 sample bottles	
2019-04-25	013-0	ROV-444	ESR - E2 South	11:29	16:24	21:27	00:08	56°05.2844‘	30°19.1219‘	2611	56°05.2804‘	30°19.1565‘	2579		
2019-04-25	013-1	N-1			19:15			56°05.3514‘	30°19.0975‘	2652				Net: snails, Kiwa crab	
2019-04-26	014-1	MUC-03	ESR - East of E2	13:34	14:35		15:36	56°07.705‘	30°04.176‘	2763				12 x 28 cm	*
2019-04-26	014-2	GC-09	ESR - East of E2	15:37	16:27		17:19	56°07.708‘	30°04.142‘	2776				5 m/5.5 m/5.06 m	*

				Time (UTC)				Begin / on seafloor			End / off seafloor				
Date	St.	Instrument	Location		on	off		Latitude	Longitude	Water	Latitude	Longitude	Water	Core length/ Penetration/ Recovery	
2019	PS119/			Begin	seafloor	seafloor	End	S	W	depth (m)	S	W	depth (m)	Remarks	
2019-04-26	015-1	GC-10	ESR - East of E2	18:08	18:52		20:12	56°06.594‘	30°09.123‘	3034				5 m/6 m/5.11 m	*
2019-04-26	015-2	MUC-04	ESR - East of E2	20:15	21:10		22:24	56°06.598‘	30°09.129‘	3034				12 x 34 cm	*
2019-04-26	016-1	CTD-04	ESR - E2 West	23:22	01:17		02:42	56°04.6241	30°19.3952	2618				22 sample bottles	
2019-04-27	017-0	ROV-445	ESR - E2 West	17:27	21:00	02:03	04:17	56°04.6217‘	30°19.4137‘	2596	56°04.6105‘	30°19.3704‘	2583		
2019-04-27	017-1	N-1			23:12			56°04.6430‘	30°19.4364‘	2591				Net: yellow chimney precipitate	
2019-04-27	017-2	IGT-1			23:42			56°04.6428‘	30°19.4368‘	2591				IGT-1: 30 °C	
2019-04-28	017-3	IGT-2			00:36			56°04.6105‘	30°19.4384‘	2591				IGT-3: 53 °C	
2019-04-28	018-1	MUC-05	ESR - E2	14:14	15:08		16:15	56°08.938‘	29°58.551‘	3258				12 x 33 cm	*
2019-04-28	018-2	GC-11	ESR - E2	16:19	17:07		19:10	56°08.953‘	29°58.546‘	3266				10 m/10 m/8.14 m	*
2019-04-29	019-1	CTD-05	ESR - E2	01:00	02:45	04:38	05:53	56°08.589‘	31°28.774‘	3349	56°08.135‘	31°28.659‘	3330	Posidonia out of service after 1.5 h, 22 samples	*
2019-04-29	020-0	ROV-446	ESR - E2 South	11:15	13:42	00:09	02:26	56°05.2769‘	30°19.1355‘	2571	56°05.2769‘	30°19.1355‘	2571		
2019-04-29	020-1	N-1			14:50			56°05.3279‘	30°19.1512‘	2641				Net red: sponge	
2019-04-29	020-2	N-2			15:34			56°05.3342‘	30°19.1026‘	2637				Net white: 3 crabs	
2019-04-29	020-3	TL-1			16:13			56°05.3343‘	30°19.1024‘	2635				TL: 3.5 - 4.1 °C at colony of snails	
2019-04-29	020-4	N-3			16:26			56°05.3325‘	30°19.1013‘	2635				Net blue: collected snails	
2019-04-29	020-5	N-4			17:45			56°05.3433‘	30°19.0849‘	2645				Net blue: dead crab	
2019-04-29	020-6	BS-1			17:52			56°05.3433‘	30°19.0837‘	2645				Claw: Paulasterias	
2019-04-29	020-7	GS-1			19:26			56°05.3049‘	30°19.1287‘	2623				Claw: sample 5 R in box „I“	
2019-04-29	020-8	IGT-1			19:32			56°05.3050‘	30°19.1287‘	2618				IGT-1: sample 6 F	
2019-04-29	020-9	IGT-2			19:43			56°05.3047‘	30°19.1292‘	2618				IGT-2: sample 7 F	
2019-04-29	020-10	TL-2			19:54			56°05.3048‘	30°19.1294‘	2624				TL: 320 °C	
2019-04-29	020-11	GS-2			20:35			56°05.3039‘	30°19.1267‘	2624				Scoop: sample 8 R shovel sample	

				Time (UTC)				Begin / on seafloor			End / off seafloor				
Date	St.	Instrument	Location		on	off		Latitude	Longitude	Water	Latitude	Longitude	Water	Core length/ Penetration/ Recovery	
2019	PS119/			Begin	seafloor	seafloor	End	S	W	depth (m)	S	W	depth (m)	Remarks	
2019-04-29	020-12	GS-3			21:08			56°05.3004‘	30°19.1516‘	2623				Claw: sample 9 R	
2019-04-29	020-13	IGT-3			23:09			56°05.2839‘	30°19.1496‘	2623				IGT-3: sample 10 F	
2019-04-29	020-14	IGT-4			23:25			56°05.2850‘	30°19.1499‘	2607				IGT-4: sample 11 F	
2019-04-29	020-15	TL-3			23:45			56°05.2864‘	30°19.1487‘	2583				TL: 343.7 °C	
2019-04-29	020-16	GS-4			23:55			???	???	???				Claw: sample 12 R	
2019-04-30	021-1	GC-12	ESR - E2 West	10:15	11:20		12:42	56°08.342‘	31°28.702‘	3363				3 m/3,5 m/3,09 m	*
2019-04-30	022-1	GC-13	ESR - E2 West	12:49	14:00		15:12	56°09.292‘	31°29.045‘	3342				10 m/10 m/6,70 m	*
2019-04-30	022-2	MUC-06	ESR - E2 West	15:13	16:15		17:22	56°09.316‘	31°29.065‘	3342				12 x 38 cm	*
2019-05-01	023-1	CTD-06	SS fore-arc	13:00	15:18		16:50	55°37.4454	27°11.5511	3640				22 sample bottles	
2019-05-05	024-1	CTD-07	Kemp Caldera	08:58	10:16		11:32	59°41.6789	28°21.0267	1417				22 sample bottles	
2019-05-06	025-1	GC-14	ESR - E9	10:08	11:31		12:38	59°52.748‘	29°28.268‘	2899				10 m/3 m/2.31 m	*
2019-05-06	025-2	MUC-07	ESR - E9	12:40	13:37		14:41	59°52.743‘	29°28.261‘	2897				12 x 24 cm	*
2019-05-06	026-1	CTD-08	Kemp Caldera	18:14	19:13		20:16	59°41.7240	28°19.6262	1620				22 sample bottles	
2019-05-07	027-1	OFOBS-04	Kemp Caldera	01:10	03:06	07:38	08:24	59°39.4227	28°21.8262	739	59°41.4807	28°20.9468	1487		
2019-05-07	028-0	ROV-447	Kemp Caldera	10:12	12:40	00:29	02:18	59°41.6740‘	28°21.0965‘	1407	59°41.6313‘	28°21.1271‘	1391		
2019-05-07	028-1	P-1			13:36			59°41.6788‘	28°21.0934‘	1418				P-9: < 1/4 full	
2019-05-07	028-2	P-2			13:44			59°41.6789‘	28°21.0929‘	1419				P-10: > 1/2 full	
2019-05-07	028-3	TL-1			14:00			59°41.6791‘	28°21.0921‘	1418				TL: 5.75 °C; 1.75 °C background	
2019-05-07	028-4	P-3			14:16			59°41.6784‘	28°21.0918‘	1418				P-11: 1/3 full	
2019-05-07	028-5	GS-1			14:38			59°41.6792‘	28°21.0927‘	1419				Claw: basalt GW into „I“	
2019-05-07	028-6	GS-2			14:53			59°41.6781‘	28°21.0953‘	1417				Claw: great wall rock into „I“ + „K“	
2019-05-07	028-7	GS-3			15:02			59°41.6783‘	28°21.0961‘	1416				Claw: sulfur „I“	
2019-05-07	028-8	IGT-1			15:20			59°41.6769‘	28°21.0948‘	1420				IGT-1: 62.95 °C; 0.1 °C ambient	
2019-05-07	028-9	P-4			16:34			59°41.6899‘	28°21.0079‘	1424				P-1: < 1/2 full	

				Time (UTC)				Begin / on seafloor			End / off seafloor					
Date	St.	Instrument	Location	Begin	on seafloor	off seafloor	End	Latitude S	Longitude W	Water depth (m)	Latitude S	Longitude W	Water depth (m)	Remarks	Core length/ Penetration/ Recovery	
2019	PS119/															
2019-05-07	028-10	P-5			16:37			59°41.6898'	28°21.0080'	1424				P-2: ~ 1/3 full (very dusty)		
2019-05-07	028-11	GS-4			16:44			59°41.6899'	28°21.0085'	1423				Claw: black chimney into „H"		
2019-05-07	028-12	P-6			17:38			59°41.6857'	28°21.0137'	1423				P-3: sediments in front of a small mound		
2019-05-07	028-13	P-7			17:40			59°41.6853'	28°21.0149'	1424				P-4: next to P-3 (right hand side)		
2019-05-07	028-14	P-8			17:43			59°41.6850'	28°21.0159'	1422				P-12: next to PC-4 (right hand side)		
2019-05-07	028-15	TL-2			17:50			59°41.6852'	28°21.0154'	1423				TL: 55.4 °C		
2019-05-07	028-16	IGT-2			18:47			59°41.6858'	28°21.0138'	1423				IGT-3: 230 °C		
2019-05-07	028-17	IGT-3			19:02			59°41.6855'	28°21.0149'	1423				IGT-4: 190 °C		
2019-05-07	028-18	GS-5			19:50			59°41.6851'	28°21.0141'	1423				Blue + red handle: scoop of sulfur + dark minerals		
2019-05-07	028-19	P-9			21:27			59°41.6925'	28°20.9807'	1427				P-5: probably only partly recoverd, most red fell out		
2019-05-07	028-20	P-10			21:32			59°41.6924'	28°20.9800'	1427				P-6: most sedimemt fell out		
2019-05-07	028-21	TL-3			21:42			59°41.6923'	28°20.9816'	1427				TL: 11-6 °C		
2019-05-07	028-22	TL-4			21:44			59°41.6923'	28°20.9811'	1427				TL: 6-1 °C		
2019-05-07	028-23	TL-5			21:53			59°41.6921'	28°20.9822'	1426				TL: 100 °C		
2019-05-07	028-24	TL-6			22:04			59°41.6914'	28°20.9948'	1425				TL: ~ 105 °C		
2019-05-07	028-25	N-1			22:53			59°41.6644'	28°21.0547'	1420				Net blue: taking living clams		
2019-05-07	028-26	TL-7			23:28			59°41.6645'	28°21.0550'	1420				TL: temperature in clam field 4.2 °C		
2019-05-08	029-1	GC-15	ESR - E9	10:00	10:57		11:58	60°02.518'	29°41.825'	2631				5 m/5 m/4.5 m	*	

				Time (UTC)				Begin / on seafloor			End / off seafloor				
Date	St.	Instrument	Location		on	off		Latitude	Longitude	Water	Latitude	Longitude	Water	Core length/ Penetration/ Recovery	
2019	PS119/			Begin	seafloor	seafloor	End	S	W	depth (m)	S	W	depth (m)	Remarks	
2019-05-08	029-2	MUC-08	ESR - E9	12:00	12:50		13:52	60°02.512‘	29°41.833‘	2631				12 x 32 cm	*
2019-05-08	030-1	PC-01	ESR - E9	15:10	16:58		19:11	59°52.743‘	29°28.248‘	2895				15 m/15 m/11.73 m	*
2019-05-09	031-1	CTD-09	ESR - E5	19:18	21:01		22:49	57°26.3629‘	30°07.1406	3639				22 sample bottles	
2019-05-09	032-1	OFOBS-05	ESR - E5	23:22	02:45	09:02	10:36	57°22.5675‘	30°07.2666	3886	57°27.7051	30°07.3269	3649		
2019-05-11	033-0	ROV-448	Kemp Caldera	10:10	12:02	15:00	16:13	59°42.0211‘	28°21.2502‘	1463	59°41.6919‘	28°20.9804‘	1425		
2019-05-11	033-1	P-1			14:04			???	???	???				P-3: ~1/3 core length	
2019-05-11	033-2	P-2			14:06			???	???	???				P-6: ~1/2 core length	
2019-05-11	033-3	N-1			14:14			59°41.6685‘	28°21.0541‘	1427				Net red: big net full, too large	
2019-05-11	033-4	TL-1			14:37			59°41.6726‘	28°21.0446‘	1423				TL: 0.3 °C	
2019-05-11	034-1	OFOBS-06	Kemp Caldera	17:00	20:20	22:42	23:50	59°40.5536	28°21.4710	1112	59°42.1525	28°21.8398	1477		
2019-05-12	035-1	CTD-10	Kemp Caldera	00:08	01:06		02:11	59°40.5469	28°21.4081	1121				for ICOS, 22 sample bottles	
2019-05-12	036-1	MUC-09	Kemp Caldera	02:38	03:18		03:58	59°41.720‘	28°19.652‘	1618				12 x ?? cm	*
2019-05-12	036-2	GC-16	Kemp Caldera	04:04	04:39		05:17	59°41.710‘	28°19.647‘	1619				3 m/3 m/1.59 m	*
2019-05-13	037-1	PC-02	ESR - E8	13:21	14:56		16:16	59°29.178‘	28°46.637‘	2637				15 m/10 m/8.67 m	*
2019-05-13	037-2	MUC-10	ESR - E8	16:17	17:07		18:24	59°29.187‘	28°46.608‘	2639				12 x 30 cm	*
2019-05-13	038-1	CTD-11	ESR - E8	18:54	20:07		21:36	59°28.3876	28°41.0975	2553				for ICOS, 22 sample bottles	
2019-05-14	039-1	OFOBS-07	Kemp Caldera	00:51	02:02	08:51	09:36	59°42.1206	28°20.5519	1540	59°42.6613	28°20.7468	1516		
2019-05-14	040-1	CTD-12	Kemp Caldera	09:58	10:42		11:30	59°42.5365	28°20.5383	1564				for ICOS, 22 sample bottles	
2019-05-14	041-1	CTD-13	Kemp Caldera	12:14	13:12		14:08	59°41.1945	28°18.9467	1575				for ICOS, 22 sample bottles	
2019-05-14	042-0	ROV-449	Kemp Caldera	14:32	16:30	01:40	03:10	59°40.5615‘	28°21.4059‘	1138	59°40.6102‘	28°21.5183‘	1162.3		
2019-05-14	042-1	IGT-1			21:19			59°40.5537‘	28°21.4674‘	1128				IGT-1: 231 °C, ambient temp. 0.05°C	

				Time (UTC)				Begin / on seafloor			End / off seafloor				
Date	**St.**	**Instrument**	**Location**		**on**	**off**		**Latitude**	**Longitude**	**Water**	**Latitude**	**Longitude**	**Water**	**Core length/ Penetration/ Recovery**	
2019	**PS119/**			**Begin**	**seafloor**	**seafloor**	**End**	**S**	**W**	**depth (m)**	**S**	**W**	**depth (m)**	**Remarks**	
2019-05-14	042-2	GS-1			21:37			59°40.5541‘	28°21.4674‘	1130				Claw: old chimney in „M“	
2019-05-14	042-3	GS-2			21:50			59°40.5551‘	28°21.4669‘	1130				Claw: second (white) chimney in „M“	
2019-05-14	042-4	IGT-2			22:02			59°40.5553‘	28°21.4675‘	1131				IGT-3: 229 °C, ambient temp. 0.6 °C	
2019-05-14	042-5	P-1			23:04			59°40.6125‘	28°21.4352‘	1172				P-2: ~1/3 full	
2019-05-14	042-6	P-2			23:08			59°40.6125‘	28°21.4330‘	1170				P-8: most sediment fell out	
2019-05-14	042-7	P-3			23:12			59°40.6125‘	28°21.4366‘	1169				P-10: ~1/3 full	
2019-05-14	042-8	TL-1			23:17			59°40.6124‘	28°21.4373‘	1171				TL: 8.7 °C and 15.25 °C, ambient T 0.3 °C	
2019-05-15	042-9	IGT-3			00:49			59°40.6099‘	28°21.5163‘	1163				IGT-4: ambient temp. 0.4 °C	
2019-05-15	042-10	TL-2			01:14			59°40.6100‘	28°21.5166‘	1166				TL: 198.25 °C	
2019-05-15	043-1	OFOBS-08	Kemp Caldera	03:40	04:39	08:54	09:30	59°42.6229	28°17.4441	1087	59°42.0187	28°20.7747	1524		
2019-05-15	044-1	CTD-14	Kemp Caldera	09:57	10:48		11:53	59°42.1077	28°18.7074	1567				for ICOS, 22 sample bottles	
2019-05-15	045-1	PC-03	Kemp Caldera	12:00	13:05		14:12	59°41.717‘	28°19.662‘	1610				15 m/5 m (bended)/2.3 m	*
2019-05-16	046-1	OFOBS-09	SS fore-arc	17:50	18:51	22:20	23:20	55°54.1595	26°46.5308	2500	55°54.4290	26°47.0416	2312		
2019-05-18	047-1	ROV-450	ESR - E2 South	10:00	12:48	19:46	21:33	56°05.2723‘	30°19.1451‘	2590	56°05.3424‘	30°19.0962‘	2643		
2019-05-20	048-1	MUC-11	ESR - E2	11:47	12:46		13:51	56°21.208‘	28°28.286‘	2909				1 x 29 cm; 1 x 48 cm	*
2019-05-20	048-2	GC-17	ESR - E2	13:51	14:51		16:10	56°21.212‘	28°28.243‘	2909				5 m/bended (‚banana‘), empty	*
2019-05-21	049-1	OFOBS	ESR - E2 South	00:05	-	-	01:37	56°05.273‘	30°19.129‘	-				Cancelled	*
2019-05-22	050-1	ROV	Kemp Caldera	00:16	-	-	01:29	59°41.633‘	28°20.856‘	-				Cancelled	*
2019-05-22	051-1	CTD-15	Kemp Caldera	01:18	01:44		02:03	59°41.648‘	28°21.076‘	138					*
2019-05-23	052-1	GC-18	ESR - E2 (WOW)	14:31	15:35		17:00	56°08.3454	31°28.7111	3355				5 m/5.5 m/5.0 m, +MTL, +Posidonia	

				Time (UTC)				Begin / on seafloor			End / off seafloor				
Date	St.	Instrument	Location		on	off		Latitude	Longitude	Water	Latitude	Longitude	Water	Core length/ Penetration/ Recovery	
2019	PS119/			Begin	seafloor	seafloor	End	S	W	depth (m)	S	W	depth (m)	Remarks	
2019-05-23	052-2	MUC-12	ESR - E2 (WOW)	17:02	18:25		19:38	56°08.3467	31°28.7155	3359				12 x 36 cm, +Posidonia	
2019-05-23	052-3	CTD-16	ESR - E2 (WOW)	19:41	21:12		22:44	56°08.3128	31°28.6718	3350				for ICOS, 22 sample bottles	
2019-05-23	053-1	MUC-13	ESR - E2 (WOW)	22:55	23:58		01:30	56°07.6967	31°28.4962	3321				11 x 43 cm, +Posidonia	
2019-05-24	054-1	CTD-17	ESR - E2 (WOW)	23:20	02:09		03:43	56°08.4573	31°28.6541	3355				for ICOS, 22 sample bottles	
2019-05-25	055-1	CTD-18	ESR - E2 (WOW)	04:10	05:42		07:16	56°09.2444	31°29.1512	3338				for ICOS, 22 sample bottles	
2019-05-25	056-1	OFOBS-10	ESR - E2 South	15:58	17:40	23:56	01:14	56°05.1782	30°18.9419	2587	56°05.5272	30°19.8528	2636		
2019-05-26	057-1	GC-19	ESR - E2 (WOW)	05:10	06:29		08:27	56°07.7085	31°28.5252	3329				10 m/10 m/7.96 m	*
2019-05-26	058-1	GC-20	Drygalski Trough	23:36	23:51		00:32	54°55.916‘	36°00.892‘	283				10 m/10 m/8.65 m, +MTL	*

Remotely Operated Vehicle: ROV
Gravity Corer: GC
Piston Corer: PC
Box Corer: BC
Multic Corer: MUC
OFOBS: OFOBS
CTD (AWI-OZE): CTDOZE
Biologic Sample: BS
Geologic Sample: GS

ROV payload
T-Stick: TS
T-Lance: TL
Gas Bubble Sampler: GBS
Fluid Sampler: IGT
Bubble Catcher: BC
Push Corer: P
Net: N
Marker: M
Autonomous scanning sonar: ASSMO
Suction Sampler: S
Bubble Image Plate: BI

* coordinates of the vessel

APPENDIX

A.1 TEILNEHMENDE INSTITUTE / PARTICIPATING INSTITUTIONS

	Address
AWI	Alfred-Wegener-Institut Helmholtz-Zentrum für Polar- und Meeresforschung Postfach 120161 27515 Bremerhaven Germany
BAS	British Antarctic Survey High Cross, Madlingley Road Cambridge CB3 OET United Kingdom
BBC	British Broadcasting Corporation Natural History Unit Whiteladies Road BS8 2LR Bristol United Kingdom
CeNak	Centrum für Naturkunde Universität Hamburg Martin-Luther-King-Platz 3 20146 Hamburg Germany
CEOAS	College of Earth, Ocean, and Atmospheric Sciences, Oregon State University 104 CEOAS Administration Building Corvallis, OR 97331-5503 USA
DWD	Deutscher Wetterdienst Geschäftsbereich Wettervorhersage Seeschifffahrtsberatung Bernhard-Nocht-Str. 76 20359 Hamburg Germany
GeoB	Department of Geosciences (FB5) University of Bremen Klagenfurterstr. 28334 Bremen Germany

	Address
GFZ	Department 2.1 - Physics of Earthquakes and Volcanoes Helmholtz Centre Potsdam German Research Centre for Geosciences (GFZ) Helmholtzstraße 7 14467 Potsdam Germany
HeliService	Heli Service International GmbH Flugbetrieb Polarstern Gorch-Fock-Str. 105 26721 Emden Germany
IGG-UG	Institut für Geographie und Geologie der Universität Greifswald Friedrich-Ludwig-Jahn-Str. 17A 17489 Greifswald Germany
IMMH	Internationales Maritimes Museum Hamburg Koreastr. 1 20457 Hamburg Germany
IPGP	Institut de Physique du Globe de Paris Sorbonne Paris Cité Observatoire Volcanologique du Piton de la Fournaise 14 RN3, km 27 97418 La Plaine des Cafres France
MARUM	Center for Marine Environmental Sciences University of Bremen Leobener Str. 28359 Bremen Germany
MPI	Max Planck Institute for Marine Microbiology Celsiusstr. 1 28359 Bremen Germany
NOCS	National Oceanography Centre Waterfront Campus European Way Southampton SO14 3ZH United Kingdom

	Address
NHM	Natural History Museum Cromwell Road London SW7 5BD United Kingdom
NOAA	National Oceanic and Atmospheric Administration Pacific Marine Environmental Lab 7600 Sand Point Way NE, Seattle, WA 98115-6349 USA
OkState	Boone Pickens School of Geology Oklahoma State University 105 Noble Research Center 74078-3031 Stillwater USA
QUB-QML	Queen's University Belfast Marine Laboratory 12-13 The Strand BT22 1PF Portaferry United Kingdom
SEE-UL	School of Earth and Environment Leeds University Woodhouse Lane LS2 9JT Leeds United Kingdom

A.2 FAHRTTEILNEHMER / CRUISE PARTICIPANTS

Name/ Last name	Vorname/ First name	Institut Institute	Beruf/ Profession	Fachrichtung/ Discipline
Ahrlich	Frauke	MARUM	Engineer	ROV
Arevalo Gonzalez	Marcelo	AWI	Scientist	Coring
Bohrmann	Gerhard	GeoB	Chief scientist	Geology
Bosiger	Yoland	BBC	Writer	Shooting
Büttner	Hauke	MARUM	Engineer	ROV
Daub	Pascal	AWI	Technician	Coring
Derrien	Allan	IPGP	PhD student	Volcanology
Diehl	Alexander	GeoB	Scientist	Geology
Franke	Maximilian	MPI	PhD student	Microbiology
Gaide	Stefanie	GeoB	Technician	Mapping
Geier	Benedikt	MPI	PhD student	Microbiology
Gischler	Michael	HeliService	Pilot	Helicopter
Hempelt	Juliane	DWD	Technician	Meteorology
Höfken	Adrian	AWI	PhD student	Geology
Jones	Christopher	OkState	PhD student	Geochemistry
Kesselring	Tina	CeNak	Veterinarian	Animal health
Koschinsky	Philipp	MARUM	Engineer	ROV
Köster	Male	AWI	PhD student	Geochemistry
Krieger	Chintara	CeNak	Student	Animal health
Kürzinger	Victoria	GeoB	PhD student	Mapping
Lensch	Norbert	AWI	Technician	Geology
Leymann	Tom	MARUM	Technician	ROV
Lichtschlag	Anna	NOCS	Scientist	Geology
Linse	Katrin	BAS	Scientist	Biology
Little	Crispin	SEE-UL	Lecturer	Paleontology
Malnati	Janice	GeoB	Technician	Geochemistry
Meschede	Martin	IGG-UG	Professor	Geology
Meyrick	Sam Lewis	BBC	Cameraman	Helicopter
Pape	Thomas	GeoB	Scientist	Geology
Pereira	Samuel	GeoB	Student	Geology

Name/ Last name	Vorname/ First name	Institut Institute	Beruf/ Profession	Fachrichtung/ Discipline
Ratmeyer	Volker	MARUM	Scientist	ROV
Rentsch	Harald	DWD	Meteorologist	Meteorology
Reuter	Christian	MARUM	Scientist	ROV
Reuter	Michael	MARUM	Technician	ROV
Richter	Nicole	IPGP	Scientist	Volcanology
Richter	Roland	HeliService	Technician	Helicopter
Riedinger	Natascha	OkState	Professor	Geochemistry
Römer	Miriam	GeoB	Scientist	Geology
Rücker	Nontje	GeoB	Student	Geology
Santos	Victor	HeliService	Technician	Helicopter
Schade	Tobias	MARUM	Technician	ROV
Schröder	Marcel	MARUM	Engineer	ROV
Sigwart	Julia	QUB-QML	Professor	Biology
Torres	Marta	CEOAS	Professor	Geochemistry
Tseng	YiTing	MARUM	PhD student	Geology
Vejzovic	Ines	GeoB	Student	Mapping
Viquerat	Sacha	CeNak	Veterinarian	Animal health
v. Neuhoff	Holger	IMMH	Curator	Outreach
v. Neuhoff	Stephanie	IMMH	Journalist	Outreach
Wintersteller	Paul	MARUM	Scientist	Mapping
Zillgen	Carsten	HeliService	Pilot	Helicopter

A.3 SCHIFFSBESATZUNG / SHIP'S CREW

No.	Name	Rank
1	Langhinrichs, Moritz	Master
2	Kentges, Felix	1. Offc.
3	Grafe, Jens	Ch. Eng.
4	Hering, Igor	2. Offc.
5	Neumann, Ralph	2. Offc.
6	Langer, Carl	2. Offc.
7	Mengel, Andreas	Doctor
8	Christian, Boris	R. Offc.
9	Krinfeld, Oleksandr	2. Eng.
10	Haack, Michael Detlev	2. Eng.
11	Fiedler, Alexander	2. Eng.
12	Christian, Boris	Elec. Eng.
13	Himmel, Frank	ELO
14	Hüttebräucker, Olaf	ELO
15	Ganter, Armin	ELO
16	Nasis, Ilias	ELO
17	Brück, Sebastian	Boatsw.
18	Henning, Jörg	Carpenter
19	Wende, Uwe	A.B.
20	Bäcker, Andreas	A.B.
21	Buchholz, Joscha	A.B.
22	Klee, Philip	A.B.
23	Köpnick, Ulrich	A.B.
24	Möller, Falko	A.B.
25	Neubauer, Werner	A.B.
26	Schade, Tom	A.B.
27	Decker, Jens	A.B.
28	Preußner, Jörg	Storek.
29	Redmer, Jens	E-Eng.
30	Gebhardt, Norman	Mot-man
31	Rhau, Lars-Peter	Mot-man
32	Schwarz, Uwe	Mot-man

No.	Name	Rank
33	Teichert, Uwe	Mot-man
34	Freiwald, Petra	Mot-man
35	Schnieder, Sven	Cook
36	Möller, Wolfgang	Cooksmate
37	Silinski, Frank	Cooksmate
38	Czyborra, Bärbel	1. Stwdess
39	Wöckener, Martina	Stwdess/N.
40	Arendt, René	2. Stwdess
41	Dibenau, Torsten	2. Steward
42	Golla, Gerald	2. Stwdess
43	Chen, Dan	2. Steward
44	Siliski, Carmen	2. Stwdess
45	Sun, Yong Sheng	Laundrym.

A.4 STATIONSLISTE / STATION LIST

Station	Date	Time	Latitude	Longitude	Depth [m]	Gear	Action	Comment
PS119_0_ Underway-1	2019-04-18	04:37	-53.65957	-53.29667	1578	ADCP_150	station start	
PS119_0_ Underway-1	2019-04-18	04:38	-53.65963	-53.29160	1580	ADCP_150	profile start	
PS119_0_ Underway-1	2019-05-29	21:02	-52.55127	-50.49679	3468	ADCP_150	profile end	
PS119_0_ Underway-1	2019-05-29	21:02	-52.55123	-50.49735	3469	ADCP_150	station end	
PS119_0_ Underway-3	2019-04-18	04:37	-53.65957	-53.29667	1578	FBOX	station start	
PS119_0_ Underway-3	2019-04-18	04:38	-53.65963	-53.29160	1580	FBOX	profile start	
PS119_0_ Underway-3	2019-05-29	21:03	-52.55103	-50.50120	3469	FBOX	profile end	
PS119_0_ Underway-3	2019-05-29	21:03	-52.55098	-50.50176	3467	FBOX	station end	
PS119_0_ Underway-4	2019-04-18	04:37	-53.65957	-53.29667	1578	HVAIR	station start	
PS119_0_ Underway-4	2019-04-18	04:38	-53.65963	-53.29160	1580	HVAIR	profile start	
PS119_0_ Underway-4	2019-05-29	21:01	-52.55152	-50.49469	3470	HVAIR	profile end	
PS119_0_ Underway-5	2019-04-18	04:37	-53.65957	-53.29667	1578	PCO2_GO	station start	
PS119_0_ Underway-5	2019-04-18	04:38	-53.65963	-53.29160	1580	PCO2_GO	profile start	
PS119_0_ Underway-5	2019-05-29	21:02	-52.55140	-50.49560	3470	PCO2_GO	profile end	
PS119_0_ Underway-5	2019-05-29	21:02	-52.55132	-50.49625	3470	PCO2_GO	station end	
PS119_0_ Underway-6	2019-04-18	04:37	-53.65957	-53.29667	1578	PCO2_SUB	station start	
PS119_0_ Underway-6	2019-04-18	04:38	-53.65963	-53.29160	1580	PCO2_SUB	profile start	
PS119_0_ Underway-6	2019-05-29	21:02	-52.55118	-50.49822	3469	PCO2_SUB	profile end	
PS119_0_ Underway-6	2019-05-29	21:03	-52.55114	-50.49936	3469	PCO2_SUB	station end	
PS119_0_ Underway-7	2019-04-18	04:37	-53.65957	-53.29667	1578	RM	station start	
PS119_0_ Underway-7	2019-04-18	04:38	-53.65963	-53.29160	1580	RM	profile start	
PS119_0_ Underway-7	2019-05-29	21:01	-52.55173	-50.49331	3469	RM	profile end	
PS119_0_ Underway-8	2019-04-18	04:37	-53.65957	-53.29667	1578	GRAV	station start	

Station	Date	Time	Latitude	Longitude	Depth [m]	Gear	Action	Comment
PS119_0_ Underway-8	2019-04-18	04:38	-53.65963	-53.29160	1580	GRAV	profile start	
PS119_0_ Underway-8	2019-05-29	21:01	-52.55162	-50.49406	3471	GRAV	profile end	
PS119_0_ Underway-9	2019-04-18	04:37	-53.65957	-53.29667	1578	SVP	station start	
PS119_0_ Underway-9	2019-04-18	04:38	-53.65963	-53.29160	1580	SVP	profile start	
PS119_0_ Underway-9	2019-05-29	21:04	-52.55092	-50.50245	3468	SVP	profile end	
PS119_0_ Underway-9	2019-05-29	21:04	-52.55088	-50.50292	3467	SVP	station end	
PS119_0_ Underway-10	2019-04-18	04:37	-53.65957	-53.29667	1578	TSG_KEEL	station start	
PS119_0_ Underway-10	2019-04-18	04:38	-53.65963	-53.29160	1580	TSG_KEEL	profile start	
PS119_0_ Underway-10	2019-04-30	10:57	-56.13951	-31.47839	3344	TSG_KEEL	profile end	
PS119_0_ Underway-10	2019-04-30	13:45	-56.15493	-31.48417	NA	TSG_KEEL	profile start	
PS119_0_ Underway-10	2019-05-08	12:31	-60.04203	-29.69697	2637	TSG_KEEL	profile end	
PS119_0_ Underway-10	2019-05-08	18:24	-59.87806	-29.47514	2903	TSG_KEEL	profile start	
PS119_0_ Underway-10	2019-05-29	21:04	-52.55084	-50.50345	3467	TSG_KEEL	profile end	
PS119_0_ Underway-10	2019-05-29	21:04	-52.55080	-50.50389	3467	TSG_KEEL	station end	
PS119_0_ Underway-11	2019-04-18	04:37	-53.65957	-53.29667	1578	TSG_ KEEL_2	station start	
PS119_0_ Underway-11	2019-04-18	04:38	-53.65963	-53.29160	1580	TSG_ KEEL_2	profile start	
PS119_0_ Underway-11	2019-04-30	10:57	-56.13957	-31.47829	3344	TSG_ KEEL_2	profile end	
PS119_0_ Underway-11	2019-04-30	13:46	-56.15503	-31.48422	NA	TSG_ KEEL_2	profile start	
PS119_0_ Underway-11	2019-05-08	12:31	-60.04205	-29.69695	2638	TSG_ KEEL_2	profile end	
PS119_0_ Underway-11	2019-05-08	18:24	-59.87803	-29.47524	2902	TSG_ KEEL_2	profile start	
PS119_0_ Underway-11	2019-05-29	21:03	-52.55111	-50.50013	3468	TSG_ KEEL_2	profile end	
PS119_0_ Underway-11	2019-05-29	21:03	-52.55108	-50.50064	3469	TSG_ KEEL_2	station end	
PS119_0_ Underway-12	2019-04-13	12:00	-53.12532	-70.85841	9.5	WST	station start	
PS119_0_ Underway-12	2019-04-13	12:02	-53.12532	-70.85841	9.5	WST	profile start	
PS119_0_ Underway-13	2019-04-18	04:37	-53.65959	-53.29397	1578	HS	station start	

Station	Date	Time	Latitude	Longitude	Depth [m]	Gear	Action	Comment
PS119_0_ Underway-13	2019-04-18	04:37	-53.65963	-53.29168	1580	HS	profile start	
PS119_0_ Underway-13	2019-05-29	21:04	-52.55075	-50.50450	3466	HS	profile end	
PS119_0_ Underway-13	2019-05-29	21:04	-52.55071	-50.50516	3467	HS	station end	
PS119_0_ Underway-14	2019-04-18	04:37	-53.65957	-53.29659	1578	PS	station start	
PS119_0_ Underway-14	2019-04-18	04:37	-53.65960	-53.29438	1578	PS	profile start	
PS119_0_ Underway-14	2019-05-29	21:05	-52.55066	-50.50585	3466	PS	profile end	
PS119_0_ Underway-14	2019-05-29	21:05	-52.55064	-50.50628	3467	PS	station end	
PS119_1-1	2019-04-20	13:11	-54.71458	-39.54122	3633	MUC	station start	
PS119_1-1	2019-04-20	14:29	-54.71386	-39.54392	3633	MUC	at depth	
PS119_1-1	2019-04-20	16:00	-54.71430	-39.54172	3632	MUC	station end	
PS119_1-2	2019-04-20	16:03	-54.71411	-39.54119	3634	GC	station start	
PS119_1-2	2019-04-20	17:21	-54.71485	-39.54142	3630	GC	at depth	
PS119_1-2	2019-04-20	19:08	-54.71256	-39.54560	3637	GC	station end	
PS119_2-1	2019-04-20	19:35	-54.70446	-39.61260	3532	GC	station start	
PS119_2-1	2019-04-20	22:42	-54.70388	-39.60277	3353	GC	station end	
PS119_3-1	2019-04-21	09:16	-54.94138	-36.24750	177	OFOBS	station start	
PS119_3-1	2019-04-21	12:01	-54.94206	-36.24702	NA	OFOBS	profile start	
PS119_3-1	2019-04-21	13:07	-54.93881	-36.26699	NA	OFOBS	profile end	
PS119_3-1	2019-04-21	13:21	-54.93925	-36.26816	NA	OFOBS	station end	
PS119_4-1	2019-04-21	16:44	-54.81448	-36.01068	NA	GC	station start	
PS119_4-1	2019-04-21	16:52	-54.81454	-36.01094	225	GC	at depth	
PS119_4-1	2019-04-21	17:30	-54.81461	-36.01015	225	GC	station end	
PS119_4-2	2019-04-21	17:31	-54.81461	-36.01015	226	GC	station start	
PS119_4-2	2019-04-21	17:44	-54.81457	-36.01078	224	GC	at depth	
PS119_4-2	2019-04-21	17:59	-54.81468	-36.01021	226	GC	station end	
PS119_5-1	2019-04-22	12:15	-54.98617	-36.23250	287	GC	station start	
PS119_5-1	2019-04-22	12:45	-54.98559	-36.23142	290	GC	at depth	
PS119_5-1	2019-04-22	14:02	-54.96424	-36.18127	252	GC	station end	
PS119_6-1	2019-04-22	15:00	-54.92510	-35.99276	290	GC	station start	
PS119_6-1	2019-04-22	16:40	-54.92304	-35.99034	290	GC	station end	
PS119_7-1	2019-04-22	17:31	-54.90278	-35.94231	319	GC	station start	
PS119_7-1	2019-04-22	17:42	-54.90271	-35.94487	319	GC	at depth	
PS119_7-1	2019-04-22	18:13	-54.90246	-35.94400	320	GC	station end	
PS119_7-2	2019-04-22	18:13	-54.90245	-35.94399	320	MUC	station start	
PS119_7-2	2019-04-22	18:22	-54.90253	-35.94437	322	MUC	at depth	
PS119_7-2	2019-04-22	19:29	-54.89955	-35.94317	319	MUC	station end	
PS119_8-1	2019-04-22	20:12	-54.86205	-35.90656	297	GC	station start	
PS119_8-1	2019-04-22	20:29	-54.86212	-35.90602	294	GC	at depth	

Station	Date	Time	Latitude	Longitude	Depth [m]	Gear	Action	Comment
PS119_8-1	2019-04-22	21:05	-54.86269	-35.90790	305	GC	station end	
PS119_9-1	2019-04-23	19:59	-56.06449	-30.32165	4867	OFOBS	station start	
PS119_9-1	2019-04-23	21:51	-56.06540	-30.32351	NA	OFOBS	at depth	
PS119_9-1	2019-04-23	22:48	-56.06548	-30.32367	3424	OFOBS	profile start	
PS119_9-1	2019-04-24	01:05	-56.10420	-30.32207	NA	OFOBS	profile end	
PS119_9-1	2019-04-24	02:17	-56.10181	-30.31025	NA	OFOBS	station end	
PS119_10-1	2019-04-24	02:43	-56.07718	-30.32316	NA	CTDOZE	station start	
PS119_10-1	2019-04-24	03:52	-56.07709	-30.32340	NA	CTDOZE	at depth	
PS119_10-1	2019-04-24	04:48	-56.07584	-30.32484	2547	CTDOZE	station end	
PS119_10-1	2019-04-24	06:17	-56.07596	-30.32480	2621	CTDOZE	station start	
PS119_10-1	2019-04-24	07:24	-56.07283	-30.32221	2640	CTDOZE	at depth	first time
PS119_10-1	2019-04-24	07:45	-56.07029	-30.32304	2663	CTDOZE	at depth	second time
PS119_10-1	2019-04-24	10:11	-56.06995	-30.31581	2661	CTDOZE	station end	
PS119_11-1	2019-04-24	16:56	-56.04385	-30.33961	2729	OFOBS	station start	
PS119_11-1	2019-04-24	19:00	-56.04333	-30.34041	2710	OFOBS	at depth	
PS119_11-1	2019-04-24	19:12	-56.04401	-30.33995	2710	OFOBS	at depth	
PS119_11-1	2019-04-24	20:55	-56.05240	-30.34226	2680	OFOBS	station end	
PS119_12-1	2019-04-24	21:05	-56.05287	-30.34244	2680	CTDOZE	station start	
PS119_12-1	2019-04-24	22:55	-56.05450	-30.33951	2673	CTDOZE	at depth	first time
PS119_12-1	2019-04-25	00:50	-56.07625	-30.31960	2588	CTDOZE	at depth	second time
PS119_12-1	2019-04-25	03:30	-56.07738	-30.31671	2581	CTDOZE	station end	
PS119_13-1	2019-04-25	11:29	-56.08806	-30.31936	2608	ROV	station start	
PS119_13-1	2019-04-25	12:43	-56.08794	-30.31786	2599	ROV	station end	Pre-Dive-Check not successful
PS119_13-1	2019-04-25	14:08	-56.08794	-30.31919	2590	ROV	station start	
PS119_13-1	2019-04-25	16:24	-56.08778	-30.31940	2616	ROV	at depth	
PS119_13-1	2019-04-26	00:08	-56.08743	-30.31063	2623	ROV	station end	
PS119_14-1	2019-04-26	13:34	-56.12752	-30.06994	2760	MUC	station start	
PS119_14-1	2019-04-26	14:34	-56.12842	-30.06960	2768	MUC	at depth	
PS119_14-1	2019-04-26	15:36	-56.12804	-30.06890	2772	MUC	station end	
PS119_14-2	2019-04-26	15:37	-56.12806	-30.06910	2771	GC	station start	
PS119_14-2	2019-04-26	16:27	-56.12846	-30.06903	2776	GC	at depth	
PS119_14-2	2019-04-26	17:19	-56.12831	-30.06926	2771	GC	station end	
PS119_15-1	2019-04-26	18:08	-56.10844	-30.15254	3011	GC	station start	
PS119_15-1	2019-04-26	18:52	-56.10989	-30.15205	3037	GC	at depth	
PS119_15-1	2019-04-26	20:12	-56.10998	-30.15181	3044	GC	station end	
PS119_15-2	2019-04-26	20:15	-56.10990	-30.15181	3047	MUC	station start	
PS119_15-2	2019-04-26	21:11	-56.10997	-30.15214	3040	MUC	at depth	
PS119_15-2	2019-04-26	22:24	-56.10967	-30.15122	3071	MUC	station end	
PS119_16-1	2019-04-26	23:22	-56.07683	-30.32491	2616	CTDOZE	station start	
PS119_16-1	2019-04-27	01:17	-56.07694	-30.32206	2618	CTDOZE	at depth	

Station	Date	Time	Latitude	Longitude	Depth [m]	Gear	Action	Comment
PS119_16-1	2019-04-27	02:52	-56.07761	-30.32334	2614	CTDOZE	station end	
PS119_17-1	2019-04-27	17:27	-56.07730	-30.32476	2585	ROV	station start	
PS119_17-1	2019-04-27	21:00	-56.07687	-30.32559	2588	ROV	at depth	
PS119_17-1	2019-04-28	04:17	-56.07861	-30.31904	2586	ROV	station end	
PS119_18-1	2019-04-28	14:14	-56.14726	-29.97594	3253	MUC	station start	
PS119_18-1	2019-04-28	15:08	-56.14896	-29.97586	3254	MUC	at depth	
PS119_18-1	2019-04-28	16:15	-56.14902	-29.97591	3258	MUC	station end	
PS119_18-2	2019-04-28	16:19	-56.14899	-29.97581	3262	GC	station start	
PS119_18-2	2019-04-28	17:07	-56.14921	-29.97576	3256	GC	at depth	
PS119_18-2	2019-04-28	19:10	-56.14836	-29.97713	3248	GC	station end	
PS119_19-1	2019-04-29	01:09	-56.14320	-31.47777	3349	CTDOZE	station start	
PS119_19-1	2019-04-29	02:45	-56.14305	-31.47950	3349	CTDOZE	at depth	
PS119_19-1	2019-04-29	05:53	-56.13647	-31.47807	3337	CTDOZE	station end	
PS119_20-1	2019-04-29	11:13	-56.08847	-30.31823	NA	ROV	station start	
PS119_20-1	2019-04-29	11:28	-56.08829	-30.31596	NA	ROV	station end	Dive-check not successful
PS119_20-1	2019-04-29	11:33	-56.08794	-30.31483	NA	ROV	station start	
PS119_20-1	2019-04-30	02:26	-56.08768	-30.31370	2650	ROV	station end	
PS119_21-1	2019-04-30	10:15	-56.13757	-31.47677	3331	GC	station start	
PS119_21-1	2019-04-30	11:20	-56.13903	-31.47836	3344	GC	at depth	
PS119_21-1	2019-04-30	12:42	-56.14009	-31.47663	NA	GC	station end	
PS119_22-1	2019-04-30	12:59	-56.15714	-31.48493	NA	GC	station start	
PS119_22-1	2019-04-30	14:00	-56.15487	-31.48408	NA	GC	at depth	
PS119_22-1	2019-04-30	15:12	-56.15497	-31.48438	NA	GC	station end	
PS119_22-2	2019-04-30	15:13	-56.15502	-31.48439	NA	MUC	station start	
PS119_22-2	2019-04-30	16:15	-56.15526	-31.48442	NA	MUC	at depth	
PS119_22-2	2019-04-30	17:22	-56.15519	-31.48391	3342	MUC	station end	
PS119_23-1	2019-05-01	13:00	-55.62471	-27.19104	3620	CTDOZE	station start	
PS119_23-1	2019-05-01	15:18	-55.62560	-27.18982	3589	CTDOZE	at depth	
PS119_23-1	2019-05-01	16:50	-55.62565	-27.18934	3598	CTDOZE	station end	
PS119_24-1	2019-05-05	08:58	-59.69463	-28.34979	1446	CTDOZE	station start	
PS119_24-1	2019-05-05	10:00	-59.69517	-28.34979	1442	CTDOZE	at depth	first time
PS119_24-1	2019-05-05	10:16	-59.69456	-28.35124	1417	CTDOZE	at depth	second time
PS119_24-1	2019-05-05	11:32	-59.69433	-28.35265	1391	CTDOZE	station end	
PS119_25-1	2019-05-06	10:08	-59.87890	-29.47092	2901	GC	station start	
PS119_25-1	2019-05-06	11:32	-59.87914	-29.47113	2902	GC	at depth	
PS119_25-1	2019-05-06	12:38	-59.87908	-29.47082	2900	GC	station end	
PS119_25-2	2019-05-06	12:40	-59.87915	-29.47098	2895	MUC	station start	
PS119_25-2	2019-05-06	13:36	-59.87906	-29.47101	2901	MUC	at depth	
PS119_25-2	2019-05-06	14:41	-59.87844	-29.47068	2896	MUC	station end	
PS119_26-1	2019-05-06	18:14	-59.69513	-28.32732	1616	CTDOZE	station start	
PS119_26-1	2019-05-06	19:13	-59.69569	-28.32731	1620	CTDOZE	at depth	

Station	Date	Time	Latitude	Longitude	Depth [m]	Gear	Action	Comment
PS119_26-1	2019-05-06	20:21	-59.69667	-28.32501	1619	CTDOZE	station end	
PS119_27-1	2019-05-07	01:10	-59.65770	-28.36413	775	OFOBS	station start	
PS119_27-1	2019-05-07	03:06	-59.65778	-28.36375	776	OFOBS	profile start	
PS119_27-1	2019-05-07	07:38	-59.69878	-28.34899	1508	OFOBS	profile end	
PS119_27-1	2019-05-07	08:24	-59.69942	-28.34802	1553	OFOBS	station end	
PS119_28-1	2019-05-07	10:12	-59.69472	-28.35206	1397	ROV	station start	
PS119_28-1	2019-05-08	02:18	-59.69094	-28.34532	1562	ROV	station end	
PS119_29-1	2019-05-08	10:00	-60.04188	-29.69665	2636	GC	station start	
PS119_29-1	2019-05-08	10:57	-60.04197	-29.69708	2638	GC	at depth	
PS119_29-1	2019-05-08	11:58	-60.04192	-29.69666	2638	GC	station end	
PS119_29-2	2019-05-08	12:00	-60.04198	-29.69668	2639	MUC	station start	
PS119_29-2	2019-05-08	12:50	-60.04187	-29.69721	2637	MUC	at depth	
PS119_29-2	2019-05-08	13:52	-60.04149	-29.69392	2638	MUC	station end	
PS119_30-1	2019-05-08	15:10	-59.88102	-29.47466	2902	PC	station start	
PS119_30-1	2019-05-08	16:58	-59.87906	-29.47080	2896	PC	at depth	
PS119_30-1	2019-05-08	19:11	-59.87426	-29.47175	2903	PC	station end	
PS119_31-1	2019-05-09	19:18	-57.44093	-30.11622	3612	CTDOZE	station start	
PS119_31-1	2019-05-09	21:01	-57.43952	-30.11932	3640	CTDOZE	at depth	
PS119_31-1	2019-05-09	22:49	-57.43920	-30.12141	3633	CTDOZE	station end	
PS119_32-1	2019-05-09	23:22	-57.37349	-30.12164	3931	OFOBS	station start	
PS119_32-1	2019-05-10	02:28	-57.37617	-30.12138	NA	OFOBS	at depth	
PS119_32-1	2019-05-10	02:45	-57.37887	-30.12162	NA	OFOBS	profile start	
PS119_32-1	2019-05-10	05:55	-57.42534	-30.12215	NA	OFOBS	at depth	
PS119_32-1	2019-05-10	09:02	-57.46735	-30.12453	NA	OFOBS	profile end	
PS119_32-1	2019-05-10	10:36	-57.46181	-30.12658	3678	OFOBS	station end	
PS119_33-1	2019-05-11	10:10	-59.70033	-28.35426	1496	ROV	station start	
PS119_33-1	2019-05-11	16:13	-59.69495	-28.34840	1463	ROV	station end	
PS119_34-1	2019-05-11	17:00	-59.67097	-28.35519	891	OFOBS	station start	
PS119_34-1	2019-05-11	17:56	-59.67548	-28.35620	NA	OFOBS	station end	Stop
PS119_34-1	2019-05-11	18:28	-59.67572	-28.35632	NA	OFOBS	station start	
PS119_34-1	2019-05-11	20:20	-59.67606	-28.35836	1131	OFOBS	profile start	
PS119_34-1	2019-05-11	21:42	-59.69203	-28.35887	1454	OFOBS	at depth	
PS119_34-1	2019-05-11	23:50	-59.69809	-28.37136	1453	OFOBS	station end	
PS119_35-1	2019-05-12	00:08	-59.67553	-28.35617	1105	CTDOZE	station start	
PS119_35-1	2019-05-12	01:06	-59.67599	-28.35787	1118	CTDOZE	at depth	
PS119_35-1	2019-05-12	02:11	-59.67606	-28.35449	1153	CTDOZE	station end	
PS119_36-1	2019-05-12	02:38	-59.69495	-28.32772	1619	MUC	station start	
PS119_36-1	2019-05-12	03:18	-59.69534	-28.32753	1619	MUC	at depth	
PS119_36-1	2019-05-12	03:58	-59.69552	-28.32745	1618	MUC	station end	
PS119_36-2	2019-05-12	04:04	-59.69508	-28.32771	1621	GC	station start	
PS119_36-2	2019-05-12	04:39	-59.69517	-28.32745	1620	GC	at depth	
PS119_36-2	2019-05-12	05:17	-59.69525	-28.32712	1620	GC	station end	
PS119_37-1	2019-05-13	13:21	-59.48551	-28.77747	2641	PC	station start	

Station	Date	Time	Latitude	Longitude	Depth [m]	Gear	Action	Comment
PS119_37-1	2019-05-13	14:56	-59.48631	-28.77722	2643	PC	at depth	
PS119_37-1	2019-05-13	16:16	-59.48654	-28.77711	2641	PC	station end	
PS119_37-2	2019-05-13	16:17	-59.48656	-28.77691	2641	MUC	station start	
PS119_37-2	2019-05-13	17:07	-59.48646	-28.77680	2642	MUC	at depth	
PS119_37-2	2019-05-13	18:24	-59.48571	-28.77876	2645	MUC	station end	
PS119_38-1	2019-05-13	18:54	-59.47307	-28.68272	2531	CTDOZE	station start	
PS119_38-1	2019-05-13	20:07	-59.47318	-28.68537	2553	CTDOZE	at depth	
PS119_38-1	2019-05-13	21:36	-59.47351	-28.68769	2558	CTDOZE	station end	
PS119_39-1	2019-05-14	00:51	-59.70600	-28.33374	1601	OFOBS	station start	
PS119_39-1	2019-05-14	02:01	-59.70183	-28.34284	1575	OFOBS	at depth	
PS119_39-1	2019-05-14	02:02	-59.70152	-28.34276	1572	OFOBS	profile start	
PS119_39-1	2019-05-14	08:38	-59.71313	-28.34468	NA	OFOBS	at depth	
PS119_39-1	2019-05-14	08:51	-59.71623	-28.34352	NA	OFOBS	profile end	
PS119_39-1	2019-05-14	09:36	-59.71346	-28.34412	NA	OFOBS	station end	
PS119_40-1	2019-05-14	09:58	-59.70982	-28.34224	NA	CTDOZE	station start	
PS119_40-1	2019-05-14	10:42	-59.70852	-28.34162	1566	CTDOZE	at depth	
PS119_40-1	2019-05-14	11:30	-59.70867	-28.34256	1560	CTDOZE	station end	
PS119_41-1	2019-05-14	12:14	-59.68773	-28.32108	1582	CTDOZE	station start	
PS119_41-1	2019-05-14	13:12	-59.68695	-28.31593	1565	CTDOZE	at depth	
PS119_41-1	2019-05-14	14:08	-59.68685	-28.31801	1573	CTDOZE	station end	
PS119_42-1	2019-05-14	14:32	-59.67767	-28.35610	1200	ROV	station start	
PS119_42-1	2019-05-15	03:10	-59.67569	-28.35758	1114	ROV	station end	
PS119_43-1	2019-05-15	03:40	-59.70477	-28.29667	1421	OFOBS	station start	
PS119_43-1	2019-05-15	04:38	-59.70987	-28.29208	1165	OFOBS	profile start	
PS119_43-1	2019-05-15	05:49	-59.70328	-28.32407	1607	OFOBS	at depth	
PS119_43-1	2019-05-15	08:54	-59.69927	-28.35266	1473	OFOBS	profile end	
PS119_43-1	2019-05-15	09:30	-59.69799	-28.35795	1427	OFOBS	station end	
PS119_44-1	2019-05-15	09:57	-59.70183	-28.31141	1567	CTDOZE	station start	
PS119_44-1	2019-05-15	10:48	-59.70196	-28.31190	1555	CTDOZE	at depth	
PS119_44-1	2019-05-15	11:52	-59.69479	-28.32888	1612	CTDOZE	station end	
PS119_45-1	2019-05-15	12:00	-59.69522	-28.32850	1602	PC	station start	
PS119_45-1	2019-05-15	13:05	-59.69529	-28.32770	1618	PC	at depth	
PS119_45-1	2019-05-15	14:12	-59.69634	-28.33417	1608	PC	station end	
PS119_46-1	2019-05-16	17:50	-55.90407	-26.77680	2473	OFOBS	station start	
PS119_46-1	2019-05-16	18:44	-55.90321	-26.77544	2480	OFOBS	at depth	
PS119_46-1	2019-05-16	18:51	-55.90363	-26.77596	2470	OFOBS	profile start	
PS119_46-1	2019-05-16	19:44	-55.90773	-26.78439	2320	OFOBS	profile end	
PS119_46-1	2019-05-16	20:09	-55.90742	-26.78338	2343	OFOBS	profile start	
PS119_46-1	2019-05-16	20:50	-55.90264	-26.77441	2485	OFOBS	profile end	
PS119_46-1	2019-05-16	20:51	-55.90259	-26.77425	2504	OFOBS	profile start	
PS119_46-1	2019-05-16	22:20	-55.90973	-26.78504	2293	OFOBS	profile end	
PS119_46-1	2019-05-16	23:20	-55.90734	-26.78374	2331	OFOBS	station end	
PS119_47-1	2019-05-18	10:00	-56.08746	-30.31938	2604	ROV	station start	

Station	Date	Time	Latitude	Longitude	Depth [m]	Gear	Action	Comment
PS119_47-1	2019-05-18	21:55	-56.08950	-30.31366	NA	ROV	station end	
PS119_48-1	2019-05-20	11:47	-56.35411	-28.47321	2910	MUC	station start	
PS119_48-1	2019-05-20	12:46	-56.35347	-28.47143	2909	MUC	at depth	
PS119_48-1	2019-05-20	13:51	-56.35320	-28.47162	2909	MUC	station end	
PS119_48-2	2019-05-20	13:51	-56.35321	-28.47182	2908	GC	station start	
PS119_48-2	2019-05-20	14:51	-56.35352	-28.47072	2907	GC	at depth	
PS119_48-2	2019-05-20	16:10	-56.35335	-28.46934	2907	GC	station end	
PS119_49-1	2019-05-21	00:05	-56.08788	-30.31882	2604	OFOBS	station start	
PS119_49-1	2019-05-21	01:37	-56.08695	-30.31906	2592	OFOBS	station end	
PS119_50-1	2019-05-22	00:16	-59.69388	-28.34760	715	ROV	station start	
PS119_50-1	2019-05-22	01:29	-59.69349	-28.35142	1417	ROV	station end	
PS119_51-1	2019-05-22	01:18	-59.69416	-28.35149	1398	CTDOZE	station start	
PS119_51-1	2019-05-22	01:44	-59.69414	-28.35127	1403	CTDOZE	at depth	
PS119_51-1	2019-05-22	02:03	-59.69335	-28.35178	1443	CTDOZE	station end	
PS119_52-1	2019-05-23	14:31	-56.13796	-31.48136	3356	GC	station start	
PS119_52-1	2019-05-23	17:00	-56.13915	-31.47759	3281	GC	station end	
PS119_52-2	2019-05-23	17:02	-56.13907	-31.47798	3284	MUC	station start	
PS119_52-2	2019-05-23	18:25	-56.13917	-31.47679	3277	MUC	at depth	
PS119_52-2	2019-05-23	19:38	-56.13905	-31.47899	3353	MUC	station end	
PS119_52-3	2019-05-23	19:41	-56.13895	-31.47887	3353	CTDOZE	station start	
PS119_52-3	2019-05-23	21:12	-56.13849	-31.47794	3340	CTDOZE	at depth	
PS119_52-3	2019-05-23	22:44	-56.13447	-31.47805	3331	CTDOZE	station end	
PS119_53-1	2019-05-23	22:55	-56.12951	-31.47753	3328	MUC	station start	
PS119_53-1	2019-05-23	23:58	-56.12848	-31.47405	3321	MUC	at depth	
PS119_53-1	2019-05-24	01:30	-56.12783	-31.47468	3323	MUC	station end	
PS119_54-1	2019-05-24	23:20	-56.13997	-31.47356	3272	CTDOZE	station start	
PS119_54-1	2019-05-25	02:09	-56.14076	-31.48145	3355	CTDOZE	at depth	
PS119_54-1	2019-05-25	03:43	-56.14351	-31.47226	3322	CTDOZE	station end	
PS119_55-1	2019-05-25	04:10	-56.15460	-31.48432	3329	CTDOZE	station start	
PS119_55-1	2019-05-25	05:42	-56.15418	-31.48358	3335	CTDOZE	at depth	
PS119_55-1	2019-05-25	07:16	-56.15289	-31.48088	3325	CTDOZE	station end	
PS119_56-1	2019-05-25	15:58	-56.08491	-30.31544	2601	OFOBS	station start	
PS119_56-1	2019-05-25	17:38	-56.08769	-30.31962	2578	OFOBS	at depth	
PS119_56-1	2019-05-25	17:40	-56.08785	-30.32149	2609	OFOBS	profile start	
PS119_56-1	2019-05-25	23:56	-56.09373	-30.33530	2663	OFOBS	profile end	
PS119_56-1	2019-05-26	01:14	-56.09627	-30.34806	2657	OFOBS	station end	
PS119_57-1	2019-05-26	05:10	-56.12745	-31.47390	3322	GC	station start	
PS119_57-1	2019-05-26	06:29	-56.12896	-31.47474	3319	GC	at depth	
PS119_57-1	2019-05-26	08:27	-56.11575	-31.48443	3417	GC	station end	
PS119_58-1	2019-05-26	23:36	-54.93055	-36.01402	290	GC	station start	
PS119_58-1	2019-05-26	23:51	-54.93193	-36.01487	288	GC	at depth	
PS119_58-1	2019-05-27	00:32	-54.93176	-36.01456	288	GC	station end	

Gear abbreviations	**Gear**
ADCP_150	ADCP 150kHz
CTDOZE	CTD AWI-OZE
FBOX	FerryBox
GC	Gravity Corer
GRAV	Sea Gravimeter
HS	Hydrosweep
HVAIR	High Volume Air Sampler
MUC	Multi Corer
OFOBS	Ocean Floor Observation and Bathemetry System
PC	Piston Corer
PCO2_GO	pCO2 GO
PCO2_SUB	pCO2 Subctech
PS	Parasound
RM	Radiation Measurements
ROV	Remotely Operated Vehicle
SVP	Sound Velocity Profiler
TSG_KEEL	Thermosalinograph Keel
TSG_KEEL_2	Thermosalinograph Keel 2
WST	Weatherstation

A.5 CORE DESCRIPTION LOGS

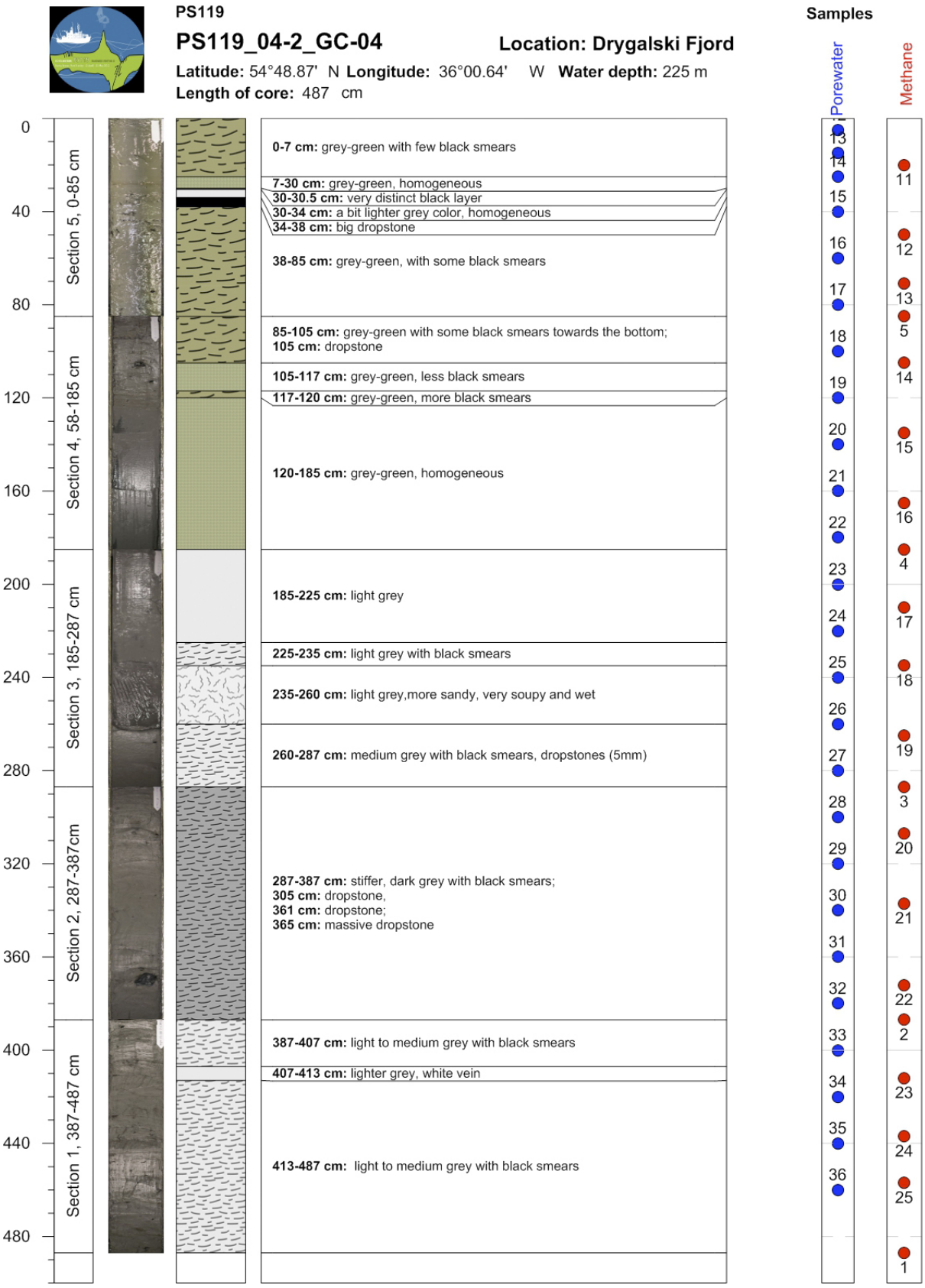

PS119

PS119_14-2_GC-09 Location: E of E2

Latitude: 56°07.708'N **Longitude:** 30°04.142' W **Water depth:** 2776 m
Length of core: 506 cm

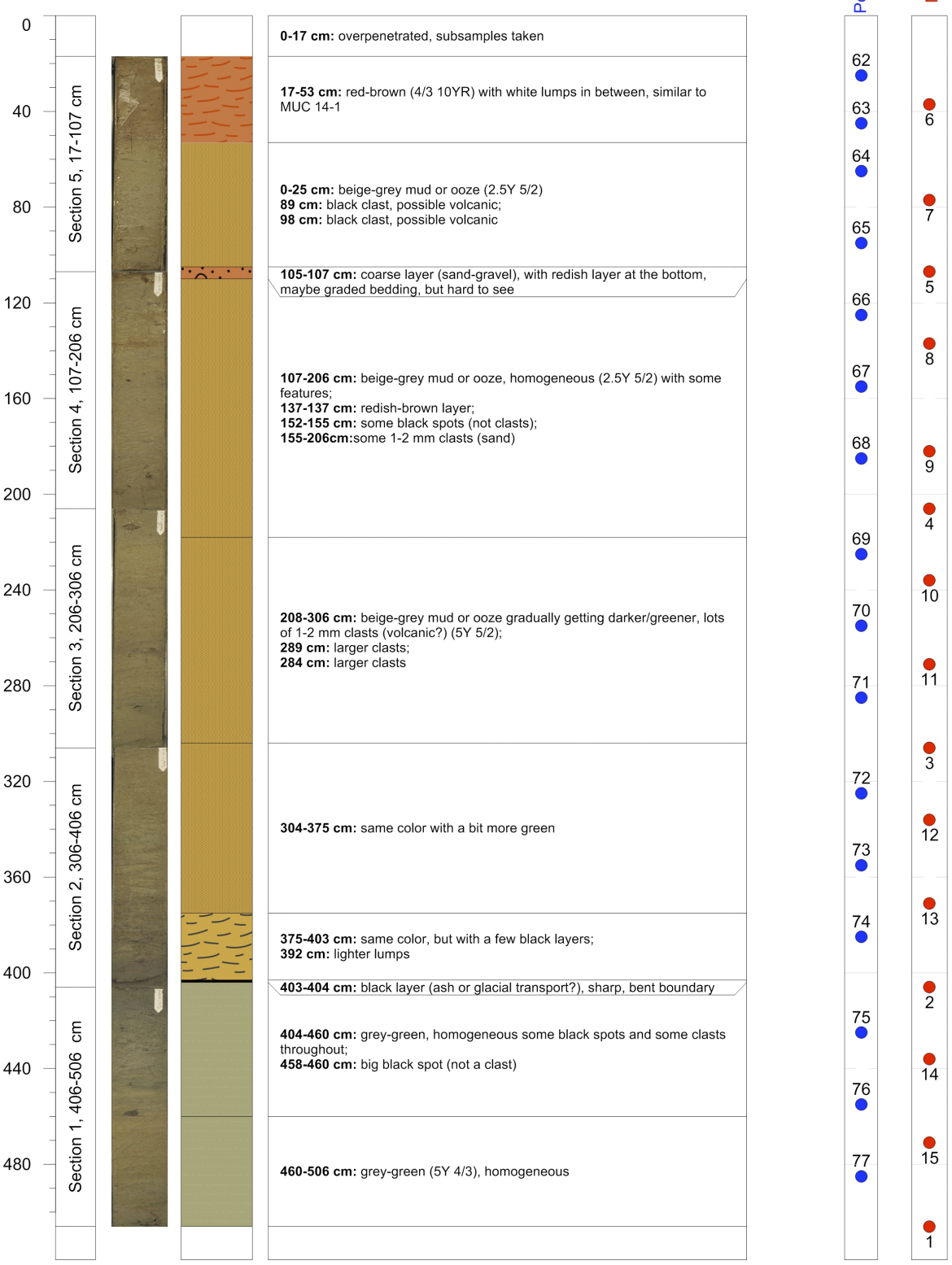

PS119

PS119_15-1_GC-10 Location: E of E2

Latitude: 56°06.598'N **Longitude:** 30°09.129' W **Water depth:** 3034 m
Length of core: 511 cm

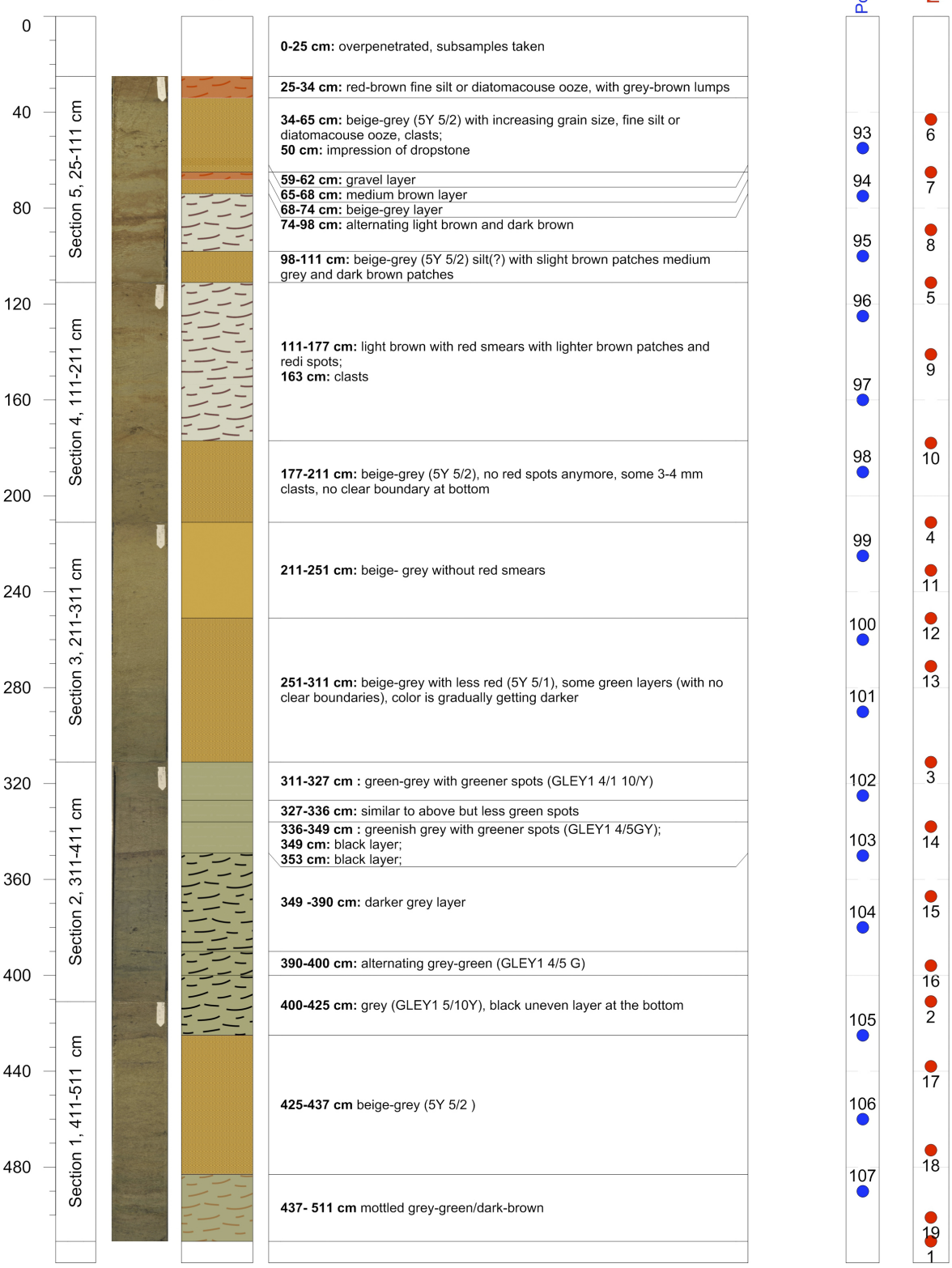

PS119

PS119_18-1_GC-11 Location: E of E2

Latitude: 56°08.953'N **Longitude:** 29°58.546' W **Water depth:** 3266 m
Length of core: 814 cm

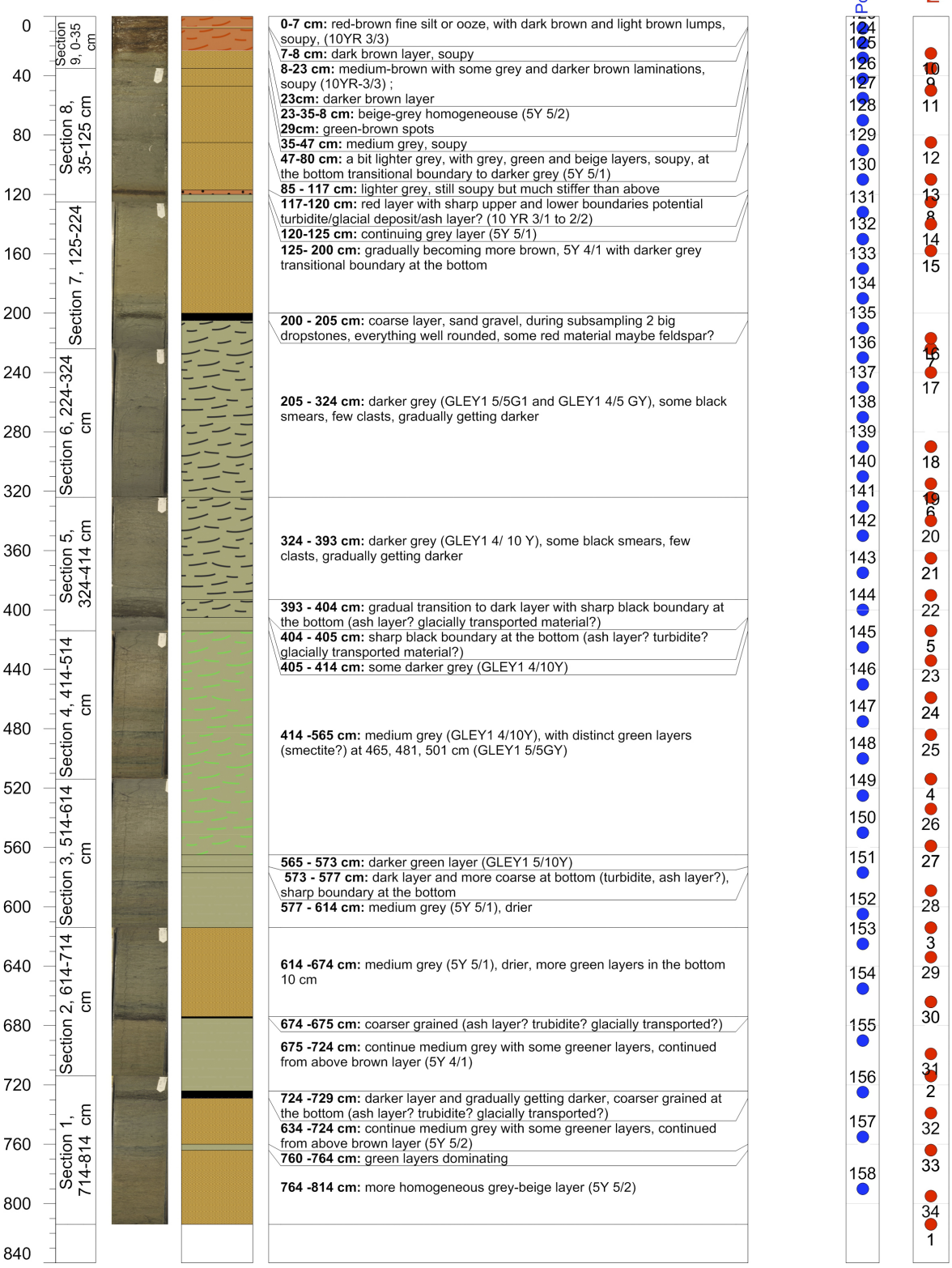

PS119

PS119_21-1_GC-12 **Location: W od ESR**

Latitude: 56°08.342'N **Longitude:** 31°28.702' W **Water depth:** 3363 m
Length of core: 309 cm

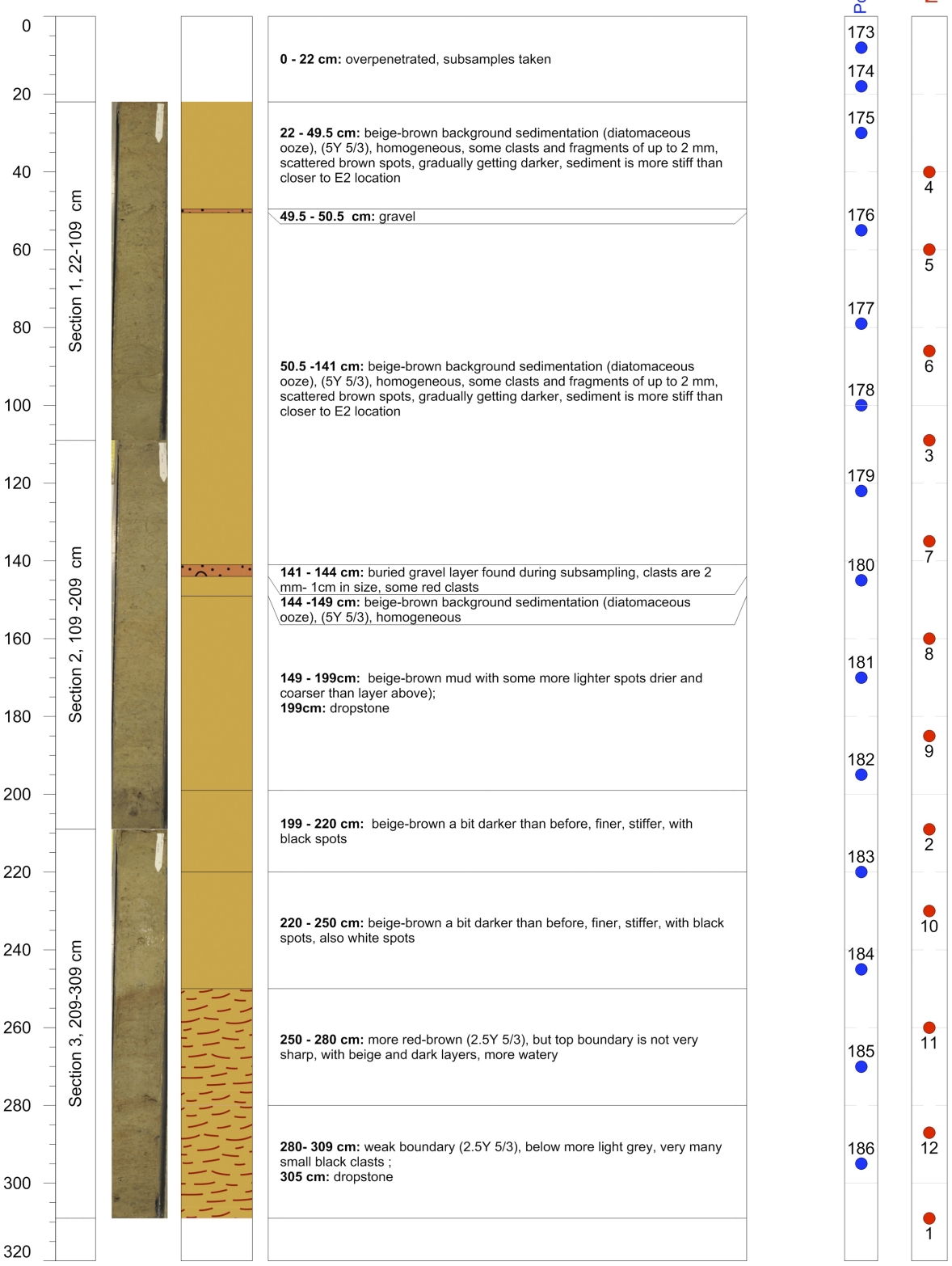

Samples

PS119

PS119_22-1_GC-13 Location: W od ESR

Latitude: 56°09.292'N **Longitude:** 31°29.045' W **Water depth:** 3342 m
Length of core: 670 cm

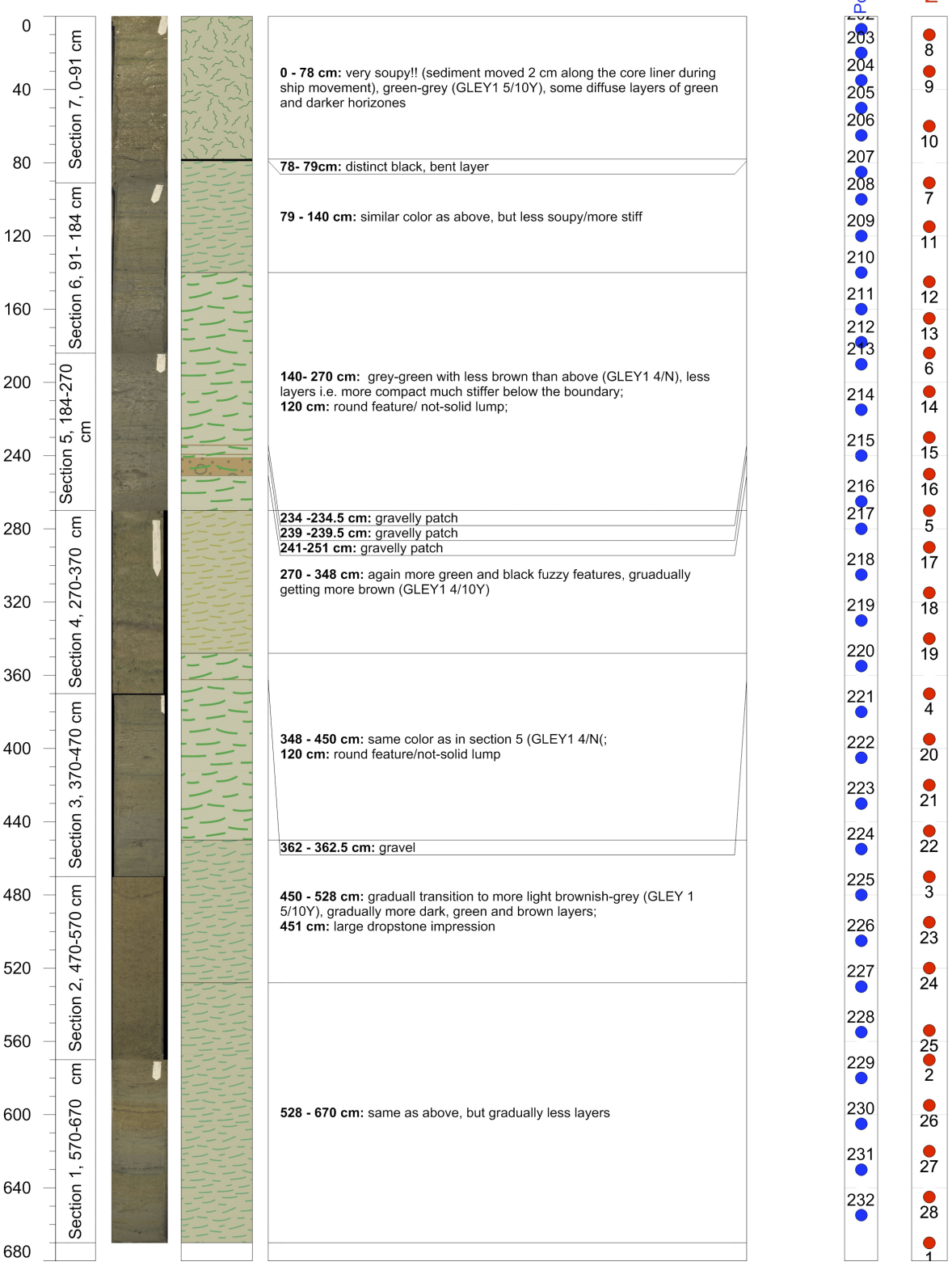

PS119

PS119_25-1_GC-14 **Location: ESR E9**

Latitude: 59°52.748'N **Longitude:** 29°28.268' W **Water depth:** 2899 m
Length of core: 231 cm

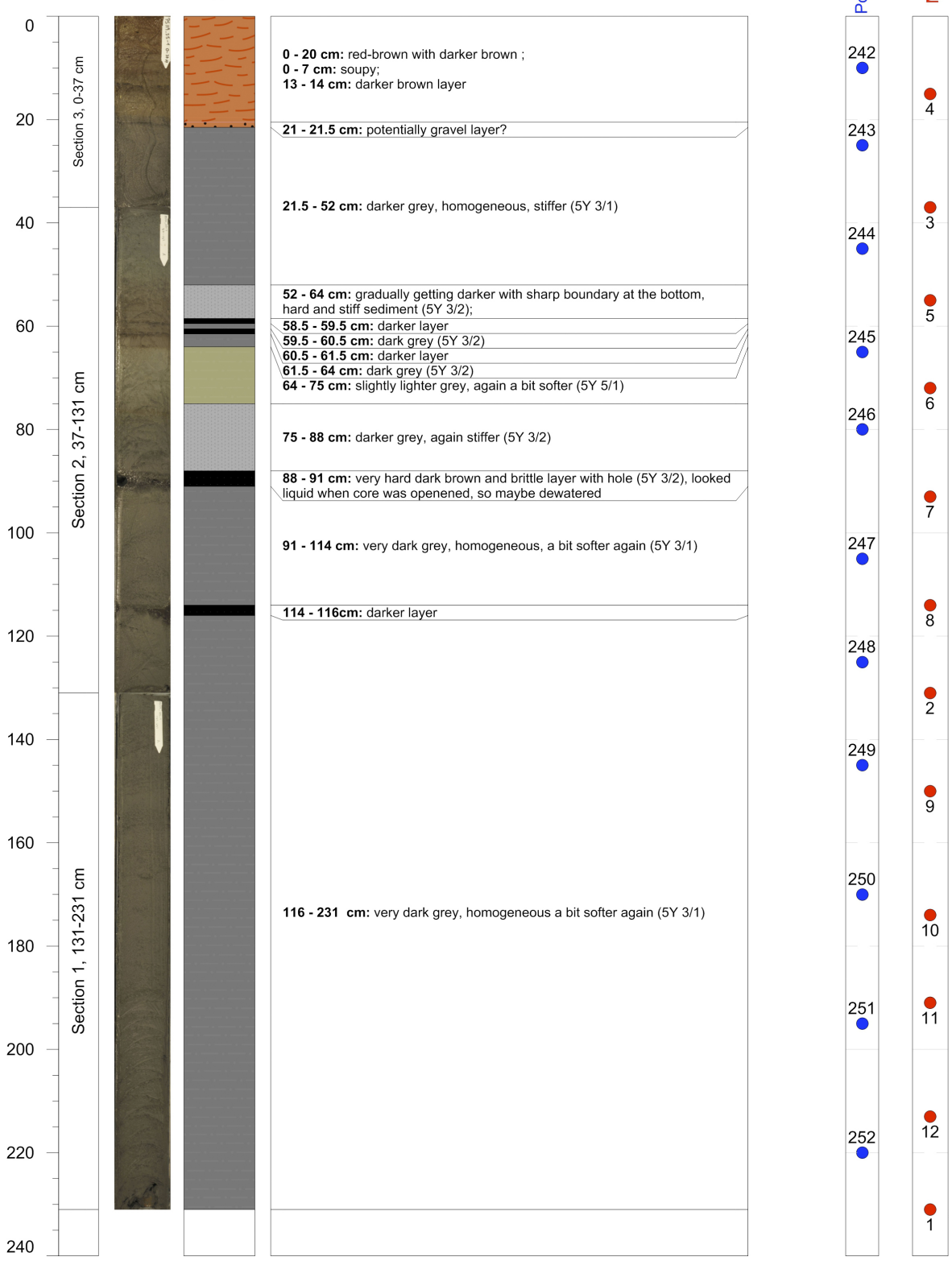

PS119

PS119_29-1_GC-15 Location: ESR E9

Latitude: 60°02.518'N **Longitude:** 29°41.825' W **Water depth:** 2631 m
Length of core: 450 cm

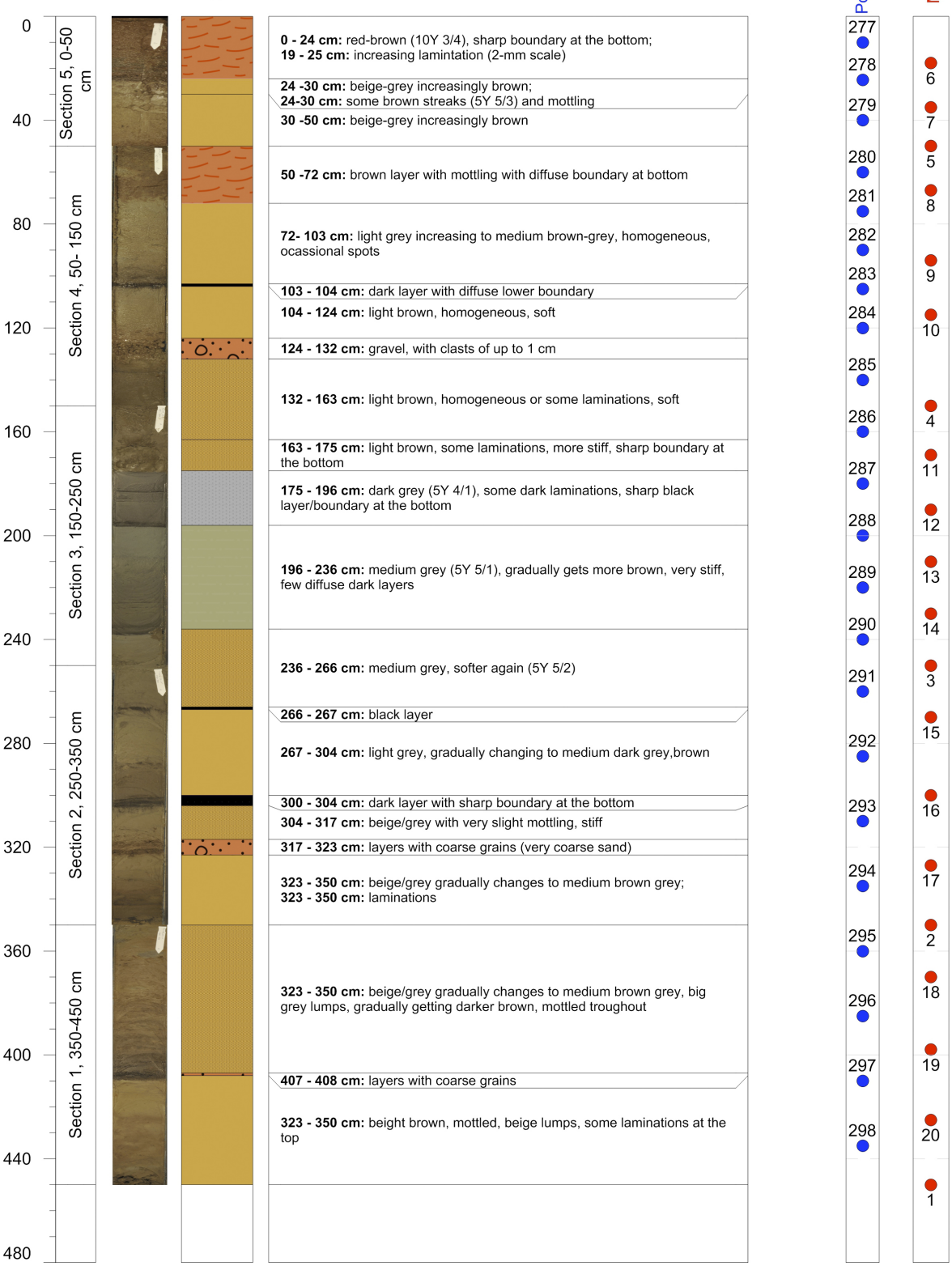

PS119

PS119_30-1_PC-1 **Location: ESR E9**

Latitude: 59°52.743'N **Longitude:** 29°28.248' W **Water depth:** 2895 m
Length of core: 1173 cm

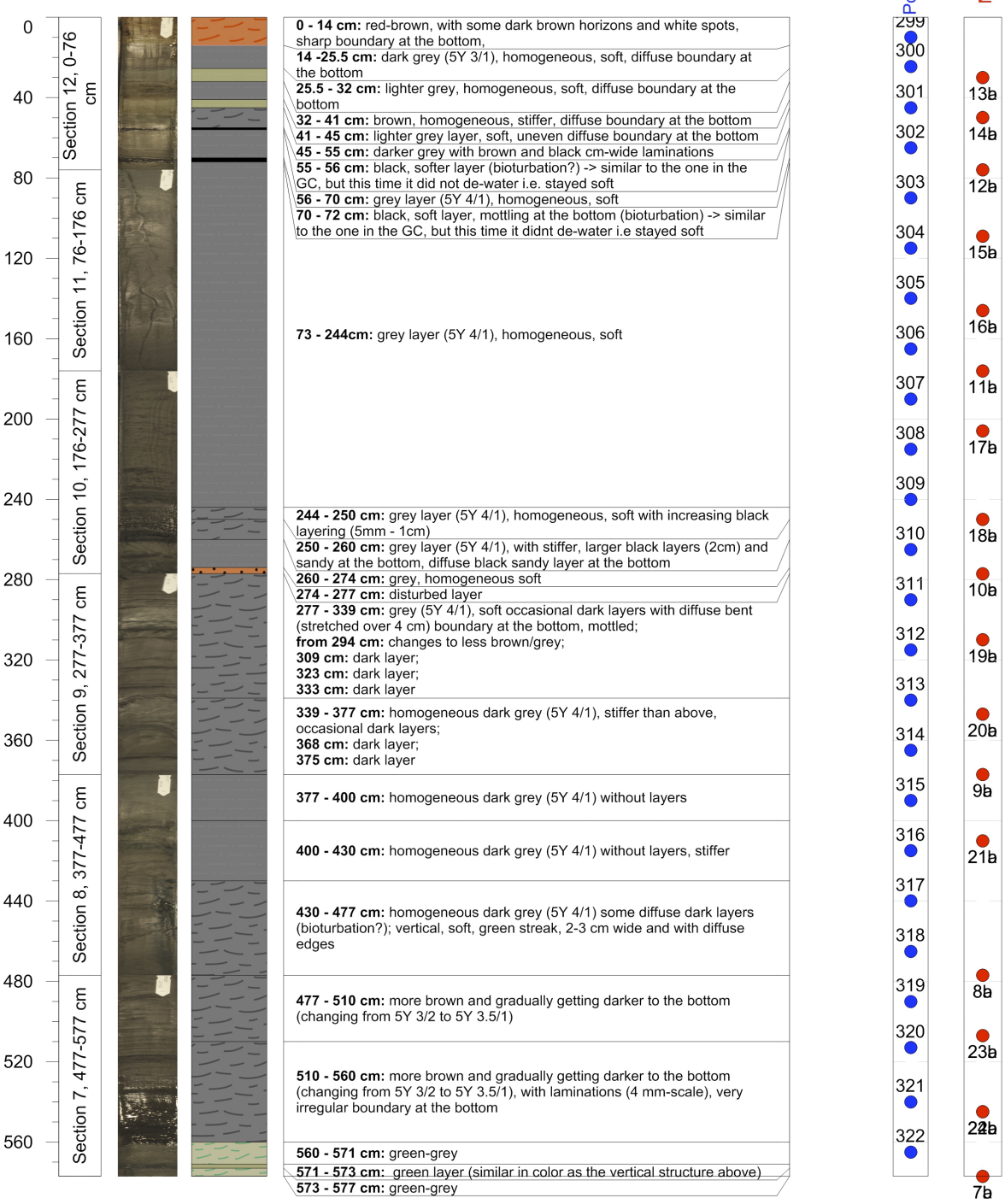

Samples

PS119

CONTINUED

PS119_30-1_PC-1 **Location: ESR E9**

Latitude: 59°52.743'N **Longitude:** 29°28.248' W **Water depth:** 2895 m

Length of core: 1173 cm

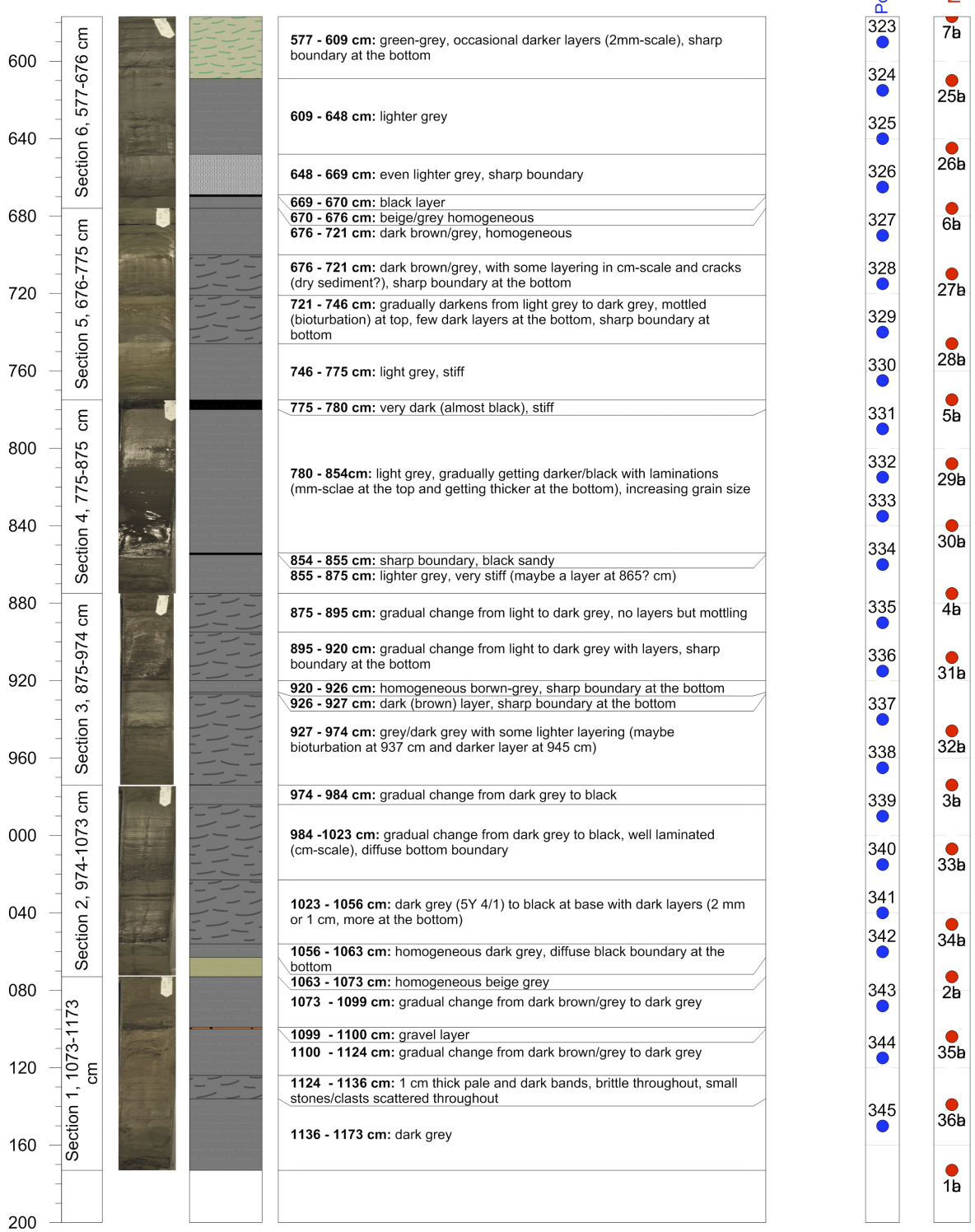

PS119

PS119_36-1_GC-16

Location: Kemp Caldera

Latitude: 59°41.710'N **Longitude:** 28°19.647' W **Water depth:** 1619 m
Length of core: 159 cm

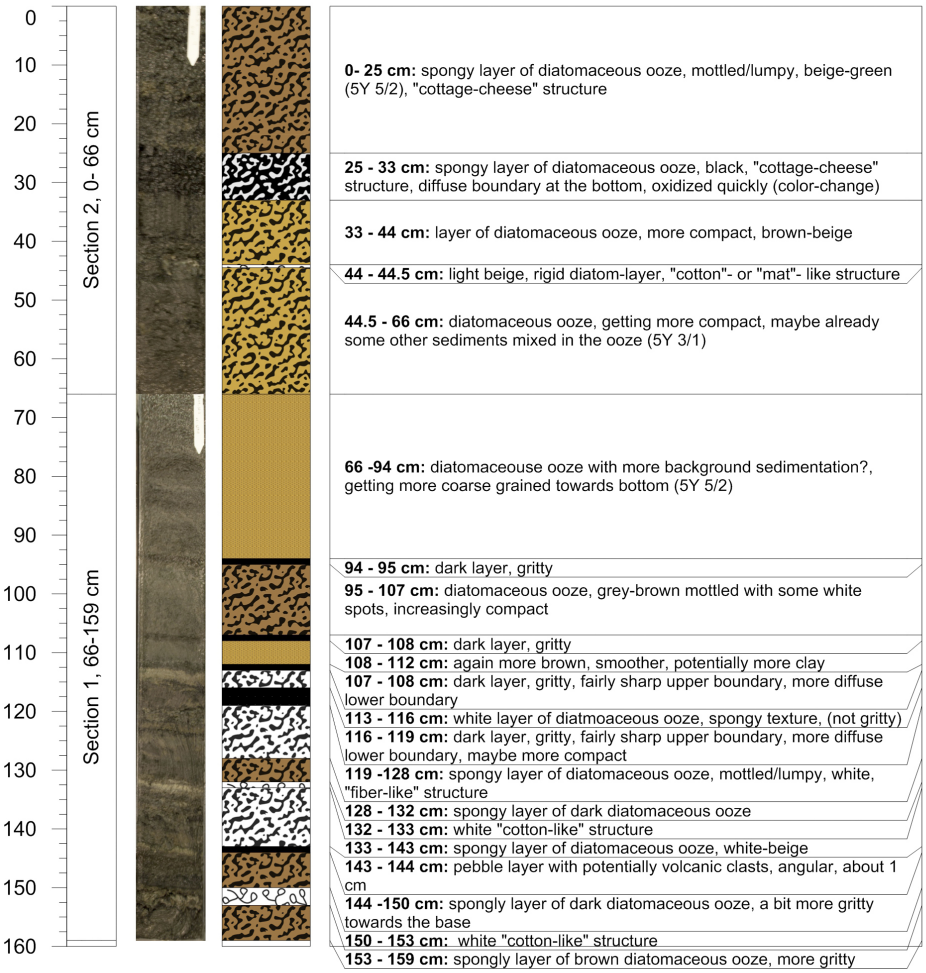

Samples

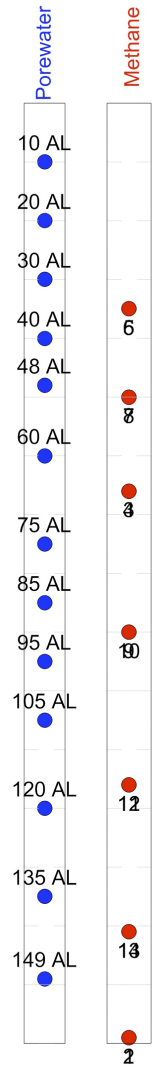

PS119

PS119_37-1_PC-2 Location: ESR E8

Latitude: 28°46.637'N **Longitude:** 59°29.178' W **Water depth:** 2637 m
Length of core: 867 cm

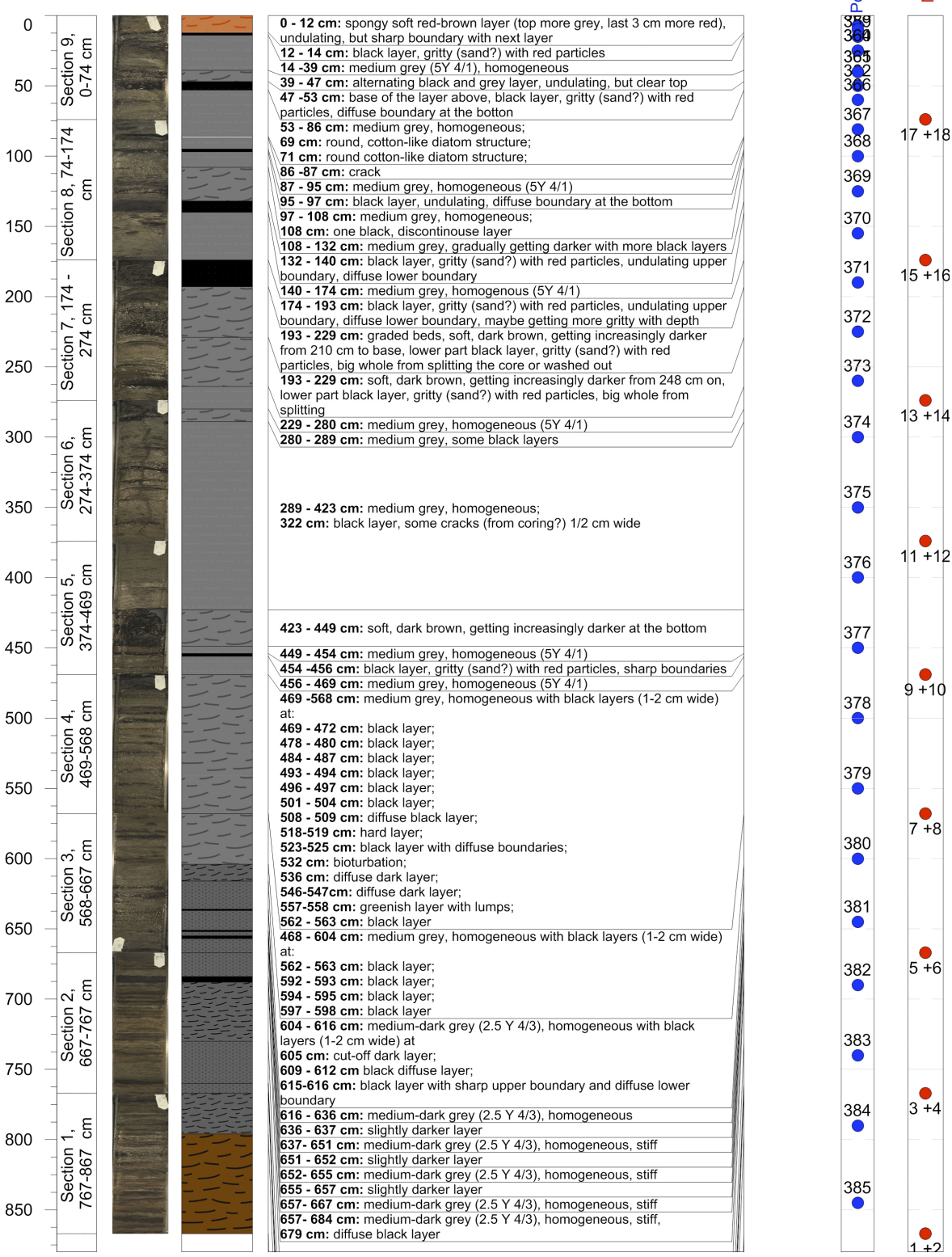

Samples

PS119

PS119_37-1_PC-2 TC

Location: ESR E8

Latitude: 28°46.637'N **Longitude:** 59°29.178' W **Water depth:** 2637 m

Length of core: 63 cm

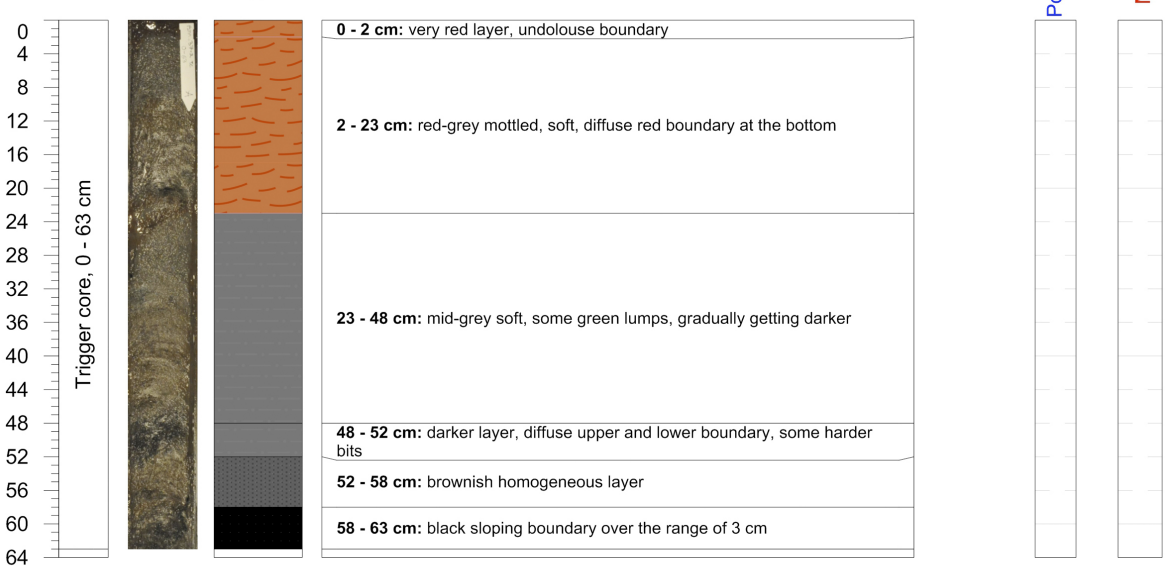

0 - 2 cm: very red layer, undolouse boundary

2 - 23 cm: red-grey mottled, soft, diffuse red boundary at the bottom

23 - 48 cm: mid-grey soft, some green lumps, gradually getting darker

48 - 52 cm: darker layer, diffuse upper and lower boundary, some harder bits

52 - 58 cm: brownish homogeneous layer

58 - 63 cm: black sloping boundary over the range of 3 cm

PS119

PS119_45-1_PC-3 Location: Kemp Caldera

Latitude: 28°19.662'N **Longitude:** 59°41.717' W **Water depth:** 1610 m
Length of core: 230 cm

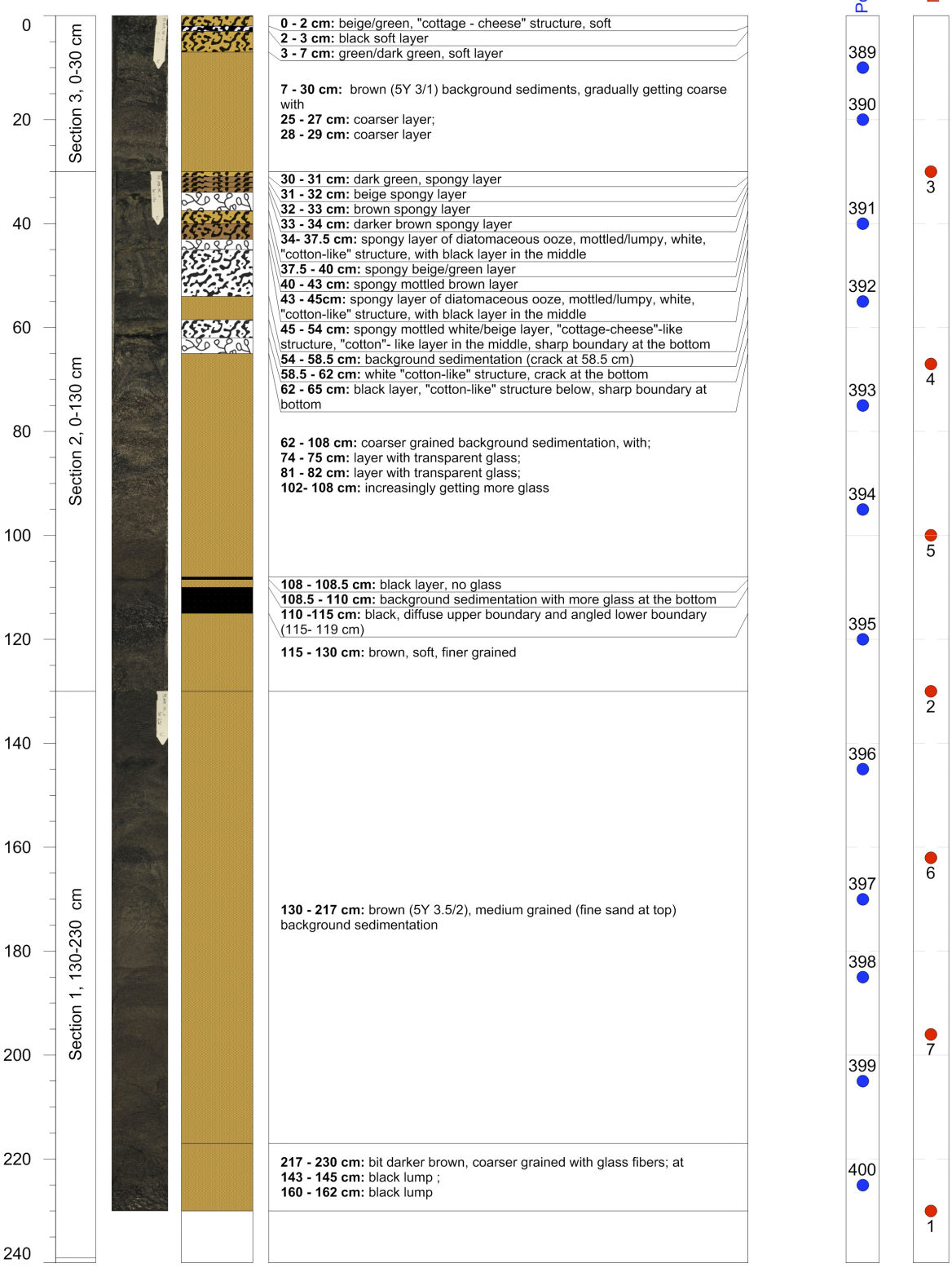

PS119

PS119_45-1_PC-3TC

Location: Kemp Caldera

Latitude: 28°19.662'N **Longitude:** 59°41.717' W **Water depth:** 1610 m

Length of core: 40 cm

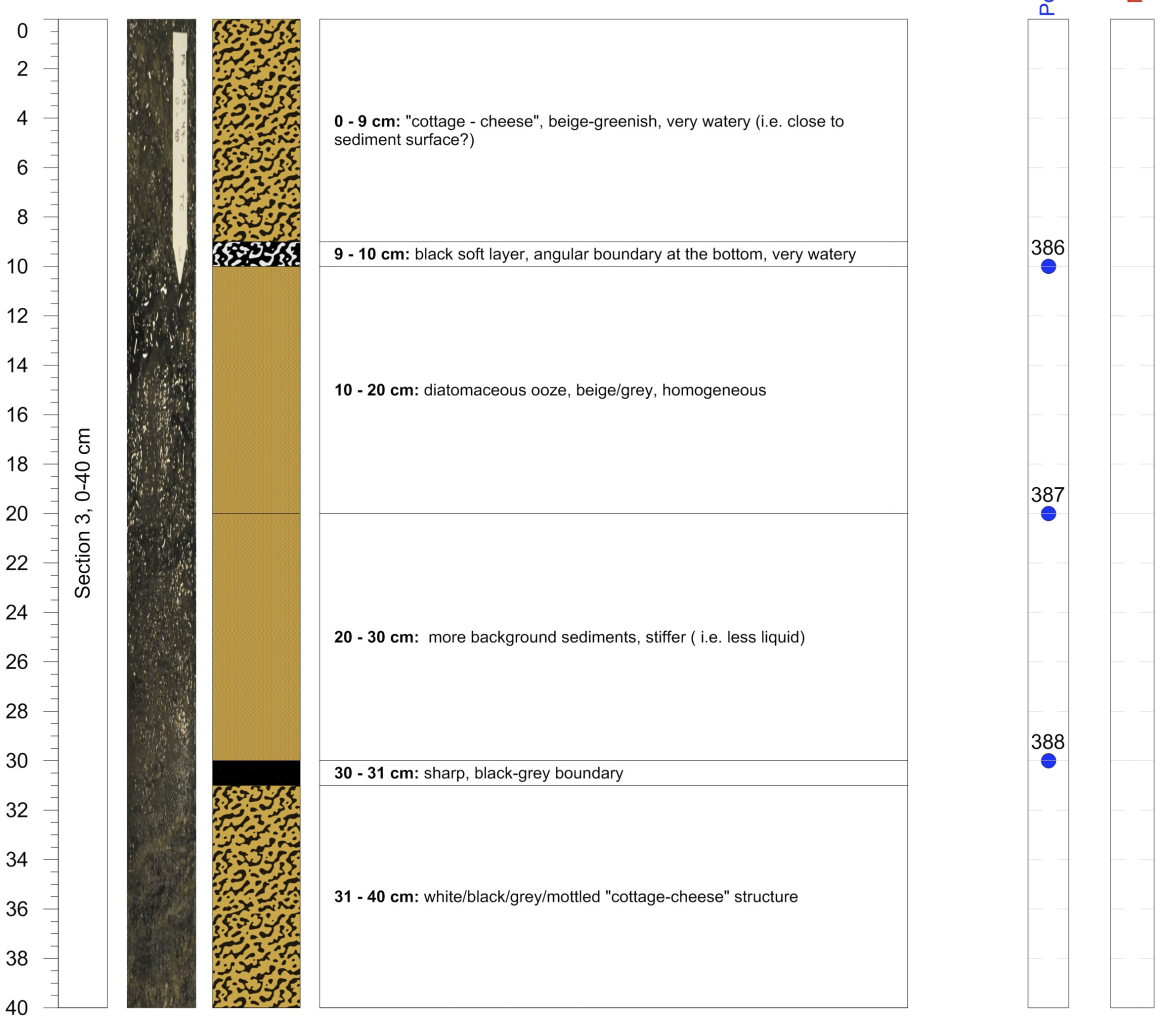

PS119

PS119_52-1_GC18

Location: ESR - E2 West (WOW)

Latitude: 31°28.7111 N **Longitude:** 56°08.3454 W **Water depth:** 3355 m

Length of core: 500 cm

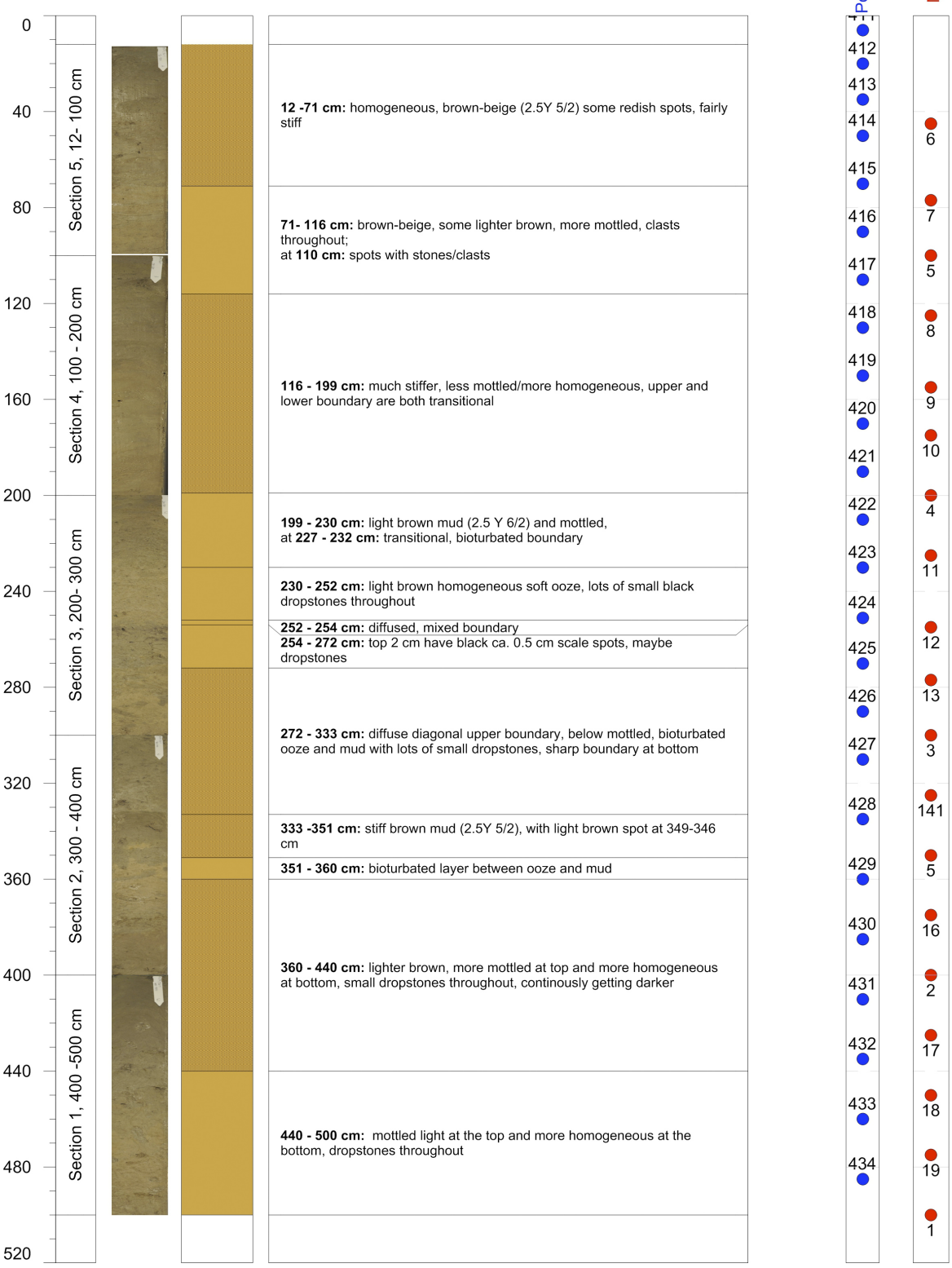

PS119

PS119_57-1_GC19

Location: ESR - E2 West (WOW)

Latitude: 31°28.5252 N **Longitude:** 56°07.7085 W **Water depth:** 3329 m

Length of core: 796 cm

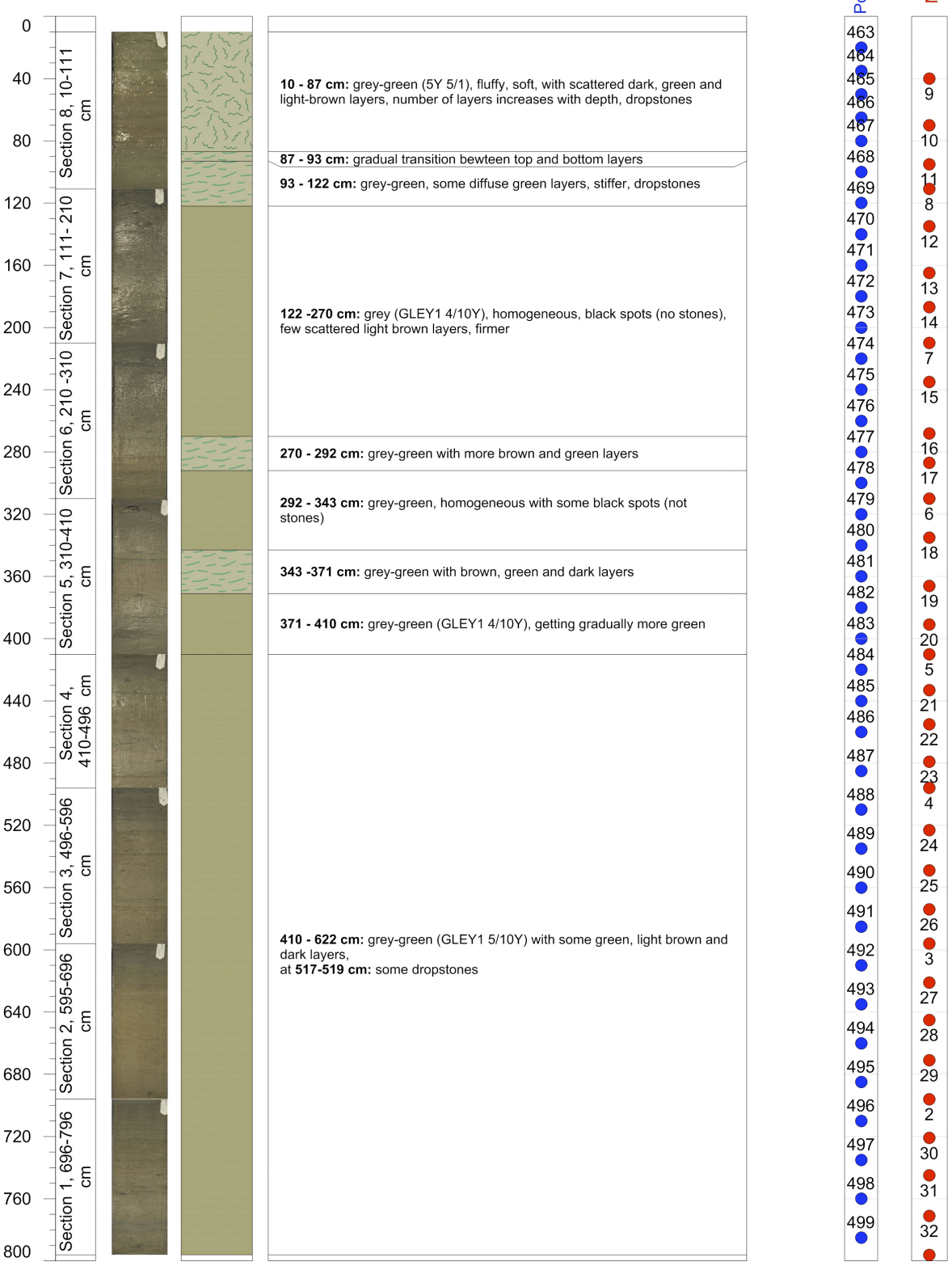

PS119

PS119_58-1_GC20 Location: Drygalski Trough

Latitude: 36°00.892'N **Longitude:** 54°55.916' W **Water depth:** 283 m
Length of core: 865 cm

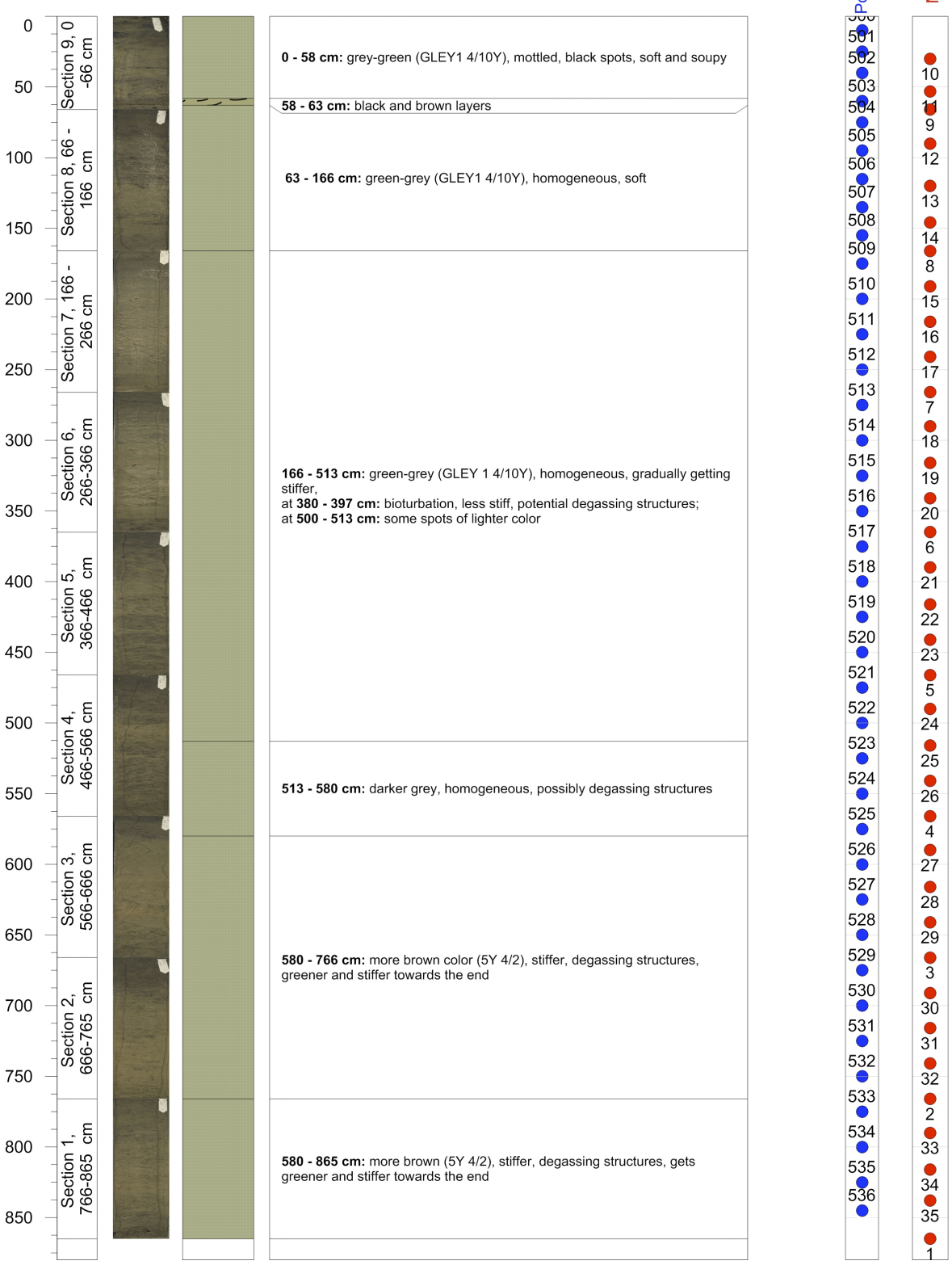

A.6 MULTI-SENSOR CORE LOGGER DATA

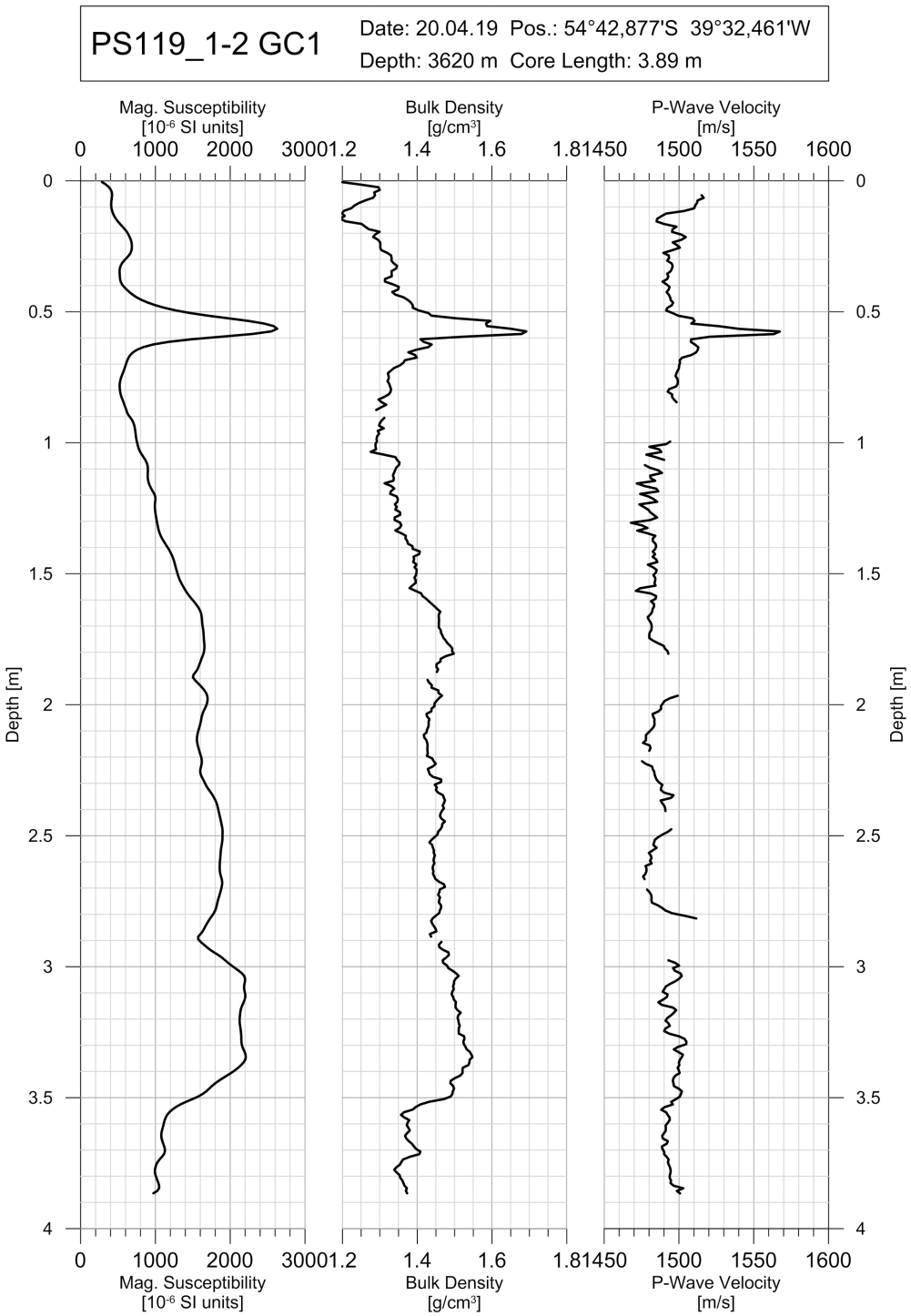

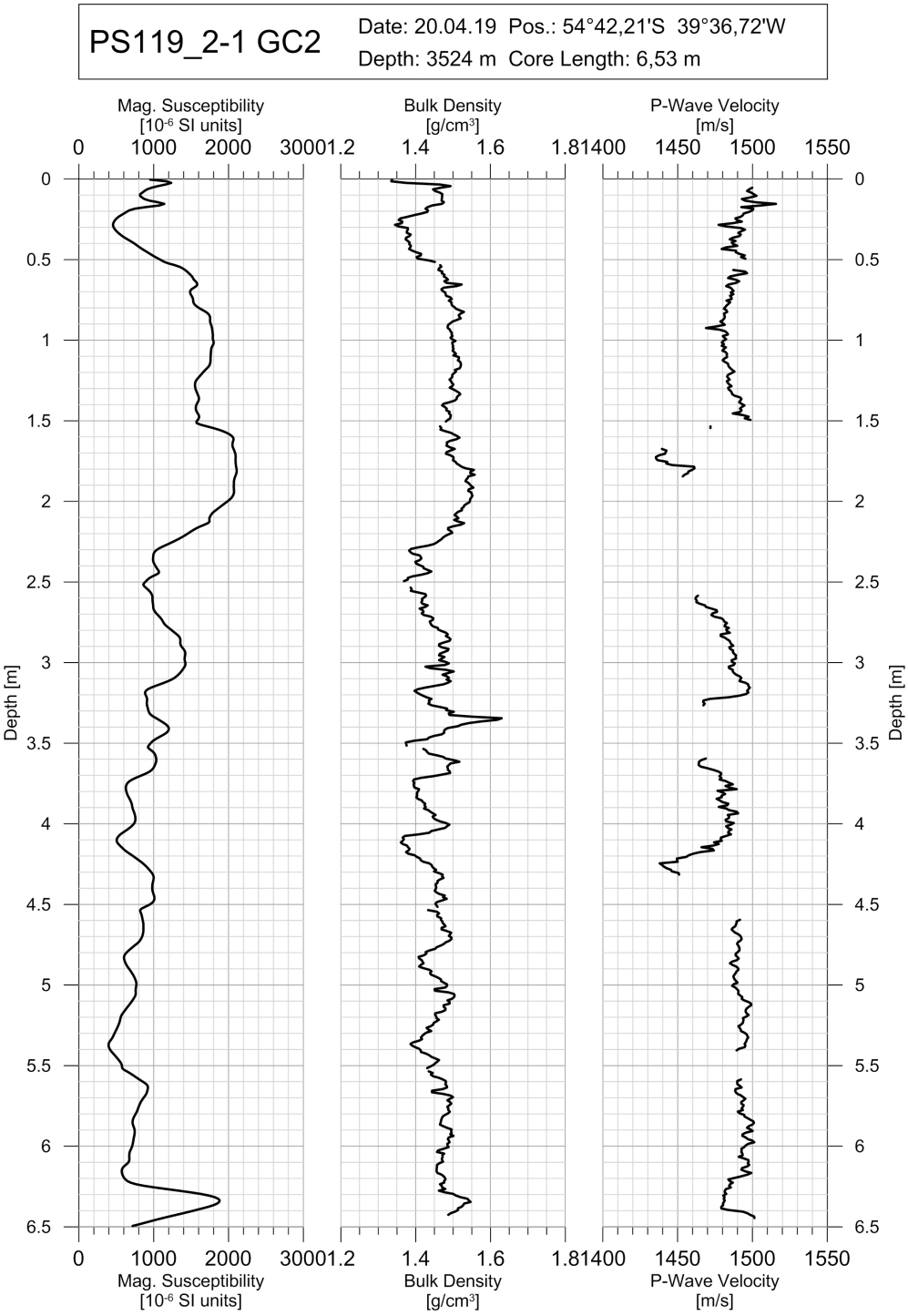
PS119_2-1 GC2
Date: 20.04.19 Pos.: 54°42,21'S 39°36,72'W
Depth: 3524 m Core Length: 6,53 m
Mag. Susceptibility
[10-6 SI units]
Bulk Density
[g/cm3]
P-Wave Velocity
[m/s]
Depth [m]
0 1000 2000 3000
1.2 1.4 1.6 1.8
1400 1450 1500 1550
0 0.5 1 1.5 2 2.5 3 3.5 4 4.5 5 5.5 6 6.5

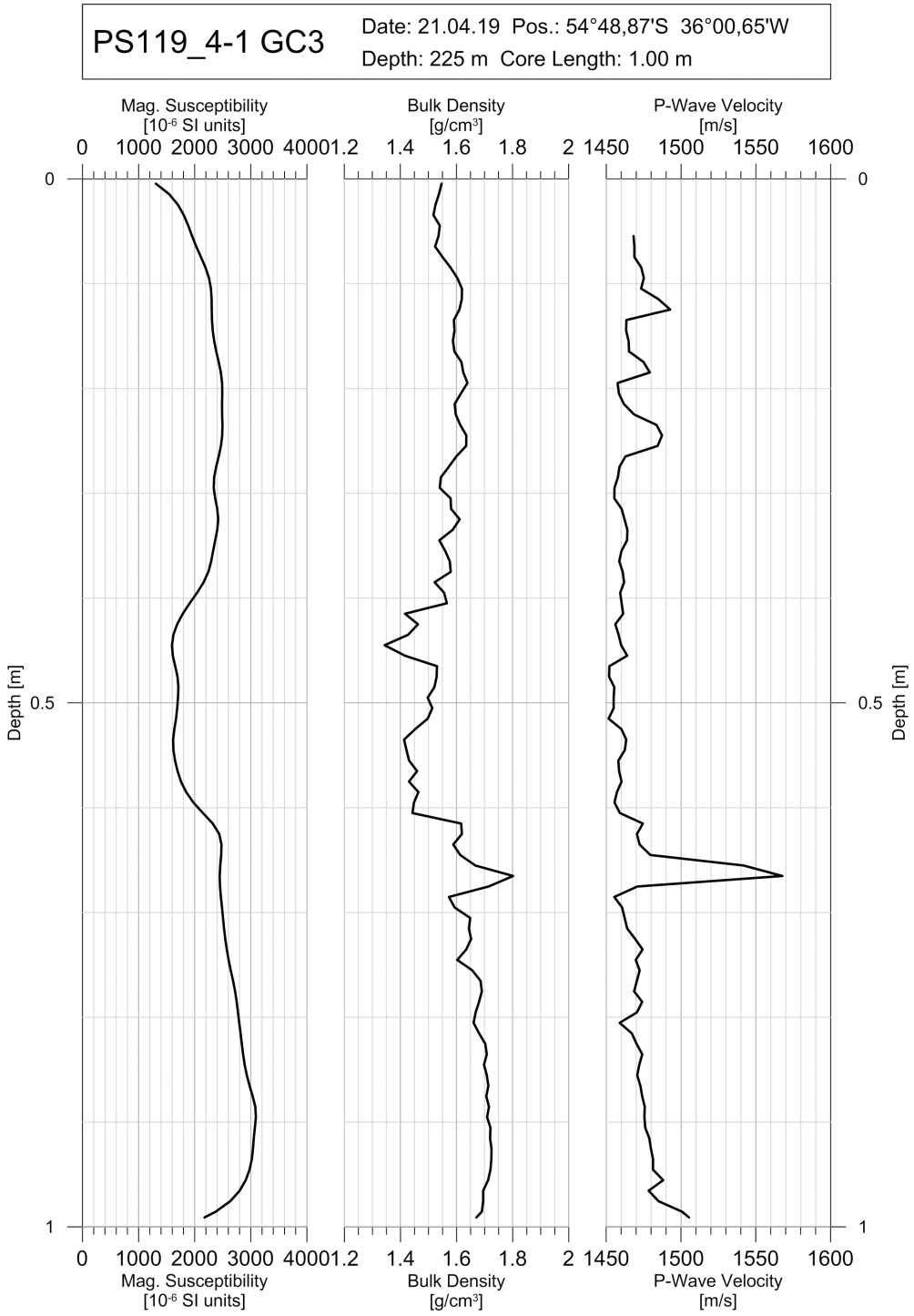
PS119_4-1 GC3
Date: 21.04.19 Pos.: 54°48,87'S 36°00,65'W
Depth: 225 m Core Length: 1.00 m
Mag. Susceptibility
[10-6 SI units]
0 1000 2000 3000 4000
Bulk Density
[g/cm3]
1.2 1.4 1.6 1.8 2
P-Wave Velocity
[m/s]
1450 1500 1550 1600
Depth [m]
0
0.5
1

PS119_4-2 GC4

Date: 21.04.19 Pos.: 54°48,87'S 36°00,64'W
Depth: 225 m Core Length: 4,87 m

top is missing

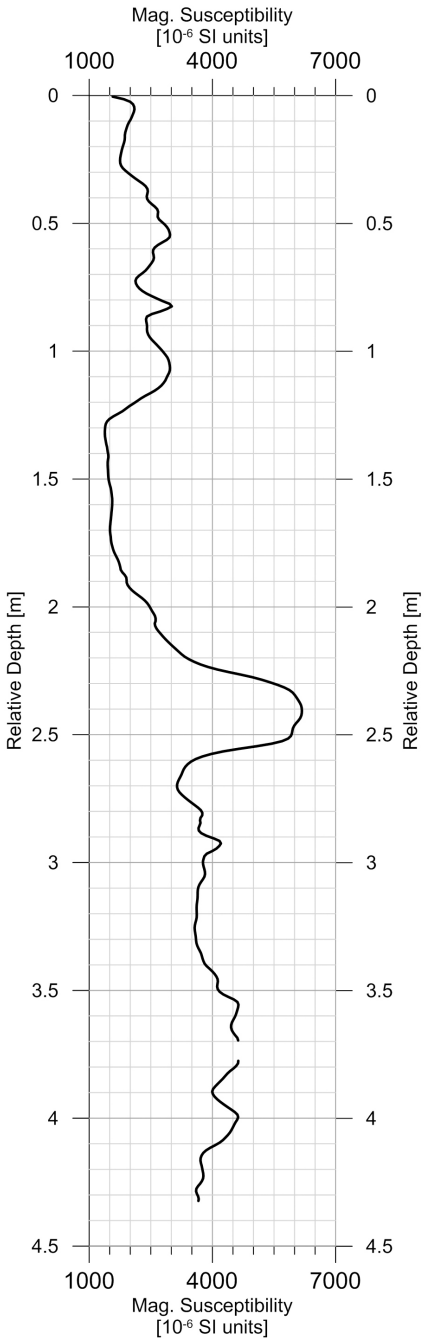

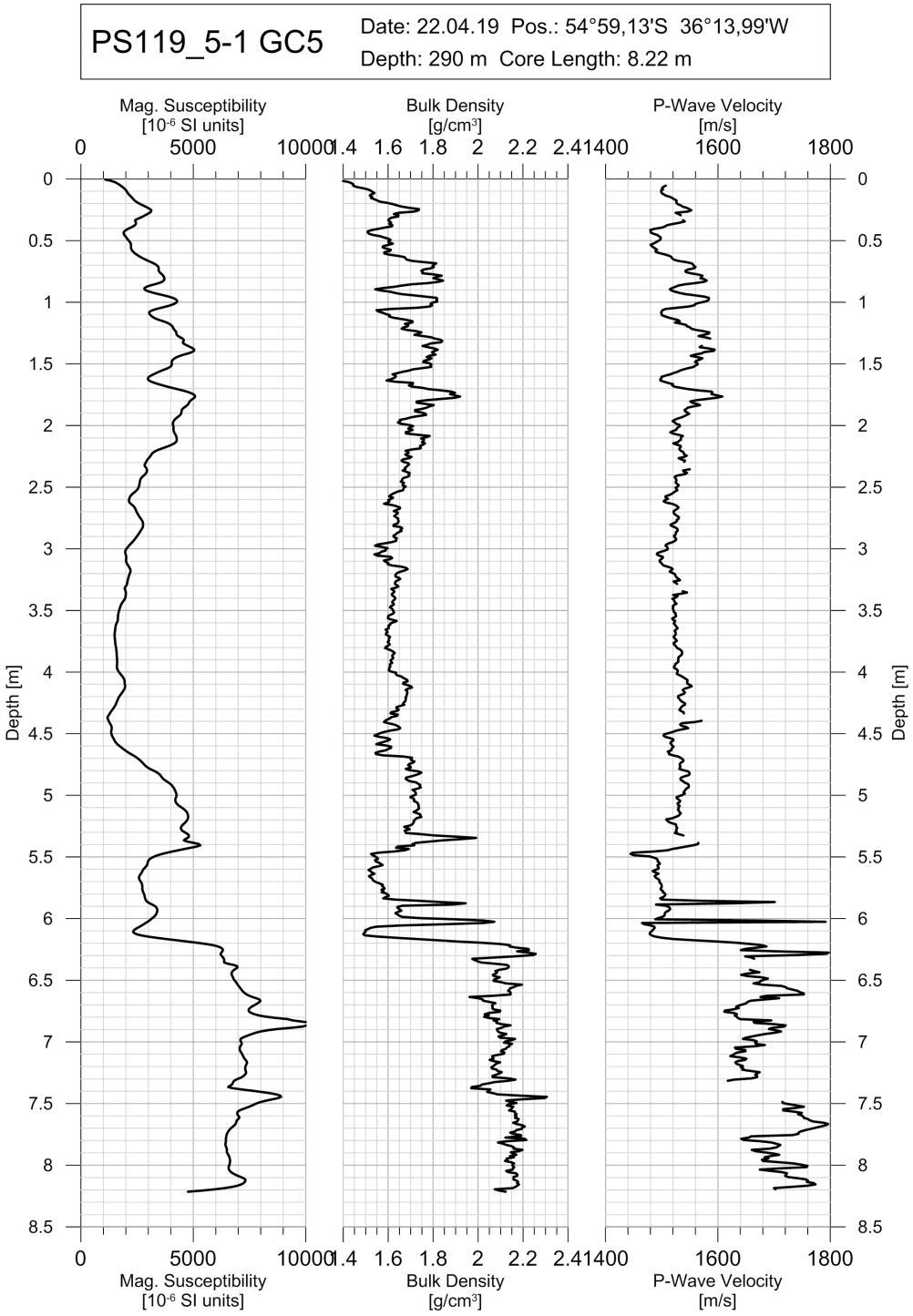
PS119_5-1 GC5
Date: 22.04.19 Pos.: 54°59,13'S 36°13,99'W
Depth: 290 m Core Length: 8.22 m
Mag. Susceptibility
[10-6 SI units]
Bulk Density
[g/cm3]
P-Wave Velocity
[m/s]
Depth [m]

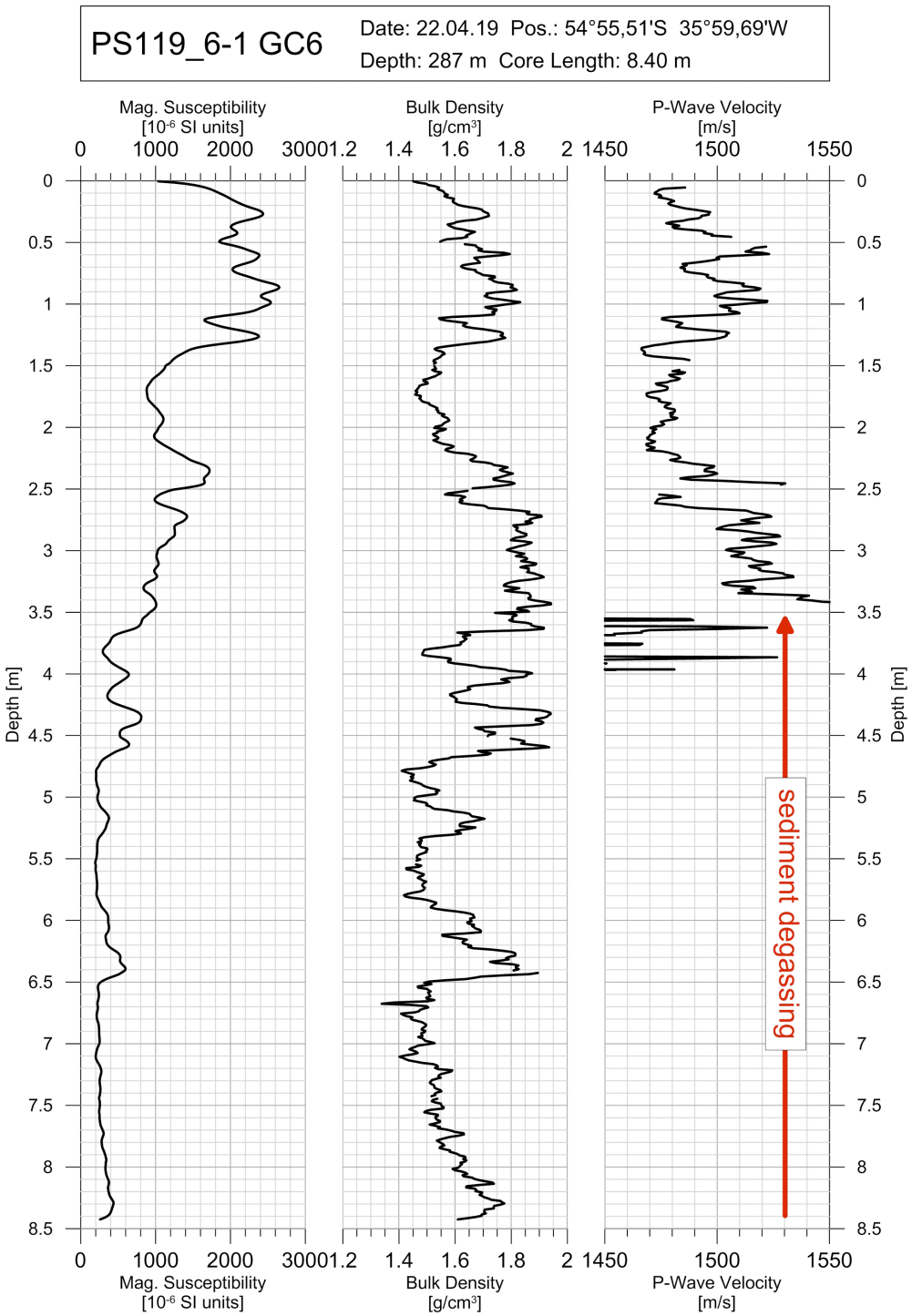
PS119_6-1 GC6
Date: 22.04.19 Pos.: 54°55,51'S 35°59,69'W
Depth: 287 m Core Length: 8.40 m
Mag. Susceptibility
[10-6 SI units]
Bulk Density
[g/cm3]
P-Wave Velocity
[m/s]
Depth [m]
sediment degassing

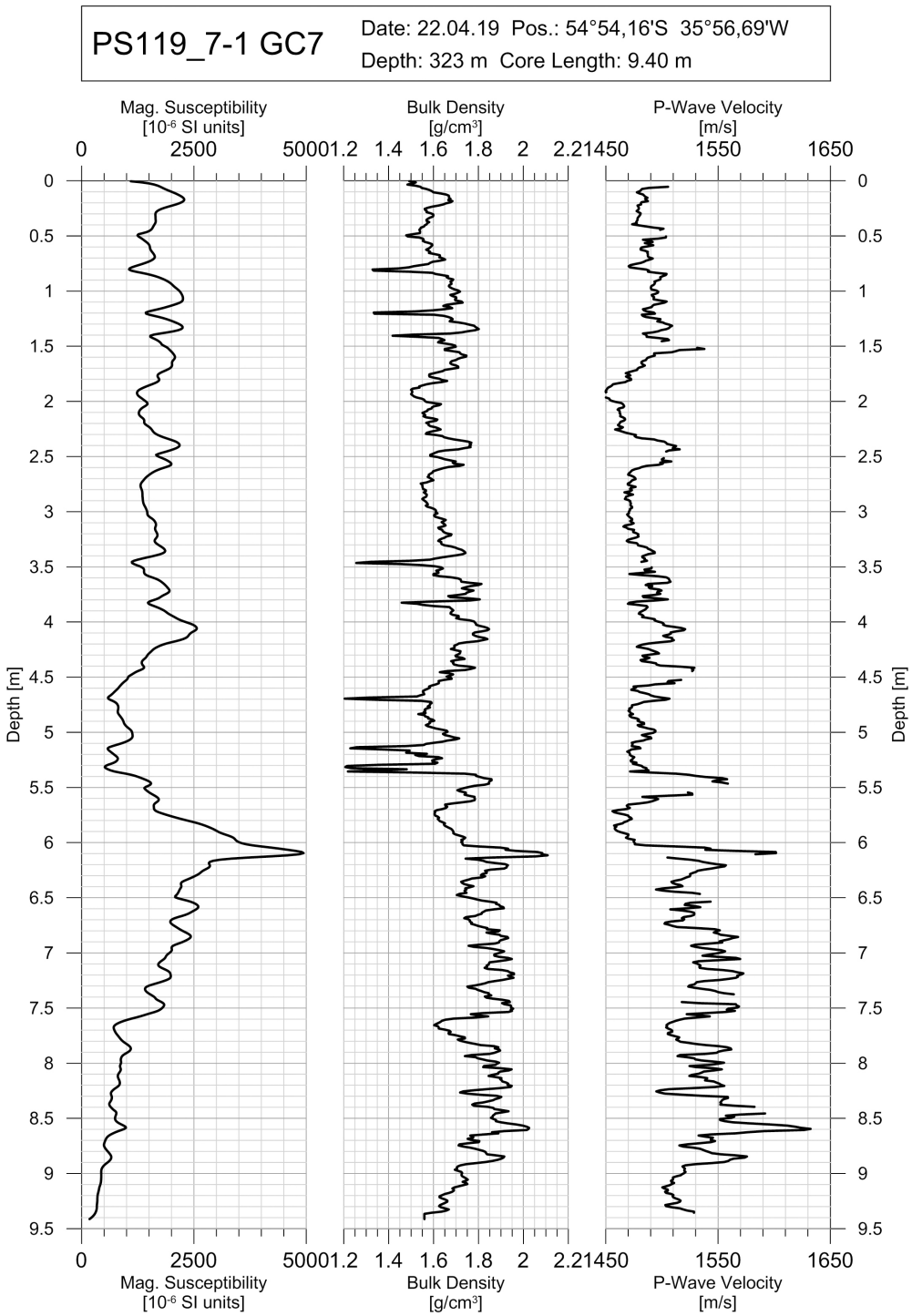
PS119_7-1 GC7
Date: 22.04.19 Pos.: 54°54,16'S 35°56,69'W
Depth: 323 m Core Length: 9.40 m
Mag. Susceptibility
[10-6 SI units]
Bulk Density
[g/cm3]
P-Wave Velocity
[m/s]
Depth [m]
0
2500
50001.2
1.4
1.6
1.8
2
2.21450
1550
1650
0.5
1
1.5
2.5
3
3.5
4
4.5
5
5.5
6
6.5
7
7.5
8
8.5
9
9.5

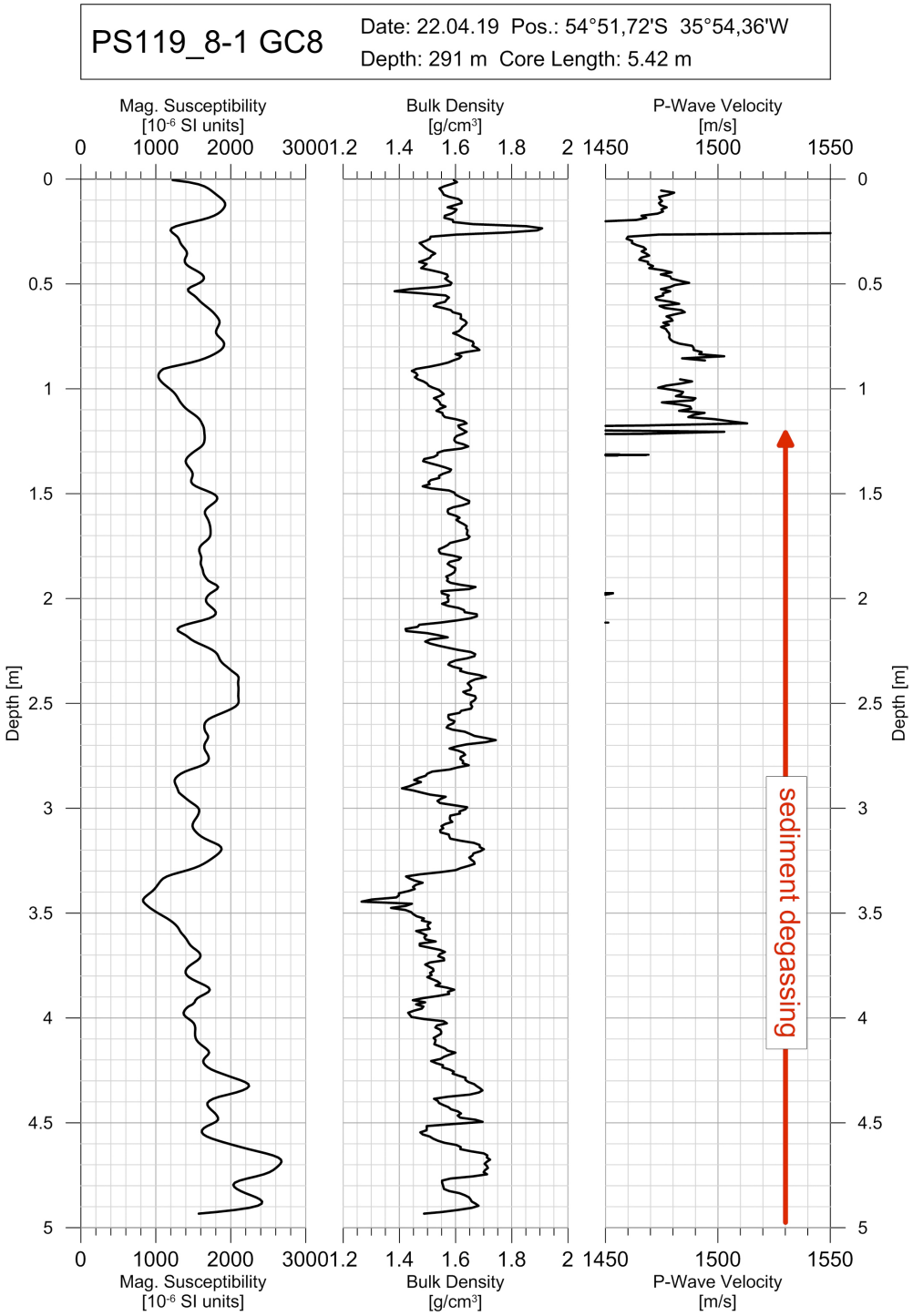
PS119_8-1 GC8
Date: 22.04.19 Pos.: 54°51,72'S 35°54,36'W
Depth: 291 m Core Length: 5.42 m
Mag. Susceptibility
[10-6 SI units]
Bulk Density
[g/cm3]
P-Wave Velocity
[m/s]
0
1000
2000
3000
1.2
1.4
1.6
1.8
2
1450
1500
1550
Depth [m]
0
0.5
1
1.5
2
2.5
3
3.5
4
4.5
5
sediment degassing

PS119_14-2 GC9 Date: 26.04.19 Pos.: 56°06,594'S 30°09,123'W Depth: 3034 m Core Length: 5,06 m

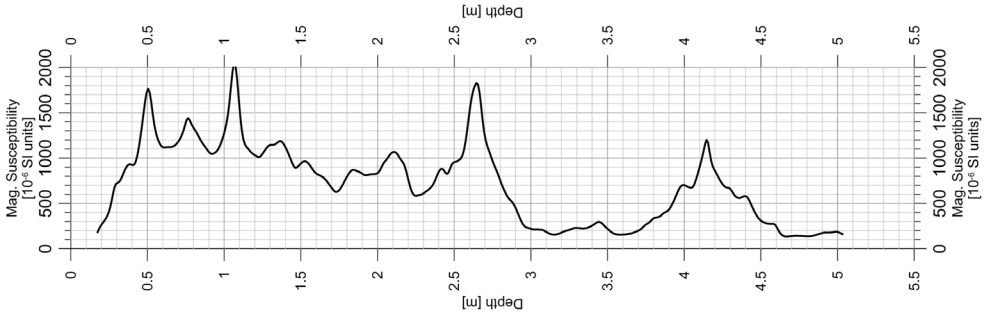

top is missing (ca. 17 cm)

PS119_15-1 GC10 Date: 26.04.19 Pos.: 56°06,598'S 30°09,129'W Depth: 3034 m Core Length: 5,11 m

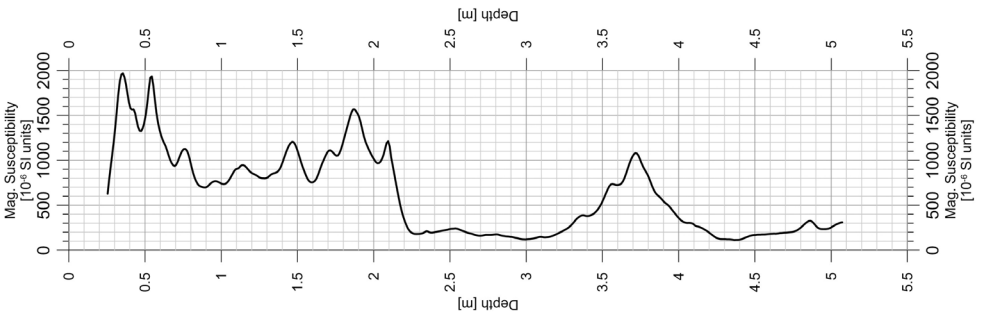

top is missing (ca. 25 cm)

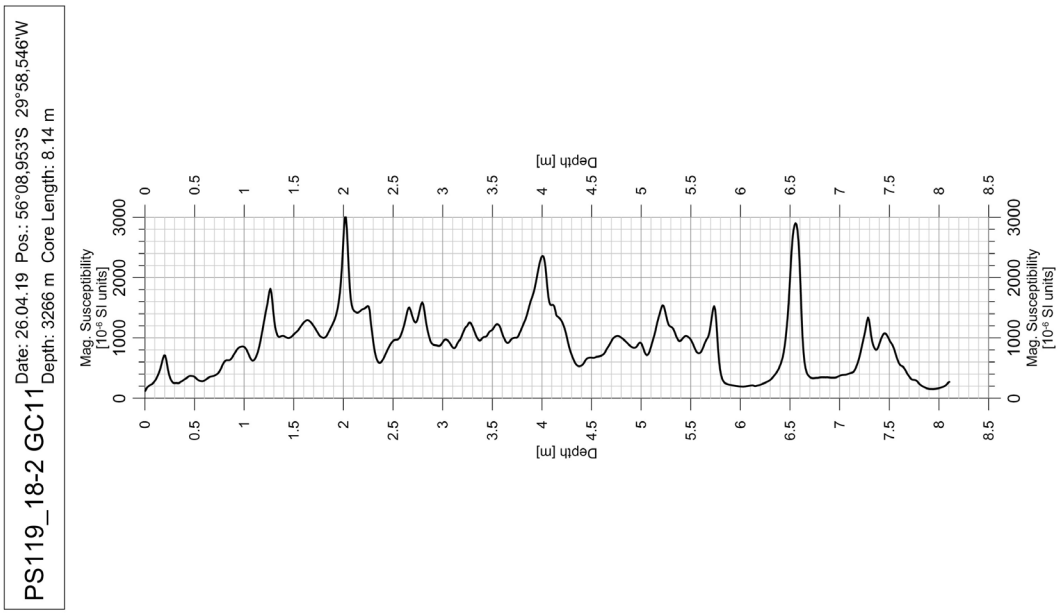
PS119_18-2 GC11
Date: 26.04.19 Pos.: 56°08,953'S 29°58,546'W
Depth: 3266 m Core Length: 8.14 m
Mag. Susceptibility
[10⁻⁶ SI units]
Depth [m]

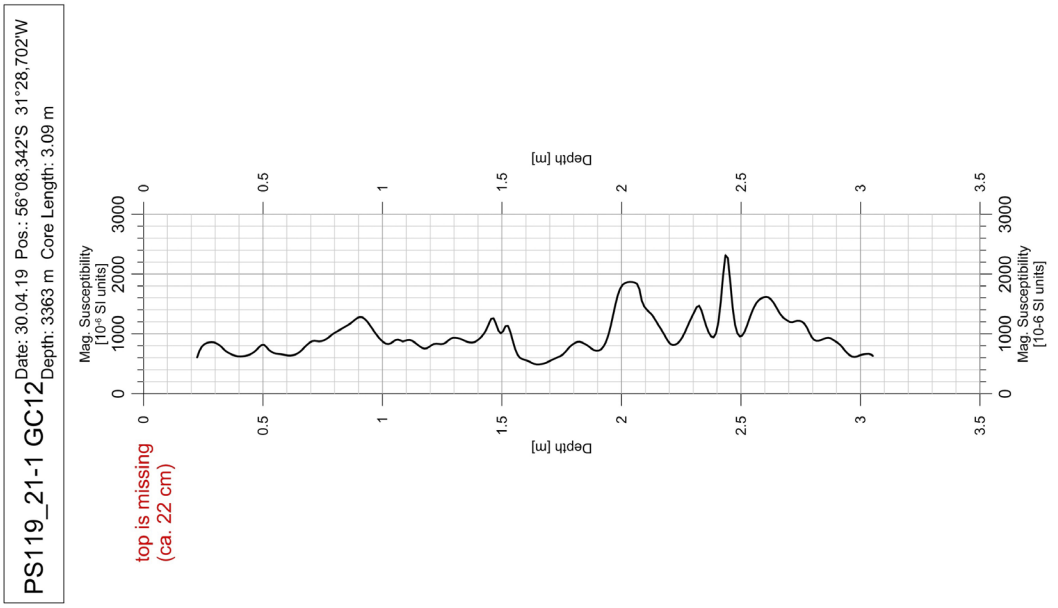
PS119_21-1 GC12
Date: 30.04.19 Pos.: 56°08,342'S 31°28,702'W
Depth: 3363 m Core Length: 3.09 m
top is missing
(ca. 22 cm)
Mag. Susceptibility
[10⁻⁶ SI units]
Depth [m]

PS119_22-1 GC13 Date: 30.04.19 Pos.: 56°09,292'S 31°29,045'W
Depth: 3342 m Core Length: 6.70 m

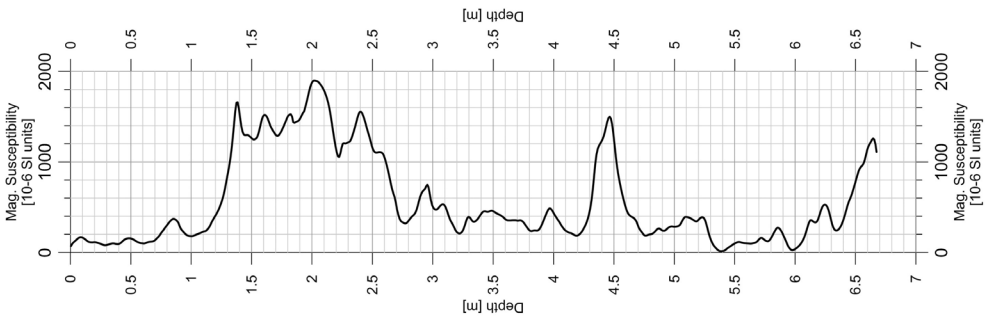

PS119_25-1 GC14 Date: 06.05.19 Pos.: 59°52,748'S 29°28,268'W
Depth: 2899 m Core Length: 2.31 m

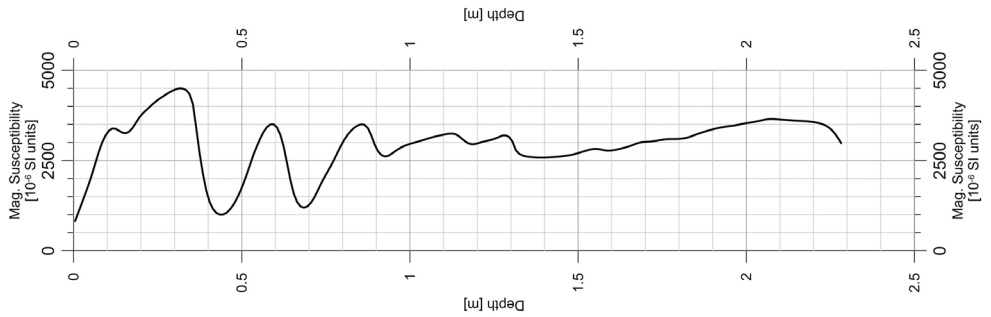

PS119_29-1 GC15 Date: 08.05.19 Pos.: 60°02,518'S 29°41,825'W
Depth: 2631 m Core Length: 4.50 m

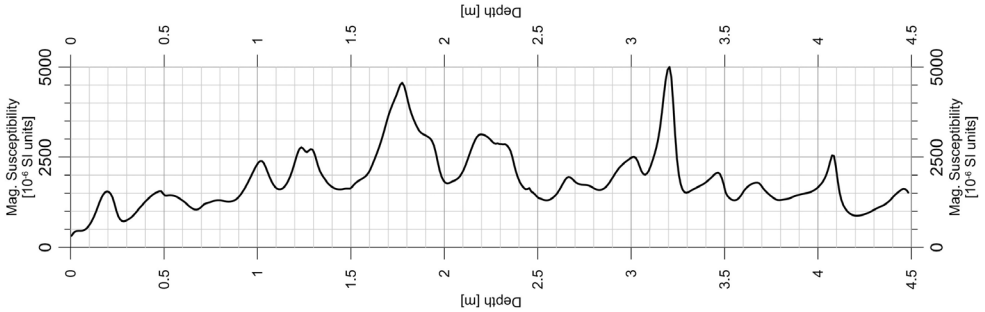

PS119_30-1 PC1 Date: 08.05.19 Pos.: 59°52,743'S 29°28,248'W
Depth: 2895 m Core Length: 11.73 m

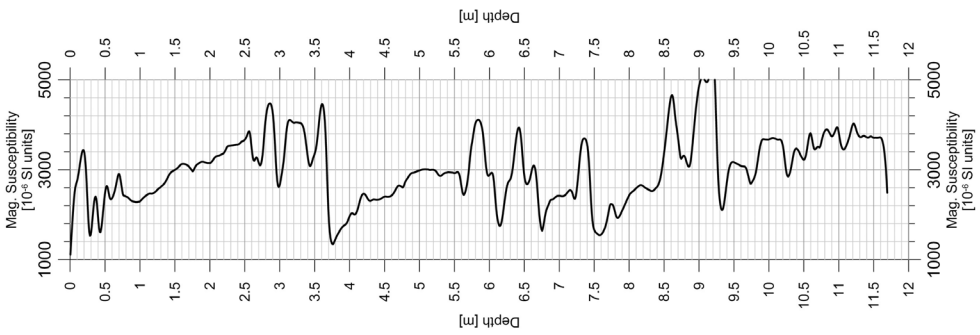

PS119_30-1 TC1 Date: 08.05.19 Pos.: 59°52,743'S 29°28,248'W Depth: 2895 m Core Length: 0.57 m

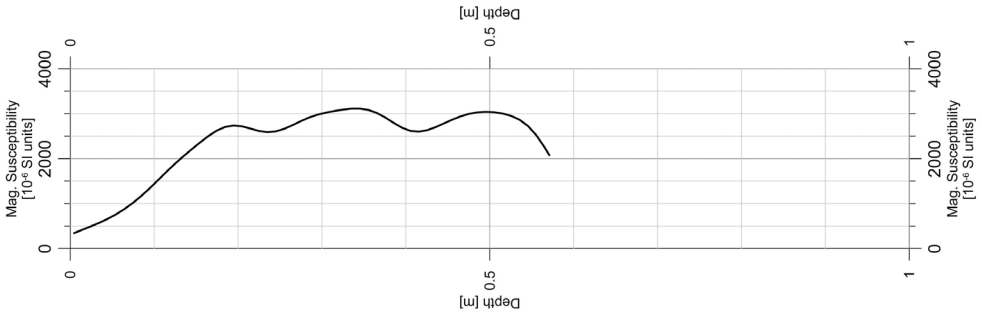

PS119_36-2 GC16 Date: 12.05.19 Pos.: 59°41,710'S 28°19,647'W Depth: 1619 m Core Length: 1.59 m

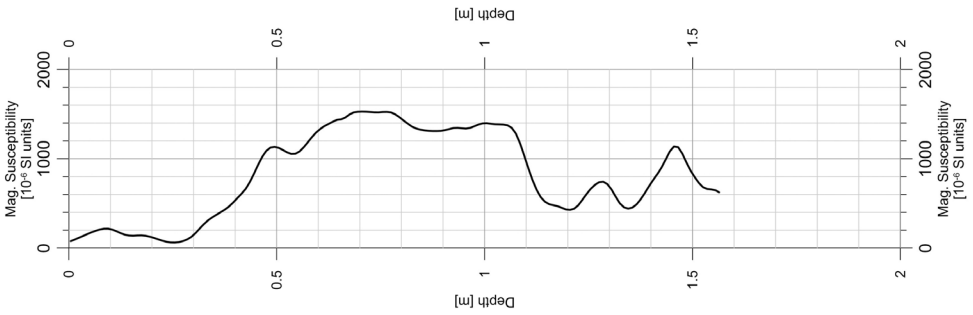

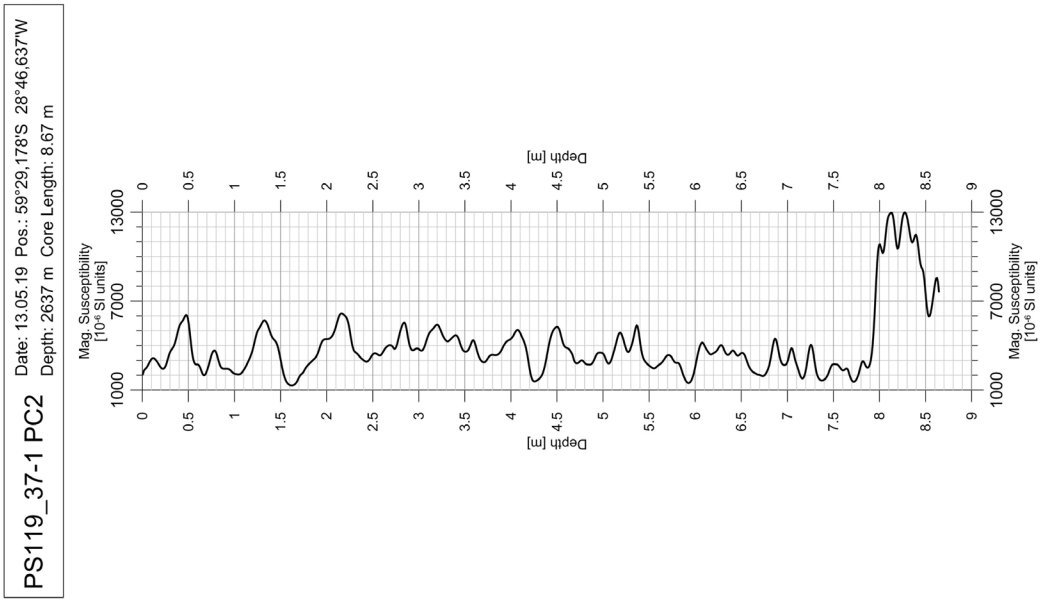
PS119_37-1 PC2
Date: 13.05.19 Pos.: 59°29,178'S 28°46,637'W
Depth: 2637 m Core Length: 8.67 m
Mag. Susceptibility [10⁻⁶ SI units]
1000
7000
13000
Depth [m]
0
0.5
1
1.5
2
2.5
3
3.5
4
4.5
5
5.5
6
6.5
7
7.5
8
8.5
9

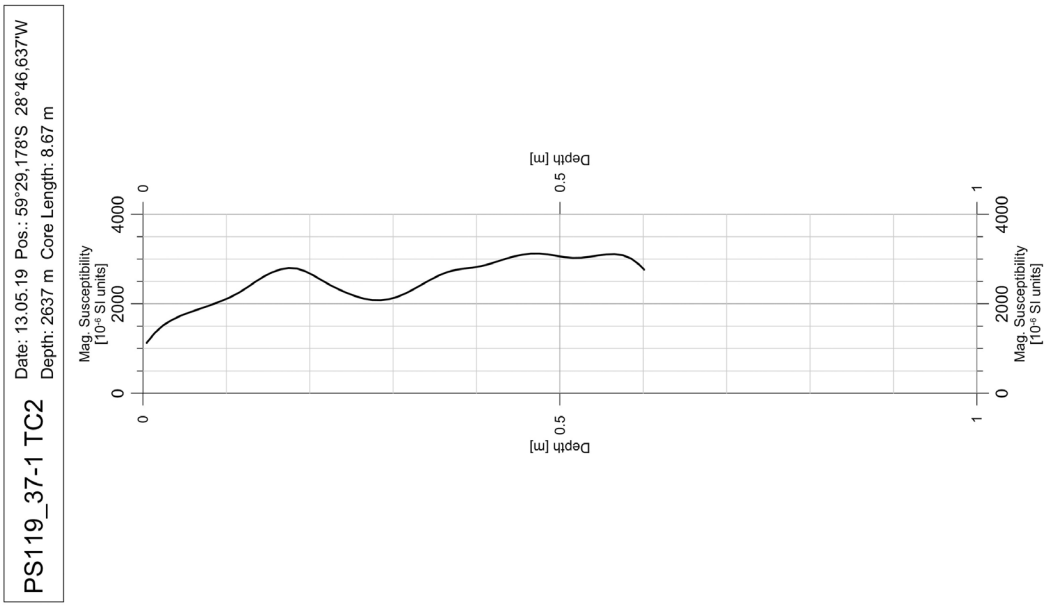
PS119_37-1 TC2
Date: 13.05.19 Pos.: 59°29,178'S 28°46,637'W
Depth: 2637 m Core Length: 8.67 m
Mag. Susceptibility [10⁻⁶ SI units]
0
2000
4000
Depth [m]
0
0.5
1

PS119_45-1 PC3 Date: 15.05.19 Pos.: 59°41,717'S 28°19,662'W Depth: 1610 m Core Length: 2.30 m

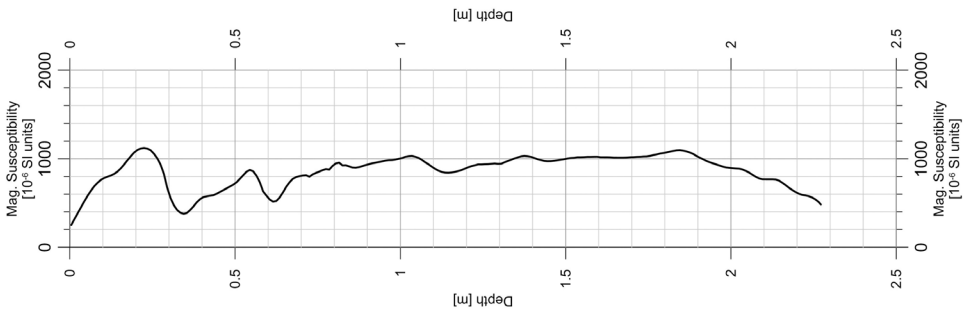

PS119_45-1 TC3 Date: 15.05.19 Pos.: 59°41,717'S 28°19,662'W Depth: 1610 m Core Length: 0.61 m

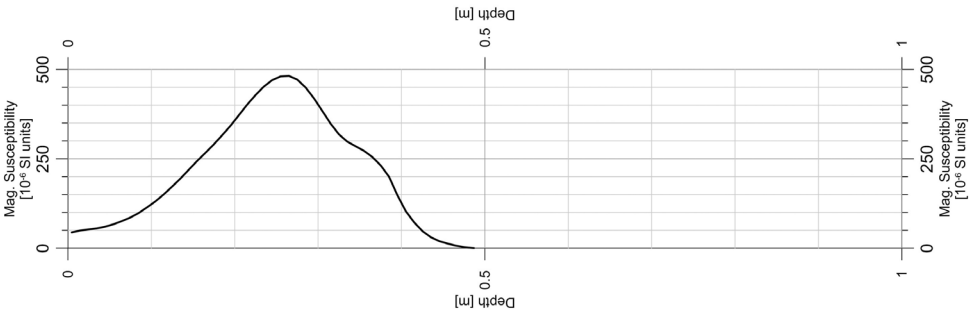

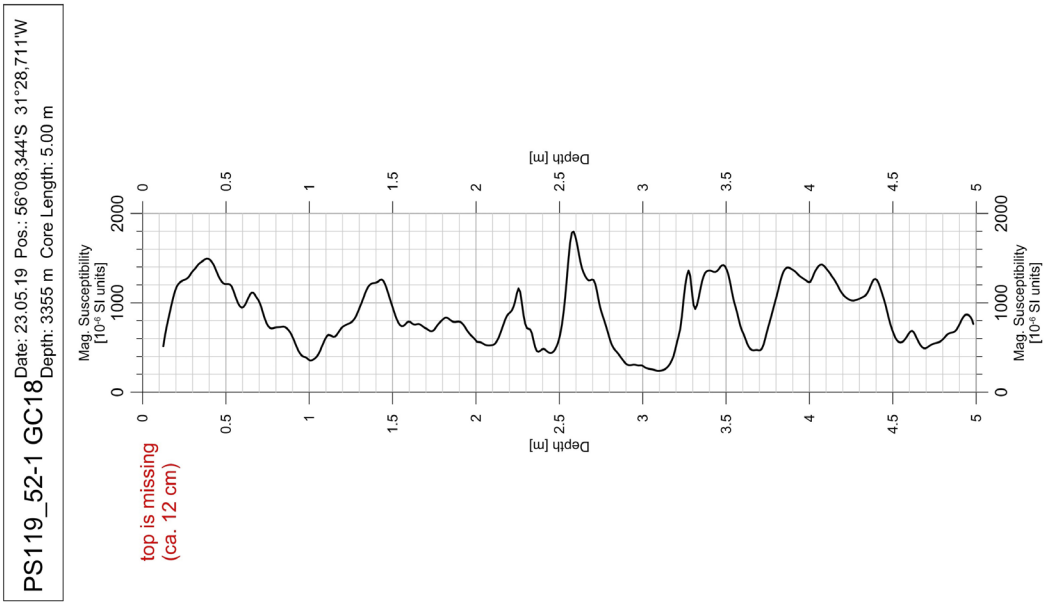
PS119_52-1 GC18
Date: 23.05.19 Pos.: 56°08,344'S 31°28,711'W
Depth: 3355 m Core Length: 5.00 m
top is missing
(ca. 12 cm)
Mag. Susceptibility
[10⁻⁶ SI units]
Depth [m]

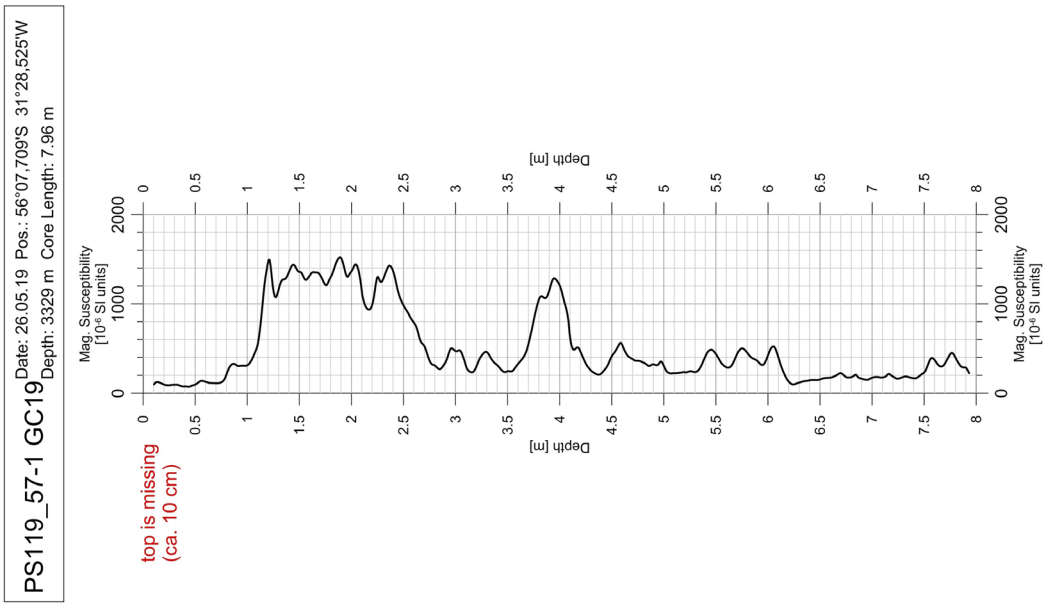
PS119_57-1 GC19
Date: 26.05.19 Pos.: 56°07,709'S 31°28,525'W
Depth: 3329 m Core Length: 7.96 m
top is missing
(ca. 10 cm)
Mag. Susceptibility
[10⁻⁶ SI units]
Depth [m]

PS119_58-1 GC20 Date: 26.05.19 Pos.: 54°55,916'S 36°00,892'W
Depth: 283 m Core Length: 8.65 m

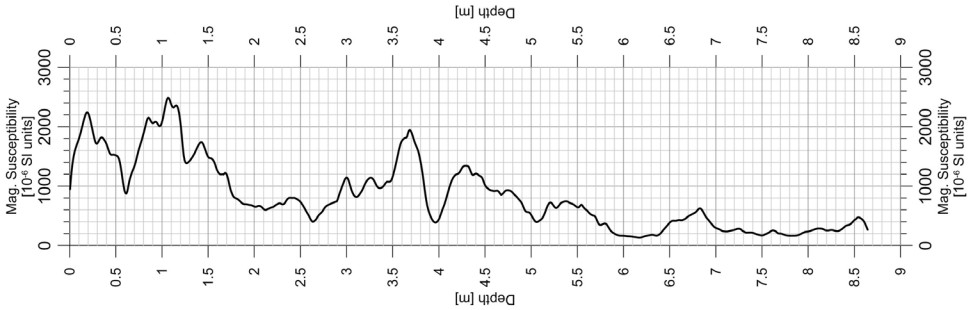

A.7 FAUNA SAMPLES

PS119	Dive	Event	Place	Area	Location	Sample	No of	Taxon	Use	Fixation	Recipient
	Quest	no				Id					
Station	MUC	no	core			PS119-	ind				
001-1	MUC-1		7	SW of SG		1		0-2 cm	microplastics	frozen	Julia (Katrin)
001-1	MUC-1		7	SW of SG		2		2-5 cm	microplastics	frozen	Julia (Katrin)
001-1	MUC-1		9	SW of SG		3		0-2 cm	biodiversity	ethanol	Katrin
001-1	MUC-1		9	SW of SG		4		2-5 cm	biodiversity	ethanol	Katrin
001-1	MUC-1		10	SW of SG		5		0-2 cm	biodiversity	ethanol	Katrin
001-1	MUC-1		10	SW of SG		6		2-5 cm	biodiversity	ethanol	Katrin
007-2	MUC-2		11	SW of SG		7		0-2 cm	microplastics	frozen	Julia (Katrin)
007-2	MUC-2		11	SW of SG		8		2-5 cm	microplastics	frozen	Julia (Katrin)
007-2	MUC-2		8	SW of SG		9		0-2 cm	biodiversity	ethanol	Katrin
007-2	MUC-2		8	SW of SG		10		2-5 cm	biodiversity	ethanol	Katrin
007-2	MUC-2		14	SW of SG		11		14-21 cm	biodiversity	ethanol	Katrin
007-2	MUC-2		2	SW of SG		12		0-2 cm	biodiversity	ethanol	Katrin
007-2	MUC-2		2	SW of SG		13		2-5 cm	biodiversity	ethanol	Katrin
013-1	Dive 444	1	net	E2_S	Schloss	14	1	Kiwa tyleri	biodiversity	ethanol	Katrin
013-1	Dive 444	1	net	E2_S	Schloss	15	15	Gigantopelta chessoia	respiratio	frozen	Katrin
013-1	Dive 444	1	net	E2_S	Schloss	16	15	Gigantopelta chessoia	respiratio	frozen	Katrin
013-1	Dive 444	1	net	E2_S	Schloss	17	20	Lepetodrilus concentricus	biodiversity	ethanol	Katrin
013-1	Dive 444	1	net	E2_S	Schloss	18	30	Lepetodrilus concentricus	biodiversity	ethanol	Katrin

PS119	Dive	Event	Place	Area	Location	Sample	No of	Taxon	Use	Fixation	Recipient
	Quest	no				Id					
Station	MUC	no	core			PS119-	ind				
013-1	Dive 444	1	net	E2_S	Schloss	19	1	Gigantopelta chessoia	proteomics	bag	Katrin
013-1	Dive 444	1	net	E2_S	Schloss	20	1	Gigantopelta chessoia	proteomics	bag	Katrin
013-1	Dive 444	1	net	E2_S	Schloss	21	3	Gigantopelta chessoia	biodiversity	ethanol	Katrin
013-1	Dive 444	1	net	E2_S	Schloss	22	15	Lepetodrilus concentricus	biodiversity	ethanol	Katrin
014-2	MUC-3		7	E of E2		23		0-2 cm	microplastics	frozen	Julia (Katrin)
014-2	MUC-3		7	E of E2		24		2-5 cm	microplastics	frozen	Julia (Katrin)
014-2	MUC-3		8	E of E2		25		0-2 cm	biodiversity	ethanol	Katrin
014-2	MUC-3		8	E of E2		26		2-5 cm	biodiversity	ethanol	Katrin
014-2	MUC-3		5	E of E2		27		0-2 cm	biodiversity	ethanol	Katrin
014-2	MUC-3		5	E of E2		28		2-5 cm	biodiversity	ethanol	Katrin
015-2	MUC-4		12	E of E2		29		0-2 cm	microplastics	frozen	Julia (Katrin)
015-2	MUC-4		12	E of E2		30		2-5 cm	microplastics	frozen	Julia (Katrin)
015-2	MUC-4		5	E of E2		31		0-2 cm	biodiversity	ethanol	Katrin
015-2	MUC-4		5	E of E2		32		2-5 cm	biodiversity	ethanol	Katrin
015-2	MUC-4		8	E of E2		33		0-2 cm	biodiversity	ethanol	Katrin
015-2	MUC-4		8	E of E2		34		2-5 cm	biodiversity	ethanol	Katrin
015-2	MUC-4		3	E of E2		35		0-2 cm	biodiversity	ethanol	Katrin
015-2	MUC-4		3	E of E2		36		2-5 cm	biodiversity	ethanol	Katrin
015-2	MUC-4		9	E of E2		37		0-2 cm	biodiversity	ethanol	Katrin

PS119	Dive	Event	Place	Area	Location	Sample	No of	Taxon	Use	Fixation	Recipient
	Quest	no				Id					
Station	MUC	no	core			PS119-	ind				
015-2	MUC-4		9	E of E2		38		2-5 cm	biodiversity	ethanol	Katrin
018-1	MUC-5		1	E of E2		39		0-2 cm	microplastics	frozen	Julia (Katrin)
018-1	MUC-5		1	E of E2		40		2-5 cm	microplastics	frozen	Julia (Katrin)
018-1	MUC-5		3	E of E2		41		0-2 cm	biodiversity	ethanol	Katrin
018-1	MUC-5		3	E of E2		42		2-5 cm	biodiversity	ethanol	Katrin
018-1	MUC-5		7	E of E2		43		0-2 cm	biodiversity	ethanol	Katrin
018-1	MUC-5		7	E of E2		44		2-5 cm	biodiversity	ethanol	Katrin
020-1	Dive 446	6	net	E2_S	non-Confusion	45	1	Paulasterias tyleri	Genetics	RNAlater	Cris Little
020-1	Dive 446	1	net	E2_S	Off vent	46	1	Cladorhiza sp.	Genetics	RNAlater	Cris Little
020-1	Dive 446	1	net	E2_S	non-Liberachi	47	1	Kiwa tyleri	biodiversity	ethanol	Katrin
020-1	Dive 446	1	net	E2_S	non-Liberachi	48	4	Gigantopelta chessoia	respiratio	frozen	Julia (Katrin)
020-1	Dive 446	1	net	E2_S	non-Liberachi	49	1	Kiwa tyleri	biodiversity	ethanol	Katrin
020-1	Dive 446	1	net	E2_S	non-Liberachi	50	1	Sericosura bamberi	biodiversity	ethanol	Katrin
020-1	Dive 446	1	net	E2_S	non-Liberachi	51	1	Sericosura cooki	biodiversity	ethanol	Katrin
020-1	Dive 446	1	net	E2_S	non-Liberachi	52	5	Lepetodrilus concentricus	biodiversity	ethanol	Katrin
020-1	Dive 446	1	net	E2_S	non-Liberachi	53	9	Provanna cooki	biodiversity	ethanol	Katrin
020-1	Dive 446	1	net	E2_S	non-Liberachi	54	1	hydrozoan	biodiversity	ethanol	Katrin

PS119	Dive	Event	Place	Area	Location	Sample	No of	Taxon	Use	Fixation	Recipient
	Quest	no				Id					
Station	MUC	no	core			PS119-	ind				
020-1	Dive 446	1	net	E2_S	non-Liberachi	55	2	Ostracoda	biodiversity	ethanol	Katrin
020-1	Dive 446	1	net	E2_S	non-Liberachi	56	1	Kiwa tyleri	biodiversity	ethanol	Katrin
020-1	Dive 446	1	net	E2_S	non-Liberachi	57	1	Kiwa tyleri	biodiversity	ethanol	Katrin
022-1	MUC-6		10	W of E2		58		0-2 cm	microplastics	frozen	Julia (Katrin)
022-1	MUC-6		10	W of E2		59		2-5 cm	microplastics	frozen	Julia (Katrin)
022-1	MUC-6		7	W of E2		60		0-2 cm	biodiversity	ethanol	Katrin
022-1	MUC-6		7	W of E2		61		2-5 cm	biodiversity	ethanol	Katrin
022-1	MUC-6		10	W of E2		62		33-36 cm	biodiversity	ethanol	Katrin
022-1	MUC-6		12	W of E2		63		0-2 cm	biodiversity	ethanol	Katrin
022-1	MUC-6		12	W of E2		64		2-5 cm	biodiversity	ethanol	Katrin
022-1	MUC-6		9	W of E2		65		0-4 cm	biodiversity	ethanol	Katrin
022-1	MUC-6		6	W of E2		66		5 cm	biodiversity	ethanol	Katrin
025-2	MUC-7		1	E of E9		67		0-2 cm	microplastics	frozen	Julia (Katrin)
025-2	MUC-7		1	E of E9		68		2-5 cm	microplastics	frozen	Julia (Katrin)
025-2	MUC-7		2	E of E9		69		0-2 cm	microplastics	frozen	Julia (Katrin)
025-2	MUC-7		2	E of E9		70		2-5 cm	microplastics	frozen	Julia (Katrin)
025-2	MUC-7		4	E of E9		71		0-2 cm	biodiversity	ethanol	Katrin
025-2	MUC-7		4	E of E9		70		2-5 cm	biodiversity	ethanol	Katrin

PS119	Dive	Event	Place	Area	Location	Sample	No of	Taxon	Use	Fixation	Recipient
	Quest	no				Id					
Station	MUC	no	core			PS119-	ind				
025-2	MUC-7		9	E of E9		71		0-2 cm	biodiversity	ethanol	Katrin
025-2	MUC-7		9	E of E9		74		2-5 cm	biodiversity	ethanol	Katrin
028-1	Dive 447	5	claw-l-K	Kemp	Great Wall	75	-	rubble	biodiversity	ethanol	Katrin
028-1	Dive 447	6	claw-l-K	Kemp	Great Wall	76	50	Lepetodrilus concentricus	biodiversity	ethanol	Katrin
028-1	Dive 447	7	claw-l	Kemp	Great Wall	77	2	Lepetodrilus concentricus	biodiversity	ethanol	Katrin
028-1	Dive 447	11	claw-H	Kemp	Toxic castle	78	29	Lepetodrilus concentricus	biodiversity	ethanol	Katrin
028-1	Dive 447	25	net-bl&w	Kemp	Live clams 1	79	1	Cocculinid sp	biodiversity	ethanol	Katrin
028-1	Dive 447	25	net-bl&w	Kemp	Live clams 1	80	7	Lysianassid sp	biodiversity	ethanol	Katrin
028-1	Dive 447	25	net-bl&w	Kemp	Live clams 1	81	16	live clams	respiration	frozen	Julia (Katrin)
028-1	Dive 447	25	net-bl&w	Kemp	Live clams 1	82	6	broken clams	Symbiosis		Benedikt
028-1	Dive 447	25	net-bl&w	Kemp	Live clams 1	83	ca. 50	cf. Sclerolinum	Genetics	RNAlater	Cris Little
028-1	Dive 447	25	net-bl&w	Kemp	Live clams 1	84	-	rubble	biodiversity	ethanol	
028-1	Dive 447	25	net-bl&w	Kemp	Live clams 1	85	2	cf. Sclerolinum	Genetics	RNAlater	Cris Little
029-2	MUC-8		4	E of E9		86		0-2 cm	microplastics	frozen	Julia (Katrin)
029-2	MUC-8		4	E of E9		87		2-5 cm	microplastics	frozen	Julia (Katrin)
029-2	MUC-8		5	E of E9		88		0-2 cm	biodiversity	ethanol	Katrin
029-2	MUC-8		5	E of E9		89		2-5 cm	biodiversity	ethanol	Katrin
029-2	MUC-8		6	E of E9		90		0-2 cm	biodiversity	ethanol	Katrin
029-2	MUC-8		6	E of E9		91		2-5 cm	biodiversity	ethanol	Katrin
033-1	Dive 448	3	net red	Kemp	Live clams 2	92	-	rubble	biodiversity	ethanol	Katrin
033-1	Dive 448	3	net red	Kemp	Live clams 2	93	-	spp from rubble	biodiversity	ethanol	Katrin

PS119	Dive	Event	Place	Area	Location	Sample	No of	Taxon	Use	Fixation	Recipient
	Quest	no				Id					
Station	MUC	no	core			PS119-	ind				
033-1	Dive 448	3	net red	Kemp	Live clams 2	94	-	rubble	biodiversity	ethanol	Katrin
033-1	Dive 448	3	net red	Kemp	Live clams 2	95	-	bacterial mat	biodiversity	ethanol	Katrin
033-1	Dive 448	3	net red	Kemp	Live clams 2	96	15	Laubiericoncha puertodeseadoi	respiration	frozen	Julia (Katrin)
033-1	Dive 448	3	net red	Kemp	Live clams 2	97	35	Laubiericoncha puertodeseadoi	respiration	frozen	Julia (Katrin)
033-1	Dive 448	3	net red	Kemp	Live clams 2	98	ca. 100	cf. Sclerolinum	Genetics	RNAlater	Cris Little
036-1	MUC-9		3	Kemp	centre	99		0-2 cm	microplastics	frozen	Julia (Katrin)
036-1	MUC-9		3	Kemp	centre	100		2-5 cm	microplastics	frozen	Julia (Katrin)
036-1	MUC-9		12	Kemp	centre	101		0-2 cm	microplastics	frozen	Julia (Katrin)
036-1	MUC-9		12	Kemp	centre	102		2-5 cm	microplastics	frozen	Julia (Katrin)
037-2	MUC-10		1	E8		103		0-2 cm	microplastics	frozen	Julia (Katrin)
037-2	MUC-10		1	E8		104		2-5 cm	microplastics	frozen	Julia (Katrin)
037-2	MUC-10		5	E8		105		0-2 cm	biodiversity	ethanol	Katrin
037-2	MUC-10		5	E8		106		2-5 cm	biodiversity	ethanol	Katrin
037-2	MUC-10		8	E8		107		0-2 cm	biodiversity	ethanol	Katrin
037-2	MUC-10		8	E8		108		2-5 cm	biodiversity	ethanol	Katrin
037-2	MUC-10		2	E8		109		0-2 cm	microplastics	frozen	Julia (Katrin)
037-2	MUC-10		2	E8		110		2-5 cm	microplastics	frozen	Julia (Katrin)

PS119	Dive	Event	Place	Area	Location	Sample	No of	Taxon	Use	Fixation	Recipient
	Quest	no				Id					
Station	MUC	no	core			PS119-	ind				
037-2	MUC-10		7	E8		111		0-2 cm	biodiversity	ethanol	Katrin
020-1	Dive 446	1	net	E2_S	non-Liberachi	112		rubble E2_S	biodiversity	ethanol	Katrin
013-1	Dive 444	1	net	E2_S	Schloss	113		Gigantopelta chessoia	biodiversity	ethanol	Katrin
013-1	Dive 444	1	net	E2_S	Schloss	114		Gigantopelta chessoia	biodiversity	ethanol	Katrin
033-1	Dive 448	3	net red	Kemp	Live clams 2	115	ca 20	Laubiericoncha puertodeseadoi	symbiosis		Benedikt
047-1	Dive 450	1	net	E2_S	Schloss	116	5	Kiwa tyleri	biodiversity	ethanol	Katrin
048-1	MUC-11		1	E of E2		117		0-4 cm	microplastics	frozen	Julia (Katrin)
048-1	MUC-11		9	E of E2		118		0-3 cm	microplastics	frozen	Julia (Katrin)
052-2	MUC-12		7	WOW		119		0-2 cm	microplastics	frozen	Julia (Katrin)
052-2	MUC-12		7	WOW		120		2-5 cm	microplastics	frozen	Julia (Katrin)
052-2	MUC-12		9	WOW		121		0-2 cm	biodiversity	ethanol	Katrin
052-2	MUC-12		9	WOW		122		2-5 cm	biodiversity	ethanol	Katrin
052-2	MUC-12		10	WOW		123		0-2 cm	biodiversity	ethanol	Katrin
052-2	MUC-12		10	WOW		124		2-5 cm	biodiversity	ethanol	Katrin
052-2	MUC-12		11	WOW		125		0-2 cm	microplastics	frozen	Julia (Katrin)
052-2	MUC-12		11	WOW		126		2-5 cm	microplastics	frozen	Julia (Katrin)
053-1	MUC-13		3	WOW		127		0-2 cm	microplastics	frozen	Julia (Katrin)

PS119	Dive	Event	Place	Area	Location	Sample	No of	Taxon	Use	Fixation	Recipient
	Quest	no				Id					
Station	MUC	no	core			PS119-	ind				
053-1	MUC-13		3	WOW		128		2-5 cm	microplastics	frozen	Julia (Katrin)
053-1	MUC-13		5	WOW		129		0-2 cm	microplastics	frozen	Julia (Katrin)
053-1	MUC-13		5	WOW		130		2-5 cm	microplastics	frozen	Julia (Katrin)

Die **Berichte zur Polar- und Meeresforschung** (ISSN 1866-3192) werden beginnend mit dem Band 569 (2008) als Open-Access-Publikation herausgegeben. Ein Verzeichnis aller Bände einschließlich der Druckausgaben (ISSN 1618-3193, Band 377-568, von 2000 bis 2008) sowie der früheren **Berichte zur Polarforschung** (ISSN 0176-5027, Band 1-376, von 1981 bis 2000) befindet sich im electronic Publication Information Center **(ePIC)** des Alfred-Wegener-Instituts, Helmholtz-Zentrum für Polar- und Meeresforschung (AWI); see https://epic.awi.de. Durch Auswahl “Reports on Polar- and Marine Research“ (via “browse”/”type”) wird eine Liste der Publikationen, sortiert nach Bandnummer, innerhalb der absteigenden chronologischen Reihenfolge der Jahrgänge mit Verweis auf das jeweilige pdf-Symbol zum Herunterladen angezeigt.

The **Reports on Polar and Marine Research** (ISSN 1866-3192) are available as open access publications since 2008. A table of all volumes including the printed issues (ISSN 1618-3193, Vol. 377-568, from 2000 until 2008), as well as the earlier **Reports on Polar Research** (ISSN 0176-5027, Vol. 1-376, from 1981 until 2000) is provided by the electronic Publication Information Center **(ePIC)** of the Alfred Wegener Institute, Helmholtz Centre for Polar and Marine Research (AWI); see URL https://epic.awi.de. To generate a list of all Reports, use the URL http://epic.awi.de and select “browse”/ ”type” to browse ”Reports on Polar and Marine Research”. A chronological list in declining order will be presented, and pdf-icons displayed for downloading.

Zuletzt erschienene Ausgaben:

Recently published issues:

736 (2019) The Expedition PS119 of the Research Vessel POLARSTERN to the Eastern Scotia Sea in 2019, edited by Gerhard Bohrmann

735 (2019) The Expedition PS118 of the Research Vessel POLARSTERN to the Weddell Sea in 2019, edited by Boris Dorschel

734 (2019) Russian-German Cooperation: Expeditions to Siberia in 2018. Edited by Stefan Kruse, Dmitry Bolshiyanov, Mikhail Grigoriev, Anne Morgenstern, Luidmila Pestryakova, Leonid Tsibizov, Annegret Udke

733 (2019) Expeditions to Antarctica: ANT-Land 2018/19 Neumayer Station III, Kohnen Station, Flight Operations and Field Campaigns, edited by Tanja Fromm, Constance Oberdieck, Tim Heitland, Peter Köhler

732 (2019) The Expedition PS117 of the Research Vessel POLARSTERN to the Weddell Sea in 2018/2019, edited by Olaf Boebel

731 (2019) The Expedition PS116 of the Research Vessel POLARSTERN to the Atlantic Ocean in 2018, edited by Claudia Hanfland and Bjela König

730 (2019) The Expedition PS110 of the Research Vessel POLARSTERN to the Atlantic Ocean in 2017/2018, edited by Frank Niessen

729 (2019) The Expedition SO261 of the Research Vessel SONNE to the Atacama Trench in the Pacific Ocean in 2018, edited by Frank Wenzhöfer

728 (2019) The Expedition PS115/2 of the Research Vessel POLARSTERN to the Arctic Ocean in 2018, edited by Ruediger Stein

727 (2019) The Expedition PS115/1 of the Research Vessel POLARSTERN to the Greenland Sea and Wandel Sea in 2018, edited by Volkmar Damm

ALFRED-WEGENER-INSTITUT
HELMHOLTZ-ZENTRUM FÜR POLAR-
UND MEERESFORSCHUNG

BREMERHAVEN

Am Handelshafen 12
27570 Bremerhaven
Telefon 0471 4831-0
Telefax 0471 4831-1149
www.awi.de

HELMHOLTZ